DESTRUCTION OF ENDOCRINE DISRUPTING COMPOUNDS IN WATER BY ADVANCED OXIDATION PROCESSES: A STUDY WITH ULTRASOUND, OZONE AND VARIOUS COMBINATIONS

by

IŞIL GÜLTEKİN

B.S. in Environmental Engineering, Yıldız Technical University, 2000

M.S. in Environmental Technology, Boğaziçi University, 2002

Submitted to the Institute of Environmental Sciences in partial fulfillment of the requirements for the degree of

Doctor

of

Philosophy

in

Environmental Technology

Boğaziçi University

2008

ACKNOWLEDGEMENTS

I would like to express my deep and sincere gratitude to my thesis supervisor Prof. Dr. Nilsun H. İnce for her guidance, friendly approach and encouragement throughout this study and beyond. She has always supported me both in academic and personal terms. She has been more than just a supervisor for me and I must say that I feel lucky to be her graduate student and to know her.

I am thankful to my jury members Prof. Dr. Miray Bekbölet, Prof. Dr. Ferhan Çeçen, Assoc. Prof. Dr. Neylan Dirilgen and Assoc. Prof. Dr. İdil Arslan Alaton for their valuable and supportive comments.

The financial support provided by the Boğaziçi University Research Fund to the projects 06S101 and 07Y103D is greatly acknowledged.

The research scholarship from German Academic Exchange Service (DAAD) for carrying out experimental work at Saarland University, Institute for Environmentally Compatible Process Technology, Saarbrücken, Germany is gratefully acknowledged.

I wish to express my special thanks to Ant Teknik Cihazlar Pazarlama ve Dış Tic. Ltd. Şti., especially Cüneyt Eler and Zafer Bayram for their help during the purchase of the HPLC instrument and technical support thereafter, which were of crucial value in the completion of the dissertation.

I warmly thank to my dear friend Dila Aksoy for her endless support and help. I owe very special thanks to Gülhan Özkösemen for her help during my laboratory studies. I would like to thank Ceyda Senem Uyguner and Nilgün Ayman Öz for their friendship and support.

The most special thanks go to my dear parents Nalan and Erdal Gültekin, and my sister Umut for their endless love, support, patience and understanding.

ABSTRACT

The presence of endocrine disrupting compounds (EDCs) in the environment is a significant health concern due to their potential to mimic the hormonal activity in wildlife. Their elimination in water by conventional water treatment methods is very difficult, so that extensive research has been recently devoted to the development of appropriate and effective methods for the complete destruction of the compounds or for removing their endocrine activities. Due to the high reactivity of hydroxyl radicals with all organic chemicals regardless of their complexity, advanced oxidation processes that are based on the onsite generation of these radicals have gained much attention in recent years for the destruction of problematic pollutants in water such as EDCs .

The aim of this study was to investigate the degradability of EDCs primarily by ultrasound, which is a novel technique of hydroxyl radical production. In addition, ozonation and hybrid techniques involving combinations of ultrasound with ozone and/or with Fenton reactions were also evaluated as alternative methods. The test compounds were selected from a group of well classified EDCs (Bisphenol-A and 4-n-Nonylphenol) and a group of non-classified but suspected EDCs (a textile dye-C.I. Acid Orange 8). The emphasis was on: i) effects of operating parameters such as EDC concentration, pH, ultrasonic frequency, the dose of chemical reagents; and ii) reaction kinetics and reaction sites.

It was found that the rate of EDC decay was pseudo-first order in all experimental systems and at all test conditions. Ozonation at pH 6 was a very effective method of converting EDCs to products, which did not exhibit endocrine disrupting properties. The efficiency of ultrasonic destruction of EDCs was largely related to the physical properties of the compounds (e.g. hydrophobicity), the applied frequency, the type of dissolved gases in the medium and the pH of the solution. Addition of OH radical sinks (e.g. carbonates, tertiary butyl alcohol) and OH radical sources (e.g. Fenton reagents, carbon tetrachloride) at the right doses was a key parameter in controlling the reactivity of EDCs under ultrasonic irradiation. Combination of ultrasound with ozone induced a synergistic effect particularly for the overall degradation or mineralization of the compounds.

ÖZET

Endokrin bozucu maddelerin (EBM) çevrede bulunmaları, bu maddelerin doğal yaşamda hormonal aktiviteyi taklit etme potansiyellerinden dolayı ciddi bir sağlık endişesi yaratmaktadır. Konvansiyonel su arıtma metotları ile giderilmeleri çok zor olduğundan, bu maddelerin tamamen parçalanması veya endokrin aktivitelerinin giderilmesi için uygun ve etkili metotların geliştirilmesi adına kapsamlı araştırmalar yapılmaktadır. Hidroksil radikallerinin organik maddelerle yüksek reaktiviteye sahip olmasından dolayı, bu radikallerin oluşumunu temel alan ileri oksidasyon prosesleri sulardaki EBM' ler gibi problemli kirleticilerin parçalanması konusunda son yıllarda önemli ölçüde ilgi çekmiştir.

Bu çalışmanın amacı, esas olarak sesüstü dalgalar ile EBM'lerin parçalanmasının incelenmesidir. Ozonlama ve sesüstü dalgaların ozon ve/veya Fenton reaksiyonları ile kombinasyonunu içeren hibrid tekniklerde alternatif metotlar olarak değerlendirilmiştir. Test maddeler tanımlanmış EBM grubundan (Bisfenol-A ve Nonilfenol) ve tanımlanmamış fakat şüpheli EBM sınıfından (tekstil boyası-C.I. Acid Orange 8) şeçilmiştir. Tezde vurgulanan konular şunlardır: (i) EBM konsantrasyonu, pH, ultrasonik frekans, eklenen kimyasal dozu gibi operasyonel parametrelerin etkisi, (ii) reaksiyon kinetiği ve reaksiyon bölgeleri.

Bütün deneysel sistemlerde ve her test koşulunda EBM parçalanmasının birinci derece kinetiğine uyduğu tespit edilmiştir. pH 6' da yapılan ozonlamanın, EBM' leri endokrin bozucu özellik göstermeyen maddelere dönüştürmede etkili bir metot olduğu görülmüştür. EBM'lerin sesüstü dalgalar ile parçalanmasının maddelerin fiziksel özelliklerine (hidrofobiklik gibi), uygulanan frekansa, ortamda bulunan çözünmüş gaz tipine ve çözeltinin pH'sına bağlı olduğu bulunmuştur. Hidroksil radikal yakalayıcılarının (karbonatlar, tert-butil alkol gibi) ve hidroksil radikal kaynaklarının (Fenton, karbon tetraklorür gibi) doğru dozlarda eklenmesinin, EBM'lerin sesüstü dalgalar altında reaktivitesini kontrol etmede önemli bir parametre olduğu görülmüştür. Sesüstü dalgaların ozon ile birleşimi maddelerin parçalanmasında veya mineralizasyonunda sinerjistik bir etki göstermiştir.

TABLE OF CONTENTS

LIST OF FIGURES

LIST OF TABLES

LIST OF SYMBOLS/ABBREVIATIONS

A	Absorbance
AOP	Advanced oxidation process
AO8	C.I. Acid Orange 8
AP	Alkylphenol
APEO	Alkylphenol polyethoxylate
BBP	Butyl benzyl phthalate
BPA	Bisphenol A
BCOz	Bubble-column ozone reactor
C	Concentration
C.I.	Color index codes
C_p/C_v	Ratio of specific heats
DBP	Dibutyl phthalate
DEHP	2-ethylhexyl phthalate
DEP	Diethyl phthalate
DMP	Dimethyl phthalate
DPP	Di-n-propyl phthalate
EDC	Endocrine disrupting compound
EST	Estrogenic activity
G	Sonochemical product yield
k’	Pseudo-first order degradation rate coefficient
k_{BPA-O3}	Bimolecular rate constant of BPA with ozone
K_La	Ozone mass transfer rate coefficient
Log K_{ow}	Octanol-water partition coefficient
M	Mass of water
NP	Nonylphenol
4-NP	4-n-Nonylphenol
NPEO	Nonylphenol polyethoxylate
•OH	Hydroxyl radical
P	Ultrasonic power
P_d	Power dissipated in the system

TOC	Total organic carbon
US	Ultrasonic irradiation
US1	20 kHz probe type ultrasonic system
US2	300 kHz plate type ultrasonic system
US3	Multi-frequency plate type ultrasonic system
USOz	Ozone-ultrasound reactor
UV	Ultraviolet irradiation
γ	Polytropic gas ratio
κ	Thermal conductivity

1. INTRODUCTION

Recently, much concern and debate have been raised over the adverse health effects on wildlife imposed by a group of chemicals known as “endocrine disrupting compounds” (EDCs), which have the potential to disrupt the normal functioning of the endocrine system. The disruption mechanism is very complex involving alteration of hormone levels, stimulation or inhibition of their production, and/or modification of the way they travel through the body. Although the information on the impacts of EDCs on human health is currently insufficient, the threat is so serious that extensive research sources are granted to this field, particularly in North America.

The presence of EDCs in the water environment is primarily due to municipal and industrial effluent discharge following incomplete/inefficient degradation in conventional treatment processes, in addition to accidental spills from manufacturing processes and leaching from final end products. EDCs may also find their way to groundwaters by percolation of rainwater through landfills and agricultural areas.

The low concentration and low biodegradability of EDCs in water is a major problem for their destruction by conventional (biological) or non-conventional (advanced/ chemical) water treatment processes. Research has shown that even trace levels of EDCs in water may result in estrogenic activity, so that adequate treatment methods must be developed to destroy them completely or to convert them to products that do not disrupt the endocrine function. It is very important that these new technologies to be developed are not limited to medium or high concentration levels of these compounds, but are capable of destroying them at extremely low concentrations, as well.

Advanced oxidation processes, which rely on the production of hydroxyl radicals in water have been recently found effective for the elimination of compounds that exist at low concentrations and that are difficult to eliminate by conventional methods. Ultrasonic irradiation is a novel method of hydroxyl radical generation, and combination of ultrasound with the more common advanced oxidation methods (e.g. ozonation, UV irradiation, Fenton reaction) is extremely effective for the destruction of recalcitrant

compounds in water. The power of such combinations is based on the synergy induced by acoustic cavitation through very unique catalytic effects.

EDCs may be evaluated under two perspectives: i) those that are distinctly classified (i.e. identified by in-vivo and in-vitro methods), and ii) those that are not so far classified, but shown to have the potential to interfere with the endocrine system in wildlife. Within these perspectives, this research is aimed to investigate the degradability of two classified EDCs, namely Bisphenol-A and Nonylphenol; and one unclassified or potential EDC, namely C.I. Acid Orange 8 (a textile dye) using ultrasound, ozone and combinations of ultrasound with ozone and/or Fenton reactions.

In that respect, the contents of this dissertation are grouped under the following topics:

- A theoretical background on advanced oxidation processes, ozonation and ultrasound (Chapter 2).
- An extensive review of endocrine disrupting compounds and their elimination from water by advanced oxidation processes (Chapter 3). The second part has been published in *Journal of Environmental Management* as a review article (Gültekin and Ince, 2007).
- A detailed description of materials, methods and optimization of the ultrasonic reactors (Chapter 4).
- An investigation of the degradability of bisphenol-A by ultrasound, ozone and ultrasound ozone combination (Chapter 5). The first part of ultrasonic destruction covers the assessment of operating parameters, as recently published in *Ultrasonics Sonochemistry* (Gültekin and Ince, 2008). The second part covers the impacts of frequency on the rate of reaction and the assessment of reaction sites. The study on ozonation of bisphenol-A is divided into two sections: the first section was presented in the fourth IWA International Conference on Oxidation Technologies for Water and Wastewater Treatment, Germany, May 2006; and the other part covering reaction kinetics, pH effects and ozone mass transfer efficiencies has been submitted and is under review. The study on ultrasound ozone combination was

presented in Cavitation and Environment: COST D32 Working Group Workshop, Dundee, June 2007.

- An investigation of the degradability of 4-n-nonylphenol by ultrasound and combinations of ultrasound with Fenton and Fenton-like reagents (Chapter 6). The study has been recently submitted and is under review.
- An investigation of the degradability of an unclassified EDC by ultrasound (Chapter 7). The first part of this study describes the research article published in *Ultrasonics Sonochemistry* (Gültekin and Ince, 2006) covering the degradation of the azo dye C.I. Acid Orange8 by ultrasound, ozone and their combination. A part of the work was presented in The First European Conference on Oxidation and Reduction Technologies for ex-situ and in-situ Treatment of Water, Air and Soil, Germany, May 2004 prior to publication. The second part covers the impacts of carbon tetrachloride and tertiary-butyl-alcohol addition and the assessment of potential reaction sites, as was recently submitted and is currently under review.
- A summary of all findings, concluding remarks and suggestions for future work (Chapter 8).

As a final remark, all research described here was carried out in Boğaziçi University, Institute of Environmental Sciences, except that one covering ozonation of bisphenol-A, which was conducted in Saarland University, Institute for Environmentally Compatible Process Technology, Germany under the research scholarship granted by German Academic Exchange Service (DAAD).

2. THEORETICAL BACKGROUND ON ADVANCED OXIDATION PROCESSES AND ULTRASOUND

2.1. Advanced Oxidation Processes

Advanced Oxidation Processes (AOPs), which involve the in-situ generation of highly potent chemical oxidants, such as the hydroxyl radical (•OH), have emerged as an important class of technologies for accelerating the oxidation and hence removal of a wide range of organic contaminants in polluted water and air (Bolton et al., 1994). AOPs are approaches that are particularly appropriate for effluents containing refractory, toxic and/or non-biodegradable materials. There are a variety of advanced oxidation processes including: (1) homogeneous ultraviolet (UV) irradiation - either direct irradiation of the contaminant or photolytic oxidation mediated by hydrogen peroxide (UV/H_2O_2), and/or ozone ($UV/H_2O_2/O_3$ or UV/O_3), (2) Fenton and photo-Fenton processes, (3) heterogeneous photocatalysis using semiconductor catalysts (e.g. UV/TiO_2), (4) ultrasonic irradiation (sonolysis), (5) supercritical water oxidation, (6) electrochemical water oxidation, (7) X-ray or gamma-ray radiolysis, (8) electron-beam irradiation. Although these technologies involve different methods of activation, as well as oxidant generation, most of them are electric-energy-driven and share the common denominator of hydroxyl radical chemistry for contaminant removal. The brief explanation of some of the common AOPs is given below.

2.1.1. Homogeneous Processes

2.1.1.1. UV/H_2O_2 Process. Generation of •OH by UV photolysis of H_2O_2 is described by the following reaction:

$$H_2O_2 + h\nu \rightarrow 2\ \bullet OH \qquad (2.1)$$

Low pressure mercury vapor UV lamps with a 254 nm peak emission are typically used to produce UV radiation, but these lamps may not be the best choice for a UV/H_2O_2 process because the maximum absorbance of UV radiation by H_2O_2 occurs at about 220

nm and because the molar absorption coefficient of H_2O_2 at 254 nm is low. If low-pressure mercury lamps are used, a high concentration of H_2O_2 is needed in the medium to generate sufficient •OH because of the low molar absorption coefficient. However, high concentrations of H_2O_2 may scavenge the •OH, making the UV/H_2O_2 less effective. To overcome this limitation, some AOP technology vendors use high intensity, medium-pressure, broad band UV lamps; others use high intensity, xenon flash lamps whose spectral output can be adjusted to match the absorption characteristics of H_2O_2 or another photolytic target (U.S. EPA, 1998).

2.1.1.2. Ozonation. Ozone can react with substances in two different ways, either indirectly or directly. The indirect reaction pathway involves radicals. The first step is the decomposition of ozone, accelerated by initiators, such as hydroxide ion (OH^-) to form secondary oxidants such as hydroxyl radicals which are non-selective in their reactions. The direct oxidation of organic compounds by ozone is a selective reaction with slow reaction rate constants, typically being in the range of 1 to 10^3 M^{-1} s^{-1}. Normally, under acidic conditions (pH < 4) the direct pathway dominates, above pH 10 it changes to the indirect (Gottschalk et al., 2000). More detailed information on ozonation is given in section 2.2.

2.1.1.3. UV/O_3 and UV/O_3/H_2O_2 Processes. UV photolysis of O_3 in water yields H_2O_2, which in turn reacts with UV radiation or O_3 to form •OH as shown below:

$$O_3 + h\nu + H_2O \rightarrow H_2O_2 + O_2 \quad (2.2)$$

$$H_2O_2 + h\nu \rightarrow 2\ \bullet OH \quad (2.3)$$

$$2\ O_3 + H_2O_2 \rightarrow 2\ \bullet OH + 3O_2 \quad (2.4)$$

Because the molar absorption coefficient of O_3 is 3300 M^{-1} cm^{-1} at 254 nm, UV photolysis of O_3 is not expected to have the same limitation as that of H_2O_2 when low pressure mercury vapor UV lamps are used (U.S. EPA, 1998).

Addition of hydrogen peroxide to the UV/O_3 process results in a net enhancement due to the dominant production of •OH radicals as shown in equations 2.5 to 2.8.

$$H_2O_2 \leftrightarrow HOO^- + H^+ \quad (2.5)$$

$$O_3 + HOO^- \rightarrow \bullet OH + O_2^{\cdot -} + O_2 \quad (2.6)$$

$$O_3 + O_2^{\cdot -} \rightarrow O_3^{\cdot -} + O_2 \quad (2.7)$$

$$O_3^{\cdot -} + H_2O \rightarrow \bullet OH + HO^- + O_2^{\cdot} \quad (2.8)$$

2.1.1.4. O_3/H_2O_2 Process. The O_3/H_2O_2 process, also known as the peroxone process, has been used for treatment of contaminated water (U.S. EPA, 2001a). H_2O_2 can initiate decomposition of O_3 with the hydroperoxide ion (HO_2^-) as shown below:

$$H_2O_2 \leftrightarrow HO_2^- + H^+ \quad (2.9)$$

$$HO_2^- + O_3 \rightarrow O_3\bullet^- + HO_2\bullet \quad (2.10)$$

$$O_3\bullet^- + H^+ \rightarrow HO_3\bullet \quad (2.11)$$

$$HO_3\bullet \rightarrow \bullet OH + O_2 \quad (2.12)$$

$$HO_2\bullet \leftrightarrow H^+ + O_2\bullet^- \quad (2.13)$$

$$O_2\bullet^- + O_3 \rightarrow O_3\bullet^- + O_2 \quad (2.14)$$

These equations may be combined to represent the overall reaction between H_2O_2 and O_3 that yields •OH as shown in equation 2.15.

$$2\ O_3 + H_2O_2 \rightarrow 2\bullet OH + 3O_2 \quad (2.15)$$

Two •OH are formed for each mole of H_2O_2 reacting with two moles of O_3. However, H_2O_2 present in quantities significantly exceeding stoichiometry is known to scavenge •OH and thereby reduce the overall effectiveness of the O_3/H_2O_2 process (Glaze et al., 1987).

2.1.1.5. Fenton and Photo-Fenton Processes. The dark reaction of ferrous iron (Fe^{2+}) with H_2O_2 to generate •OH is known as the Fenton`s reaction (equation 2.16). The •OH formed either react with Fe^{2+} to produce ferric iron (Fe^{3+}) (equation 2.17) or can react with and initiate oxidation of organic pollutants. This process is most effective at pH levels less than or equal to 3 (Walling, 1975; Pignatello, 1992).

$$Fe^{2+} + H_2O_2 \rightarrow Fe^{3+} + OH^- + \bullet OH \quad (2.16)$$

$$\bullet OH + Fe^{2+} \rightarrow Fe^{3+} + OH^- \quad (2.17)$$

Decomposition of H_2O_2 is also catalyzed by Fe^{3+} (Walling, 1975). In this process, H_2O_2 is decomposed to the water molecule and O_2, and a steady-state concentration of Fe^{2+} is maintained during the decomposition as shown in equations 2.18 and 2.19.

$$Fe^{3+} + H_2O_2 \rightarrow Fe^{2+} + \bullet HO_2 + H^+ \quad (2.18)$$

$$\bullet HO_2 + Fe^{3+} \rightarrow Fe^{2+} + H^+ + O_2 \quad (2.19)$$

The rate of removal of organic pollutants and the extent of mineralization with the Fe^{2+}/ H_2O_2 and Fe^{3+}/H_2O_2 reagents are improved considerably by irradiation with near-UV radiation and visible light (Ruppert et al., 1993). This process is called the photo-Fenton reaction. Photo-enhancement of reaction rates is likely because of (1) photo-reduction of Fe^{3+} to Fe^{2+}; (2) photo-decarboxylation of ferric carboxylate complexes; (3) photolysis of H_2O_2 (U.S. EPA, 2001a).

2.1.2. Heterogeneous Processes and Radiation Techniques

2.1.2.1. Heterogeneous Photocatalysis. Degradation and mineralization of organic pollutants by heterogeneous photocatalysis occur in the presence of semiconductor photocatalysts, the most widely used one being titanium dioxide (TiO_2). When TiO_2 absorbs a photon of energy equal to or greater than its band gap width, an electron is excited from the valence band to the conduction band (e^-_{CB}) leaving behind an electron vacancy or "hole" in the valence band (h^+_{VB}). The combination of the electron in the conduction band and the hole in the valence band is referred to as an electron-hole pair, which subsequently migrates to the semiconductor surface and initiates chemical reactions (U.S. EPA, 1998). The primary photocatalytic mechanism is believed to proceed as follows:

$$TiO_2 + h\nu \rightarrow e^-_{CB} + h^+_{VB} \quad (2.20)$$

At the TiO_2 surface, the holes react with either H_2O or OH^- from water dissociation to form •OH (equations 2.21 and 2.22). An additional reaction may occur if the electron in the conduction band reacts with O_2 to form superoxide radical ions ($O_2•^-$) (equation 2.23). Superoxide radical ion can then react with H_2O to provide additional •OH, OH^- and O_2 (U.S. EPA, 1998).

$$h^+_{VB} + H_2O \rightarrow •OH + H^+ \quad (2.21)$$

$$h^+_{VB} + OH^- \rightarrow •OH \quad (2.22)$$

$$e^-_{CB} + O_2 \rightarrow O_2•^- \quad (2.23)$$

2.1.2.2. Gamma-Ray and X-Ray Processes. Gamma-rays are high energy photons (electromagnetic radiation) that are emitted by excited atomic nuclei in transition to a state of lower excitation. The most common source of gamma rays is radioactive decay of radioisotope cobalt 60 (^{60}Co), which emits gamma rays at energies of 1.17 and 1.33 million electron volts (MeV) as it decays to nickel 60 and has a half life of 5.27 years. X-rays are also high energy photons that are generated by accelerating high energy electrons in the form of an electron-beam against a material with a high energy number (U.S. EPA, 2001a).

When gamma rays and X-rays collide with irradiated water, high energy (secondary) electrons are generated along the trajectory of the photons which can initiate several thousand reactions as they dissipate energy in irradiated medium. The reactions result in the formation of three primary reactive species responsible for organic compound destruction, namely hydroxyl radical, hydrogen radical and aqueous electrons (U.S. EPA, 2001a).

Gamma rays and X-rays have high penetration depths within irradiated water. The effective water penetration depths of 1.25 MeV gamma-rays and 1 MeV X-ray are about 76 cm and 27 cm, respectively (Gray and Cleland, 1998; Bailey and Lackner, 1995). Therefore, both gamma-rays and X-rays can be used to treat flowing waste streams as well as containerized liquid wastes.

2.1.2.3. Electron-Beam Irradiation. The electron-beam (E-beam) process involves irradiation of water with a beam of high-energy electrons produced by an electron

accelerator. Electron accelerators can provide electron energies in the range of 0.1 to 10 MeV. High energy E-beams of about 2 MeV are used for irradiation of water (U.S. EPA, 2001a). The depth to which E-beam can penetrate irradiated water is significantly less than the depths associated with gamma rays and X-rays. A 1 MeV electron deposits its energy in water within a depth of 4 millimeters (Bailey and Lackner, 1995). As a result, E-beams are typically used to treat contaminated water of relatively shallow depths. Like gamma rays and X-rays, E-beam irradiation of water causes formation of same three primary reactive species responsible for degradation of organic compounds.

2.1.3. Ultrasonic Cavitation

Ultrasonic cavitation is a novel technique in AOP practices which results in very unique and extreme conditions generated by ultrasonic waves in liquid media, leading to a remarkably suitable medium for high energy chemistry, which is called “sonochemistry”. Sonochemistry derives principally from acoustic cavitation; the formation, growth and implosive collapse of bubbles in a liquid. Under well-established conditions, these extremes not only promote the oxidative destruction of target contaminants via free radical reactions, but also provide an excellent medium for their thermal decomposition in the gas phase. Hence, the production of free radical species by sonochemical irradiation extends the goals of AOP beyond aqueous phase oxidative destruction to gaseous decomposition, owing to very special effects generated by the formation and collapse of acoustic cavities in sonicated water (Ince et al., 2001). In Section 2.3, more detailed information on ultrasonic irradiation is given.

2.2. Ozonation

Ozone applications have increased enormously both in number and diversity since the first full scale application of ozone for the disinfection of drinking water in Nice in 1906. Ozone is a strong oxidant with a high oxidation potential of 2.07 Volts. The main areas where ozone is used in water and wastewater treatment applications include (i) disinfection, (ii) oxidation of inorganic compounds, (iii) oxidation of organic compounds including taste, odor, color removal and (iv) particle removal.

Due to its electronic configuration, ozone undergoes different reactions in water. These reactions can be divided into three categories (Beltran, 2004):

- Oxidation-reduction reactions
- Dipolar cycloaddition reactions
- Electrophilic substitution reactions

In an alkaline medium, free radicals are formed yielding hydroxyl radicals which are extremely reactive with any organic matter present in water. For this reason, ozone reactions in water can be classified as direct and indirect reactions. Direct reactions are the true ozone reactions, that is, the reactions the ozone molecule undergoes with any other type of chemical species. Indirect reactions are those between the hydroxyl radicals, formed from the decomposition of ozone, with compounds present in water. Direct and indirect reaction pathways lead to different oxidation products and are controlled by different types of kinetics (Gottschalk et al., 2000; Beltran et al., 2004).

2.2.1. Indirect Reaction

The indirect reaction pathway involves radicals. The first step is the decomposition of ozone, accelerated by initiators, such as hydroxide ion (OH^-) to form secondary oxidants such as hydroxyl radicals which are non-selective in their reactions ($k=10^8$-10^{10} $M^{-1}s^{-1}$). The radical pathway is very complex and is influenced by many substances. The indirect reaction mechanism can be divided into three steps:

Initiation step. The reaction between hydroxide ions and ozone leads to the formation of superoxide anion radical ($O_2\bullet^-$) and hydroperoxyl radical ($HO_2\bullet$).

$$O_3 + OH^- \rightarrow O_2\bullet^- + HO_2\bullet \quad (2.24)$$

Propagation Step.

$$HO_2\bullet \leftrightarrow O_2\bullet^- + H^+ \quad (2.25)$$

$$O_3 + O_2\bullet^- \rightarrow O_3\bullet^- + O_2 \quad (2.26)$$

$$O_3\bullet^- + H^+ \leftrightarrow HO_3\bullet \quad (2.27)$$

$$HO_3\bullet \rightarrow \bullet OH + O_2 \quad (2.28)$$

$$\bullet OH + O_3 \rightarrow HO_4\bullet \quad (2.29)$$

$$HO_4\bullet \rightarrow HO_2\bullet + O_2 \quad (2.30)$$

With the decay of $HO_4\bullet$ into oxygen and hydroperoxide radical, the chain reaction can start anew. Substances which convert $\bullet OH$ into superoxide radicals ($O_2\bullet^-$, $HO_2\bullet$) promote the chain reaction; they act as chain carriers, the so-called promoters. Organic molecules (R) can also act as promoters. Some of them contain functional groups which react with $\bullet OH$ and form organic radicals $R\bullet$.

Termination Step. Some organic and inorganic substances react with $\bullet OH$ to form secondary radicals which do not produce $HO_2\bullet$ and $O_2\bullet^-$. These inhibitors generally terminate the chain reaction.

$$\bullet OH + CO_3^{2-} \rightarrow OH^- + CO_3\bullet^- \quad (2.31)$$

$$\bullet OH + HCO_3^- \rightarrow OH^- + HCO_3\bullet \quad (2.32)$$

Another possibility to terminate the chain reaction is the reaction of two radicals:

$$\bullet OH + HO_2\bullet \rightarrow O_2 + H_2O \quad (2.33)$$

2.2.2. Ozone Generation

Since ozone is an unstable molecule, it has to be generated on-site. The various methods of ozone production differ in their working principles and ozone sources. The methods and their differences are summarized in Table 2.1.

Ozone production from ambient air or pure oxygen in an electrical discharge chamber is the most widespread technology for ozone generation. Electrical discharge ozone generators ionize molecular oxygen by applying high power alternating current to the gas. Air or pure oxygen can be used as a feed gas, at either ambient or elevated

pressure. Ozone is formed by recombination of ionized oxygen atoms and unionized molecular oxygen.

Table 2.1. Overview of types of ozone generation, working principles and fields of application (Gottschalk et al, 2000).

Method of Ozone Generation	**Working Principle**	**Ozone Source**	**Field of Application**
Electrical	Electrical Discharge (ED)	Air or O_2	Common standard from laboratory to full-scale
Electrochemical	Electrolysis (EL)	Water (highly purified)	Laboratory to small industrial scale
Photochemical ($\lambda < 185$ nm)	Irradiation (abstraction of electrons)	O_2 (air), water (drinking water quality or highly purified)	New technology, laboratory to full-scale
Radiation Chemistry	X-rays, radioactive γ-rays	Water (highly purified)	Very seldom, solely experimental
Thermal	Light arc ionization	Water	Very seldom, solely experimental

2.2.3. Reactors Used for Ozonation

Bubble columns (BCs) and stirred tank reactors (STRs) are the most frequently used types of ozone reactors. Bubble columns can be roughly assumed to behave like perfectly mixed reactors with respect to the liquid phase, provided the ratio of height (h) to diameter (d) is small ($h/d \leq 10$). The advantage of BCs is an increased level of the dissolved ozone concentration in the reactor, which is especially important in the case of low contaminant concentrations and /or low reaction rate constants, i.e. typical of drinking water applications. STRs are frequently used in lab-scale ozonation, partially due to the ease in modeling completely mixed phases, but they are very seldom used in full-scale applications (Gottschalk et al., 2000).

Ozone can be introduced into the reactor with different types of gas diffusers. Ring pipes, porous diffusors, porous membranes, injector nozzles and static mixers can be employed. The different types of diffusers are mainly characterized by the diameter of the

bubbles (d_B) produced; e.g. micro (d_B=0.01-0.2 mm), small (dB ≈ 1 mm) or big (d_B ≈ 2.5 mm) bubbles (Calderbank, 1967).

2.2.4. Mass Transfer of Ozone into Solution

The most important phenomena in ozonation applications is the mass transfer of ozone from gas phase to into the liquid phase. During the transfer of ozone from gas to liquid, the following stages are processed: diffusion of ozone across the gas/liquid phase, dissolving into the liquid, diffusion into the liquid. Mass transfer of ozone is affected by operating conditions, i.e concentration of ozone in the gas phase, type of ozone reactor and diffuser, solution volume, temperature, turbulence as well as chemical reactions. Depending on the relative rates of reaction and mass transfer, a chemical reaction can change the ozone concentration gradient that develops in the laminar film, normally increasing the mass transfer coefficient, which in turn increases the mass transfer rate.

2.3. Ultrasound

2.3.1. Historical Background

The chemical application of ultrasound, “sonochemistry” has become an exciting new field of research during the past decade. However, the history of sonochemistry begins in the late 1800s. The phenomenon of cavitation was first identified and reported in 1894 by Sir John I. Thornycroft and Sidney W. Barnaby. This discovery was the result of investigations into the inexplicably poor performance of a newly built destroyer, H.M.S Daring (of high-speed torpedo boats). The top speed of the ship was below specifications despite the high revolutions of the propeller. The problem was traced to an incorrect setting of the propeller blades resulting in inefficient thrust. It was found that, during the rapid motion of the propeller blade through the water, the trailing edge produced sufficient negative pressure to pull the water molecules apart and create tiny microbubbles (cavities). These bubbles subsequently collapsed with the release of intense local energy causing erosion in the metal surface of the propeller. By increasing the propeller size and reducing its rate of rotation, they could minimize this difficulty of "cavitation". As ship speeds increased, however, this became a serious concern and the Royal Navy commissioned Lord

Rayleigh to investigate. He confirmed that the effects were due to the enormous turbulence, heat, and pressure produced when cavitation bubbles imploded on the propeller surface. Despite the earlier studies, the renaissance of sonochemistry occurred in the 1980's, soon after the advent of inexpensive and reliable laboratory generators of high-intensity ultrasound. Scientists now know that the chemical effects of ultrasound are diverse and include substantial improvements in both stoichiometric and catalytic chemical reactions (Mason and Peters, 2002; Suslick, 2006).

2.3.2. Ultrasonic Frequencies

Ultrasound is defined as any sound having a frequency higher than that to which the human ear can respond (i.e. above 16 kHz). The uses of ultrasound can be divided broadly into three distinct regions:

i) low frequency or conventional power ultrasound (20-100 kHz);
ii) medium-frequency, or “sonochemical-effects” ultrasound (200-2000 kHz); and
iii) high frequency, or diagnostic ultrasound (2-10 MHz).

The use of power ultrasound has been well known in fields such as cleaning, plastic welding, emulsification, solvent degassing and cutting. High frequency ultrasound is used in medical imaging and chemical analysis. It is the medium frequency range where sonochemical effects are observed which are largely linked to the formation of free radical species. In fact, it is important to note that the range available for sonochemistry has been extended to 2 MHz with the development of high power equipment capable of generating cavitation within liquid systems at these higher frequencies (Mason and Lorimer, 2002).

Ultrasound is transmitted to a liquid by using different equipments involving baths, probe and disk systems. The essential device in the generation of ultrasound is the transducer. A transducer is any device which is capable of converting one form of energy into another. There are three main types of ultrasonic transducers for sonochemistry: gas-driven, liquid-driven and electromechanical. The most common type used in ultrasonic systems is electromechanical which is based on piezoelectric technology. Piezoelectric transducers convert electrical energy to ultrasonic vibrations by either expanding or

contracting as a result of the applied electrical charge (Mason and Luche, 1997; Mason and Peters, 2002).

2.3.3. Sonochemistry and Acoustic Cavitation

The term sonochemistry is used to describe a subject in which sound energy is used to affect chemical processes. The chemical effects of ultrasound occur as a result of the "cold boiling" phenomenon termed acoustic cavitation, which is the production of microbubbles in a liquid when a large local negative pressure is applied. Ultrasound is transmitted through a medium via pressure waves by inducing vibrational motion of the molecules which alternately compress and expand the molecular structure of the medium due to a time-varying pressure (Mason, 1990). Compression cycles exert a positive pressure on the liquid pushing the molecules together, while the expansion (rarefaction) cycles exert a negative pressure pulling the molecules away from one another. Therefore, the distance among the molecules varies as the molecules oscillate around their mean position. When the intensity of ultrasound in a liquid is increased, a point is reached where the negative pressure developed in the rarefaction cycle of the wave is sufficient to overcome the critical molecular distance to hold the molecular structure intact. As a result, the liquid breaks apart to form acoustic cavities, made of vapor and gas-filled microbubbles (Mason, 1990; Dahlem et al., 1998). These cavities are called cavitation bubbles as this process is called cavitation and the point where it starts cavitation threshold. The phenomenon "acoustic cavitation" consists of at least three distinct and successive stages: nucleation, bubble growth (expansion), and under proper conditions implosive collapse (Suslick, 1990). Development and collapse of cavitation bubbles can be seen in Figure 2.1 (Suslick, 2006).

The first stage, also known, as "cavity formation" is a nucleated process, by which cavitational nuclei are generated from microbubbles trapped in micro crevices of suspended particles within the liquid (Suslick, 1990; Reisse, 1995). In the second stage, the bubbles grow and expand in a manner restricted by the intensity of the applied sound wave. With high-intensity ultrasound, a small cavity grows rapidly through inertial effects, whereas at lower intensities the growth occurs through "rectified diffusion", proceeding in a much slower rate, and lasting many more acoustic cycles before expansion (Suslick,

1990). The third stage of cavitation occurs only if the intensity of the ultrasound wave exceeds that of the "acoustic cavitation threshold" (typically a few watts cm^{-2} for ordinary liquids exposed to 20 kHz). The cavitation threshold is defined such that when very low power ultrasound is passed through a liquid and the power is gradually increased; a point is reached at which the intensity of sonication is sufficient to cause cavitation in the liquid. It is only at powers above the cavitation threshold that sonochemistry can occur because only then can the great energies associated with cavitational collapse be released into the liquid (Mason and Peters, 2002). At this condition, the microbubbles overgrow to the extent where they can no longer efficiently absorb energy from the sound environment to sustain themselves, and implode violently, therefore, in a so-called "catastrophic collapse" (Ince et al., 2001; Mason, 1990; Suslick et al., 1990).

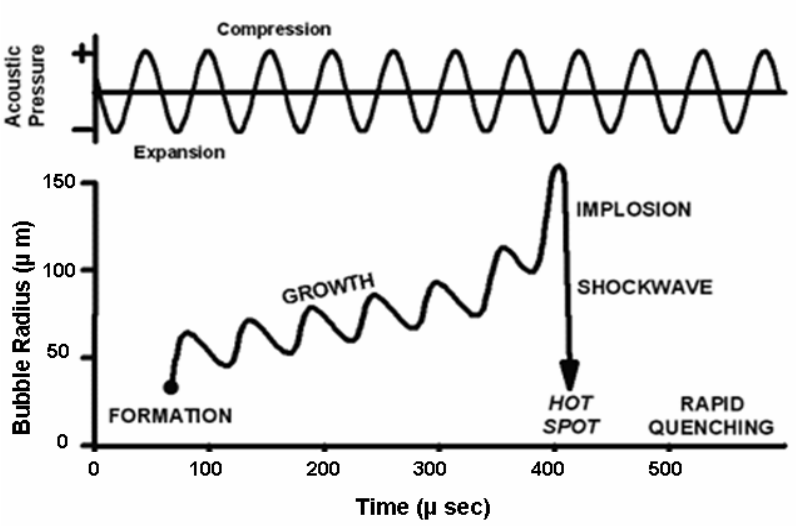

Figure 2.1. Development and collapse of cavitation bubbles (Suslick, 2006).

It is reported that during this collapse stage, such extremes of temperatures and pressures are released that the entrapped gases undergo molecular fragmentation - the underlying phenomenon in homogenous sonochemistry (Hung and Hoffmann, 1998). Furthermore, it has been observed that just before the catastrophic collapse of compressed gas-filled cavities in water, the bubbles produce a flash of light called "sonoluminescence", as detected by a peak at 310 nm and a broad continuum throughout the visible (Ince et al., 2001; Crum, 1994; Verrall et al., 1988). The spectrum of sonoluminescent water was associated with the formation of high-energy species (e.g. excited hydroxyl radicals) from molecular fragmentation of compressed gases, rather than with black body radiation

(Suslick et al., 1990; Crum, 1994; Lepoint-Mullie et al., 1996). Hence, like photochemistry, sonochemistry involves the introduction of very large amounts of energy in a short period of time, but the type of molecular excitation is thermal, unlike the electronic excitation felt by molecules in photochemical processes (Suslick, 1990). It is further reported that sonochemistry lies in between "high-energy" and "molecular" physics, requiring therefore, the use of microscopic description of matter (Reisse, 1995).

There are different theories that explain the violent collapse of cavitation microbubbles. Nevertheless, all the theories rely on that the origin of sonochemical effects is cavitation.

The most popular and widely accepted theory is the "Hot Spot Theory", which suggests that the collapse is so rapid that the compression of the gas and vapor inside the bubble is adiabatic so that no thermal exchange can occur between a bubble's interior and the surrounding liquid (Rayleigh, 1917; Noltingk and Neppiras, 1950). Consequently, the temperatures and pressures within a collapsing microbubble can reach values as high as 4200-5000 K and 1000 atm, respectively just before fragmentation (Dahlem et al., 1998; Suslick, 1990). It is also reported that the localized "hot spot" generated by the rapid collapse of acoustic cavities is very short-lived (less than 10 μs), implying the existence of extremely high heating and cooling rates in the vicinities of 10^{10} K s^{-1} (Mason, 1999; Suslick, 1990). Substituents trapped inside or around a collapsing bubble are also subjected to these extremes.

The second most accepted, "Electrical Theory" by Margulis (Margulis, 1992; Margulis, 1995) suggests that during bubble formation and collapse, enormous electrical field gradients are generated and these are sufficiently high to cause bond breakage and chemical activity.

The "Plasma Theory" by Lepoint and Mullie (1994) also suggests that extreme conditions associated with the fragmentative collapse is due to intense electrical fields and seems not to involve a true implosion. They compared the origin of cavitation chemistry to corona-like discharge caused by a fragmentation process and supported and indicated the formation of micro plasmas inside the bubble.

The “Supercritical Theory” recently proposed by Hoffmann (Hua et al., 1995) suggests the existence of a layer in the bubble-solution interface where temperature and pressure may be beyond the critical conditions of water (647 K, 22.1 MPa) and showed that supercritical water is obtained during the collapse of cavitation bubbles generated sonolytically.

The violent collapse of cavitation microbubbles results in physical and chemical effects in the liquid. Three different phenomena are responsible for physical effects, namely shock wave, liquid jet and acoustic streaming (Dahlem et al, 1998). Low frequency ultrasonic waves are often associated with better physical treatment and less importantly with chemical effects. The high-frequency range has significant chemical importance. Physical effects can enhance the reactivity of a catalyst by enlarging the surface area or accelerate a reaction by proper mixing of reagents. Chemical effects give rise to enhancement in reaction rates due to the formation of highly reactive radical species upon bubble collapse.

It is reported that a great majority of sonochemical systems, having potential industrial applications involve heterogeneous reactions, where enhancement of chemical reactivity is associated with the physical effects of ultrasound such as heat and mass transfer, surface activation, and phase mixing (Suslick, 1990; Reisse, 1995; Leighton, 1994; Serpone et al., 1994). Sonocatalysis of liquid-liquid heterogeneous reactions is based on the mixing effect of acoustic streaming, which promotes the emulsification of non-miscible liquids by enhancing reaction rates upon increased interfaces (Reisse, 1995). When the heterogeneous system is made of a solid-liquid biphasic medium, catalysis of reactions is a consequence of the disruption of the solid by the jetting phenomenon associated with the collapse of cavitation bubbles. It is important to note that many of such effects are observed when the heterogeneous medium is irradiated with low frequency, or power ultrasound at the 20-100 kHz range (Ince et al., 2001).

On the other hand, homogenous sonochemistry induced by ultrasonic irradiation of homogenous fluids is a direct outcome of the extreme conditions generated in collapsing microbubbles (Ince et al., 2001; Reisse, 1995). Such extremes are reported to produce very unique catalytic effects, arising from inherent advantages of the system such as: (i) the

ability to generate high-energy species and (ii) the mimicry of autoclave reaction conditions (i.e. high temperatures and pressures) on a microscopic scale (Ince et al., 2001; Suslick, 1990). These catalytic effects start in the "microreactors" (cavities), which are made of microbubbles filled with vapor of the liquid medium and/or dissolved volatile solutes and gases diffused into them (Mason and Cordemans, 1998). During the collapse of these cavities in pure aqueous systems, gaseous water molecules entrapped in expanded microbubbles are fragmented as in pyrolysis to generate highly reactive radical species such as hydroxyl radicals and hydrogen atoms (Riesz and Mason, 1991).

The formation of hydroxyl radicals and hydrogen atoms in sonicated water has been demonstrated in various laboratories, using combined spin trapping and electron paramagnetic resonance (EPR) techniques; the Weissler reaction; fluorescence measurements from 2-hydroxy-terephthalate produced by hydroxylation of aqueous terephthalate ion; 5,5-dimethylpyrroline-N-oxide (DMPO) trapping; and sonoluminescence measurements based on the oxidative degradation of luminol to aminophtalate under the action of sonochemically produced hydroxyl radicals (Pétrier et al., 1992; Mason et al., 1994; Weissler et al., 1950; Negishi, 1961; Hart and Henglein, 1985; Riesz et al., 1990). In non-aqueous organic solvents or aqueous media containing volatile organic gases and solutes, cavitational collapse not only results in hydroxyl and hydrogen radicals, but also in organic radical species, as confirmed by experimental studies with electron spin resonance (ESR) spectroscopy (Seghal et al., 1982).

2.3.4. The Sites of Sonochemical Reactions

Three regions exist in ultrasonically irradiated liquids in which a reaction can take place: (i) the gaseous phase inside the bubble, (ii) the interfacial sheath between the gaseous bubble and the surrounding liquid and (iii) the bulk solution (Weavers et al., 1998, Suslick et al., 1986). The physical conditions in each of these regions are largely different. It is then important to know where a reaction takes place to determine the activation mechanism, which is primarily based on the physicochemical properties of the compound.

The pyrolysis of water molecules in a collapsing cavity results in the formation of hydroxyl and hydrogen radicals, which undergo a number of chain reactions. The

hydroxyl radicals generated by water sonolysis may either react in the gas phase or recombine at the cooler gas liquid interface and/or in the bulk solution during cavity collapse to produce hydrogen peroxide and water (Riesz and Mason, 1991; Fischer et al., 1986). The reaction mechanisms are shown below:

$$H_2O \rightarrow))) \bullet OH + \bullet H \text{ (pyrolysis)} \quad (2.34)$$

$$\bullet OH + \bullet H \rightarrow H_2O \quad (2.35)$$

$$2\bullet OH \rightarrow H_2O + O \quad (2.36)$$

$$2\bullet OH \rightarrow H_2O_2 \quad (2.37)$$

$$2\bullet H \rightarrow H_2 \quad (2.38)$$

If the solution is saturated with oxygen, peroxyl and additional hydroxyl radicals are formed in the gas phase (due to the decomposition of molecular oxygen), and the recombination of the former at the cooler sites (interface or the solution bulk) produces more hydrogen peroxide, as shown (Ince et al., 2001; Makkino et al., 1982; Petrier et al., 1994):

$$O_2 + \bullet H \rightarrow \bullet O_2H \quad (2.39)$$

$$O_2 \rightarrow))) O + O \quad (2.40)$$

$$O + H_2O \rightarrow \bullet OH + \bullet OH \quad (2.41)$$

$$\bullet O_2H + \bullet O_2H \rightarrow H_2O_2 + O_2 \quad (2.42)$$

In water or effluent treatment practices, organic pollutants may be destroyed either at the first two sites upon combined effects of pyrolytic decomposition and hydroxylation, or in the solution bulk via oxidative degradation by hydroxyl radicals and hydrogen peroxide (Weavers et al., 1998). The extent of oxidation reactions in the latter site is directly related to the quantity of available uncombined hydroxyl radicals in solution, which in turn is a matter of the life time and collapse duration of the bubbles, as well as the geometry of the reactor (Ince et al., 2001).

2.3.5. Types of Cavitation

2.3.5.1. Transient Cavitation. Transient cavitation bubbles are voids or vapor filled bubbles that exist for one, or at most a few acoustic cycles, expanding to a radius of at least twice their initial size, before collapsing violently on compression often disintegrating into smaller bubbles. These smaller bubbles may act as nuclei for further bubbles, or if of sufficiently small radius they can simply dissolve into the bulk of the solution under the action of the very large forces due to surface tension. During the lifetime of the transient bubble, it is assumed that there is no time for any mass flow, by diffusion of gas, into or out of the bubble, whereas evaporation and condensation of liquid is assumed to take place freely. If there is no gas to cushion the implosion, a very violent collapse will result (Mason and Lorimer, 2002).

2.3.5.2. Stable Cavitation. Stable cavitation bubbles are thought to contain mainly gas and some vapor that oscillate about some equilibrium size for many acoustic cycles. The time scale over which they exist is sufficiently long that mass diffusion of gas, as well as thermal diffusion, with consequent evaporation and condensation of the vapor can occur, resulting in significant long term effects (Mason and Lorimer, 2002).

2.3.6. Parameters Influencing the Sonochemical Reactivity

Since sonochemistry takes its origin in cavitation, the reactivity depends on the characteristics of the bubbles. Their sizes and lifetime, and the content of the gaseous phase depend on acoustic factors (frequency, intensity, pulse), properties of the solvent (vapor pressure, viscosity, surface tension), properties of the solute (vapor pressure, solubility, octanol-water partition coefficient) and external factors (saturating gas, external applied pressure, ambient temperature, addition of solids).

2.3.6.1. Acoustic Factors.

Frequency. The rate of free radical transfer from the bubble interior (and its interfacial sheath) into the solution bulk depends on the lifetime and collapse duration of the cavities, and therefore, to the intensity of the ultrasonic pressure, the geometry of the reactor and the

frequency of the applied ultrasound waves. The behaviour of cavitation bubbles**,** i.e. their lifetime and size shows variations with ultrasonic frequency. Cavitation bubbles reach to an unstable size (resonant size) just before they implode violently. The resonant size of the bubbles is inversely related to the frequency as shown in the following equation (Leighton, 1994):

$$R_r{}^2 = \frac{3\kappa P_0}{\rho \omega_r{}^2} \tag{2.43}$$

where R_r is the resonant bubble radius, κ is the polytropic index (C_p/C_v), P_0 is the hydrostatic pressure, ρ is the density of the solution and ω_r is the resonant frequency. Lower frequencies create bubbles with higher resonant radius which have longer lifetimes resulting in more violent collapse due to the build-up of more energy (Mason, 1990; Petriér et al., 1994). On the other hand, smaller bubble sizes with shorter lifetimes occur at higher frequencies. Although the cavitation intensity decreases with increasing frequency as a result of less sonolytic fragmentation of water molecules, more radicals could be ejected into the bulk solution because radicals will have less time to recombine inside the bubble due to lower bubble lifetime.

The resonance radius of a bubble excited by low frequency waves is reported to be ~170 μm (at 20 kHz), and the cavities entrapping such bubbles are said to be "stable" or long-lived, with average life times of ~10 μs (Mason, 1990; Petriér et al., 1994). In this kind of cavitation, the collapse stage is delayed till after the elapse of a number of compression and rarefaction cycles, during which sufficient volumes of volatile solutes and solvent vapors within the liquid may flow into the gas phase (Mason, 1990). The delayed growth and long collapse duration of gas-filled bubbles allow radical scavenging and recombination reactions at the interfacial sheath (as shown by equations 2.35, 2.36, 2.37, 2.38), thus inhibiting the mass transfer of hydroxyl radicals into the solution bulk (Barbier et al., 1996). Hence, low frequency ultrasound is expected to induce effects only for hydrophobic solutes, which easily diffuse into the cavity bubbles to undergo pyrolytic destruction inside the collapsing bubble, or hydroxylation and thermal decomposition at its interfacial sheath, where pressure gradients and temperatures are still high enough to induce thermolytic fragmentation.

On the contrary, the resonance radii of bubbles excited by medium frequency (200-1000 kHz) ultrasound waves are extremely small (4.6 μm at 500 kHz), giving rise to very short-lived (0.4 μs on the average) and mainly void or vapor-filled "transient" cavitations (Ince et al., 2001; Mason, 1999). The pressures and temperatures developed in such cavities are much higher than found in "stable" cavities, and larger energies are released into the surrounding liquid during their more rapid and violent collapse (Henglein, 1987; Suslick, 1990). Furthermore, such cavitations are so short-lived and the collapse is so rapid that the time for appreciable degree of radical scavenging reactions in the hot bubble or at the interfacial region is insufficient. As a consequence, medium frequency waves are highly effective for oxidation reactions in the liquid bulk, due to the highly probable ejection of uncombined hydroxyl radicals into the surrounding liquid during collapse (Ince et al., 2001; Mason et al., 1994; Barbier et al., 1996).

It should be remembered that, lower frequency ultrasound produces more violent collapse, leading to higher localized temperatures and pressures. However, current research indicates that higher frequencies lead to higher oxidation reaction rates. Beckett and Hua (2001) have postulated that the degree of heat generated upon collapse would be most intense at lower frequencies but there would be more cavitation events and thus more opportunities for the free radicals to be produced and diffuse into the bulk media with increasing frequency. Thus, there should be an optimum frequency where the competing effects balance.

Power Intensity. The sonochemical reactions strongly depend on the intensity of the sound waves. The intensity of sonication relates directly to the amplitude of vibration of the ultrasonic source. In order to induce cavitation, the acoustic intensity must exceed a threshold value. In general, an increase in intensity provides an increase in sonochemical effects but the energy input to the system cannot be increased indefinitely for the followings reasons: (i) when a large amount of ultrasonic power enters a system, a great number of cavitation bubbles are generated in the solution. Many of these will coalesce forming larger, more long-lived bubbles. These will certainly act as a barrier to the transfer of acoustic energy through the liquid, (ii) at high vibrational amplitude, the source of ultrasound will not be able to maintain contact with the liquid throughout the complete

cycle. Technically this is known as decoupling, and results in a great loss in efficiency of transfer of power from the source to the medium (Mason and Peters, 2002).

Pulse. When sonicating a liquid, there is a rapid build-up of standing oscillating bubbles whose dimension depends on the frequency. In order to avoid their accumulation, which causes inefficiency of energy propagation and heat evolution in the medium, ultrasonic irradiation is intermittently interrupted (Mason and Cordemans, 1998). The formation of bubbles and their activity is altered by the pulse width (a small number of cycles), shape of waveform and the interval between the pulses. The effect of pulsed ultrasound depends especially on the ratio between pulse width and interval (Mason and Peters, 2002).

2.3.6.2. Properties of the Solvent. The solvent used in sonochemistry is of great importance because the physical characteristics of the medium will dictate the amount of power which can be transmitted into the system via cavitational collapse. The rates of sonochemical reactions can be increased, at least within some limits, by lowering the vapor pressure of the solvent or by choosing a less volatile one. In addition, the surface tension and the viscosity (which affects energy penetration and bulk heating) of the solvent must be taken into account which are modified when a solute is present (Petrier and Luche, 1998). The formation of voids or vapor-filled microbubbles in a liquid requires that the negative pressure in the rarefaction region must overcome the natural cohesive forces acting within the liquid. It follows therefore that cavitation is more difficult to produce in viscous liquids or liquids with high surface tensions, where the forces are stronger and waves with greater amplitude and hence greater intensity will be necessary (Mason and Lorimer, 2002).

2.3.6.3. Properties of the Solute. Physicochemical properties of solutes, i.e. vapor pressure (or Henry's constant), solubility and octanol-water partition coefficient (Log K_{ow}) play an important role in the selection of the right frequency range for achieving appreciable degrees of decontamination (Suslick, 1990; Hua and Hoffman, 1997). Hydrophobic chemicals with high vapor pressures have a strong tendency to diffuse into the gaseous bubble interior, so that the most effective reaction site for their destruction is the bubble-liquid interface and/or the gaseous bubble itself (Kontronarou et al., 1991; Drijivers et al., 1999). Hence, irradiation of aqueous solutions contaminated with volatile pollutants by power ultrasound at 20-100 kHz (whereby long-lived "stable" cavities are generated) is a

very effective decontamination method, owing to its potential to render pyrolytic destruction of the solutes in the gas and gas-liquid phase (Ince et al., 2001; Kontronarou et al., 1991). In contrast, hydrophilic compounds with low vapor pressures and low concentrations tend to remain in the bulk liquid during irradiation, due to the repulsive forces exerted to-and-from the slightly hydrophobic bubble surfaces. The major reaction site for these chemicals, therefore, is the liquid medium, where they may be destroyed by oxidative degradation, provided that sufficient quantities of hydroxyl radicals are ejected into the solution during cavitational collapse. As stated previously, maximum radical transfer into the bulk medium occurs when the collapse is "transient", or when sonication is carried out via medium frequency ultrasound waves. Moreover, at this frequency and at high concentrations of such solutes, an additional destructive pathway via thermal decomposition was observed, as demonstrated by the formation of pyrolysis products along with hydroxylated intermediates during sonolysis at 300-500 kHz (Vinodgopal et al., 1998). The extent of destruction by pyrolytic fragmentation of non-volatile contaminants is directly related to their concentration and hydrophobicity, which dictates their ability to migrate towards the bubble and/or to accumulate at the bubble-liquid interface (Serpone et al., 1994). Consequently, the probable site for thermal decomposition of non-volatile solutes is the interfacial bubble sheath, at which solutes may accumulate via adsorptive processes during the formation and growth of acoustic cavities. At appreciable concentrations, the adsorptive tendency of non-volatile solutes on non-polar surfaces of cavity bubbles was verified by the exhibition of saturation type kinetics, typical of Langmuirian behaviour, which is commonly proposed for describing photocatalytic process kinetics (Serpone et al., 1994).

2.3.6.4. External Factors.

Saturating gas. The injection of a gas throughout sonication is important since it enhances the number of cavitational events in the liquid by creating liquid defects and serving as nuclei for cavitation, and hence lowering the cavitation threshold (Mason and Cordemans, 1998). At the beginning of sonication of any liquid, gas which is normally entrapped or dissolved in the liquid promotes cavitation. However, the first effect of cavitation in solution is degassing so that over the first few minutes of sonication, cavitation becomes less extensive. For this reason, it is a common practice to bubble the liquid continuously

with a gas during sonication to maintain a constant gas flow into the bubbles so as to sustain the "extreme" conditions of collapse (Ince et al., 2001).

The selection of the gas is also of significance because it may change the reaction efficiency in relation to its physical properties. The final temperature of a collapsing bubble is closely related to: (i) a gas parameter, called the "polytropic gas ratio (γ)", i.e. the ratio of specific heats (C_p/C_v) of ambient gases entrapped in the bubble which determines the heat released upon bubble collapse (Noltingk and Neppiras, 1950; Riesz et al., 1990), (ii) the thermal conductivity of the gas which determines the heat dissipated to the surrounding environment; and (iii) the solubility of the gas. Higher collapse temperatures are favored in the presence of gases with higher polytropic gas ratio, lower thermal conductivity and lower solubility.

Assuming adiabatic bubble collapse, the maximum temperatures and pressures within the collapsed cavitation bubbles are predicted by Noltingk and Neppriass from approximate solutions of Rayleigh-Plesset equations as follows (Noltingk and Neppiras, 1950; Neppiras, 1980):

$$T_{max} = T_0 \left[\frac{P_a(\gamma - 1)}{P_v} \right] \tag{2.44}$$

$$P_{max} = P_v \left\{ \frac{P_a(\gamma - 1)}{P_v} \right\}^{\left[\gamma / \gamma - 1 \right]} \tag{2.45}$$

where T_0 = ambient (experimental) temperature in the bulk, P_v = pressure in the bubble at its maximum size or the vapor pressure of the solution, P_a = pressure in the bubble at the moment of collapse (acoustic pressure), γ = polytropic gas ratio.

As can be seen from these equations, higher temperatures and pressures are generated in the presence of gases with higher polytropic gas ratios. For this reason, monatomic gases (He, Ar, Ne) with higher γ are used in preference to diatomic gases (N_2, air, O_2) with lower γ (Riesz et al., 1990). In addition, the extent of sonochemical effects depends upon the thermal conductivity of the gas, i.e. the greater the thermal conductivity

of the gas, the more heat (formed in the bubble during collapse) will be dissipated to the surrounding liquid, decreasing T_{max}. Thermal conductivity of rare gases decreases in the order: Xe < Kr < Ar < Ne < He. Despite the equal γ ratios of Argon and Helium, much higher yields of pyrolysis products were detected with the former, as attributed to its 10-fold lower thermal conductivity (Colarusso and Serpone, 1996). It must be noted that increasing the gas content of a liquid not only leads to more facile cavitation but also a reduction in the intensity of the of the shock wave created on bubble collapse as a result of the greater cushioning effect in the microbubble. The solubility of the gas also affects the cavitation conditions; the greater the solubility of the gas, the greater the amount which penetrates into the cavitation bubble and the smaller intensity of the shock wave (Mason and Lorimer, 2002).

Ambient temperature. Lowering the bulk solution temperature has been shown to actually increase the effect of sonication (Beckett and Hua, 2001). This is due to a decrease in the vapor pressure of the solvent, which leads to an increase in the intensity of the bubble. At low vapor pressure, less vapor has an opportunity to diffuse into the bubble which favors the more violent collapse. Also, as liquid temperature decreases, the amount of gas dissolved increases and the vapor pressure of the liquid decreases. Very volatile solvents lead to relatively high pressures in the bubble and also "cushion" the collapse (Adewuyi, 2001).

External applied pressure. Increasing the external pressure means that a greater rarefaction pressure is required to initiate cavitation. Consequently, bubble formation under such conditions will require a higher acoustic intensity than that required under atmospheric pressure leading to a larger intensity of cavitational collapse and subsequently an enhanced sonochemical effect (Mason and Peters, 2002).

Addition of solids as catalysts. The addition of solid catalysts, such as glass beads, ceramic disks, SiO_2, Al_2O_3 and talc into the reaction medium is another common method for enhancing cavitation effects. Furthermore, the presence of such material is reported to be especially useful for micronization of species (in ultrasonic cell disruption), and for the abrasion, activation and alteration of the chemical properties of catalyst surfaces during ultrasonic irradiation of liquid media (Mason and Cordemans, 1998).

Addition of hydroxyl radical scavengers. The presence of hydroxyl radical scavengers adversely affects the sonochemical rate of reactions. Two well-known scavengers are carbonate (CO_3^{2-}) and tert-butanol which scavenge hydroxyl radicals in the bulk liquid and the bubble-liquid interface, respectively. The reactions of CO_3^{2-} and tert-butanol with hydroxyl radicals are as follows (Buxton et al., 1988):

$$\bullet OH + CO_3^{2-} \rightarrow OH^- + CO_3\bullet^- \qquad k = 3.9 \times 10^8\ M^{-1}\ s^{-1} \qquad (2.46)$$

$$\bullet OH + (CH_3)_3COH \rightarrow H_2O + CH_2C(CH_3)_2 + (CH_3)_3CO\bullet \qquad k = 6.0 \times 10^8\ M^{-1}\ s^{-1} \qquad (2.47)$$

It was also reported that upon high-temperature pyrolysis during ultrasonic irradiation, thermal decomposition of tert-butanol is essentially a methyl-radical system and can be represented as in the following (Tauber et al., 1999a):

$$(CH_3)_3COH \rightarrow\rightarrow 3\ \bullet CH_3 + CO + H\bullet \qquad (2.48)$$

Addition of hydroxyl radical preservers. Addition of chemical reagents such as ferrous sulfate, carbon tetrachloride (CCl_4) into the solution has been demonstrated to enhance the efficiency of sonochemical decay processes. Upon ferrous sulfate addition, the decomposition of sonochemically produced H_2O_2 is accelerated through Fenton's reaction (equation 2.48) and thus additional •OH radicals are produced.

$$Fe^{2+} + H_2O_2 \rightarrow Fe^{3+} + OH^- + \bullet OH \qquad (2.49)$$

$$CCl_4 +))) \rightarrow \bullet Cl + \bullet CCl_3 \rightarrow\rightarrow HOCl + HCl \qquad (2.50)$$

Enhancement of sonochemical reactions in the presence of carbon tetrachloride is due to the production of HOCl, HCl and chlorine containing radicals, all of which are strong oxidizing agents (Wang et al., 2007). In addition, the reaction of CCl_4 with hydrogen atoms prevents the combination of H and OH radicals ($k_{CCl4\text{-}H} = 3.8 \times 10^7\ M\ s^{-1}$, $k_{H\text{-}OH} = 4 \times 10^{10}\ M\ s^{-1}$; Buxton et al., 1988), thereby increasing the concentration of OH radicals to attack target compounds.

2.3.7. Determination of Ultrasonic Power in a Reaction Medium

An ultrasonic system transforms electrical energy into mechanical energy, which is then transmitted into the sonicated reaction medium. However, not all of the energy produces physical and chemical effects. Part of it is lost in the generation of heat, is reflected and is consumed in sound re-emission. Only the remaining acoustic energy is absorbed by the liquid to produce cavitation. Therefore, the power output of the ultrasonic generator can not be used as an indication of the acoustic power delivered into the solution. In a pure liquid, one might assume that almost all the mechanical energy produces heat. Among the methods for the estimation of the amount of ultrasonic energy that is transferred to the solution, calorimetry is the most common which involves a measurement of the initial rate of heating produced when a system is irradiated by ultrasound (Mason, 1999). The method involves the measurement of the temperature T against time t for about 30 seconds, using a thermocouple placed in the reaction vessel. From T versus t data, the temperature rise dT/dt, can be estimated either by curve-fitting the data to a polynomial in t, or by constructing a tangent to the curve at time zero. The ultrasonic power (P_d) actually entering the system can then be calculated by substituting the value of dT/dt into Equation 2.51 (Mason, 1999; Mason and Cordemans, 1998; Mason et al., 1992):

$$P_d = (dT/dt).C_p.M \qquad (2.51)$$

where P_d= power dissipated in the system (W), (dT/dt)= the temperature rise at certain time interval (ºC/sec), C_p= heat capacity of water (4.1840 J g^{-1} $ºC^{-1}$) , and M= mass of water in the reaction vessel (g).

The dissipated power in the reaction medium that is measured by calorimetry is then used to determine the efficiency of the system either by calculating the ultrasonic intensity which is equal to the dissipated power per unit emitting area (W cm^{-2}), or the ultrasonic density (W mL^{-1}), i.e. dissipated power per total mass of the solvent (water) in the reactor.

3. THEORETICAL BACKGROUND ON ENDOCRINE DISRUPTORS AND LITERATURE REVIEW ON THEIR REMOVAL BY ADVANCED OXIDATION PROCESSES

3.1. Endocrine Disruption

3.1.1. Background Information

There is a growing concern about the possible harmful consequences of exposure to chemicals that exert hormonal activity and are capable of modulating or disrupting the endocrine system of humans and animals (Metzler and Pfeiffer, 2001). These pollutants, referred to collectively as endocrine disrupting compounds (EDCs) are also described with other terms such as environmental estrogens, endocrine disruptors, endocrine modulators, ecoestrogens, environmental hormones, hormone-related toxicants, endocrine-active compounds. EDCs comprise a large and still increasing number of natural and anthropogenic agents with diverse chemical structures.

An endocrine disruptor is any substance that has the potential to interfere with the normal hormone function in animals and humans. U.S. Environmental Protection Agency (1997) defines endocrine disruptor as an exogenous agent that interferes with the synthesis, secretion, transport, binding, action or elimination of natural hormones in the body that are responsible for the maintenance of homeostasis, reproduction, development and/or behavior.

Although the general interest in endocrine disruption is relatively recent, scientific interest dates back to as early as 1930s with the discovery that certain compounds can mimic the endogenous hormones of animals and some synthetic chemicals were estrogenic (Walker and Janney, 1930; Cook et al., 1934; Stroud, 1940). In 1962, the effect of toxic contaminants in the environment came to public attention through Rachel Carson's book, "Silent Spring", in which the detrimental effects of pesticides, particularly the organochlorine pesticide DDT on wildlife was reported (Carson, 1962). It was in 1980s

when it was first reported that gulls living in areas contaminated with DDT exhibited abnormal reproductive system development (Fry and Toone, 1981; Fry et al., 1987). Possible links between organochlorine pesticides and endocrine disruption was provided by researchers in Florida, who discovered reproductive disorders in alligators in Lake Apopka (Guillette et al., 1994; Guillette et al., 1996). The adverse impacts of EDCs on wildlife species raised concerns about their potential effects on humans. In 1996, "Our Stolen Future", a book written by Colborn et al. (1996) attracted great attention in public and scientific community which highlighted the health and environmental threats created by man-made chemicals that interfere with hormones in wildlife and humans. Probably the most convincing evidence that synthetic chemicals can act like hormones comes from the diethylstilbestrol (DES) experience. The drug DES, a strong synthetic estrogen banned since the 1970s, was given to pregnant women during critical fetal development to prevent miscarriages. Daughters and sons of women who took the drug have higher reproductive problems and cancer rates than those not exposed to DES in the womb (Herbst et al., 1971; Gill et al., 1979). In addition, laboratory studies confirmed that DES causes reproductive problems and cancer in male and female mice. The unanticipated sensitivity of the developing human reproductive system to DES clearly demonstrates that the human embryo/fetus is not immune to insult by exogenous chemicals that act as hormones (Jintelmann et al., 2003). Based on the findings in wildlife and DES experience, it is thought that EDCs may be responsible for some reproductive problems in both women and men, as well as for the increase in the frequency of certain types of cancer such as breast, testicular and prostate cancer. EDCs have also been linked to developmental deficiencies and learning disabilities in children. Because hormone receptor systems are similar in humans and animals, effects observed in wildlife species raise concerns of potential human health effects (EPA, 2001b).

3.1.2. Endocrine System and Mechanisms of Disruption

The endocrine system is made up of glands, hormones, and target cells that comprise a complex network of chemical signals and messages controlling many immediate and lifelong bodily responses and functions. Hormones produced by the endocrine system act as messengers, working with the nervous system to tell cells how and when to: (i) maintain the body's internal steady state (nutrition, metabolism, excretion,

water and salt balance), (ii) react to stimuli from outside the body, (iii) regulate growth, development and reproduction, (iv) produce, use and store energy. In order to send messages, hormones lock into receptors and, like a key in a lock, send the required signal. At very low concentrations, synthetic compounds that mimic hormones can insert themselves into the receptor and affect the normal hormone function inside the body (Daborn, 1999).

There are mainly four different mechanisms of disruption. Endocrine disruptors can either, (i) mimick the action of naturally-produced hormones, estrogens and androgens (the male hormones), and thereby setting off similar chemical reactions in the body (agonistic action) (chemicals that act like estrogen are called estrogens), (ii) block, prevent and/or alter hormonal binding to hormone receptors, thereby preventing the action of normal hormones (antagonistic action) (chemicals that block or antagonize hormones are labeled anti-estrogens or anti-androgens), (iii) affect the synthesis, transport, metabolism and excretion of hormones, thus altering the concentrations of natural hormones, (iv) modify the making and function of hormone receptors (Jintelmann et al., 2003). Well-known examples of agonists are the synthetic estrogens DES and ethinylestradiol which are estrogen copycats. Typical antagonists for hormone receptors are the herbicides linuron, vinclozolin and their metabolites, or the pharmaceutical tamoxifen, which compete for binding sites at the androgen and estrogen receptors, respectively (Jintelmann et al., 2003).

Environmental estrogens are the most commonly discussed, but chemicals can also act as androgens and thyroid hormones (regulating metabolism and growth). Such chemicals will most drastically affect the reproductive organs, brain, thyroid, liver, kidney and immune system (Daborn, 1999).

3.1.3. Types of Endocrine Disruptors

3.1.3.1. Classified Endocrine Disruptors. Endocrine active compounds comprise both naturally occurring substances and man-made chemicals, and their chemical structures are surprisingly diverse (Metzler and Pfeiffer, 2001). Classified endocrine disruptors can be given as follows:

i. Natural hormones, which include

estrogen (responsible for female sexual development),

progesterone and testosterone (=androgens: responsible for male sexual development)

phytoestrogens (substances that occur naturally in some plants, such as soybeans, which display estrogen-like activity when ingested by the body. Examples are genistein and daidzein).

ii. Man-made substances

ii.1. Synthetically produced hormones, identical to natural hormones, such as oral contraceptives, hormone-replacement treatment which have been designed intentionally to interfere with and modulate the endocrine system.

ii.2. Man-made chemicals: The most common known man-made endocrine disrupting chemicals are:

Pesticides (DDT, endosulfan, methoxychlor)

Highly Chlorinated Compounds (Polychlorinated biphenyls (PCBs), dioxin, furan)

Alkylphenols (nonylphenol, octylphenol)

Plastic Additives (Bisphenol-A, phthalates)

Heavy Metals (cadmium, arsenic, lead, mercury).

3.1.3.2. Non-classified but Potential Endocrine Disruptors. There are many industrial chemicals that have the potential to disrupt the endocrine system. However, these chemicals have not yet been proven as endocrine disruptors.

As research increases with different classes and structures of chemicals, new findings of endocrine disrupting activity related to those compounds are documented. Some of the chemical classes of non-classified endocrine disruptors include various phenolic compounds, napthols, napthalenes, benzene and derivatives, anilines and derivatives and synthetic dyes (IEH, 2005). Among these chemical classes, synthetic dyes are of great significiance which are employed in a wide range of processes in textile, paper, food, cosmetics, petroleum products and pharmaceutical industries. Based on the chemical structure of the chromophoric group, synthetic dyes are classified as azo, nitro,

anthroquinone, triarylmethane, xanthene, heterocyclic or indigo dyes (Zollinger, 1987). Among all dyes, azo dyes account for 65% of the commercial dye market. They are characterized by the presence of the azo group (-N=N-) attached to two substituents, mainly benzene or naphthalene derivatives, containing electron withdrawing and/or donating groups. The major sources of azo dyes in the environment are effluents from the textile industry. Due to their high solubility in water, azo dyes can be transported over very long distances once they are discharged into streams and rivers. Most of the dyes are found to be resistant to conventional wastewater treatment processes. Their destruction is important because under anaerobic conditions, the azo linkage is reduced to generate aromatic amines which can be toxic and potentially carcinogenic. Examples of carcinogenic azo dyes include C.I. Direct Black 38, C.I. Direct Blue 6 and C.I. Direct Brown 95 (U.S. DHEW, 1978). In addition to the carcinogenic effects of azo dyes, research on endocrine disruption has shown that some dye intermediates such as 1,5 naphthalenediamine results in thyroid adenomas; some aniline-based dyes such as 2-chloroaniline, 4,4-dioxydianiline, dimethylaniline are adrenal disruptors; some dyes such as C.I. Basic red 9 monohydrochloride is an adrenal and thyroid carcinogen (IEH, 2005). Moreover, C.I. Basic red 9 monohydrochloride and the azo dye, C.I. Direct Blue 218 were reported as suspected endocrine toxicants (RTECS, 1997). Based on carcinogenic and endocrine disruption data, some of the azo dyes could be reasonably anticipated to be endocrine disruptors and research must be expanded for the determination of endocrine activities of dyes.

3.2. Synthetic Endocrine Disruptors in the Environment and Their Removal by Advanced Oxidation Processes

This section is devoted to the review of synthetic endocrine disruptors in the environment and their removal by advanced oxidation processes which was published in Journal of Environmental Management in 2007 (Gultekin and Ince, 2007).

3.2.1. Introduction

Disruption of the endocrine system in living organisms by synthetic organic chemicals has been of great concern in recent years due to the recognition that the environment is contaminated with numerous EDCs that exert hormonal activity (Metzler and Pfeiffer, 2001). An endocrine disruptor by definition is an exogenous agent that interferes with the synthesis, secretion, transport, binding, action and elimination of natural hormones in the body, which are responsible for the maintenance of homeostasis, reproduction, development and behavior (U.S. EPA, 2001b).

The primary function of an endocrine system is to transform various exogenous stimuli into chemical messengers and hormones, resulting in appropriate gene expressions and synthesis of proteins and/or activation of already existing tissue-specific enzyme systems (Jintelmann et al., 2003). The three major endocrine disruption endpoints are estrogenic (compounds that mimic or block natural estrogens), androgenic (compounds that mimic or block natural testosterone), and thyroidal (compounds with direct and/or indirect impacts on the thyroid) (Snyder et al., 2003). EDCs are linked to a variety of adverse health effects in wildlife, such as hormone-dependent cancers, reproductive system disorders and reduction in reproductive fitness (Fry et al., 1987; Synder et al., 2003; Alum et al., 2004). Endocrine disruptors may be natural or more commonly synthetic, all with very diverse chemical structures (Metzler and Pfeiffer, 2001). The most prominent classes of chemicals that contain EDCs are natural estrogens, phytoestrogens, pesticides (methoxychlor), surfactants (nonylphenol), plasticizers (diethylphthalate, BPA), and organohalogens (PCBs and dioxin) (U.S. EPA, 2001b).

The majority of endocrine disrupting compounds are ubiquitous as they may be present in all compartments of the environment (water, air, soil and sediments) upon imperfect manufacturing processes and/or leaching from final end products. Sources of surface water contamination with EDCs are sewage effluents from domestic and industrial facilities and industrial effluent discharges (Gomes and Lester, 2003). The major source of EDCs in domestic sewage is the daily produced male and female hormones and/or ingested synthetic steroids, which are excreted with urine and discharged into municipal systems, where they may be partially removed by biochemical oxidation before being released to surface waters as active estrogens (Deborde et al., 2005; D'Ascenzo et al., 2003; Panter et al., 1999; Ternes et al., 1999). The concentration of EDCs in surface waters is variable. Ranges of ng L^{-1} are reported in some sites for natural synthetic hormones (Ying et al., 2002a; Belfroid et al., 1999) and μg L^{-1} for alkylphenols and bisphenols (Blackburn and Waldock, 1995; Ahel et al., 1994). Such levels were found to induce feminization in male fish and intersex induction (Gray and Metcalfe, 1997). Although some researchers have reported a relation between reproductive abnormalities in animals and exposure to EDCs in real cases (Guilette et al., 1994; Andersson et al., 1988; Morrison et al., 1985), there is no apparent correlation established so far between EDC exposure and reproductive disorders in humans except for published reports during the last decade on the increase in estrogen dependent cancers and the reduction in human sperm production (Herbst et al., 1989; Mocarelli et al., 1996). The risk for groundwater contamination arises from infiltration of rainwater through landfills and percolation from agricultural areas (Gomes and Lester, 2003). Despite their low concentration in the aquatic environment, the EU has labeled hormone-like chemicals as "hazardous" due to the fact that even a trace amount of them is sufficient to initiate estrogenic activity.

Conventional water and wastewater treatment plants are inefficient for substantially removing many EDCs. For this reason, it is essential that future research focus on the investigation of appropriate treatment methods that can be integrated into water and wastewater treatment facilities to prevent the release of EDCs into the natural waters. The research with advanced oxidation processes during the last decade has shown that they are promising techniques for the removal of refractory pollutants from effluents of bio-treatment plants and/or surface waters. Hence, the aim of this study was to review and compare published research on the degradability of common endocrine disroptors, namely

bisphenol A, nonylphenol and phthalates by light and dark advanced oxidation techniques and to point out if available the efficacy of the studied method for the degradation and estrogenic activity removal of the parent compound.

3.2.2. Overview of Industrial Endocrine Disruptors

Among numerous endocrine disrupting compounds used in industrial processes, the three major classes that have recently received scientific and public interest as the most potential disruptors are bisphenols, alkylphenols and phthalates. The common feature of all is that they are produced in massive quantities, and a substantial fraction is released into the environment.

3.2.2.1. Bisphenols. The prototype of bisphenols is bisphenol A (BPA), which is used mainly as a monomer for the production of polycarbonate, epoxy and unsaturated polyester-styrene resins, flame retardants, fungicides, antioxidants and rubber chemicals. In addition, BPA is consumed as a resin in dental fillings, as coatings on cans, as powder paints and as additives in thermal paper (Fromme et al., 2002; Staples et al., 1998). Some researchers have shown that BPA could stimulate proliferation and synthesis of progesterone receptors of human breast cancer MCF-7 cells, displace estradiol from estrogen receptors, induce synthesis of vitellogenin in cultivated trout liver cells and provoke transcription of recombinant yeast cells (Perez et al., 1998; Pawlowski et al., 2000; Routledge and Sumpter, 1996). The estrogenic potency in vitro is 10^{-3} to 10^{-4} relative to that of estradiol, and $4x10^{-4}$ to 10^{-5} in vivo relative to that of diethylstilbestrol (Jintelmann et al., 2003).

BPA is released into the aquatic environment from industrial discharges, landfill leachate and water streams containing plastic debris (Yamamoto and Yasuhara, 1999; Yamamoto et al., 2001). The concentration range shows regional variations, not exceeding parts per billion levels in natural waters, but reaching much higher values in streams contaminated with industrial discharges.

3.2.2.2. Alkylphenols. Alkylphenols (AP) are used as antioxidants and plasticizers, and in the production of alkylphenol polyethoxylates (APEO) - the most widely used non-ionic

surfactants (that comprise 6% of total surfactant production worldwide) (Metzler and Pfeiffer, 2001, Nimrod and Benson, 1996). Of all the APEO production, about 80% is released to the market as nonylphenol polyethoxylates (NPEOs) (Ying et al., 2002b), which are widely used in the production of plastics, textiles and agricultural chemicals, and in household goods such as detergents, paints, pesticides and cosmetics (Naylor et al., 1992; Nimrod and Benson, 1996). Accordingly, a large majority of the research related to APEO and AP destruction in the water environment is focused on nonylphenols (NP), which enter the environment through wastewater streams with NPEOs. Under anaerobic conditions such as those found in sewers, sediments, and bio-treatment operations at wastewater treatment plants, NPEO is oxidized to NP, which is recognized with its stability, aquatic toxicity and estrogenic activity (Comber et al., 1993; McLeese et al., 1981; Soto et al., 1995). Research has shown that the degradation products of many APEO surfactants that are discharged with wastewater treatment plant effluents are estrogenic (Routledge and Sumpter, 1996).

3.2.2.3. Phthalates. Phthalates represent a class of chemical compounds used most widely as plasticizers for polyvinyl chloride (PVC) resins and cellulose film coating. To a minor extent they have also found application in cosmetics, insect repellents and propellants (Vitali et al., 1997). There are about sixty different phthalates produced and consumed worldwide for very diverse purposes. The most important one in terms of production and consumption is 2-ethylhexyl phthalate (DEHP), which is used mainly in improving technical properties of plastic materials such as PVC, and to a minor extent in the production of cosmetics, adhesives, paints and other daily used chemicals (Metzler and Pfeiffer, 2001). Other prominent phthalates are butyl benzyl phthalate (BBP) and dibutyl phthalate (DBP), which have found application in vinyl floor tiles and plasticizers, respectively (Metzler and Pfeiffer, 2001). Phthalates are easily transported to the environment during manufacture, disposal and leaching from plastic materials, in which they are bonded non-covalently to allow the required degree of flexibility (Nilsson, 1994). The short-chained phthalates, dimethyl phthalate (DMP) and diethyl phthalate (DEP) are among the most frequently identified phthalates in diverse environmental samples including surface marine waters (Tan, 1995; Fatoki and Vernon, 1990), freshwaters (Vitali et al., 1997; Staples, 2000) and sediments (Tan, 1995; Thuren, 1986). Epidemiological studies with humans have shown that phthalates induce adverse health effects such as

disorders in male reproductive tract, breast and testicular cancers and neuroendocrine system disruption (Spelsberg and Riggs, 1987; Sharpe and Shakkebaek, 1993).

3.2.3. Advanced Oxidation Processes (AOPs) as Potential Methods of EDC Destruction in the Water Environment

AOPs are those processes that involve in-situ generation of highly reactive species such as the hydroxyl radical, which is the most powerful oxidizing species after fluorine with an oxidation potential of 2.80 V (Parsons and Williams, 2004). Unlike many other radicals, hydroxyl radical is nonselective and thus readily attacks a large group of organic chemicals to convert them to less complex and less harmful intermediate products. At sufficient contact time and proper operation conditions, it is practically possible to mineralize the target pollutant to CO_2, which is the most stable end product of chemical oxidation. The remarkable advantage of AOPs over all chemical and biological processes is that they are totally "environmental-friendly" as they neither transfer pollutants from one phase to the other (as in chemical precipitation, adsorption and volatilization) nor produce massive amounts of hazardous sludge (as in activated sludge processes) (Ince and Apikyan, 2000).

The most common AOPs developed for water and wastewater remediation are presented in Table 3.1.

Table 3.1. Most common AOPs evaluated for water and wastewater treatment.

Advanced Oxidation Processes	
Photochemical Processes	**Non-Photochemical Processes**
• UV oxidation processes	• Ozonation
UV/H_2O_2	• Fenton
UV/O_3	• Ultrasound (US)
$UV/H_2O_2/O_3$	US/H_2O_2, US/O_3, US/Fenton
UV/Ultrasound	• Electrochemical oxidation
• Photo-Fenton	• Supercritical water oxidation
• Photocatalysis	• Ionizing radiation
• Sonophotocatalysis	• Electron-beam irradiation
• Vacuum UV (VUV)	• Wet-air oxidation
• Microwave	• Pulsed Plasma

Some of these processes such as photolysis with more than 3000 applications in Europe (as a disinfection process) and a large number in the US (for treating groundwater pollutants) are commercially available (Parsons and Williams, 2004). Other processes such as combinations of H_2O_2, O_3 and UV, Fenton's reagent, super-critical water oxidation and ionizing radiation have all been used at full scale. Photocatalysis and ultrasound have been assessed only at laboratory bench and pilot scales. It should be noted that research on the application of AOPs in dual or triple combinations of individual processes offer significant kinetic and performance advantages.

Methods of AOP employed in studying the degradability of endocrine disruptors in water are: i) direct (with UV) and indirect photolysis (with UV/O_3, UV/H_2O_2, UV/Fenton, UV/Fenton/oxalate); ii) photocatalysis with TiO_2 or other semiconductors; and iii) dark advanced oxidation reactions with ozone, electrochemical processes and ultrasonic cavitation.

3.2.3.1. Destruction of Bisphenol A by Advanced Oxidation Processes.

Direct and indirect photolysis with UV. UV photolysis has been one of the most widely investigated advanced oxidation methods of BPA destruction based on the facts that UV irradiation is a common practice of drinking water treatment, and photolysis is the main abiotic degradation pathway of organic matter in natural waters. The following is an overview and evaluation of such research carried out for destroying BPA.

Rosenfeldt and Linden (2004) studied the degradability of BPA by low and medium pressure mercury UV lamps and reported 5% and 10-25% reduction by direct photolysis, respectively. However, exposure of the same samples to UV/H_2O_2 at a fluence rate of 1000 mJ cm^{-2} (typical of the irradiation rate in water treatment plants) resulted in more than 90% BPA destruction regardless of the UV source. They also recorded nearly 100% reduction in estrogenic activity (EST) by UV/H_2O_2 application. A similar study reported by Chen et al. (2006) has shown that a low pressure UV lamp even when operated at 5000 mJ cm^{-2} is ineffective alone, while the efficacy is improved to 80 and 78% for BPA and EST removal, respectively in the presence of 10 mg L^{-1} H_2O_2. The important operation parameter in the UV/H_2O_2 process is the concentration of H_2O_2, which should be

maintained high enough to ensure sufficient OH radicals in solution and low enough to prevent the reaction of excess H_2O_2 with OH radicals. The impact of H_2O_2 concentration as reported by Chen et al. (2006) was such that while 97% BPA and EST removal was obtained at 25 mg L^{-1} H_2O_2, no further enhancement was obtained when the concentration was doubled.

The composition of the water containing the contaminant is a crucial parameter of system efficiency in AOP. In accordance, Neamtu and Frimmel (2006a) reported that the degradation and reduction in EST activity of BPA by 254 nm UV irradiation was more efficient in purified or surface water than in sewage water due to the presence of competing substances in the latter. They also observed a decline of EST in both matrices with increased irradiation time. In another study related to the impact of water composition, Zhan et al. (2006) reported that the degradation of BPA in the presence of natural humic substances by solar radiation was faster than in pure water. Consequently, they suggested a mechanism to the decay process that involved the: i) production of excited BPA molecules leading to direct photolysis; and ii) production of hydroxyl radicals from photoreactive components of humic substances leading to indirect photolysis. The impact of water matrix was further investigated by Zhou et al. (2004) in synthetic samples containing BPA and ferric oxalate (Fe-Ox) complexes exposed to a high pressure Hg lamp. Based on the phenomenon that Fe-Ox complexes in atmospheric waters produce H_2O_2, which react with Fe(II) to generate OH radicals according to Fenton reaction (Zepp et al., 1992), they found that maximum efficiency in their system was obtained at pH=3.5 in a Fe/Ox molar ratio of 10:120. They also reported that total mineralization (160 min exposure) in these conditions was 24% as opposed to 7.3% mineralization in the absence of oxalate.

The potential of Fenton reaction in UV photolysis of BPA was also studied by Katsumata et al. (2004) using a Xe lamp emitting UV light at $\lambda<300$ nm. The study showed that maximum destruction could be accomplished at pH=3.5-4.0 with a H_2O_2-Fe(II) ratio of 10 (by M), at which 50% mineralization was possible in 24 h. The optimal ratio of H_2O_2/Fe(II)/BPA for complete degradation of BPA was reported as 9:0.9:1.

Finally, indirect photolysis of BPA was investigated by Irmak et al. (2005) via an O_3/UV technique using a low pressure Hg UV lamp. They observed that at a dose of

$18.7x10^{-3}$ mmol min^{-1} O_3, BPA was completely converted consuming 1.40 and 1.49 mmol O_3 in the presence and absence of UV irradiation during 75 and 80 min exposure, respectively.

Photocatalysis with TiO_2. Photocatalytic reactions via photo-generated holes of TiO_2 have been thoroughly investigated for water remediation during the last couple of decades. Under near UV irradiation, TiO_2 is photoactivated to form active oxygen species (e.g. OH radicals) on surfaces of the crystal, and the radicals readily react with a wide range of organic moieties to ultimately produce CO_2. The apparent advantage of this method over homogeneous AOPs discussed above is its outstanding potential to render complete mineralization. Studies reported in the literature on photo-decomposition of BPA in the presence of TiO_2 involve the use of powder, sheet or composite TiO_2 films and comparative assessment of the degree of BPA decay, EST reduction and mineralization. A number of studies are devoted to modification and optimization of the system via variations such as replacement of the artificial light source by solar irradiation; introduction of rotating or composite TiO_2-metal sheets, addition of chemical reagents; deposition of metals and/or reticulated carbon; and hybridization of the photoreactor with low-pressure submerged membranes. The following discussion covers a critical review of the literature on TiO_2-catalyzed photolytic decomposition of BPA.

Ohko et al. (2001) reported the degradation of BPA in TiO_2 aqueous suspensions irradiated by a Xe lamp. They found that total disappearance and mineralization required 15 h and 20 h, respectively and all intermediate products vanished within that time. They also reported that transcriptional estrogenic activity in response to human estrogen receptor was reduced to less than 1% of the initial activity within 4 h. The reaction pathway for the process as proposed by Watanabe et al. (2003) followed an initial attack of OH and OOH radicals on the two methyl groups and the subsequent cleavage of the methyl moieties to produce simple aldehydes, acids and carbon dioxide. In an attempt to improve the efficiency of the process, Wang et al. (2006) added β-cyclodextrin (β-CD) and monitored the degree of decomposition and mineralization of BPA. Under optimum conditions (β-CD= $4.4x10^{-5}$ M, pH= 6), the rate of decomposition was accelerated by 23% upon β-CD addition, while complete and 37% mineralization was obtained, respectively in the presence and absence of β-CD during a total contact of 120 min. The improvement was

attributed to enhanced adsorption of BPA on TiO_2 surfaces and weakening of the bond energy between atoms of BPA molecule via "inclusion interactions" with β-CD. Another study aimed to improve the efficiency of BPA decomposition in illuminated suspensions of TiO_2 was conducted by Horikoshi et al. (2004) in a plain, thermal and microwave-assisted non-thermal hybrid system. It was found that while 67% mineralization was accomplished in the plain reactor in 90 min, the efficiency was increased to 90% in the hybrid reactor with either microwave irradiation or external heating. Different reaction byproducts in thermal and microwave irradiation routes were attributed to adsorption mode variations of BPA on TiO_2 particle surface.

Enhancement of BPA decomposition in suspensions of TiO_2 was further studied by Xie and Li (2006) using i) a TiO_2/Ti film electrode; ii) a gold deposited TiO_2 film; and iii) a reticulated vitreous carbon (RVC) electrode that continuously generated H_2O_2. The study showed that gold deposition enhanced photocatalytic and photoelectrocatalytic activities under both UV and visible irradiation by improving the efficiency of e^-/h^+ separation on the conduction band of TiO_2. Furthermore, the use of RVC cathode was found to significantly assist the photoelectrocatalytic reaction and improve the degree of BPA degradation.

Chiang et al. (2004) compared the efficiency of plain and platinized TiO_2 on photolytic decomposition and mineralization of BPA at pH 3 and 10. They found that at optimized Pt loading, the photocatalytic activity of the solution could be enhanced by 3-6 times at both pH. The relatively low degree of mineralization at pH 10 was attributed to the negative charge on TiO_2 surfaces (that inhibits adsorption) and the presence of carbonate ions (that scavenge OH radicals) formed during oxidation of organic carbon. On the other hand, Coleman et al. (2005) reported that enhancement of photocatalytic activity by immobilization of TiO_2 on Pt or Ag was dependent on the concentration of BPA and that platinization was ineffective in weakly concentrated solutions, typical of natural waters. They reported that platinum accelerated the rate of mineralization only if the concentration of BPA was larger than 50 mg L^{-1}. In a similar attempt to enhance the overall degree of decomposition in TiO_2 catalytic process, Nakashima et al. (2002) studied the photocatalytic decay of BPA in the presence of immobilized TiO_2 particles on still and rotating polytetrafluoroethylene (PTFE) mesh sheets illuminated by black fluorescence.

They found that the rate of decomposition was twice faster in the presence of rotating sheets as a consequence of enhanced mass transfer of BPA to TiO_2 surfaces upon rotational motion. Finally, Lee et al. (2004) investigated the efficiency of BPA destruction in an immobilized TiO_2 film prepared by a sol-gel method and located on the external surface of a glass tube. Their results showed that highest BPA removal was achieved when titanium-sol solution was used as a binder. The optimum coating number and the film thickness for maximum yield was 3 and 5.29 μm, respectively. While 68% BPA removal was observed with single coating, the fraction increased to 98% in the presence of 3-fold coating, above which the efficiency was reduced by increased competition for UV radiation.

A study devoted to configuration of the photoreactor for practical applications in water purification was conducted by Zhang et al. (2003) in a tubular ceramic reactor, with inner surface coated with Pt-loaded TiO_2 film and irradiated with a UV lamp located longitudinally in the center. The water contaminated with BPA was circulated through the reactor during air injection. It was found that the proposed reactor had higher photocatalytic activity in the presence of optimal aeration conditions than conventional reactors and 100% BPA removal was possible in 4 h during aeration at 1 $dm^3\ min^{-1}$.

The feasibility of photocatalytic systems using artificial light sources was questioned by Kaneco et al. (2004), who investigated the impact of natural solar radiation as an alternative to the costly and energy-intensive artificial sources, and identified the optimal values of the catalyst dose, initial BPA concentration, temperature and light intensity. It was found that TiO_2-catalyzed processes aimed to destroy BPA in aqueous media were most economic at C_0 (BPA)= 20 mg L^{-1}, TiO_2= 10 mg L^{-1}, T= 40°C, pH= 6.0, and solar light intensity= 0.35 mW cm^{-2}. The authors reported complete mineralization in 11 h at these optimal conditions.

Although photocatalysis by TiO_2 seems to be an effective method for the overall degradation of BPA, some researchers were concerned about the practicality of the process related to the relative difficulty of separating the catalyst powders and/or crystals from solution at the end of treatment. A study devoted to this problem was conducted by Fukahori et al. (2003), who attempted to modify TiO_2 crystals by combining them with a strong adsorbent-zeolite to form a paper like composite. They found that without UV

irradiation, TiO_2-zeolite composite sheets were much more efficient in BPA removal than free TiO_2 sheets and powders, whereas in the presence of black light, powders were more effective. By contrast, mineralization was highest in the presence of illuminated TiO_2-zeolite sheets, which the authors attributed to the adsorptive removal of the oxidation intermediates onto zeolite surfaces. In conclusion, composite sheets were strongly recommended for removing BPA from water due to: i) their larger efficiency than ordinary TiO_2 sheets for mineralization, ii) their potential to capture the intermediate byproducts, preventing release into water; and iii) their unproblematic separation from solution.

A similar attempt to ease the separation and recovery of sub-micron sized TiO_2 catalysts from the treated solution was conducted by Chin et al. (2007) in a hybrid system combining photocatalysis and membrane filtration in a single module. The system consisted of a low-pressure submerged hollow fiber membrane reactor in direct contact with TiO_2 and BPA and irradiated by black light fluorescent lamps. Aeration was applied to reduce the fouling of the submerged membrane and to keep the medium in suspension. It was found that 97% of BPA was degraded after 70 min, and 90% of it was mineralized after 100 min contact with the hybrid system. An intermittent frequency (ratio of off-time to on-time) of 0.1 was reported as the optimum value to stabilize the sustainability of the membrane, and an aeration rate of 0.5 L min^{-1} was the optimum for providing excess dissolved oxygen and for improving the mass transfer process.

Dark advanced oxidation reactions with ozone, ultrasound and electrochemical processes.
Ozonation has been one of the most widely investigated techniques of advanced oxidation owing to the fact that it is commonly used in a large number of water treatment plants as a clarifying and disinfecting agent. The mechanism of organic matter removal in ozonated waters is either direct oxidation by molecular ozone or indirect oxidation by OH radicals that are formed by the decomposition of ozone in alkaline conditions. In natural waters, a large fraction of these radicals (which are much less selective and much more reactive than ozone) are scavenged by the water matrix (von Gunten, 2003); therefore the principle pathway of oxidation is direct reaction of ozone with the contaminant. The literature on BPA destruction by ozone is focused on the investigation of reaction kinetics, estrogenic activity and the operation parameters such as ozone feed rate and pH, which dictates the distribution of molecular and radical species. Byproduct analysis of dark ozone processes

in water containing BPA has not been published so far, but is under investigation in our laboratory. The following discussion covers a critical review of published research on ozone-based destruction of BPA in water.

Lee et al. (2003) studied the degradation of BPA at pH= 2, 7 and 12 and found that the rate was sensitive and proportional to the ozone feed rate, but insensitive to pH and the concentration of BPA. They found that even at extreme alkaline conditions (e.g. pH=12), where OH radicals are expected to dominate over O_3, the rate of degradation remained unchanged, as a consequence of the mass transfer resistances, the deprotanation of BPA, and the competition of •OH with ozone. Moreover, the addition of H_2O_2 was found to suppress the reaction by the competition between BPA and H_2O_2 for O_3 and OH radicals. The direct rate constant of BPA-O_3 reaction at pH 2 and 12 was estimated as $1.3x10^4$ $M^{-1}s^{-1}$ and $1.6x10^9$ $M^{-1}s^{-1}$, respectively. In another study devoted to kinetics of BPA decomposition by ozone in the presence of a strong •OH scavenger, Deborde et al. (2005) found that the apparent rate was minimum at pH<5 and maximum at pH>10. The reactivity of ozone with BPA and its two ionized species was reported as $1.68x10^4$, $1.06x10^9$ and $1.11x10^9$ $M^{-1}s^{-1}$, respectively.

Some researchers were concerned with the practicality of ozonation process in real water treatment plants. A study related to this problem was conducted by Alum et al. (2004) by monitoring the concentration and estrogenic activity of BPA during 120 min ozonation at conditions similar to those of drinking water treatment plants. They found that 99% of BPA was converted with an initial ozone concentration of 30 μM in less than 2 s. However, the level of estrogenicity increased during initial contact, declined after subsequent contact and stabilized after 60 min, signifying that the oxidation byproducts had higher estrogenic activity than BPA and some residual estrogenic response remains after treatment. Behavior of BPA in oxidative water treatment facilities was also studied by Lenz et al. (2004), who reported 1.4 mg L^{-1} as the optimum O_3 concentration for complete BPA destruction and 5 min as the sufficient contact time for removing the endocrine activity without the formation of adsorbable organic halogens.

On the other hand, Irmak et al. (2005) showed that in laboratory conditions with a much higher BPA concentration and continual ozone injection, ozonation was more

efficient in removing 17β-estradiol (which is used as an indicator of estrogenic activity) from water than removing BPA. They found that the stoichiometric molar ratio and contact time for complete conversion of BPA (0.40 mM) by ozone were 14.94 and 80 min, respectively, and the ratio was 1.68 times larger than that required for complete removal of 17β-estradiol. Disagreement in the changes observed in estrogenic or endocrine activities in different laboratories is due to variations in the applied assay or technique and differences in the method of response evaluation.

Finally, Kamiya et al. (2005) investigated the impact of competing organic compounds in sewage effluents on the efficiency of BPA destruction, EST activity and toxicity reduction by ozone. They found that BPA could be successfully decomposed by ozonation with the typical dose (3-5 mg L^{-1}) regardless of the presence of other organic substances. They also reported that EST activity could be declined to below detection limit even with 1 mg L^{-1} ozone, which was sufficient to reduce the aquatic acute toxicity in real sewage as well.

The literature on BPA removal from water by electrochemical processes (EC), which carry out oxidation and reduction reactions on surfaces of electrodes at electrode-electrolyte interface, is limited. Some of these processes are “direct” applied without the addition of chemical reagents and some are “indirect” involving the addition of chemicals and generation of highly powerful oxidizing species. The study of Korshin et al. (2006) is about a direct EC process (in 0.01 M NaCl electrolyte) using an undivided flow-through cell with a PbO_2 anode and a stainless steel cathode. The efficiency of the process was tested by monitoring the concentration of chloroacetic acids, TOC and adsorbable organic halogens (TOX) in the effluent. The study showed that under the experimental conditions employed, EC-treatment of BPA resulted in the formation of identified and non-identified chlorinated byproducts. Mono-chloroacetic acid was reported as the primary identified product (5.9%), while the non-identified part of TOX was comprised of aromatic chlorinated forms of BPA, which were resistant to degradation by EC and would likely resist similar conditions in drinking water treatment plants. In the study of Jiang et al. (2005), a direct electrochemical oxidation process using graphite felt-titanium and titanium-graphite felt-stainless steel as the electrodes was tested on crude and bio-treated wastewater to investigate its efficiency for BPA destruction. They reported that while bio-

treatment with post sedimentation could lower BPA concentration from several hundreds to a hundred ng L^{-1}, levels as low as 1-100 ng L^{-1}could be achieved with electrochemical treatment.

An indirect EC process using the Fenton reaction as the source of hydroxyl radicals and involving the generation of Fenton's reagent was tested by Gözmen et al. (2003). It was found that conversion of BPA increased with increasing $[Fe^{2+}]$/[BPA] molar ratio, and replacement of ferrous/ferric pair with cuprous/cupric pair resulted in faster BPA degradation and faster mineralization. However, ferrous/ferric pair was more efficient in terms of conversion and total mineralization versus the charge utilized.

The use of ultrasonic pressure waves in water to generate hydroxyl radicals is a novel technique, which promotes the formation, growth and violent implosion of cavitation bubbles with the outcome of extreme local conditions (5000 K, 2000 atm) and high energy chemistry (Suslick, 1990; Ince et al., 2001). The presence of impurities in water such as solids and dissolved gases largely enhances the efficiency of chemical reactions as a consequence of reduced cavitational threshold (Mason, 1999). The literature on ultrasonic means of BPA destruction is limited to a couple of investigations. Kitajima et al. (2006) studied the effect of dissolved gases during sonication of BPA samples at 500 kHz and found that the rate of degradation increased in the order O_2>Ar>air>N_2. Ioan et al. (2007) compared Fenton and sono-Fenton processes in an ultrasonic bath operated at 43-47 kHz. They found that the degradation of BPA by the Fenton process was much faster in the presence of ultrasound than in its absence, and the rate was further enhanced with increasing concentrations of Fe^{2+} and decreasing levels of pH.

Overview of reaction conditions and oxidation byproducts. Throughout the review, we found that differences in the applied experimental conditions in different studies are the principle reason for the variations in final outputs and conclusions. Although descriptive experimental features of the articles discussed so far have already been specified in the text, a comparative list of all is given in Table 3.2.

Table 3.2. Summary of reaction conditions for BPA removal from water by AOP.

Concentration	Reaction Conditions	Reference
Direct and Indirect Photolysis with UV		
23.3 μM	1 kW MP[a] or four 15 W LP[b] Hg lamps; H_2O_2= 0-25 ppm; UV fluence= 0-1500 mJ cm^{-2}.	Rosenfeldt and Linden, 2004.
60 μM	15 W LP Hg lamp (253.7 nm); H_2O_2= 0-50 ppm; UV fluence=100-5000 mJ cm^{-2}; pH=5.3.	Chen et al., 2006.
520 μM	15 W LP Hg lamp (254 nm); H_2O_2: 0-750 μM; pH=6.7; photonic flux= $4.25x10^{-6}$ einstein s^{-1}.	Neamtu and Frimmel, 2006a.
44 μM	500 W MP Hg vapor lamp (365 nm); I[c] = 0.525 mW cm^{-2}; humic acids= 10 mg l^{-1}.	Zhan et al., 2006.
8.8-44 μM	125 W HP[d] Hg lamp (≥365 nm); pH=3-8, [Fe(III)]:[Ox]=10/30,10/60, 10/120 (μM/μM).	Zhou et al., 2004.
44 μM	990 W Xe lamp (<300 nm), I= 0.5 mWcm^{-2}; pH=2-4.5; Fe(II)=0-$4x10^{-5}$ M; H_2O_2= 0-$4x10^{-4}$ M.	Katsumata et al., 2004.
400 μM	15 W LP Hg lamp; O_3 fed at 10.3-18.7 mmol min^{-1}; pH=5.25.	Irmak et al., 2005.
Photocatalytic Processes with TiO_2		
Concentration	**Reaction Conditions**	**Reference**
175 μM	200 W Hg-Xe lamp (365 nm), I= 10 mW cm^{-2}; 1 g L^{-1} TiO_2.	Ohko et al., 2001.
100 μM	75 W Hg lamp (360 nm), I= 2.5 mW cm^{-2}; pH= 4.4; TiO_2= 2 g L^{-1}.	Watanabe et al., 2003.
22-88 μM	250 W metal halide lamp (≥365 nm); 1 g L^{-1} TiO_2; β-CD[e]= 0 – $17.6x10^{-5}$ M; pH 2-12.	Wang et al., 2006.
100 μM	250 W Hg lamp, I= 0.9 mW cm^{-2}; TiO_2= 2 g L^{-1}; pH= 6.7; MW[f] power= 300 W.	Horikoshi et al., 2004.
49.3 μM	8 W MP Hg UV lamp (365 nm), I= 0.68 mW cm^{-2}, 110 W HP Na vapor lamp (450-650 nm), intensity=49 mW cm^{-2}; Anode: TiO_2/Ti or Au-TiO_2/Ti; cathode: RVC or Pt; pH= 6.17.	Xie and Li, 2006.
88 μM	20 W black fluorescent lamp (355 nm); 0.1 g L^{-1} platinized TiO_2; TiO_2: Degussa P25, Hombikat UV100, Milennium PC50; pH= 3, 10.	Chiang et al., 2004.
5.6 μM, 224.4 μM	15 W black fluorescent lamp (350 nm); TiO_2= 1 g L^{-1}, bare and coated with silver or platinum; pH= 3.	Coleman et al., 2005.
0.396 μM	15 W black fluorescent lamps (x2); I= 0.24 mW cm^{-2}; bare and TiO_2-modified PTFE mesh sheets.	Nakashima et al., 2002.
44 μM	6 W black light blue lamp (365 nm); aeration= 3 L min^{-1}; immobilized TiO_2 particles; pH= 4.5; T= 30ºC.	Lee et al., 2004.
20.24 μM	30 W Hg lamp (254 nm); ceramic tube (inner surface coated with Pt-loaded TiO_2 and water-glass); solution flow=1.25 m^3 h^{-1}; aeration=1 L min^{-1}.	Zhang et al., 2003.
0-440 μM	Solar illumination, I= 0-1.7 mW cm^{-2}; TiO_2= 0-20 g L^{-1}; pH= 2-10; T= 10-70ºC.	Kaneco et al., 2004.
100 μM	Hg-Xe lamp (365 nm); I=2 mW cm^{-2}; TiO_2 powder or TiO_2-zeolite sheet (2 g L^{-1}).	Fukahori et al., 2003.

Table 3.2. (continued)

44 µM	8 W black light fluorescent lamps (x4); TiO_2= 0.5 g L^{-1}, Flux=100 L m^{-2} h^{-1}; aeration = 0.2-4 L min^{-1}; pH=4.	Chin et al., 2007.
Dark advanced oxidation with ozone, electrochemical and ultrasonic processes		
Concentration	**Reaction Conditions**	**Reference**
4.4-44 µM	O_3 feed= 0.4-2 mg min^{-1}; pH= 2, 7, 12; H_2O_2= 1-10 mM (added batch-wise or continuously).	Lee et al., 2003.
0.1 µM	O_3 generated from pure O_2; ozonation from a liquid O_3 stock solution (40 mg L^{-1}).	Alum et al., 2004.
400 µM	O_3 generated from oxygen, fed at 10.3-18.7 mmol min^{-1}; pH=5.25.	Irmak et al., 2005.
0.002 µM, 0.44 µM	O_3 generated from pure O_2, fed through bubble diffusors; target O_3 concentration= 1.4 mg L^{-1}.	Lenz et al., 2004.
2.2 µM, 88 µM	O_3 generated from pure O_2; fed at 30 mL min^{-1}.	Kamiya et al., 2005.
20 µM	Anode: cobalt-coated PbO_2; cathode: stainless steel; current density= 0-50 mA cm^{-2}.	Korshin et al., 2006.
700 µM	anode: platinum gauze; cathode: carbon felt; $[Fe^{2+}]/[BPA]_0$=1.42-7.14; $[Cu^{2+}]/[BPA]_0$=1.4-7.1.	Gözmen et al., 2003.
220 µM	US[g] frequency=500 kHz, power=120 W.	Kitajima et al., 2006.
110 µM	US bath, frequency=43-47kHz, power=500 W; H_2O_2= 7 mg L^{-1}; $FeSO_4.7H_2O$= 1.4, 2.5 mg L^{-1}; pH= 4.0, 5.0, 6.5.	Ioan et al., 2007.

[a] Medium pressure.
[b] Low pressure.
[c] Intensity.
[d] High pressure.
[e] Cyclodextrin.
[f] Microwave.
[g] Ultrasound.

One of the major concerns of BPA destruction by AOP is the final product of oxidation, because in some cases the product might still exert endocrine activity and/or might be more toxic than the parent compound. As a consequence, some of the published research was coupled with byproduct analysis, while others only with endocrine or estrogenic activity testing via bioassay techniques. In general, analysis of estrogenic activity showed that the effluent either exhibited no hormonal activity or much less that of the original sample.

A list of oxidation byproducts that were identified in studies discussed so far is given in Table 3.3. The list shows that phenol and p-hydroquinone were the two most commonly observed products regardless of the AOP technique. Hydroxyacetophenone was identified in photo-Fenton and photocatalytic processes, while methylbenzofuran was

observed in photo-Fenton, some TiO_2 and ozonation processes. It was proposed that the initial step in the reaction mechanism of photocatalytic processes was adsorption of two OH moieties or BPA itself on TiO_2 surface, followed by •OH attack on the two phenyl carbons to produce short and long chain structures leading finally to oxalic, formic and acetic acids (Watanabe et al., 2003; Horikoshi et al., 2004; Wang et al., 2006). The proposed reaction mechanisms for homogeneous processes involved initiation either by direct attack of •OH to BPA, or hydroxylation followed by abstraction of a hydrogen atom from phenolic hydroxyl groups to form quinone-like compounds, which by further oxidation ended up in aliphatic acids (Fukahori et al., 2003; Kaneco et al., 2004; Katsumata et al., 2004).

Table 3.3. Identified byproducts of BPA oxidation by various AOPs.

AOP method	**By-product**	**Reference**
Indirect Photolysis (with H_2O_2)	Phenol 1,4-dihydroxylbenzene 1,4-benzoquinone Acetate oxalate	Neamtu and Frimmel, 2006a.
Indirect Photolysis (with Fenton's reagent)	4-hydroxyacetophenone methylbenzofuran p-hydroquinone Phenol p-quinone	Katsumata et al., 2004.
Indirect Photolysis (with ferric and carboxylate ions)	BPA-o-catechol BPA-semiquinone BPA-o-quinone	Zhou et al., 2004.
Indirect Photolysis (with natural humic substances)	monohydroxylated BPA p-hydroquinone 4-isopropenylphenol Glycerol 2-hydroxy-propanoic acid	Zhan et al., 2006.
Photocatalysis with TiO_2 (immobilized particles)	1,1-ethenylidenebis-benzene 4-isopropylphenol 4-tert-butylphenol Phenol	Lee et al., 2004.
Photocatalysis with TiO_2 (suspension)	4-isopropylphenol	Watanabe et al., 2003.
Photocatalysis with TiO_2 (plain suspension, microwave irradiation, thermal)	**plain** 4-hydroxyacetophenone 4-hydroxyphenyl-2-propanol **microwave** 4-hydroxyacetophenone 4-hydroxybenzaldehyde 3-hydroxy-1,3,5-hexadiene	Horikoshi et al., 2004.

Table 3.3. (continued)

	thermal 4-hydroxyacetophenone 4-hydroxyphenyl-2-propanol 4-hydroxybenzaldehyde Phenol Hydroquinone	
Photocatalysis with TiO_2 (suspension)	3-(4-hydroxyphenyl)-3-methyl-2-oxobutanoic acid 4-vinylphenol 4-hydroxyacetophenone	Ohko et al., 2001.
Photocatalysis with TiO_2 (suspension, solar radiation)	p-hydroxyacetophenone Methylbenzofuran phenol	Kaneco et al., 2004.
Photocatalysis with TiO_2 (suspension)	p-hydroxyacetophenone p-hydroxybenzaldehyde p-hydroxy-α-methylstyrene hydroquinone	Fukahori et al., 2003.
Ozonation	p-tert-butylphenol 2-methyl-2,3-dihydrobenzofuran hydroquinone n-butyl-acetate	Gültekin et al., unpublished data.
Electrochemical Oxidation (EC-generated Fenton's reagent)	m-monohydroxylated BPA o- monohydroxylated BPA dihydroxylated BPA phenol catechol hydroquinone benzoquinone resorcinol 4-isopropenylphenol 4-hydroxy mandelic acid 4-hydroxy benzoic acid Butendionic acid 4-oxobutenoic acid Acetic acid Formic acid	Gözmen et al., 2003.
Sonolysis	2,3-dihydro-2-methylbenzofuran	Kitajima et al., 2006.

3.2.3.2. Destruction of Nonylphenol by Advanced Oxidation Processes. Published literature on the removal of nonylphenols from water by AOP is limited, focusing on their degradability by indirect photolysis, photocatalytic oxidation, ozonation and sonolysis. There is a wider scope of research on the degradability of NPEOs by AOP; however the review presented in the following three sections is devoted to nonylphenols only for the fact that they are more toxic and more persistent than the ethoxylated form and they exhibit estrogenic activity unlike the ethoxylates.

Direct and indirect photolysis with UV. There is only one source of literature on direct photolysis of NP- the study of Neamtu and Frimmel (2006b), who investigated the decomposition of NP under a solar simulator equipped with a Xe lamp. They found that the rate of decay increased with pH elevations as a consequence of the larger photoreactivity of the deprotonated molecule; but it decreased with elevations in initial NP concentration. The effect of H_2O_2 addition (indirect photolysis) was to accelerate the reaction, the intermediate byproducts of which were phenol and 1,4-dihydroxylbenzene. Addition of bicarbonate and nitrate ions retarded and enhanced the rate of degradation upon excess consumption and production of OH radicals (by NO_3^- photolysis), respectively.

Another study focusing on indirect photolysis was conducted by Chen et al. (2007) to evaluate the performance of a UV/H_2O_2 process for the removal of endocrine activity in a mixed EDC solution containing NP. The efficacy of the process was assessed by monitoring EST using an in vitro yeast screen assay and an *in vivo* fish assay. Kinetics of EST removal in both assays followed pseudo-first order rate law regardless of the water matrix, but the rate was faster in deionized water than in river water, which the authors attributed to a lower steady state OH radical concentration in the latter due to excess consumption by dissolved organic constituents. They also reported that the rate of EST activity removal in the in vivo assay was faster than that in the in vitro, to be explained by differences in pharmacokinetic properties of the assays and to highlight the significance of applying at least two tests for reliable results.

Photocatalysis. The majority of published research on advanced oxidation of NP is about photocatalytic methods, using plain or various modifications of TiO_2 and other catalysts. Pelizetti et al. (1989) showed that photocatalytic degradation and mineralization of 4-NP is faster than that of phenol and p-n-propylphenol as a consequence of larger adsorption of NP on surfaces of TiO_2 pellets. They proposed that the reaction was initiated by •OH attack on the benzene ring resulting in the production of low molecular weight intermediates and CO_2. Ike et al. (2002) compared heterogeneous and homogeneous degradation of NP by photocatalysis in TiO_2 suspension and ozonation, and reported 90% and 75-80% degradation in 30 min and 6 min, respectively.

Kohtani et al. (2003) modified the TiO_2 process by using a solar simulator and replacing the catalyst with $BiVO_4$ (capable of splitting water to H_2 and O_2) to study the degradation of 4-n-NP. They found that the compound was adsorbed perpendicularly on $BiVO_4$ surface, while a mono-molecular layer covered over and the nonyl group faced to the surface. Thus, the long alkyl chain acted as the anchor on the hydrophobic $BiVO_4$ surface and thus zero-order kinetics predominated. Monitoring of the estrogenic activity showed that EST remained constant during the first 60 min, decreased afterwards and disappeared completely in 140 min. The major and minor oxidation byproducts were cis,cis-4-alkyl-6-oxo-2,6-hexadienoic acid and 4-alkylcatechol and 4-(1-alkenyl)phenol, respectively. In another study, the same research group investigated the effect of loading silver fine particles on $BiVO_4$ and found that photocatalytic properties were strongly enhanced by the presence of silver oxides that partly covered the silver surface (Kohtani et al., 2005).

The study by Kurinobu et al. (2007) is about the photocatalytic decomposition of NP using fine magnetic photocatalyst particles with a core-shell structure of three layers, Fe_3O_4, SiO_2 and TiO_2. They found that in the absence of UV irradiation, NP was nearly all adsorbed on the magnetic particles during the first 5 min. Irradiation of the suspension by black light after 120 min resulted in complete NP removal. They also reported 100% recovery of the particles (using a high gradient magnetic separation filter) as an indicator of cost effectiveness of the process.

Dark advanced oxidation reactions. Studies on destruction of nonylphenols by dark advanced oxidation techniques such as ozonation are limited. Lenz et al. (2004) found that in a solution containing 1.4 mg L^{-1} ozone, the concentration of 4-NP (C_0= 1-200 μg L^{-1}) could be reduced to less than 20 ng L^{-1} within 5 min and the estrogenic activity to less than 95% of the original. A similar study by Kim et al. (2005) showed that despite the rapid breakdown of 4-NP by 1 h ozonation, the concentration of dissolved organic carbon remained constant throughout. They also reported that total yield of aldehydes was directly related to the quantity of ozone in solution, while the predominance of acetaldehyde and formaldehyde over all other aldehydes was stable over all tested ozone concentrations. The kinetics of ozone-mediated oxidation of NP was studied by Deborde et al. (2005) with 4-n-NP over a pH= 2.5-10.5 in the presence of t-butyl alcohol and reported that the rate was

minimum at pH<5 and maximum at pH>10. The observation was justified by estimation of the second order rate constants, which showed that the rate was 4.5 orders of magnitude larger at the alkaline level. A most recent study by Ning et al. (2007) also reports the kinetics of NP degradation by direct ozonation at pH=2. The stoichiometric factor was estimated as 1.3 (mol O_3:mol NP) and the apparent rate constant as 3.90×10^4 $M^{-1}s^{-1}$, which is in good agreement with the value reported by Deborde et al. (2005) as 3.80×10^4 $M^{-1}s^{-1}$. The reaction pathway proposed was initiated by the addition of one hydroxyl group at the *ortho*-position of the aromatic ring, leading to the formation of hydroxyl-alkylphenol.

Yim et al. (2003) investigated the degradation of nonylphenol in water by ultrasonic irradiation at 200 kHz under argon, oxygen and air atmospheres and compared it with the degradation of butyl-, pentyl- and octylphenols. They found that the rate of sonochemical oxidation was directly proportional to the length of the alkyl chain and fastest for all in argon saturated solutions. Addition of a strong •OH scavenger (t-butanol) to solution was found to decelerate the reaction to signify the dominant role of OH radicals in the overall degradation process. However, addition of just sufficient quantities of Fe(II) and Fe(III) under O_2 atmosphere largely accelerated the degradation and mineralization of NP, which the authors attributed to the presence of dissolved O_2 that acted as an extra source of OH radicals in the presence of ferric and ferrous catalysts.

Overview of reaction conditions and oxidation byproducts. A comparative list of experimental conditions employed in studies reviewed so far for NP is given in Table 3.4. As stated for BPA, discrepancies in the observed data in different laboratories for a given process are due to differences in the applied conditions and the analyzed parameters. Note the large variation in the test concentration, which is a major control parameter in the overall efficiency of an advanced oxidation system. Note also that we could not provide a table of byproducts list as we did for BPA, because byproducts as reported only in a couple of articles were pointed out in the text.

Table 3.4. Summary of reaction conditions for NP removal from water by AOP[a].

Direct and Indirect Photolysis with UV		
Concentration	**Reaction Conditions**	**Reference**
25.5 μM	1000 W Xe short-arc lamp; H_2O_2= 10,20,50 mM; pH= 5.4, 8.5; HCO_3^-= 725 mg L^{-1}; NO_3^-= 61 mg L^{-1}.	Neamtu and Frimmel, 2006b.
0.18 μM	15 W LP Hg UV lamps (x4), (253.7 nm); fluence= 0-2000 mJ cm^{-2}; H_2O_2= 10 mg L^{-1}.	Chen et al., 2007.
Photocatalysis		
Concentration	**Reaction Conditions**	**Reference**
210 μM	1500 W Xe lamp (340 nm); TiO_2= 2 g L^{-1}.	Pelizetti et al., 1989.
0.9-14.5 μM	4 W LP Hg lamp (253.7 nm); TiO_2= 2 g L^{-1}; aeration= 4 L min^{-1}; O_3= 17 g m^{-3}, flow=0.03 L min^{-1}	Ike et al., 2002.
200 μM	1000 W Xe arc lamp (>400 nm); I= 24 mW cm^{-2}; Catalyst: $BiVO_4$= 4 g L^{-1}; pH= 13.	Kohtani et al., 2003.
200 μM	Visible light (>400 nm); I= 18 mW cm^{-2}; 4 g L^{-1} Ag-loaded $BiVO_4$; pH=13.	Kohtani et al., 2005.
4.54 μM	Black light (352 nm), I=2.6 mW cm^{-2}; TiO_2=5 g L^{-1} as magnetic particles.	Kurinobu et al., 2007
Dark advanced oxidation reactions		
Concentration	**Reaction Conditions**	**Reference**
$4.54x10^{-3}$ μM, 0.908 μM	O_3 generated from pure O_2; fed through bubble diffusors; target O_3 concentration= 1.4 mg L^{-1}.	Lenz et al., 2004.
2.8 μM	O_3 stock solution produced from pure O_2; $[O_3]/[NP]$= 0-10.4 (M:M).	Kim et al., 2005.
4 μM	O_3 stock solution produced from pure O_2 -dissolved O_3= 18 mg L^{-1}; pH=2.	Ning et al., 2007.
30 μM	US frequency=200 kHz, I=6 W cm^{-2}; Fe(II)-Fe(III)=0-200 μM.	Yim et al., 2003.

[a] Abbreviations "LP", "I", "US" same as defined for Table 3.2.

3.2.3.3. Destruction of Phthalates by Advanced Oxidation Processes.

Direct and indirect photolysis with UV. Direct and indirect methods of photolysis have been more frequently investigated for destroying phthalates than for nonylphenols. These methods consist of exposing the phthalate solution to short or medium wavelength UV radiation in the absence and presence of chemical reagents (e.g. ferric salts and ozone), identification of the operating parameters, the reaction byproducts and/or determining the estrogenic activity. The following discussion covers a brief review of such literature.

Photodegradation by solar radiation is a major natural destruction pathway of non-biodegradable organic compounds in aquatic systems. A study devoted to the investigation of the degradability of di-n-propyl phthalate (DPP) by natural and artificial photolysis was

conducted by Okamoto et al. (2006) and found surprisingly that both solar and artificial radiation (Hg arc) resulted in the formation of the same estrogenic byproduct. The impact of radiation wavelength on the reaction was further examined by using a Xe arc lamp with emissions at 225, 260, 275, 290 and 310 nm. It was found that estrogenic byproduct formation was a maximum with 290 nm irradiation and zero with 225 nm. They also reported that addition of H_2O_2 to enhance the reaction supported the formation of this undesired byproduct.

Lau et al. (2005) investigated direct photolysis of DBP under monochromatic UV irradiation at 254 nm over a pH range of 3-11. They observed that the rate of photolysis slowed down after 20-30 min of irradiation by a factor related to the applied pH level. The retardation was attributed to the competition between intermediate products and DBP for photons in the 254 nm band. The six major byproducts identified were mono butyl phthalate (MBP), MBP-derived ketone (or aldehyde), MBP-derived alcohol, butyl benzoate, benzoic acid and phthalic acid, the latter being the dominant product at all test pH. The authors concluded that the applied method rendered both detoxification and inhibition of endocrine activity.

Another such study carried out by Oh et al. (2006) was focused on comparison of direct and indirect photolysis (with ozone) of DEP under 254 nm UV radiation with Hg low pressure lamps. The authors reported that while only 22% destruction was possible with direct photolysis, complete conversion of DEP was attained upon dosing 1.5 mg L^{-1} min^{-1} ozone to the photoreactor. The addition of t-butanol was found to lower the efficiency of the UV/O_3 indirect system, showing the dominance of OH radicals in the degradation pathway. More than 93% mineralization was reported for indirect method at an ozone dose of 4 mg L^{-1} min^{-1}. Monitoring of the EST activity showed that even after complete removal of the parent compound, the effluent exhibited weak EST activity due to the presence of residual byproducts.

The majority of indirect methods studied so far for phthalate destruction is about the Fenton reaction and variations of it. Bajt *et al.* (2001) investigated the photolysis of DBP in the presence of Fe^{3+} and reported 85% destruction in 90 min irradiation by an artificial light source at 365 nm. The control parameter was the concentration of

monomeric Fe^{3+} hydroxyl complex $Fe(OH)^{2+}$ due to its high photoactivity that resulted in the formation of additional hydroxyl radicals. The authors also reported that solar radiation was twice more effective than artificial light in the mineralization of the compound. The advantage of this process over conventional photo-Fenton processes is that there is no need for H_2O_2 addition and the concentration of Fe^{2+} remains stable, acting as a continual source of OH radicals. A similar study with solar light-induced degradation of DEP in the presence of Fe^{3+} was conducted by Mailhot et al. (2002), who reported that the compound degraded only via OH radicals that were formed upon excitation of $Fe(OH)^{2+}$ as previously observed by Bajt et al. (2001), and the radiation source had no affect on the efficiency. Total mineralization after 3-d irradiation was 85%. The degradation of DEP was initiated by •OH attack on the aromatic ring, while that of DBP involved a major and a minor attack at the alkyl chain and the aromatic ring, respectively (Mailhot et al., 2002; Bajt et al., 2001). Differences in reaction sites and reaction pathways are obviously due to differences in the length of the alkyl chain, which dictates the number of available reaction sites.

The study of Zhao et al. (2004) compares the efficiencies of dark and photo-Fenton processes for the degradation of DMP and reports that the compound was degraded by both of the processes, but with a 2-fold faster rate by the light reaction. The optimum Fe^{2+} and H_2O_2 concentrations for the photo-Fenton process were 1.67×10^{-4} M and 5×10^{-4} M, respectively, at which 81% of DMP was oxidized in 120 min. The reported optimal reagent doses are in perfect agreement with the observation of Yang et al. (2005) for DEP, which was slightly less degradable (75.8%) under the same optimal conditions due to its larger alkyl chain. The most recent literature on the photo-Fenton process is the study of Chiou et al. (2006a) with DBP. It was found that at pH=3 with a H_2O_2 addition rate of 4.74×10^{-5} mol min^{-1} L^{-1} and a Fe^{3+} concentration of 4.50×10^{-4} mol L^{-1}, 92% mineralization was possible in 90 min.

Finally, the study of Xu et al. (2007) is about the operating parameters of UV/H_2O_2 process for the destruction of DEP using a low pressure Hg lamp emitting UV radiation at 254 nm. The authors reported that at optimized conditions (UV intensity= 133.9 μW cm^{-2}; H_2O_2= 20 mg L^{-1}), 99% of the parent compound was removed in 40 min. The reaction rate was directly proportional to the concentrations of DEP and H_2O_2, and to the intensity of UV radiation and temperature. A direct linear relation between the reaction rate and the

H_2O_2 concentration is due to the fact that H_2O_2 was maintained below the critical level, above which it would compete with the target compound for OH radicals and retard its rate of oxidation (Ince, 1999).

Photocatalysis with TiO_2. The literature on photocatalytic destruction of phthalates describes variations in the form of TiO_2 catalyst, optimization of the operating parameters, and less frequently identification of the reaction byproducts. The earliest study is about the degradability and oxidation byproducts of dialkyl phthalates in TiO_2 suspension (Hustert and Moza, 1988). The authors found that mono and di-hydroxylated byproducts were formed upon oxidation of phthalates containing shorter alkyl chains (dimethyl and diethyl), whereas hydroxylated byproduct formation was insignificant in the oxidation of phthalates with longer alkyl chains (dibutyl and di-ethyl-hexyl). In a recent study by Kaneco et al. (2006), the same byproducts were identified for the destruction of DBP in TiO_2 suspension and found that optimum values of the catalyst concentration, temperature and pH were 50 $\mu g\ ml^{-1}$, 20°C, and 6.0, respectively.

Muneer et al. (2001) have also focused on setting of the operation parameters such as pH, concentration, and type or quantity of TiO_2 particles for the degradation of DEP. The efficiency defined as the ratio of the degradation rate to the incident light intensity was found to increase with pH increase and reached a maximum at pH 6, which is close to the zero point charge of TiO_2. The authors concluded that DEP conversion efficiency could be enhanced by raising the concentration of TiO_2 and/or that of DEP. Although the addition of electron acceptors such as hydrogen peroxide, bromate and persulfate did not render a significant enhancement in the rate of DEP conversion, the degree of mineralization was remarkably increased in the presence of bromate. A more recent study describing the use of TiO_2 particles immobilized on silicate glass beads, as reported by Chiou et al. (2006b) for DBP showed that 75% conversion and 70% mineralization was possible in 80 min regardless of the pH level. Hence, unlike most studies reporting pH as a critical parameter, the influence of pH within a range of 4.5 – 9.0 was found insignificant in this study, as attributed to the scavenging of excess OH radicals (generated in alkaline pH) by carbonate species.

The study of Ooka et al. (2003) compared the efficiency of untreated and hydrothermally treated TiO_2 pillared clays on the degradation of DBP, DEP, DMP and BPA, reporting that the process was enhanced with increasing hydrophobicity of the phtalate (DBP>BPA>DEP>DMP) and with hydrothermal treatment of the clays. In a subsequent study, the authors further compared the effectiveness of four different hydrophobic TiO_2 pillared clays on the degradation of DBP and DMP, and found that the degradation of both compounds was enhanced with increasing surface hydrophobicity of the clays, by which the adsorptive capacity also increased (Ooka et al., 2004).

Dark advanced oxidation reactions. The literature on dark advanced oxidation processes of phthalate destruction is limited to ozonation and ultrasound processes. A study by Li et al. (2005) showed that the rate of ozone-based destruction of DBP is directly proportional to the applied ozone dose and is fastest during the first 15 min of reaction. The authors found that mineralization was much slower than oxidation of the parent compound, and attributed it to the formation of organic acids with low reactivity with ozone. Addition of UV light and/or UV/TiO_2 increased both the rate of degradation and the fraction of mineralization upon photo-decomposition of O_3 and/or photoactivation of TiO_2, respectively to generate active oxygen species.

There is also research with catalytic ozonation processes to enhance the biodegradability and/or the mineralization of phthalates. One such study compares the efficiency of a bio-treatment process applied to the effluent of a plain ozonation and a granular activated carbon-catalyzed ozonation process for the treatment of DMP, DEP, DBP and DEHP (Li et al., 2006). The authors found that pre-ozonation with activated carbon improved ozone utilization and the biodegradability of the effluent, resulting in nearly 100% removal of DMP and DEP (and more than 93% of the others) in the effluent of the bio-process. More recently, Yunrui et al. (2007) have compared the efficiencies of Al_2O_3 and Ru/Al_2O_3–catalyzed ozonation processes for the destruction of DMP. They found the catalysts were ineffective in the oxidation of DMP by ozone, but very effective in the mineralization of the ozonated byproducts, as the CO_2 formation increased by 3 fold and 1.5 fold in the presence of Ru/Al_2O_3 and Al_2O_3, respectively. Continuous monitoring of the total organic carbon and component leaching for 42 h showed that catalytic activity of Ru/Al_2O_3 remained constant with time, while that of Al_2O_3 decreased upon leaching.

There are two published articles in the literature about ultrasonic destruction of phthalates. The earlier one is by Yim et al. (2002), who investigated the degradation of phthalic acid esters (DMP, DEP and DBP) at 200 kHz. They reported that the rate of all was pseudo-first order with half-lives of 17.9, 11.8 and 6.9 min, respectively, and the reaction site was either the gas-liquid interface (pH 4-11) or the cavitation bubble (pH>11). More recently, Psillakis et al. (2004) studied the decomposition of six phthalate esters at 80 kHz. They showed that higher molecular mass phthalates such as DBP, BBP, DEHP and di-octyl phthalate (DOP) were readily degradable by ultrasound for complete removal in 30-60 min contact, while less hydrophobic DMP and DEP were much more resistant, requiring prolonged sonication for complete destruction. Addition of NaCl was found to enhance the rate of degradation in more polar DMP, DEP, DBP and BBP upon decreased solubility, which promotes diffusion of the compounds from the bulk solution to the bubble-water interface, where they meet a much denser cloud of hydroxyl radicals. On the other hand, salt addition was reported to decelerate the degradation of non-polar esters such as DEHP and DOP to be explained by reduced number of cavity bubbles upon alteration of the vapor pressure.

Overview of reaction conditions and oxidation byproducts. A comparative list of experimental conditions employed in studies reviewed so far for phthalates is summarized in Table 3.5. Similar to the conditions of BPA and NP, the largest variation is in the concentration of the test compound. There are also vast variations in the applied light intensity in UV-based reactions and in the concentration of the TiO_2 catalyst. However, the concentration of iron and H_2O_2 in Fenton processes lies within same orders of magnitude. Byproduct analysis was rarely carried out for phthalate destruction by AOP, and the only information is the formation of monohydroxylated and/or dihydroxylated derivates (Hustert and Moza, 1988; Bajt et al., 2001; Mailhot et al., 2002 ; Kaneco et al., 2006).

Table 3.5. Summary of reaction conditions for phthalate removal from water by AOP[a].

Direct and Indirect Photolysis with UV		
Compound/concentration	**Reaction conditions**	**Reference**
DPP/250 μM	Solar, artifical UV irradiation (Hg arc-254 nm, 0.94 mW cm^{-2} or Xe arc:225, 260, 275, 290, 310 nm, 0.07, 0.16, 0.28, 0.34, 0.48 mW cm^{-2}; H_2O_2= 15 μM.	Okamoto et al., 2006.
DBP/2-10 μM	35 W-254 nm phosphorcoated LP Hg lamps (x8), I = $1.5x10^{-6}$ einstein L^{-1} s^{-1}; pH= 3-11.	Lau et al., 2005.
DEP/100 μM	3 W LP Hg arc lamp (254 nm); I= 0.4 W L^{-1}; O_3 dose= 1.5, 4 mg l^{-1} min^{-1}, fed at 0.5 L min^{-1}; pH= 7.	Oh et al., 2006.
DBP/30 μM	125 W HP Hg lamp (365 nm); Fe(III)= $3x10^{-4}$ M; pH=3.1.	Bajt et al., 2001.
DEP/260 μM	125 W HP Hg lamp (365 nm) or natural sunlight; Fe(III)= $3.05x10^{-4}$ M.	Mailhot et al., 2002.
DMP/51.5 μM	150 W HP Hg lamp; Fe(II)=0-$3.3x10^{-4}$ M; H_2O_2= 0-$8.3x10^{-4}$ M; pH=2-6.	Zhao et al., 2004.
DEP/45 μM	160 W HP Hg lamp; Fe(II)=0-$3.3x10^{-4}$ M; H_2O_2= 0-$10x10^{-4}$ M; pH=1-6.	Yang et al., 2005.
DBP/18 μM	8 W UV (312 nm) lamps (x2); I=120 μW cm^{-2}; pH=2-4, Fe(III) =9-54 $x10^{-5}$ M, H_2O_2= 4-$55x10^{-6}$ M min^{-1}; T=25ºC.	Chiou et al., 2006a.
DEP/4.5 μM	30 W (254 nm) UV lamps(x10); I=21-134 μW cm^{-2}; H_2O_2=2.5-30 mg L^{-1}; T=15-31ºC.	Xu et al., 2007.
Photocatalysis with TiO_2		
Compound/concentration	**Reaction conditions**	**Reference**
DBP/18 μM	990 W Xe lamp (<300 nm); I=1.8 mW cm^{-2}; TiO_2= 0-0.3 g L^{-1}; pH= 1-10; T= 10-40ºC.	Kaneco et al., 2006.
DEP/ 100-1000 μM	500 W HP Hg lamp (320 nm); I=110 μmol photon L^{-1} min^{-1}; TiO_2=0.5-5 g L^{-1}; pH= 3-9.	Muneer et al., 2001.
DBP/9-45 μM	8 W UV lamp (365 nm); I = 1.67 mW cm^{-2}; 150 g TiO_2/glass; pH= 4.5-9.0; sample circulation=10 ml min^{-1}.	Chiou et al., 2006b.
DBP/144 μM, DEP/180 μM, DMP/ 206 μM	Black light lamp (365 nm); I= 0.80 mW cm^{-2}; TiO_2= 1.2 g L^{-1}.	Ooka et al., 2003
DBP/144 μM DMP/206 μM	Black light lamp (365 nm); I= 0.80 mW cm^{-2}; TiO_2= 1.2 g L^{-1}	Ooka et al., 2004
Dark advanced oxidation reactions with ozone and ultrasonic processes		
Type and concentration	**Reaction conditions**	**Reference**
DBP/54 μM	Ozone feed = 12.5, 25.0, 50.0 mg h^{-1}; pH=6.4; 15 W LP UV lamp (254 nm); I=40 mW cm^{-2}; carbon-modified TiO_2 thin films.	Li et al., 2005.

Table 3.5. (continued)

DMP/593 µM, DEP/754µM, DBP/106.8 µM, DEHP/23 µM	O_3 generated from pure O_2; 100 g GAC in ozone reactor; EBCT-BAC[b] reactor = 15 min.	Li et al., 2006.
DMP/31 µM	Ozone feed = 118 mg O_3 h^{-1}; gas flow= 400 mL min^{-1}; Ru/Al_2O_3 catalyst= 10 g l^{-1}; pH=6.6, T= 15ºC.	Yunrui et al., 2007
DMP, DEP, DBP/100 µM	US frequency=200 kHz; US power I = 6 Wcm^{-2}; pH= 4-12.	Yim et al., 2002.
DMP/0.206 µM, DEP/ 0.180 µM, DBP/0.144 µM, BBP/0.128 µM, DEHP, DOP/0.102 µM	US frequency=80 kHz; US power=75 W, 150 W.	Psillakis et al., 2004.

[a] Abbreviations "LP", "HP", "I", "US" same as defined for Table 2.
[b] Empty bed contact time in biological activated carbon reactor.

3.2.4. Conclusions

The increasing consumption of endocrine disrupting compounds worldwide has raised significant public concern due to their initiation of hormone-like activities even in trace concentrations in surface waters. Research has shown that advanced oxidation processes, which generate very active oxidative species such as the hydroxyl radical, are promising tools for the destruction of such compounds in water, particularly bisphenol-A, nonylphenol and phthalates. The most commonly investigated method of advanced oxidation for destroying endocrine disrupting compounds in water is photocatalysis with titanium dioxide, while there is sufficient literature on ozonation, direct and indirect photolysis, electrochemical oxidation and ultrasonic irradiation, as well. However, more research is required particularly with hybrid processes to make advantage of synergistic effects and to investigate the impacts of interfering agents and chemical structures before proposing advanced oxidation as a viable solution to the treatment of these compounds in water.

A large majority of the reviewed articles involved studied the behavior of a single chemical tested in much higher concentrations than detected in the water environment, whereas endocrine disruptors exist in mixtures of multi components rather than as a single component. In present, the difficulty of working with concentrations in micro and nano gram l^{-1} levels to simulate the environment is due to the limitations in available analytical instruments, but the problem will be solved in the future with promising developments in

instrumentation and detection limits. As a final remark, it should be noted that recent developments in bioassay techniques used for screening the effluent endocrine activity provide excellent support to the evaluation of the overall performance of the treatment processes.

4. MATERIALS AND METHODS

4.1. Materials

4.1.1. Test Compounds

Bisphenol A, 4-n-Nonylphenol and C.I. Acid Orange 8 with chemical structures given below were purchased in solid form from Aldrich in >99% purity, from Riedel-de-Häen in 99.9% purity and from Aldrich in 65% purity, respectively.

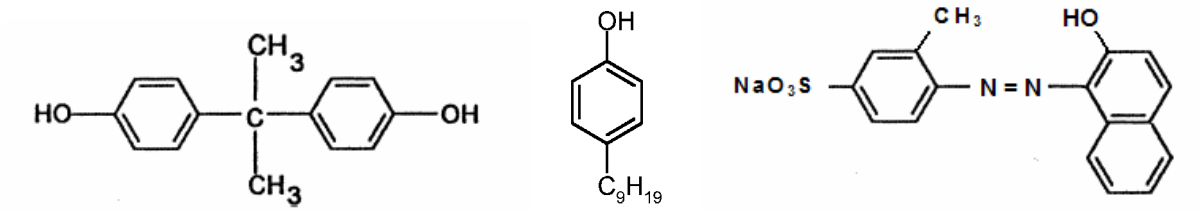

Bisphenol-A	4-n-Nonylphenol	C.I. Acid Orange 8
MW=228.29 g mol^{-1}	MW=220.35 g mol^{-1}	MW=364.4 g mol^{-1}

Figure 4.1. Molecular structures of Bisphenol-A, 4-n-Nonylphenol and C.I. Acid Orange 8.

4.1.2. Reagents

All test solutions were prepared in ultrapure water produced by a Millipore Milli-Q gradient system. HPLC-grade methanol and HPLC-grade acetonitrile were obtained from Merck to prepare stock solutions of 4-n-Nonylphenol and to use as a mobile phase in HPLC, respectively. The reagents sulfuric acid (H_2SO_4, Merck), sodium hydroxide (NaOH, Merck), sodium carbonate (Na_2CO_3, Merck), tert-butanol (Acros Organics), carbon tetrachloride (CCl_4, Merck), iron(II) sulfate heptahydrate ($FeSO_4.7H_2O$, Merck), cupric sulfate ($CuSO_4.5H_2O$, EM Science), hydrogen peroxide (H_2O_2, 35% w/w, Merck) and potassium indigo trisulfonate (Sigma-Aldrich) were all analytical grade. Air, argon and oxygen were obtained from BOS Istanbul with >99% purity.

4.1.3. Experimental Set-ups

4.1.3.1. Ultrasonic Reactor Systems.

20 kHz probe type **(US1)**. The system (Figure 4.2) is made of a 100 mL glass cell (Sonoplus) surrounded by a water-cooling jacket to keep the solution at constant temperature (25±0.5 ºC), a probe type transducer (Bandelin Sonoplus HD220) with a probe tip area of 1.13 cm^2 emitting ultrasonic waves at 20 kHz and a 180 W generator to convert electrical power into ultrasonic energy. The horn is submerged 3 cm from the top of the cell, which has an effective volume of 80 mL. The system is mounted in a polyurethane isolating material to prevent excessive noise.

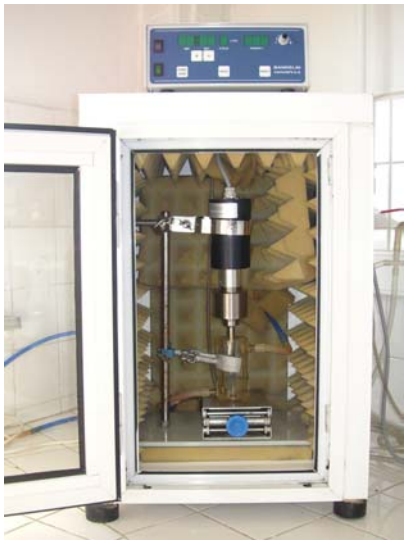

Figure 4.2. Photographic view of US1 (20 kHz probe type reactor).

300 kHz plate type **(US2)**. The system (Figure 4.3) is made of a 150 mL glass cell surrounded by a water-cooling jacket to keep the solution at constant temperature (25±0.5 ºC), a plate type piezoelectric transducer with a vibrational area of 9.6 cm^2, which emits ultrasonic waves at 300 kHz and a 25 W generator to convert electrical power into ultrasonic energy (Undatim Ultrasonics, Belgium).

Figure 4.3. Photographic view of US2 (300 kHz plate type reactor).

Multi-frequency plate type **(US3)**. The system (Figure 4.4) is made of a 500 mL glass cell surrounded by a water-cooling jacket to keep the solution at constant temperature (25±0.5 ºC), a multi-frequency plate type piezoelectric transducer with a vibrational area of 22 cm^2 emitting ultrasonic waves at 577, 861 and 1145 kHz, and a generator with an output power capacity of 120 W (Ultraschall, Germany).

Figure 4.4. Photographic view of US3 (multi-frequency plate type reactor).

4.1.3.2. Ozone Reactors.

Bubble-column reactor **(BCOz).** This is a semi-batch system made of a 5-liter cylindrical chamber of 65 cm depth and 10 cm diameter (Figure 4.5). Ozone is injected into the contactor through a micro-porous diffuser (10-16 μm) located at the bottom of the cylinder during continuous generation from dry pure oxygen by an Anseros COM-CD-HF-1 model ozone generator.

Figure 4.5. Photographic view of BCOz (bubble-column reactor).

Ozone-ultrasound reactor **(USOz).** The system is a modified US2 (Figure 4.6) fed by onsite generated ozone from dry pure oxygen (Ozone Lab 100 model generator, Ozone Services) that is introduced into the glass reactor through a teflon tube.

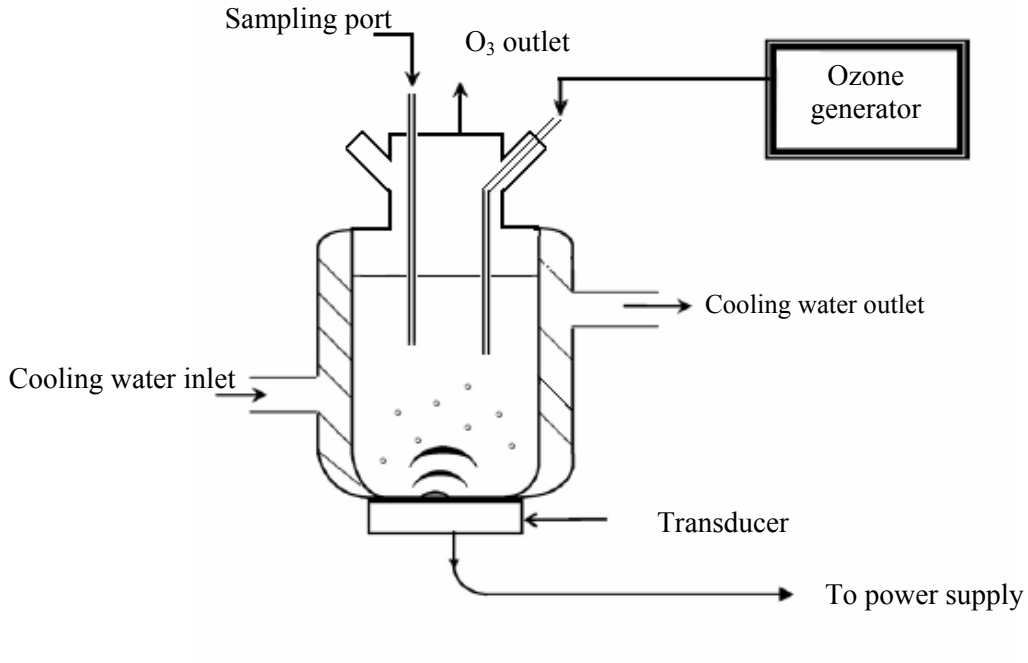

Figure 4.6. Schematic diagram of USOz.

4.1.4. Optimization of Ultrasonic Systems

Calorimetric measurements were carried out for the three ultrasonic reactors at different power outputs and reaction volumes as described in section 2.3.7 for determining the optimum working conditions.

4.1.4.1. Optimization of US1. The generator was operated at 10, 20, 30, 40, 50, 60 and 70% of its total capacity (180 W). Higher outputs were not tested to avoid damage to the probe by excess heating. The power dissipated in solution at each test output was monitored in 80 mL milli-Q water by 4-min calorimetric analysis. The results are presented in Table 4.1.

Table 4.1. Temperature increase in US1 during sonication of 80 mL milli-Q water for 4 min under varying generator power outputs.

Time, s	Power output, %						
	P= 10%	P=20%	P=30%	P=40%	P=50%	P=60%	P=70%
	Temperature, ^{o}C						
0	18.00	22.00	21.00	23.00	21.00	22.00	23.00
30	21.00	25.00	25.00	26.50	26.00	27.00	28.50
45	22.00	26.50	26.50	29.00	28.00	29.50	31.00
60	22.00	28.00	28.00	30.50	30.50	32.00	33.00
90	23.00	30.50	31.00	34.00	35.00	37.00	38.00
120	24.50	33.50	34.00	38.00	39.00	42.00	43.50
150	25.00	36.00	37.50	42.00	43.00	47.50	50.50
180	27.50	39.00	40.50	45.50	47.50	51.50	55.00
210	28.00	41.50	43.00	49.00	51.50	55.50	58.00
240	30.50	44.00	47.00	53.50	55.00	59.50	63.00

The plot of T versus time (Figure 4.7) provided an estimate of the rate of temperature rise (dT/dt) via fitting of the best polynomial to the observed data set. Values of dT/dt as estimated from the slope of the fitted curves are summarized in Table 4.2. These values were then inserted in Equation 2.51:

$$P_d = 0.111\frac{^{o}C}{\text{sec}} x 4.182\frac{J}{g\,^{o}C} x 80g = 37.3W \quad \text{(at 30\% power output)} \tag{4.1}$$

to estimate the power that was dissipated in solution at each test condition. The results are presented in Table 4.3.

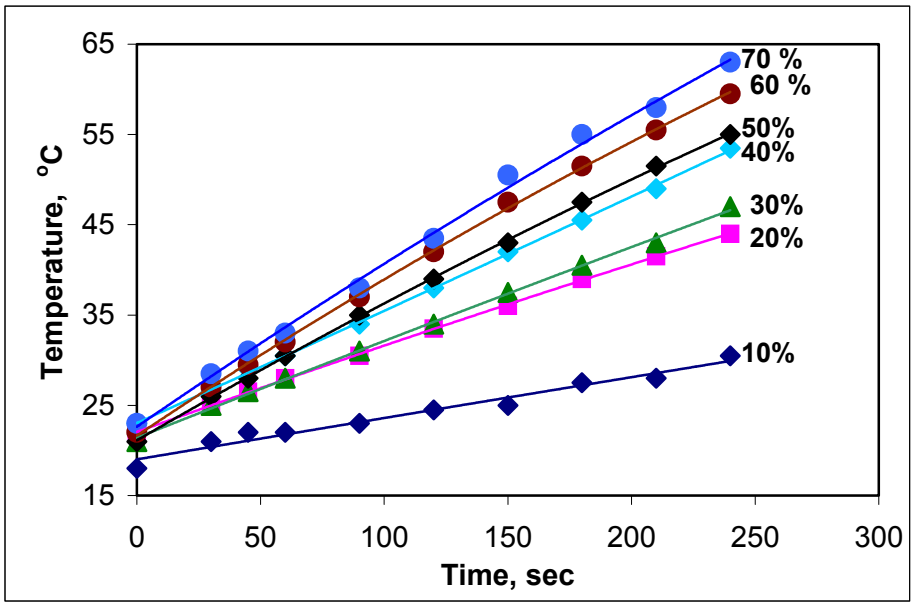

Figure 4.7. The raise in temperature in 80 mL water in US1 at varying power outputs.

Table 4.2. The temperature raise in water estimated from the slopes of the straight lines in Figure 4.7.

Applied Power (% of maximum)	P= 10%	P=20%	**P=30%**	P=40%	P=50%	P=60%	70%
dT/dt, ^{o}C/sec	0.046	0.099	**0.111**	0.126	0.157	0.180	0.184

Table 4.3. The effective power dissipated in solution at each power output in US1.

Applied Power (as % of 180 W)	P= 10%	P=20%	P=30%	P=40%	P=50%	P=60%	70%
Power in solution, W	15.4	33.0	**37.3**	42.1	52.4	60.2	61.6

The relation between the applied power and the power deposited per unit volume of solution is presented in Figure 4.8.

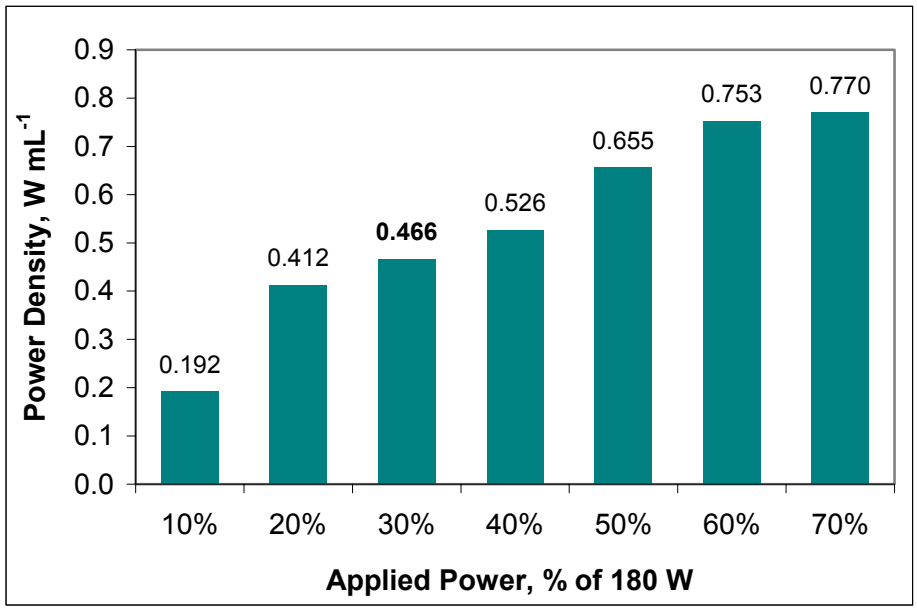

Figure 4.8. Power density as a function of the applied power.

Calorimetric measurements were repeated for three other test volumes to select the most effective reaction volume. The results are tabulated in Table 4.4. The working volume and power are selected as 80 mL and 54 W (30%), respectively that corresponds to dissipation of 37.3 W in solution.

Table 4.4. Combined impacts of solution volume and generator output on the quantity of ultrasonic power dissipated in solution.

Generator power, W	**Power dissipated, W**			
	70 mL	**80 mL**	**90 mL**	**100 mL**
18.00 (10%)	14.13	15.40	17.80	19.61
36.00 (20%)	31.59	32.97	33.76	36.51
54.00 (30%)	38.61	37.25	39.78	43.95
72.00 (40%)	44.00	42.07	44.38	47.68
90.00 (50%)	50.21	52.42	53.79	56.67
108.00 (60%)	59.22	60.22	63.65	65.95
126.00 (70%)	63.55	61.59	66.17	69.42

4.1.4.2. Optimization of US2. The ultrasonic generator was operated at 5, 10, 15, 20, 25 W power outputs. The power dissipated in solution at each test output was monitored in 100 mL milli-Q water by 5-min calorimetric analysis. The results of 25 W operation are presented in Table 4.5.

Table 4.5. Temperature increase in US2 during sonication of milli-Q water for 5 min under a power output of 25 W.

Time, s	0	30	60	90	120	150	180	210	240	270	300
Temperature, ^{o}C	16	17.5	18.5	20	21	22	23	24	25	25.5	26.5

The plot of T versus time (Figure 4.9) provided an estimate of the temperature rise (dT/dt) via fitting of a polynomial to the observed data set. The value of dT/dt was 0.0454 °C s^{-1} from the fitted curve.

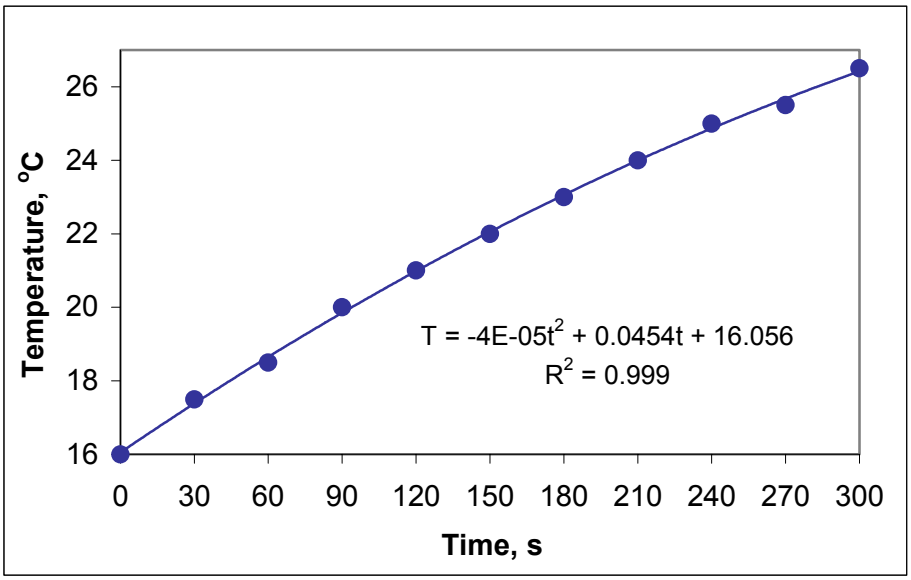

Figure 4.9. Temperature rise during 5 minute sonication of 100 mL milli-Q water at 25 W generator output in US2.

The power dissipated in solution was calculated using Equation 2.51 and found that the power density was 0.190 W mL^{-1}.

Calorimetric measurements were repeated for different reactor volumes (other than 100 mL) and the results are tabulated in Table 4.6. The maximum dissipated power in US2 was 19 W, which corresponded to an output power of 25 W and a reactor volume of 100 mL. The power density as a function of system volume for an input power of 25 W is presented in Figure 4.10.

Table 4.6. Impact of solution volume on the power dissipated in solution in US2.

Generator power, W	Power in solution, W		
	100 mL	125 mL	150 mL
5.00	1	-	2
10.00	7	4	4
15.00	9	7	6
20.00	12	13	11
25.00	19	14	12

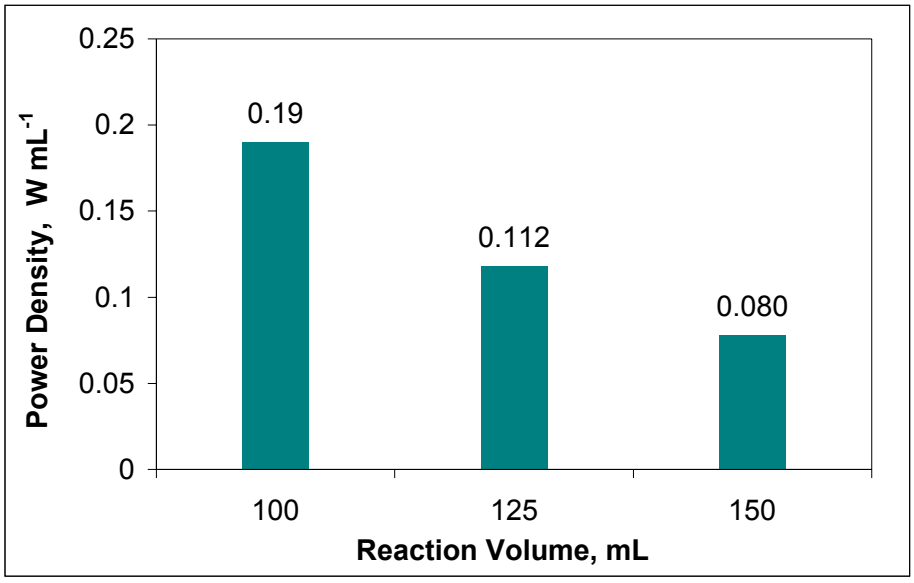

Figure 4.10. Power density as a function of reaction volume for an applied power of 25 W in US2.

4.1.4.3. Optimization of US3. The ultrasonic generator was operated at 76, 92, 100 and 108 W power outputs for each test frequency which corresponded to 63, 77, 83 and 90% of the maximum power (120 W) supplied by the generator, respectively. Lower outputs were not

tested due to very low power dissipation below a power output of 76 W. The power dissipated in solution at each test output was monitored in 250 mL milli-Q water by 10-min calorimetric analysis at each test frequency. The results are presented in Table 4.7.

Table 4.7. Temperature increase in US3 during sonication of 250 mL milli-Q water for 10 minutes under varying power outputs.

Time, s	Power output, %											
	577 kHz				861 kHz				1145 kHz			
	63%	77%	83%	90%	63%	77%	83%	90%	63%	77%	83%	90%
	Temperature, ºC											
0	28.6	29.5	27.0	27.8	30.2	31.1	26.0	26.3	24.4	24.5	27.2	27.1
30	29.1	30.2	27.9	29.9	31.0	31.8	27.3	27.3	24.9	25.3	28.3	28.7
60	29.6	32.1	29.1	31.9	31.5	32.6	28.5	28.9	25.3	26.4	29.9	30.4
90	29.9	33.2	30.4	33.5	31.9	33.5	29.8	30.5	25.7	27.4	31.2	32.1
120	30.4	34.1	32.1	34.8	32.4	34.5	30.5	32.2	26.3	28.3	32.5	33.5
150	30.8	35.0	33.3	36.0	32.8	35.4	32.2	33.6	26.7	29.5	33.7	35.2
180	31.2	35.8	34.7	37.1	33.3	36.2	33.3	35.2	27.3	30.4	34.9	36.6
210	31.9	36.7	35.6	38.8	33.7	37.3	34.7	36.5	27.8	31.2	36.0	38.0
240	32.2	37.5	36.8	40.1	34.3	38.1	35.8	38.1	28.3	32.1	37.5	39.4
270	32.4	38.1	37.7	41.1	34.7	39.0	37.1	39.6	28.5	33.0	38.5	40.7
300	32.7	39.0	38.4	42.4	35.2	39.8	38.2	41.0	29.0	33.7	39.5	42.0
330	33.1	39.6	39.4	43.3	35.6	40.7	39.4	42.4	29.5	34.8	40.7	43.4
360	33.5	40.1	40.1	44.3	36.0	41.6	40.5	43.7	30.0	35.6	41.7	44.6
390	33.9	40.9	41.1	45.2	36.5	42.4	41.7	45.0	30.4	36.3	42.6	45.7
420	34.4	41.5	41.8	46.2	36.9	43.1	42.6	46.4	30.7	37.1	43.9	46.9
450	34.8	42.2	42.6	47.1	37.5	43.9	43.7	47.7	31.2	37.8	44.8	48.1
480	35.2	43.0	43.4	47.9	37.8	44.8	44.8	48.8	31.6	38.5	45.8	49.5
510	35.6	43.5	44.1	48.7	38.2	45.4	45.7	50.0	32.1	39.3	46.9	50.7
540	35.8	44.1	44.8	49.4	38.6	46.2	46.8	51.3	32.4	40.1	47.7	51.9
570	36.4	44.8	45.4	50.2	39.0	47.0	47.7	52.4	32.7	40.7	48.6	52.7
600	36.8	45.2	46.0	50.8	39.5	47.9	48.5	53.6	33.2	41.4	49.6	53.7

The plot of T versus time for each set provided an estimate of the temperature rise (dT/dt) via fitting of a polynomial to the observed data set. An example of a polynomial fit for 861 kHz at a power output of 100 W (83%) in 250 mL reaction volume is presented in Figure 4.11. The values of dT/dt were estimated from the slopes of fitted curves for each

power output at all frequencies (Table 4.8) and dissipated powers were calculated by using equation 2.51 (Table 4.9).

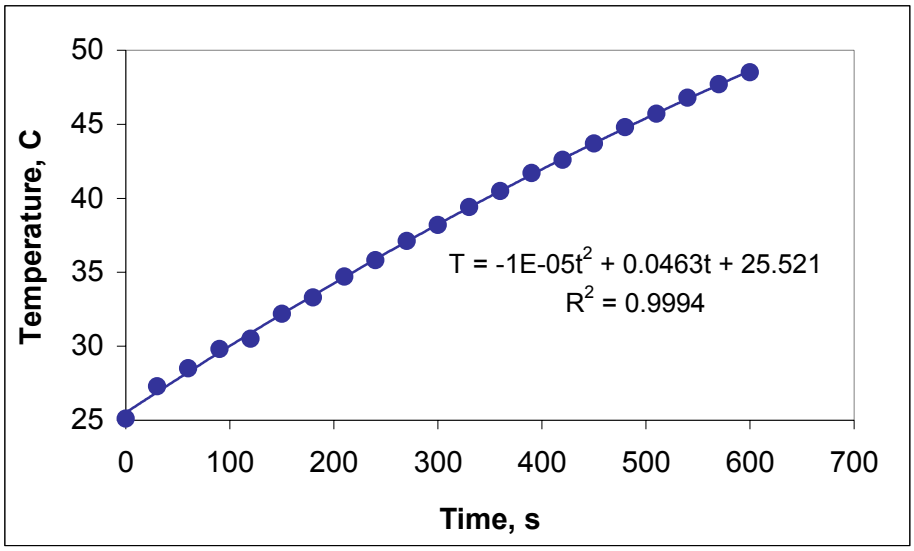

Figure 4.11. Temperature rise during 10 min sonication of 250 mL milli-Q water at 100 W output in US3.

Table 4.8. The values of dT/dt for each power output in US3.

Applied power (as % of 120 W)	**Power in solution, W**		
	577 kHz	**861 kHz**	**1145 kHz**
63%	0.014	0.017	0.017
77%	0.036	0.031	0.035
83%	0.047	0.046	0.047
90%	0.056	0.054	0.055

Table 4.9. Power dissipated in solution at each output power in US3.

Applied power (as % of 120 W)	**Power in solution, W**		
	577 kHz	**861 kHz**	**1145 kHz**
63%	14.74	17.57	17.46
77%	37.43	32.72	36.38
83%	48.83	48.41	48.93
90%	58.34	56.67	57.29

Calorimetric determination of the dissipated power was also carried out in four other volumes (other than 250 mL) and the results are tabulated in Table 4.10.

Table 4.10. Combined impacts of solution volume (V) and generator output on the power dissipated in solution in US3.

V mL	**Power in solution, W**											
	577 kHz				**861 kHz**				**1145 kHz**			
	63%	**77%**	**83%**	**90%**	**63%**	**77%**	**83%**	**90%**	**63%**	**77%**	**83%**	**90%**
200	11.63	37.97	-	52.02	15.39	31.11	-	55.37	16.31	32.54	-	51.52
250	14.74	37.43	**48.83**	58.34	17.56	32.73	**48.41**	56.67	17.46	36.38	**48.93**	57.29
300	15.68	44.16	-	61.98	17.56	33.87	-	56.21	18.19	35.88	-	57.71
350	11.86	50.06	-	63.82	18.15	36.30	-	57.23	20.05	34.10	-	59.13
400	20.91	44.33	-	71.76	17.73	35.97	-	61.06	15.72	30.78	-	62.90

The working volume and the power output was selected as 250 mL and 83% for all frequencies for the following reasons: i) to prevent excess heating at lower volumes, ii) to compare the performance at similar power densities.

4.1.4.4. Summary of Optimization Experiments. A summary of all optimization results for the three reactors is presented in Table 4.11.

Table 4.11. Optimum reactor parameters.

Reactor	**Power Applied, W**	**Power Dissipated in Solution, W**	**Volume, mL**
US1	54	37.30	80
US2	25	18.99	100
US3	100	48.83(577 kHz), 48.41(861 kHz), 48.93(1145 kHz)	250

4.2. Methods of EDC Removal

4.2.1. Bisphenol-A

4.2.1.1. Preparation of Test Solutions. A stock bisphenol-A solution of 450 μM was prepared in ultra-pure milli-Q water and stored in the dark at 4 ºC. Test samples of various strengths were prepared by diluting from the stock using milli-Q water.

4.2.1.2. Procedure. Experiments were carried out in US2, US3, BCOz and USOz. Prior to sonication, the test solutions were bubbled with air, argon or oxygen for 1 h and the same gas was continually sparged into the solution throughout sonication. The experiments were conducted at natural pH of the solutions except when investigating the effect of pH. Samples were withdrawn from the reactors at frequent time intervals for BPA analysis by high-pressure liquid chromatography (HPLC).

4.2.1.3. Analytical Methods.

HPLC analysis. Bisphenol-A was analyzed by a Shimadzu LC-20AT HPLC using a SPD-20A UV-vis detector set at 220 nm and an Inertsil ODS-3V column (150 mm x 4.6 mm, 5 μm). The method was isocratic and a mixture of acetonitrile-milli-Q water solution (50:50 by volume) at a flowrate of 1 mL min^{-1} was used as the mobile phase throughout analysis. Sample injection volume was 100 μL and the retention time of BPA was 5.4 min. For analysis of the experiments carried out in Germany, a Shimadzu LC-10ATVP HPLC with a photo diode array detector set at 220 nm (Shimadzu SIL-10ADVP) equipped with a Hypersil ODS column (250 mm x 3 mm, 3 μm, Macherey-Nagel) was used. The method and mobile phase were the same as described above. In this case, the flow rate of the mobile phase was 0.5 mL min^{-1} and BPA retention time was 5.2 min. A calibration curve was prepared using BPA concentrations in the range of 0.2-100 μM.

Total organic carbon analysis. Total organic carbon (TOC) was monitored using a Shimadzu TOC-V CSH analyzer operating in the non-purgeable organic carbon (NPOC) mode. The instrument was calibrated by standard solutions of KHP (1-10 ppm). Samples were acidified with HCl to pH 1-2 and purged for 1.5 min prior to injection with

instrument grade air to ensure that all carbonate, bicarbonate and carbonic acid are removed as carbon dioxide (in gas form) from the solution. For TOC measurements in Germany, an Elementar model high TOC/TNb analyzer operating in NPOC mode was used. All samples were measured in triplicate.

Hydrogen peroxide analysis. The concentration of hydrogen peroxide (H_2O_2) was analyzed by the potassium iodide method described by Klassen et al. (1994). The method is based on the reaction of iodide (I^-) with H_2O_2 to form triiodide ion (I_3^-), which has a strong absorbance at 351 nm. The analysis of H_2O_2 at concentrations as low as 1 mM is conveniently made by determining the yield of I_3^- formed when H_2O_2 reacts with KI in a buffered solution containing ammonium molybdate tetrahydrate as a catalyst. Two solutions (A and B) were prepared as described below and 2.5 mL from each solution was mixed with 1 mL of sample and diluted to 10 mL to record the absorbance at 351 nm.

Solution A: 33 g of KI, 1g of NaOH and 0.1 g of ammonium molybdate tetrahydrate were diluted to 500 mL with milli-Q water. The solution was stirred for 1 h to dissolve the molybdate and kept in the dark to prevent the oxidation of I^-.

Solution B: 10 g of potassium hydrogen phtalate was dissolved in 500 mL to serve as the buffer solution.

Gaseous ozone analysis. Initial ozone concentrations in the gas phase were measured by an Anseros Ozomat GM-6000-PRO model analyzer and recorded by Anseros OZOLAB Amacs software (Germany).

Dissolved ozone analysis. The aqueous ozone concentration was analyzed by the indigo colorimetric method (APHA/AWWA/WPCP, 1992). The method is based on the decolorization of indigo by ozone in solution. The decrease in absorbance is linear with increasing ozone concentration. Two solutions (indigo stock and indigo reagent) were prepared as described below:

Indigo stock solution: 77 mg potassium indigo trisulfonate ($C_{16}H_7N_2O_{11}S_3K_3$) and 0.1 mL concentrated phosphoric acid were diluted to 100 mL with milli-Q water. The stock

solution is stable for about 4 months when stored in the dark, and should be discarded when absorbance at 600 nm of a 1:100 dilution falls below 0.16.

Indigo reagent solution: 25 mL indigo stock solution, 2.5 g sodium dihydrogen phosphate (NaH_2PO_4), and 1.75 mL concentrated phosphoric acid were diluted to 250 mL with milli-Q water.

10 mL indigo reagent and 10 mL sample were mixed and diluted to 100 mL with milli-Q water. Blank sample was prepared in the absence of sample. The absorbance of both solutions were measured at 600 nm and the aqueous ozone concentration was calculated by the following equation:

$$\text{mg } O_3 / \text{L} = \frac{100 \times \Delta A}{f \times b \times V} \qquad (4.2)$$

where ΔA is the difference in absorbance (600 nm) between blank and sample, b is the path length of cell (cm), V is the volume of the sample (mL), and *f* is the proportionality constant which is 0.42 ± 0.01/cm/mg/L ($\Delta \in$ = 20 000 M^{-1} cm^{-1}) at 600 nm compared to the ultraviolet absorption of pure ozone of $\in$ = 2950 M^{-1} cm^{-1} at 258 nm.

Gas chromatography-mass spectrometry analysis. By-products of BPA (in BCOz) were analyzed by a Shimadzu QP5000 gas chromatography-mass spectrometry (GC-MS). Samples were extracted by solid phase extraction (SPE) as proposed by Kaneco and co-workers (2004) prior to GC-MS analysis. SPE cartridges (C_{18} PAH, Chromabond) were placed on the vacuum manifold and conditioned with 10 mL of solvent mixture containing dichloromethane and ethyl acetate (1:1 by volume), 10 mL of methanol and 10 mL of milli-Q water. The sample was loaded into the cartridge at a flow rate of 5 mL min^{-1}. The cartridge was dried and the retained compounds were eluted by 4x5 mL (1:1 by volume) of a solvent mixture of dichloromethane and ethyl acetate. The eluting solution was concentrated under gentle nitrogen flow before introduction to GC-MS. The GC-MS was equipped with a Factor Four (Varian) column (60 mm x 0.25 mm, 0.25 μm) and operated at the following conditions: injector temperature 300ºC, column temperature program 100ºC (1 min), 100-300ºC (7ºC min^{-1}) and 300ºC (10 min), carrier gas Helium flowing at

1.1 mL min^{-1}, interface temperature 250ºC. Analyses were performed in the electron impact (EI) mode at 70 eV using the scan mode. Wiley 221 and NIST 107 spectra libraries were used to identify the products.

4.2.2. 4-n-Nonylphenol

4.2.2.1. Preparation of Test Solutions. A stock 4-n-nonylphenol solution of 8700 μM was prepared in HPLC-grade methanol and stored in the dark at 4 ºC. Test samples of various strengths were prepared by diluting from the stock using ultra-pure milli-Q water.

4.2.2.2. Procedure. Experiments were conducted in US1 and US3. The test solutions were bubbled with air, argon or oxygen for 1 h prior to sonication and the same gas was continuously sparged into the solution throughout sonication. The experiments were run at natural pH of the solutions except when investigating the effect of pH. In some experiments, salts of iron(II) sulfate heptahydrate and cupric sulfate were added to the solutions. Samples were withdrawn from the reactor at frequent time intervals for 4-NP analysis by HPLC.

4.2.2.3. Analytical Methods.

HPLC analysis. 4-n-nonylphenol was analyzed by a Shimadzu LC-20AT HPLC using a SPD-20A UV-vis detector set at 220 nm and an Inertsil ODS-3V column. A mixture of acetonitrile- milli-Q water solution (80:20 by volume) at a flowrate of 2 mL min^{-1} was used as the mobile phase throughout analysis. Sample injection volume was 50 μL and the retention time of NP was 5.2 min. A calibration curve was prepared using 4-NP concentrations in the range of 0.2-500 μM.

Gas chromatographic analysis. By-products of 4-NP (in US1) were analyzed by an Agilent 6890N gas chromatograph (GC) with flame ionization detector (FID) detector.

4.2.3. C.I. Acid Orange 8

4.2.3.1. Preparation of Test Solutions. A stock AO8 solution of 3 mM was prepared in boiling milli-Q water during magnetic stirring, and stored in the dark at 4ºC. Test concentrations of various dye strengths were prepared from the stock by proper dilutions with milli-Q water.

4.2.3.2. Procedure. Experiments were carried out in US2 and USOz. The test solutions were aerated prior to sonication and sparged continuously with argon during sonication. The pH of all solutions after saturation with air was 5.0 and no pH adjustment was made in any test scheme. The performance of the systems for color decay was assessed by the degree of reduction in the maximum absorbance of the dye in the visible band (490 nm), while aromatic and naphthol ring degradation were determined by the abatements at UV-254 and UV-312 nm bands, respectively. The impacts of carbon tetrachloride and tert-butanol on decolorization and UV abatement were investigated in US2.

4.2.3.3. Analytical Methods.

Spectrophotometric analysis. The visible and UV absorbance of effluent samples were analyzed using a Unicam Hελios Alpha/Beta double beam spectrophotometer.

Hydrogen peroxide and total organic carbon analysis. These analyses were carried out as described in section 4.2.1.3.

5. BISPHENOL-A

5.1. Ultrasound

5.1.1. Operational Parameters

The study presented in this section (5.1.1) is a copy of the paper entitled "Ultrasonic Destruction of Bisphenol-A: The Operating Parameters", published in Ultrasonics Sonochemistry (Gultekin and Ince, 2008).

5.1.1.1. Background. The issue of endocrine disruption has recently received much public and scientific concern due to the detection and identification of many endocrine disrupting compounds (EDCs) in the environment. Evidence indicating adverse impacts of these compounds in wildlife has also raised concern of potential health effects in humans, particularly as hormonal malfunctions. More recently, increased incidence of some cancer types and reproductive system dysfunctions in humans have been linked to EDC exposures (U.S. EPA, 2001b).

Among numerous EDCs used in industrial processes, bisphenol-A (BPA) is one of the most popular, owing to its large consumption in the production of polycarbonate and epoxy resins, flame retardants, and many specialty products (Staples et al., 1998). The discharge of BPA into the water environment occurs unintentionally during handling, unloading, heating and accidental spills. Animal studies with BPA have shown that it exhibited weak estrogenic activity (Harris et al., 1997); increased the rate of proliferation of breast cancer cells (Krishnan et al., 1993), induced acute toxicity to a number of freshwater and marine species (Alexander et al., 1988); resulted in prostate enlargement in mice (vom Saal et al., 1998), and changed the pituitary function in rats (Steinmetz, 1997). Human studies have shown that BPA was present in the serum of adults (Takeuchi and Tsutsumi, 2002) and was detected in 95% of urine samples in a test population of 394 (Calafat et al., 2005).

Environmental scientists concerned with contamination of natural waters with BPA have been searching for alternative methods to render complete or considerable destruction of the compound. Among these, advanced oxidation processes (AOPs) such as heterogeneous photocatalysis with TiO_2, Fenton and photo-Fenton processes and ozonation have been the most common (Chiang et al., 2004; Katsumata et al., 2004; Deborde et al., 2005). The literature on ultrasonic means of BPA destruction is limited to a couple of investigations (Kitajima et al., 2006; Ioan et al., 2007).

Ultrasonic irradiation of liquids gives rise to cavitation bubbles, which during compression/rarefaction cycles grow and expand by entrapping volatile vapors and gases in the medium. When the bubbles become too large to sustain themselves, they undergo violent implosions resulting in local hot spots with extreme temperatures and pressures (Suslick, 1990). Organic compounds exposed to ultrasound may undergo degradation via thermal and/or chemical reactions depending on the degree of solute's partitioning between the gaseous bubble and the aqueous solution. The degradation of highly and moderately volatile compounds takes place in the gas phase by molecular fragmentation and at the interfacial sheath by oxidative destruction, respectively. If the compound is largely hydrophilic and unable to diffuse out of the bulk liquid, degradation is governed merely by aqueous phase oxidation reactions (Suslick, 1990; Mason, 1999).

The objective of this study was to investigate the degradability of BPA by ultrasonic irradiation at 300 kHz and to select the operating parameters of optimum efficiency. The method involved selection of the working BPA concentration based on maximum rate of sonochemical decay, followed by assessing the role of pH and sparge gases. Potential sites of reaction were investigated by monitoring the rate of decay in the presence of various quantities of sodium carbonate and t-butanol, which are strong scavengers of hydroxyl radicals in the bulk liquid and the bubble-liquid interface, respectively.

5.1.1.2. Materials and Methods. Bisphenol A (Molecular Mass=228.29 g mol^{-1}) was obtained from Aldrich in > 99 % purity and used as received. HPLC-grade acetonitrile (Merck) was used as a mobile phase in HPLC, respectively. The reagents H_2SO_4, NaOH, t-butanol and Na_2CO_3 were all analytical grade. Sonication was carried out in a 150 mL

glass reactor surrounded by a water-cooling jacket and consisting of a plate type transducer connected to a 25 W generator emitting ultrasonic waves at 300 kHz. The ultrasonic power density in the reactor was 0.190 W mL^{-1} as determined by calorimetric analysis (Mason et al., 1992).

Test samples of 100 mL were prepared in ultra pure milli-Q water, and aerated for 1-h before exposure to ultrasound. The pH of all samples following aeration was nearly constant at 6.0 - 6.3. The operating concentration was found by sonicating 10, 20, 40, 60 and 100 μM BPA for 60 min while monitoring the concentration of BPA within every 5 min. Impacts of pH and sparge gases were tested during sonication of the selected test concentration at pH=3.0, 6.0 and 10.5 and in the presence of argon, air and oxygen bubbling, respectively. The effect of hydroxyl radical scavengers on the rate of decay was investigated by adding increasing quantities of sodium carbonate and t-butanol and/or by varying the molar ratio of scavenger to BPA in the test samples during sonication.

BPA was analyzed by a Shimadzu LC-20AT HPLC using a SPD-20A UV-vis detector set at 220 nm and an Inertsil ODS-3V column. A mixture of acetonitrile- milli-Q water solution (50:50 by volume) at 1 mL min^{-1} was used as the eluate throughout analysis. Hydrogen peroxide was measured colorimetrically by the potassium iodide method (Klassen et al., 1994).

5.1.1.3. Results and Discussion.

Effect of concentration. Normalized plots of concentration-time data and the fitted curves to the first-order rate equation ($C=C_0e^{-k't}$) for 10, 20, 40, 60 and 100 μM BPA are presented in Figure 5.1. It was found that increases in concentration within the low range (e.g. 10 μM - 20 μM) resulted in much sharper decreases in the rate of degradation than increases in the higher range, as typical of saturation type kinetics proposed in the literature for the degradation of concentrated solutions of hydrophilic compounds by ultrasound (Kidak and Ince, 2006; Serpone et al., 1994).

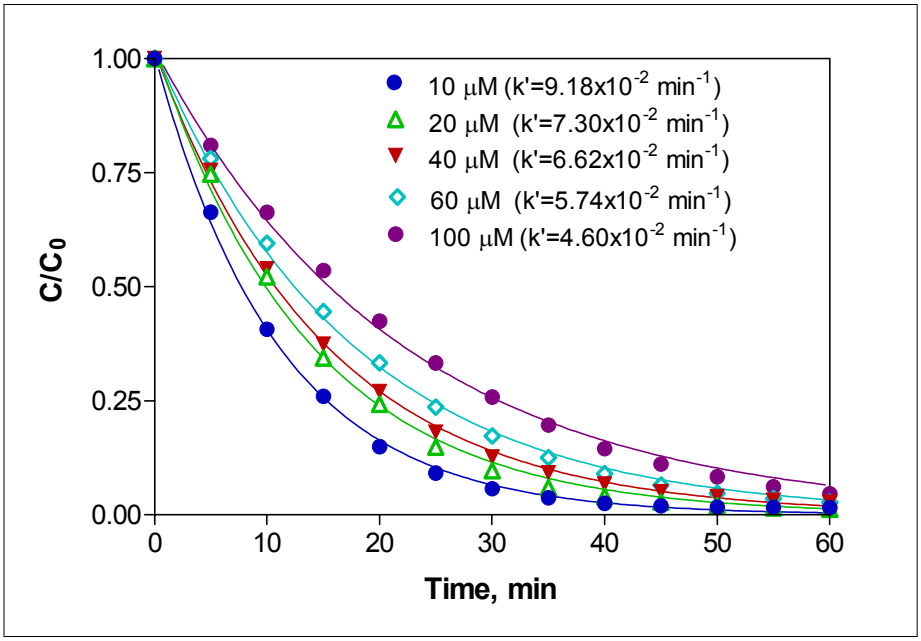

Figure 5.1. Effect of concentration on sonochemical decay of BPA under 0.15 L min^{-1} air injection. The solid lines are the fit of data to $C/C_0 = e^{-k't}$, where C_0 and C are concentrations (μM) of BPA at time zero and t, respectively; and k' is the pseudo 1st order decay rate constant (min^{-1}).

The sonochemical "product yield" and its variation with the initial BPA concentration were estimated by:

$$G = \frac{\Delta M \times V}{E} \qquad (5.1)$$

where: G is the yield (mole J^{-1}), ΔM is the difference in the number of moles of BPA at t=0 and t= 60 min (mole L^{-1}), V is the solution volume (L) and E is the energy deposited in the reactor (J), as estimated from calorimetric data. The plot of G against concentration is presented in Figure 5.2. The fact that sonochemical yield increases proportionally with concentration despite the increased competition for hydroxyl radicals in the bulk solution shows that at higher concentrations decomposition occurs not only in the bulk liquid but also at the bubble-liquid interface.

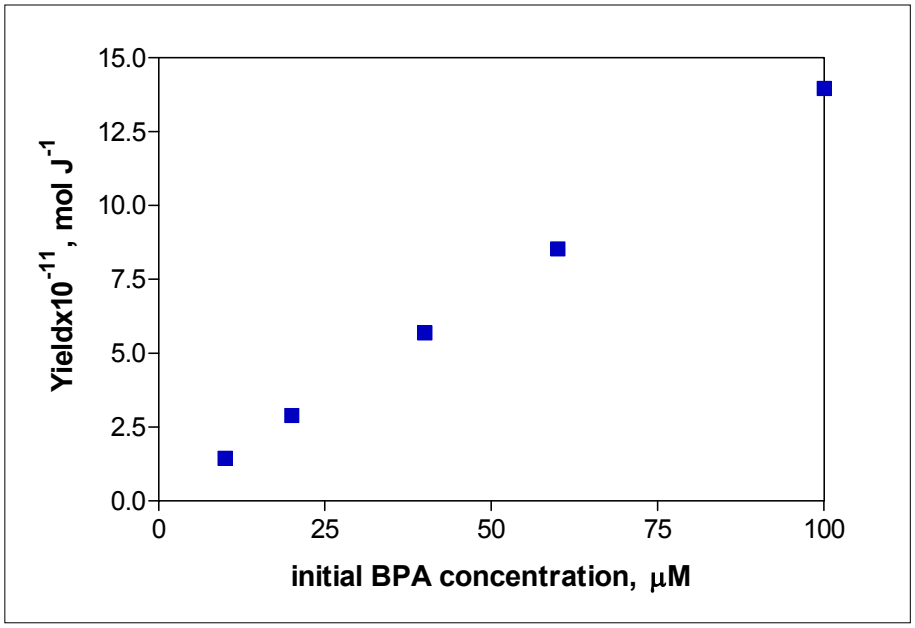

Figure 5.2. The response of 60-min "product yield" to increases in BPA concentration.

Effect of pH. The effect of pH was investigated by sonication of 10 µM BPA at pH=3.0, 6.0 and 10.5 during air bubbling. The results and estimated pseudo-first order decay rate coefficients are presented in Figure 5.3.

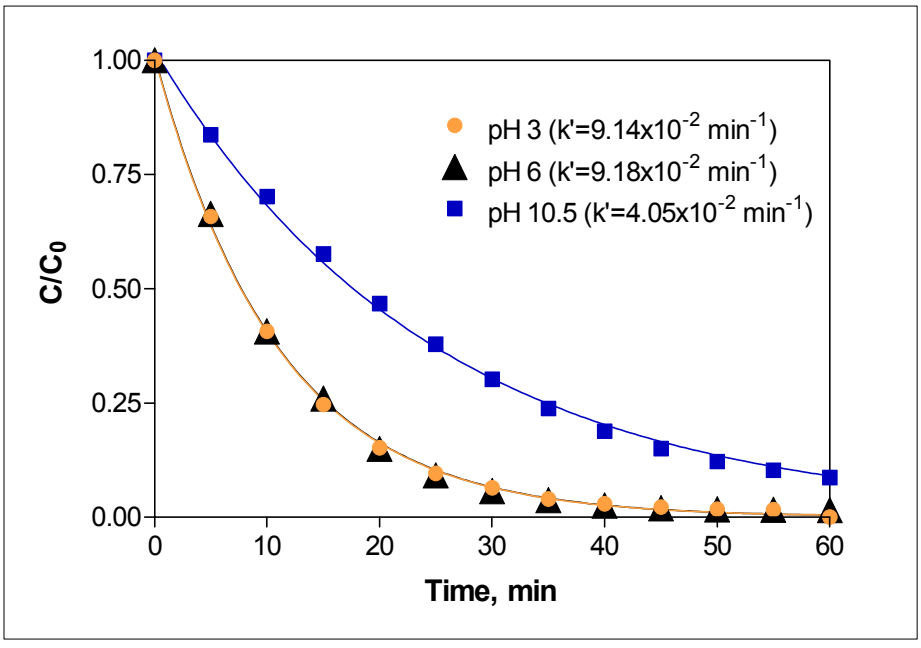

Figure 5.3. Effect of pH on sonochemical degradation of BPA at C_0 =10 µM.

The data reveal that the rate was unaffected by pH variations within acidic to near-neutral region, but remarkably decelerated upon elevation to alkaline levels. The sonochemical product yield was also adversely affected by increases in pH from neutral to highly alkaline level, as G was $1.46x10^{-11}$, $1.44x10^{-11}$ and $1.34x10^{-11}$ mol J^{-1} at pH 3.0, 6.0 and 10.5, respectively.

To explain these findings, we checked the dissociation constant of BPA and found that there are two distinct values, one at $pK_{a1} = 9.6$ and the other at $pK_{a2} = 10.2$ (Kosky and Guggenheim, 1991). Hence, at pH 3 and 6, the compound exists mainly in molecular form, whereas at pH 10.5 it is completely ionic, which due to the negative sign is much more hydrophilic than the neutral state and thus is less likely to approach the negatively charged cavity bubbles. As a consequence, the faster decomposition of BPA at pH 3 and 6 than that at pH=10.5 is due to the more likely diffusion of the molecule at lower pH to the bubble-liquid interface, where the concentration of hydroxyl radicals is a maximum. A more detailed discussion of pH effect on sonochemical decomposition of aromatic compounds can be found in the literature (Kidak and Ince, 2006; Ince and Tezcanli-Güyer, 2004).

Effect of saturating gas. Gas injection during sonication is a common tool to enhance cavitation and selection of the right gas is very important, because it may change the reaction efficiency in relation to its physical properties. The relative gas impact was tested by continuous injection of argon, air or oxygen at equivalent flow rates and monitoring the concentration of BPA. Normalized plots of BPA concentration against time during air, argon and oxygen injection are presented in Figure 5.4.

The data showed that the rate of BPA degradation was affected by the injected gas type, being fastest in the presence of air and slowest in that of oxygen. In general, different sonochemical efficiencies in presence of different gases are explained by differences in polytropic gas ratios and thermal conductivities. It is well known that high polytropic gas ratio (γ) and low conductivity (κ) favor higher collapse temperatures (Neppiras, 1980). In accordance, the values of γ and κ for Ar, air and oxygen (γ=1.67, κ=$177x10^{-4}$ W m^{-1} K^{-1}; γ=1.40, κ=$262x10^{-4}$ W m^{-1} $K^{-1}$and γ=1.40, κ=$267x10^{-4}$ W m^{-1} K^{-1}, respectively (Perry and Green, 1984) suggest that maximum collapse temperature is expected in the presence of argon, and lower/equivalent temperatures in the presence of air or oxygen. Nevertheless,

the observed decay coefficient during air bubbling is not consistent with this rule, and must therefore be explained via other parameters.

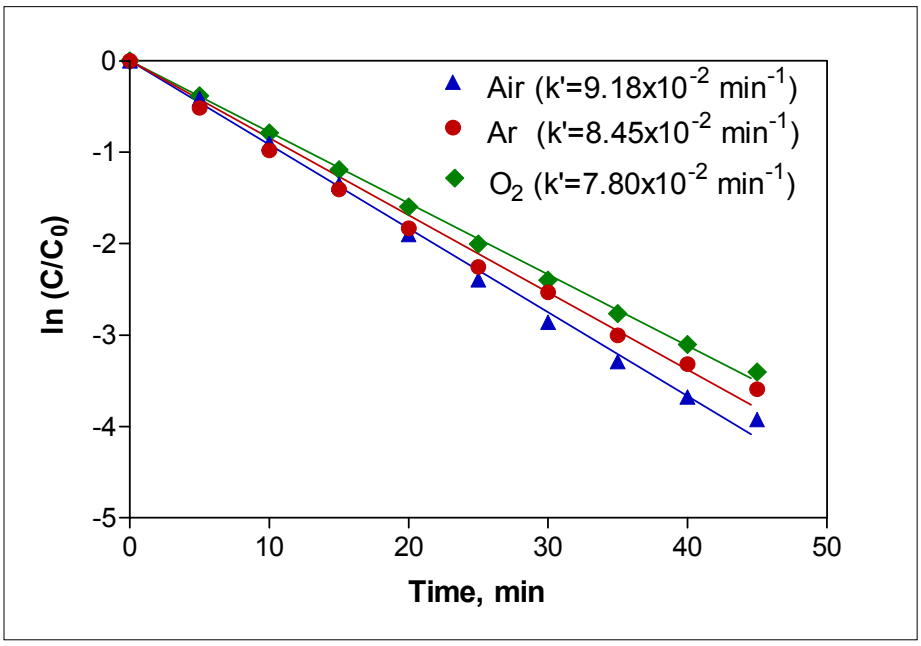

Figure 5.4. Relative rates of BPA decomposition during argon, air and oxygen bubbling (C_0=10 μM, gas flow rate=0.15 L min^{-1}). The solid lines represent linear regression of the data within 45 min reaction time.

The following reactions take place when sonication is carried out during air injection (Petrier et al., 1992; Hart and Henglein, 1986; Mead et al., 1976; Hart et al., 1986):

$$H_2O +))) \rightarrow \ \bullet OH + \bullet H \quad (5.2)$$

$$N_2 + \bullet OH \rightarrow N_2O + \bullet H \quad (5.3)$$

$$N_2O + O \rightarrow 2NO \quad (5.4)$$

$$\bullet H + N_2O \rightarrow N_2 + \bullet OH \quad (5.5)$$

$$\bullet OH + N_2O \rightarrow 2NO + \bullet H \quad (5.6)$$

$$3N_2O + H_2O \rightarrow 2HNO_3 + 2N_2 \quad (5.7)$$

$$HNO_3 + \bullet H \rightarrow \bullet NO_2 + H_2O \quad (5.8)$$

$$HNO_3 + \bullet OH \rightarrow \bullet NO_3 + H_2O \quad (5.9)$$

Finally, nitric acid undergoes thermal fragmentation in the collapsing bubbles to form additional nitrite, nitrate and hydroxyl radicals:

$$HNO_3 +))) \rightarrow \bullet OH + \bullet NO_2 \quad (5.10)$$

$$HNO_3 +))) \rightarrow \bullet H + \bullet NO_3 \quad (5.11)$$

Reactions 5.2-5.11 suggest that the rapid decomposition of BPA in the presence of air despite its less favorable physical properties than argon is due to: i) generation of nitric acid that enhances the reaction by lowering the solution pH; ii) formation of excess •OH and other radicals such as $\bullet NO_2$ and $\bullet NO_3$, which are considerably reactive with aromatic compounds ($k_{\bullet Nox} = 10^7\ M^{-1}\ s^{-1}$; $k_{\bullet OH} = 10^{12}\ M^{-1}\ s^{-1}$, (Gogate and Pandit, 2004)).

On the other hand, the relative rate of BPA decay in presence of Ar and oxygen is consistent with the general rule about the impact of gas properties despite the fact that some excess radicals (e.g. •OH and $\bullet HO_2$) are also generated in O_2-saturated solutions. The consistency must be due to the fact that the reactivity of HO_2 radicals with aromatic compounds is 2-3 orders of magnitude lower than that of NO_x (Bielski et al., 1985).

H_2O_2 formation. Ultrasonic irradiation of water results in the formation of hydrogen peroxide by recombination of OH radicals that form upon water fragmentation. The concentration of hydrogen peroxide in solution, therefore, is an indirect measure of the concentration of hydroxyl radicals ejected into the bulk liquid. Figure 5.5 shows the net production of H_2O_2 during 60 min sonication with 10, 40 and 100 μM BPA. It was found that the rate of H_2O_2 accumulation was largest in the control reaction (ultrasound in milli-Q water containing no BPA) and decreased with the addition of increasing concentrations of BPA, by scavenging reactions. Note that at 40 and 100 μM BPA, the rate of accumulation reached a steady level after 40 min sonication, showing that the rate of •OH consumption by recombination and scavenging reactions was nearly equivalent to the rate of its production. This observation is a clear indication of •OH-mediated oxidation as one of the decomposition pathways of BPA.

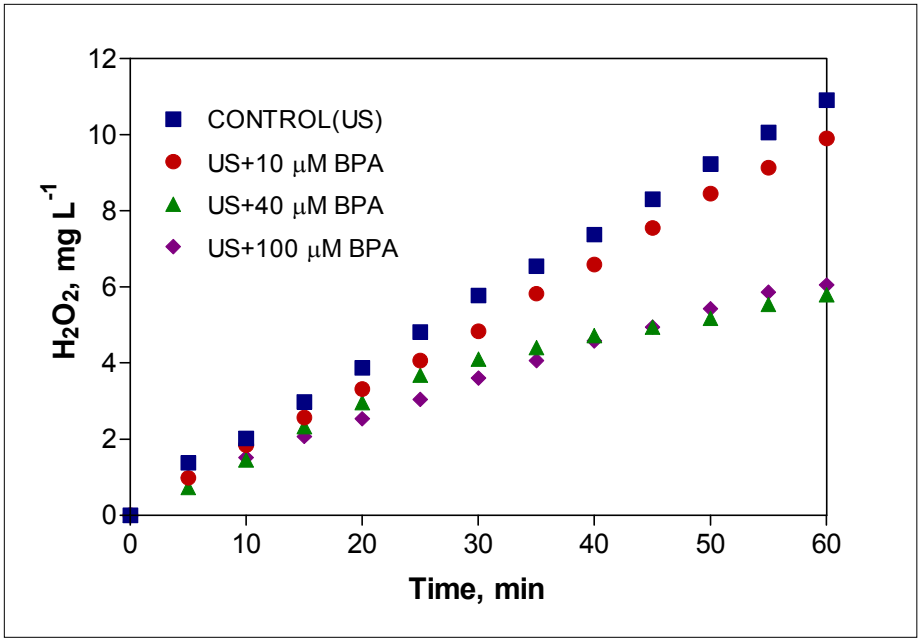

Figure 5.5. Accumulation of H_2O_2 during sonication of ultra pure milli-Q water with and without BPA.

Effect of hydroxyl radical scavengers. It is well known that ultrasonic decomposition of organic compounds is a function of their physicochemical properties such as vapor pressure/solubility and octanol-water partition coefficient. The three potential sites for chemical reactions in ultrasonically irradiated liquids are: (1) the cavitation bubble; (2) the interfacial sheath between the bubble and the surrounding liquid and (3) the solution bulk (Ince et al., 2001). Given that BPA is a slightly volatile and moderately soluble compound (p_i=4.0x10^{-8} mm Hg; solubility=120 mg L^{-1}; (Howard, 1989)) with log K_{ow} = 3.40 (Bayer-Leverkusen, 1993), the major decomposition pathway is expected to be oxidation by hydroxyl radicals in the bulk solution, while a minor one may involve decomposition at the interfacial region or surfaces of collapsing bubbles, where the concentration of hydroxyl radical is a maximum. At very high concentrations, thermal fragmentation may also occur as some of the molecules will likely diffuse into the hot bubble interiors.

To assess the potential reaction sites of hydroxyl radical-mediated oxidation of BPA, we monitored its degradation in the presence of carbonate (p_i=negligible, $k_{\bullet OH}$=3.9x10^8 M^{-1} s^{-1} (Buxton et al., 1988)), and t-butanol (p_i=31 mm Hg (Sigma-Aldrich, 2004), $k_{\bullet OH}$=6.0x10^8 M^{-1} s^{-1} (Buxton et al., 1988)), which are well-known scavengers of

OH radicals in the bulk liquid and the bubble-liquid interface, respectively. It was found that at micro-molar levels, the presence of scavengers did not alter the rate of BPA degradation and at low milli-molar levels (0.1-0.5 mM) the rate was slowed down by no more than 10%. At carbonate concentrations of 1, 5 and 10 mM, the degree of deceleration was increased to 18.5%, 40.1% and 40.0%, respectively. The stability of the rate above 5 mM CO_3^{2-} must be due to the salting out effect, by which the hydrophobicity of BPA is increased and some of it is diffused to the interfacial sheath for further oxidation.

In case of t-butanol addition at 1, 5 and 10 mM, the degradation was found to decelerate by 15%, 51.4% and 74.4%, respectively. This observation clearly indicates that BPA undergoes oxidation not only in the bulk liquid but also in the interfacial sheath, where the competition for OH radicals increases as the quantity of t-butanol relative to that of BPA is increased. The pseudo-first order decay coefficients of BPA in the presence of 1, 5 and 10 mM carbonate and t-butanol are listed in Table 5.1.

Table 5.1. Relative impacts of •OH scavengers on the rate of 10 μM BPA decay.

Scavenger Concentration	**k'x10^{-2}, min^{-1}**	
	CO_3^{2-}	**t-C_4H_9OH**
1 mM	7.44±0.07	7.74±0.06
5 mM	5.41±0.05	4.44±0.12
10 mM	5.54±0.08	2.34±0.04

The values listed in Table 5.1 show that the relative impact of t-butanol on the rate of BPA decomposition was larger than that of carbonate. Hence, we carried out a more thorough investigation of t-butanol impact by varying its molar ratio to that of BPA. In the first experimental set, the rate of decay was monitored in t-butanol:BPA mixtures of 10, 50, 100, 500 and 1000 (μM:μM), where the concentration of BPA was kept constant at 10 μM. It was found that in each case the reaction was decelerated only during the first 5-8 min of sonication (data not shown) and the degree of deceleration was proportional to the quantity of t-butanol added. However, in all cases the 60-min fraction of BPA removal was unaffected by the quantity of t-butanol in solution, except when it was ≥5000 μM. The results are plotted in Figure 5.6 in a bar chart. In accordance, we concluded that: i) t-butanol quickly decomposes by oxidation and/or thermal fragmentation so that there is no

competition during continued sonication; ii) the quantity of OH radicals in the bulk liquid is unlimited within the experimental conditions employed; iii) the reaction of t-butanol with OH radicals is not competitive with that of BPA unless at very high t-butanol relative concentrations.

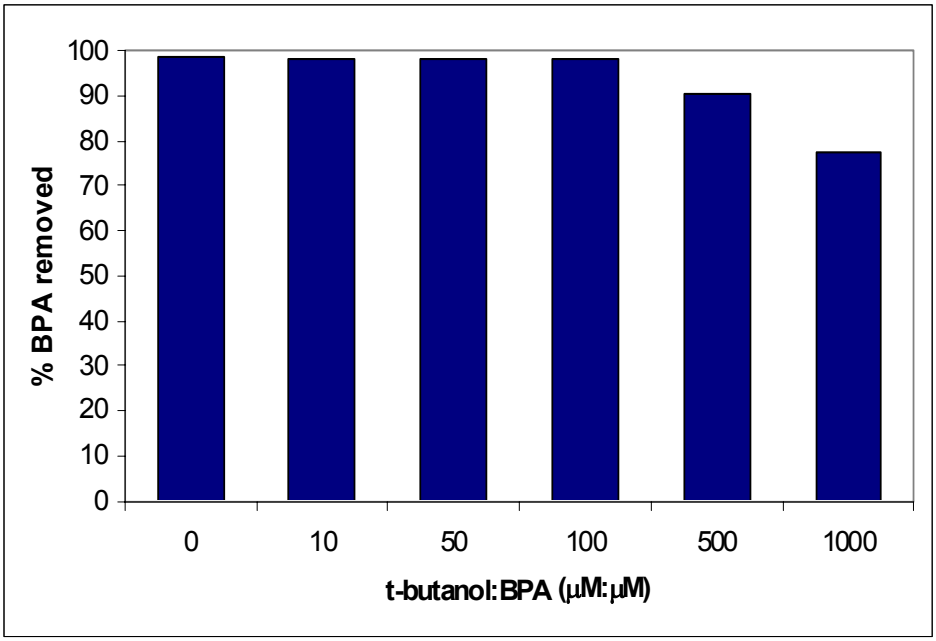

Figure 5.6. Relative fractions of BPA decay in mixtures of t-butanol:BPA (BPA=10μM, t=60 min).

In the second experimental set, we monitored the degree of 60 min decomposition in t-butanol:BPA mixtures of 10 and 100 (by μM), where BPA concentration was kept constant at 100 μM and that of t-butanol was varied accordingly. The results are listed in Table 5.2. The drastic decrease in the degree of BPA removal by a 10-fold increase in the relative concentration of t-butanol in the mixture is a clear indication of i) interfacial reactions of BPA at high concentrations and ii) the competition between t-butanol and BPA for OH radicals. The figures inserted in parenthesis in Table 5.2 are the observed fractions of decomposition in mixtures of the first set, where the molar ratios were 10 and 100 again, but the concentration of BPA was 10 μM. Note that the competition for •OH was insignificant at 10 μM BPA regardless of the t-butanol level, and/or the reaction occurred mainly in the bulk liquid at low BPA concentrations.

Table 5.2. The fraction of BPA decay at varying relative t-butanol: BPA concentrations.

Molar ratio (μM:μM)	% BPA removed
10 (1000 t-B/100 BPA)	94.09 (98.35)
100 (10000 t-B/100 BPA)	48.08 (98.28)

5.1.1.4. Conclusions. The sonochemical product yield for the decomposition of BPA at 300 kHz was found to increase linearly with the input BPA concentration, as a consequence of the possibility of reaction sites other than the bulk liquid at more concentrated solutions. Acidic to near-neutral pH and injection of air render faster decomposition than alkaline pH, and argon or oxygen injection. The lower rate of hydrogen peroxide accumulation in BPA solutions than in ultra pure deionized water is an evidence of OH radical-mediated oxidation as the major destruction pathway. The impact of carbonate and t-butanol as strong scavengers of OH radicals was insignificant at low concentrations of the scavengers, but significant when the fraction of scavenger to BPA was large. Finally, the degree of rate inhibition was much larger in the presence of large concentrations of t-butanol than carbonate, showing the significance of interfacial reactions in the destruction pathway of BPA.

5.1.2. Effect of Frequency and Pulsed Mode of Irradiation

5.1.2.1. Background. Sonochemistry takes its origin in cavitation, indicating that sonochemical reactivity depends on the characteristics of the cavity bubbles, which in turn are dependent on the applied frequency. The resonant size of a bubble is inversely proportional to the magnitude of the frequency, as was expressed earlier by equation 2.42. In that respect, low frequency ultrasound supports the formation of stable cavities with large radii and long lifetimes, whereas transient, small sized and short-lived cavities are generated under high frequency ultrasound.

Ultrasonic irradiation of water results in a rapid build-up of cavitation bubbles in the medium, which may lead to accumulation of bubbles, evolution of excess heat and inefficiency of energy transmission undesired heat evolution (Mason and Cordemans,

1998). To prevent these undesired conditions, ultrasound is applied in the "pulsed" mode, which means intermittent interruption of sonication within short intervals.

The study described in the following sections was aimed to investigate: i) the relative efficiencies of 577, 861, and 1145 kHz, ii) the potential reaction sites (as the bulk liquid or the interfacial sheath) and iii) the impact of pulse sonication on the degradation of BPA. The method involved exposing of 10 μM of BPA to US3 while monitoring the concentrations of BPA, H_2O_2 and TOC. The effect of pulsed ultrasound was tested at 861 kHz by varying the ratio of pulsed length to interval length.

5.1.2.2. Experimental. Sonication was carried out in US3, which is a multi-frequency reactor as described previously. The power density in the reactor was 0.195, 0.194 and 0.196 W mL^{-1} at 577, 861 and 1145 kHz, respectively. Air was used as the sparge gas to enhance bubble formation and to compensate for degassing effects.

Test solutions of 250 mL containing 10 μM BPA were prepared in ultra pure milli-Q water and aerated for 1-h before exposure to ultrasound. The pH of the solutions after saturation with air was 6.0 and no pH adjustment was made in any test scheme. Sonication time in each test was 60 min and samples were collected at various intervals for analysis of BPA, H_2O_2 and TOC. The potential reaction sites were investigated by monitoring the concentration of BPA during sonication in the presence of 1 mM and 10 mM tertiary butyl alcohol, which is a strong scavenger of hydroxyl radicals at the bubble-liquid interface. The effect of pulse sonication was tested by varying the pulse length between 10-5000 ms and the interval length between 1-5000 ms.

5.1.2.3. Results and Discussion.

Sonochemical rate. The effect of frequency on the rate of BPA decomposition by ultrasound is presented in Figure 5.7. It was found that the reaction was most rapid at 861 kHz, less at 1145 kHz and least at 577 kHz. This finding indicates that there exists an optimum frequency at which the interactive effects of bubble life, bubble size and OH radical concentration are maximum.

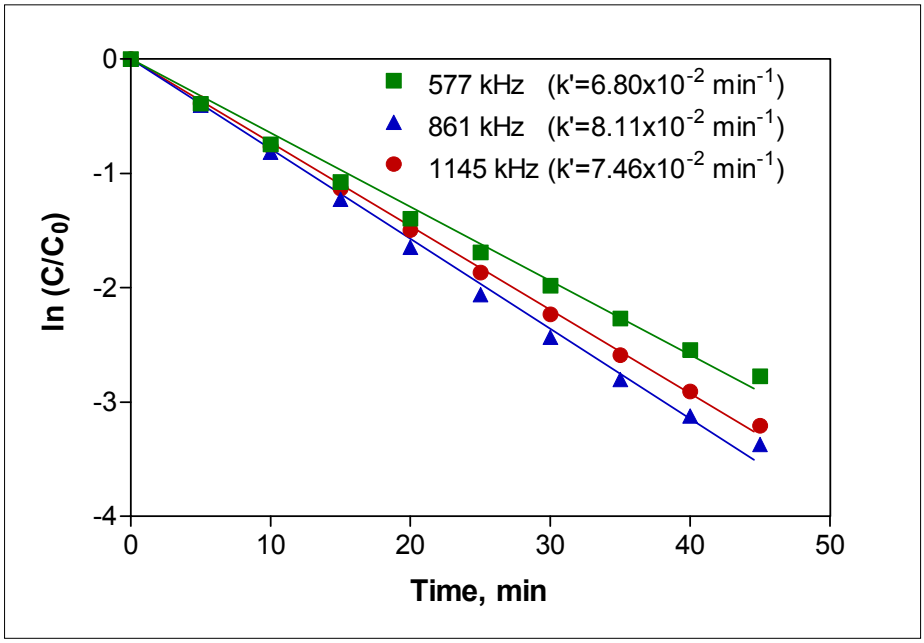

Figure 5.7. Log-linear decay of BPA at varying ultrasonic frequencies (C_0=10 μM, air flow rate=0.15 L min^{-1}).

Sonochemical product yield. A more important indicator of frequency effect is the sonochemical product yield G, which takes into account the change in mass of the compound per unit energy deposited, as was defined by Equation 5.1. Calculation of product yields at each frequency showed that the yield was only slightly affected by frequency, as G was $1.44x10^{-11}$, $1.49x10^{-11}$ and $1.46x10^{-11}$ mol J^{-1} at 577, 861 and 1145 kHz, respectively.

Accumulation of hydrogen peroxide. To further examine the effect of frequency, the generation of hydrogen peroxide was monitored in the absence and presence of BPA as an indirect measure of hydroxyl radicals in the bulk solution. It was found that the concentration of H_2O_2 linearly increased at all frequencies, as shown in Figure 5.8 for 60 min sonication. The results show that the rate of H_2O_2 formation was a maximum at 861 kHz in the absence of BPA and at 577 kHz in its presence.

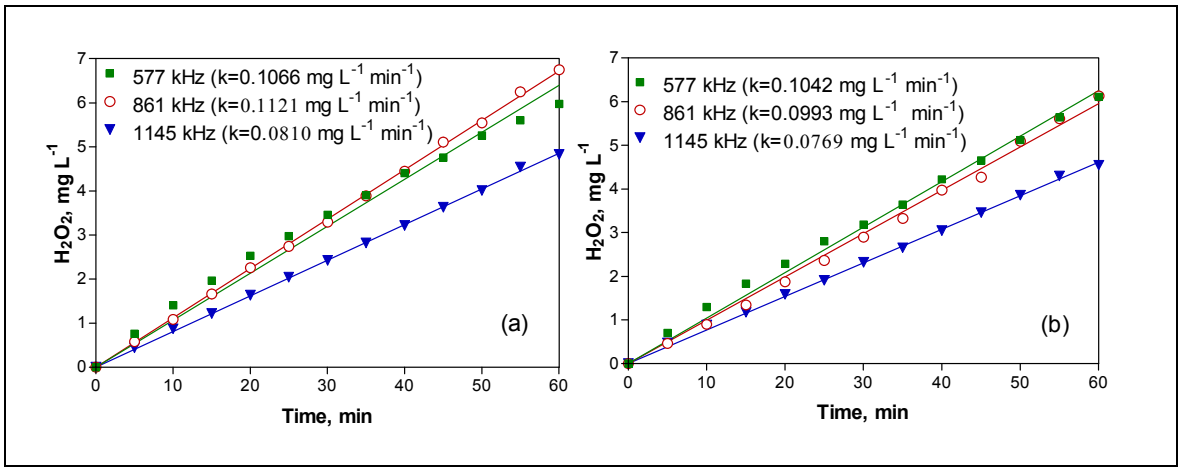

Figure 5.8. Frequency-related build-up of hydrogen peroxide in ultra pure water (a) and ultra pure water spiked with 10 µM BPA (b).

A summary of BPA rate constants, 60-min sonochemical yields and H_2O_2 formation rates is presented in Table 5.3 for comparative evaluation of the test frequencies.

Table 5.3. Comparison of BPA decay rates, 60-min sonochemical yields and H_2O_2 formation rates at 577, 861 and 1145 kHz ultrasound.

Frequency kHz	**k' min^{-1}**	**$Gx10^{-11}$ mol J^{-1}**	**H_2O_2 formation rate mg $L^{-1}min^{-1}$**
577	6.80	1.44	0.1042
861	8.11	1.49	0.0993
1145	7.46	1.46	0.0769

As discussed earlier in section 2.3.6.1, lower frequencies support longer-lived bubbles with higher energy. As the frequency increases bubble size, bubble energy and bubble life time are all reduced, but the rate of •OH ejection to the bulk solution increases (due to shortness of the time for their recombination). In addition, more frequent oscillations per unit time result in enhanced mass transfer in and out of the bubbles (Beckett and Hua, 2001). However, when the frequency is too high the resonant size of a bubble may be insufficient for complete pyrolysis of water molecules to produce sufficient hydroxyl radicals. Thus, there exists an optimum frequency range at which the bubble size is large enough to provide the best conditions for the violent collapse of cavity bubbles.

Selecting 861 kHz as the optimum frequency, the sites of reaction were assessed by sonication of BPA at 861 kHz in the presence of 1 mM and 10 mM tert-butanol. The results are presented in Table 5.4 in terms of the pseudo-first order rate constants.

Table 5.4. Effect of tert-butanol on the rate of BPA decay at 861 kHz.

Test Condition	**$k'x10^{-2}$ (min^{-1})**
Control (t-butanol=0)	8.11
t-butanol=1 mM	7.35
t-butanol=10 mM	2.18

It was found that in the presence of 1 mM tert-butanol the rate of reaction was decelerated only by 9.4 %, while in that of 10 mM the deceleration was 73 %. The data clearly indicate that in addition to the bulk liquid the bubble-liquid interface is a significant reaction site during sonochemical decomposition of BPA. The large inhibition observed at the higher dose of tert-butanol is not only due to excessive consumption of OH radicals at the interfacial area but also to the rapid decomposition of tert-butanol to volatile byproducts. The latter results in: (i) reduced number of adsorption sites at the interfacial sheath (competitive adsorption) and (ii) reduced bubble temperature upon diffusion and accumulation of the byproducts in the gaseous bubbles (the cushioning effect).

Mineralization. Total organic carbon measurements during 60 min sonication of 10 μM BPA at each frequency showed that no mineralization occurred within that time. This is not surprising, since mineralization is a much longer process than oxidation of the parent compound. However, TOC reduction after 8 h sonication was also found insignificant. It was then concluded that at very low or trace concentrations, mineralization of BPA is not possible by ultrasonic irradiation. To verify this hypothesis, we monitored the TOC of a 100 μM BPA solution during 8 h sonication at 861 kHz. The data as presented in Figure 5.9 show that total mineralization was 6 % after 2 h sonication, which provided 99% BPA elimination, and about 30 % after 8 h sonication.

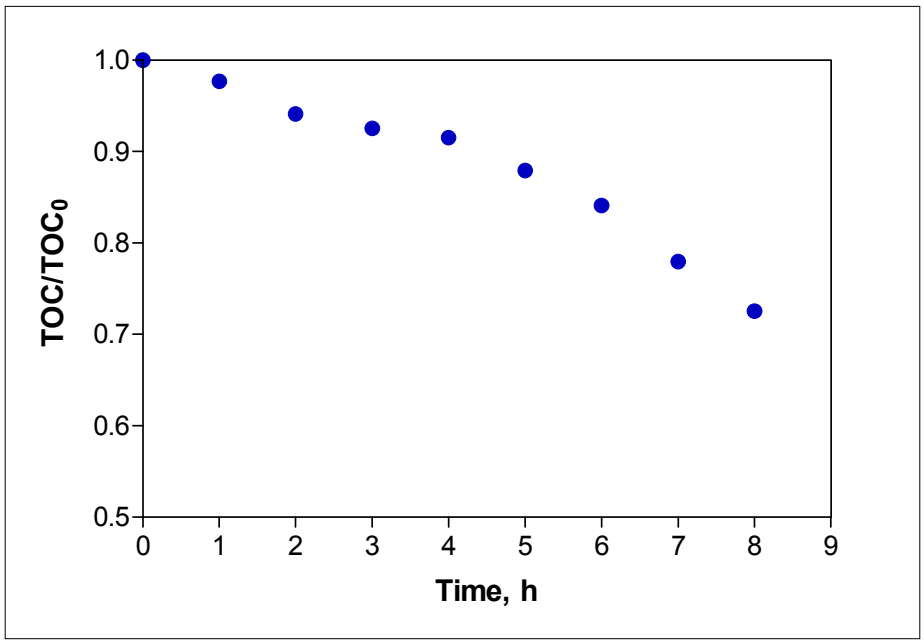

Figure 5.9. Normalized plot of TOC destruction in 100 μM BPA by sonication at 861 kHz.

Effect of pulsed ultrasound. Factors that affect the efficiency of pulsed ultrasound are "activation time", i.e. the time required to produce chemically active gas bubbles; and "deactivation time", i.e. the time during which the bubbles and the nuclei contained in the solution are decayed. When the pulse length is shorter than the activation time, chemical reactions do not occur because cavitation bubbles do not find sufficient time for growth and implosion. Correspondingly, when the interval length is longer than the deactivation time, activation of the system is vanished and the following pulse has to reactivate the system again (Henglein et al., 1989).

Experiments were conducted by varying the pulse and interval lengths at 15 min sonication periods. The conditions were fixed as follows: applied pulse lengths: 10, 100, 250, 500, 1000, 2000 and 5000 ms; applied interval lengths: 1, 10, 50, 100, 500, 1000, 2500 and 5000 ms. Pulse conditions and the observed BPA elimination fractions at each are tabulated in Table 5.5.

Table 5.5. Relative fractions of BPA elimination under various pulse-mode applications.

Pulse length, ms	Interval length, ms	On/Off ratio (P/I)	% BPA removal
10	1	10	1.8
10	10	1	0.6
100	10	10	55.1
100	100	1	33.2
100	500	0.2	14.2
100	1000	0.1	8.4
250	10	25	63.5
500	10	50	67.9
500	50	10	64.2
500	100	5	59.2
1000	10	100	68.9
1000	50	20	65.7
1000	100	10	64.2
1000	1000	1	41.3
1000	5000	0.2	15.5
2000	1000	2	54.2
5000	1000	5	64.4
5000	2500	2	54.1
5000	5000	1	42.1

The data show that at all pulse lengths, the degree of BPA elimination decreased with increasing interval time or decreasing on/off ratios. In addition, the efficiency of elimination was not a function of the P/I ratio, but that of the pulse length. For example, at a constant P/I ratio of 10, the fraction of elimination varied between 1.8% and 64.2%, corresponding to a pulse duration of 10 ms and 1000 ms, respectively. Note that BPA elimination was insignificant at very short pulse lengths (10 ms) due to the insufficient build-up of activation in the solution. Maximum elimination was obtained at P/I=100, corresponding to a pulse length of 1000 ms and an interval of 10 ms. Hence, the efficiency of pulsed irradiation increased as the length of pulse was enlarged and that of the interval was shortened. This means that at short pulse lengths, cavitation bubbles could not be activated to produce sufficient collapse conditions as energy and radical species. Comparing the maximum fraction of elimination in 15 min pulse operation (68.9%) with that of 15 min continuous sonication (70.7%), we can say that the pulse mode is slightly more effective since it consumed only 14.85 min of the generator time, whereas the other consumed full time. However, at 5000 ms pulse and 1000 ms interval lengths, the fraction

of elimination was 64.42% and the generator on-time was 12.5 min, which may be considered a more significant advantage over continuous sonication.

5.1.2.4. Conclusions. The results of the present study showed that ultrasonic frequency affects the rate of BPA degradation, but not necessarily the sonochemical product yield. The rate constant was largest at 861 kHz due to the optimum bubble size and life time that produced the most effective collapse conditions. Mineralization at very low BPA concentrations was insignificant even by extended sonication, but 30 % complete at higher concentrations within 8 h. Pulsed mode of sonication provided an advantage over continuous sonication, but the selection of pulse and interval lengths was extremely important of the efficiency of the application.

5.2. Ozonation

This section covers contents of the manuscript entitled “Destruction of Bisphenol-A in Water by Ozonation” that was submitted in October 2007 and is currently under review.

5.2.1. Background

Bisphenols are among the most common synthetic EDCs, and the prototype is bisphenol A, which is widely used in the production of polycarbonate and epoxy resins, unsaturated polyester-styrene resins and flame retardants (Fromme et al., 2002). The estrogenic potency in vitro is 10^{-3}-10^{-4} relative to that of estradiol, and $4x10^{-4}$-10^{-5} in vivo relative to that of diethylstilbestrol (Jintelmann et al., 2003). BPA also induces acute toxicity to a number of marine and freshwater species such as shrimps and minnow; and water flea and green algae in the range of 1-10 mg L^{-1}, respectively (Alexander et al., 1988).

BPA is accumulated in surface waters by industrial wastewater discharge from plastics-producing plants, domestic sewage and leaching from landfill sites that contain large quantities of plastics (U.S. EPA, 2001b; Crain et al., 2007). The concentration of BPA in surface waters varies by location, as 0.0005-0.41 μg L^{-1} is the range reported in Germany (Fromme et al., 2002) and 12, 19, 21 μg L^{-1} are the maxima detected in USA, Japan and the Netherlands (Kolpin et al., 2002; Belfroid et al., 2002), respectively. The concentration range reported for hazardous waste landfill leachate is 1.3-17200 μg L^{-1}, while that in sediments is 0.01-0.19 mg kg^{-1} (Yamamoto et al., 2001; Fromme et al., 2002).

Ozonation is a common advanced oxidation technique for the removal of recalcitrant organic compounds in water as well as for disinfection, decolorization and detoxification purposes (Alvares et al., 2001; Alaton and Caglayan, 2006; Anotai et al., 2006).

The aim of this study was to investigate the degradability of bisphenol A in water by ozonation to identify the operation parameters, the mass transfer and reaction rate constants, mineralization efficiency and the oxidation byproducts. The work is aimed to

fulfil the gap in the literature on identification of the intermediate products and assessment of the overall degradation or mineralization process.

5.2.2. Experimental

Experiments were carried out in a closed semi-batch reactor (BCOz), as described previously. The mass flow rate of the gas mixture (O_2/O_3) was 0.15 $m^3 h^{-1}$ in all runs. Test solutions of 2000 mL were prepared by dilution of a formerly prepared stock solution with ultra-pure milli-Q water. All samples were originally slightly acidic (pH=6.0) and ozonated without buffering except when the effect of pH on mineralization was tested. Reactor samples were collected within frequent intervals for analysis of BPA, dissolved ozone and total organic carbon. The mass transfer rate of ozone was estimated by injecting a constant flow of gaseous ozone into milli-Q water initially at pH 6 and monitoring the aqueous ozone concentration over time. The overall degradation or mineralization of BPA and the impact of pH were assessed by monitoring the total organic carbon residual at pH 3, 6 and 11 during 60 min ozonation. In all cases, the residual ozone in effluent samples was quenched by the addition of sodium thiosulfate.

5.2.3. Results and Discussion

5.2.3.1. Effects of BPA Concentration and the Contact Time. Aqueous solutions of 22, 44, 88 and 176 μM BPA were ozonated for 30 min at an oxygen flow rate of 2.5 L min^{-1} yielding an influent gaseous ozone concentration of 1.62 g m^{-3} (4.05 mg min^{-1}), and the disappearance of BPA was assessed by monitoring the residual BPA and UV-visible spectra of the samples that were withdrawn from the reactor within 1 min intervals. Although the selected test concentrations are higher than the range reported for fresh water systems, similar and larger values are found in wastewater streams originating from BPA producing and consuming facilities, as well as in landfill leachate (Yamamoto et al., 2001). Moreover, the test concentrations here are within the reported range in the literature for ozonation of BPA in water (0.002 μM-400 μM).

It was found that the rate of reaction followed pseudo-first order kinetics with rate constants of 0.71, 0.66, 0.45 and 0.27 min^{-1} for 22, 44, 88 and 176 μM BPA, respectively.

The data are plotted in Figure 5.10. The inset at the top right corner represents the UV spectrum of 44 μM BPA before and during ozonation.

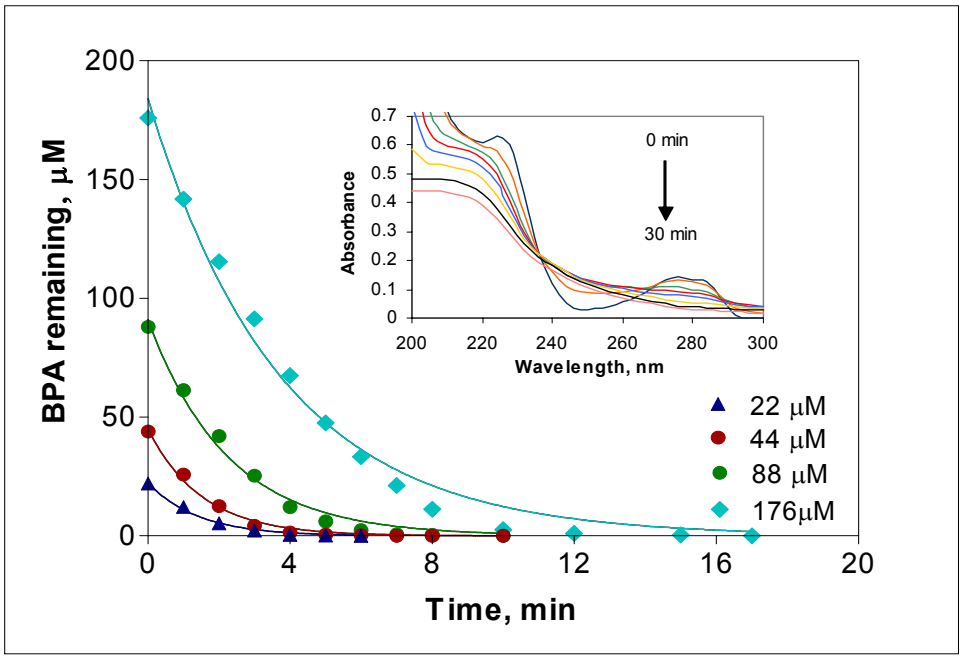

Figure 5.10. Effect of concentration on the rate of BPA decay by ozonation at 4.05 mg min^{-1}. The inserted plot shows absorption abatement in UV band (200-300 nm) of 44 μM BPA during 30 min ozonation.

5.2.3.2. Ozone Addition. Ozone was added to a solution of 44 μM BPA at 1.62, 2.56, 3.18 and 4.12 g m^{-3} of gaseous ozone inlet concentrations, which corresponded to addition rates of 4.05, 6.40, 7.95 and 10.30 mg min^{-1}, respectively. The degradation of BPA at each condition is presented in Figure 5.11 in normalized concentration against time. In all cases, pH declined rapidly to 4.0 within the first 2 min and remained relatively stable thereafter. The pseudo-first order reaction rate constants increased linearly with increasing rates of ozone addition, as shown by the inset at the top right corner of the figure. It was found that complete conversion of BPA in each case (at ozone addition rates of 4.05, 6.40, 7.95 and 10.30 mg min^{-1}) was accomplished at specific ozone doses of 2.01, 1.90, 1.58 and 1.51 mg/mg BPA, respectively.

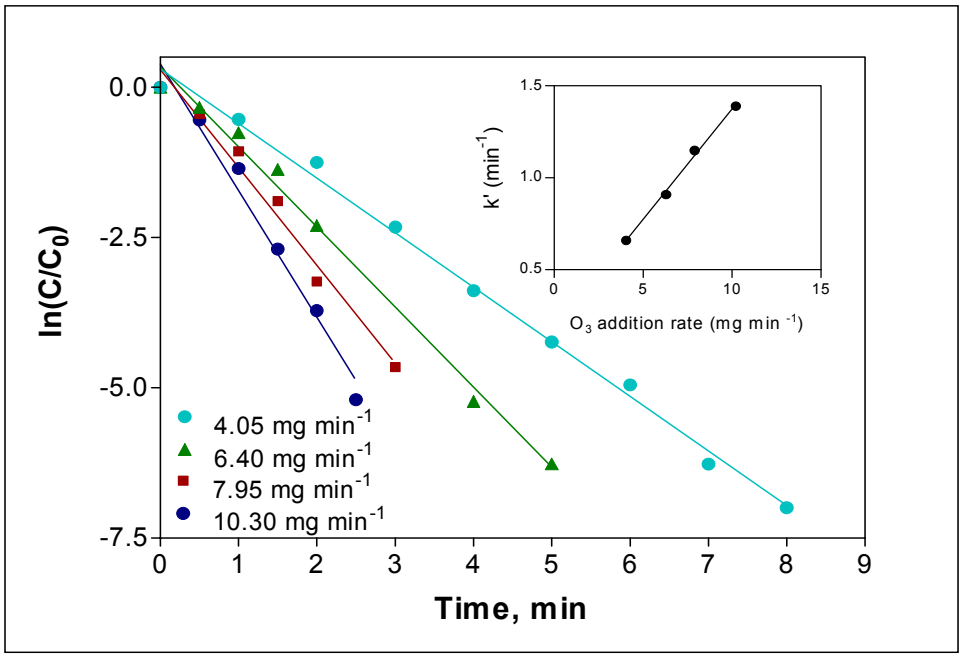

Figure 5.11. Effect of ozone addition rate on the decomposition of BPA (pH_0=6, C_0= 44 μM).

Based on the fact that the rate of oxidation in ozonated solutions is limited by the mass rate of ozone transfer in solution, we estimated the mass transfer rate coefficient of ozone in milli-Q water at 20°C and pH=6.0 (which remained constant for the first 7 min) during 60 min ozonation at a constant ozone addition rate of 4.05 mg min^{-1}. The variation of aqueous ozone concentration in the test solution is presented in Figure 5.12. It was found that during the first 10 min the concentration of O_3 inclined steeply; between 10 and 20 min the inclination was slow; and with further addition it began to stabilize, reaching ultimately an average value of 0.74 mg L^{-1}. The mass transfer rate coefficient (K_La) was estimated by linear regression analysis of 7-min data of $ln[(C^*-C_t)/C^*]$ and time, where C^* is the observed maximum concentration of ozone at 20°C and C_t is the observed ozone concentration at time t. The result of regression analysis is given Figure 5.13. The value of K_La in the specified conditions was estimated as 0.25 min^{-1}.

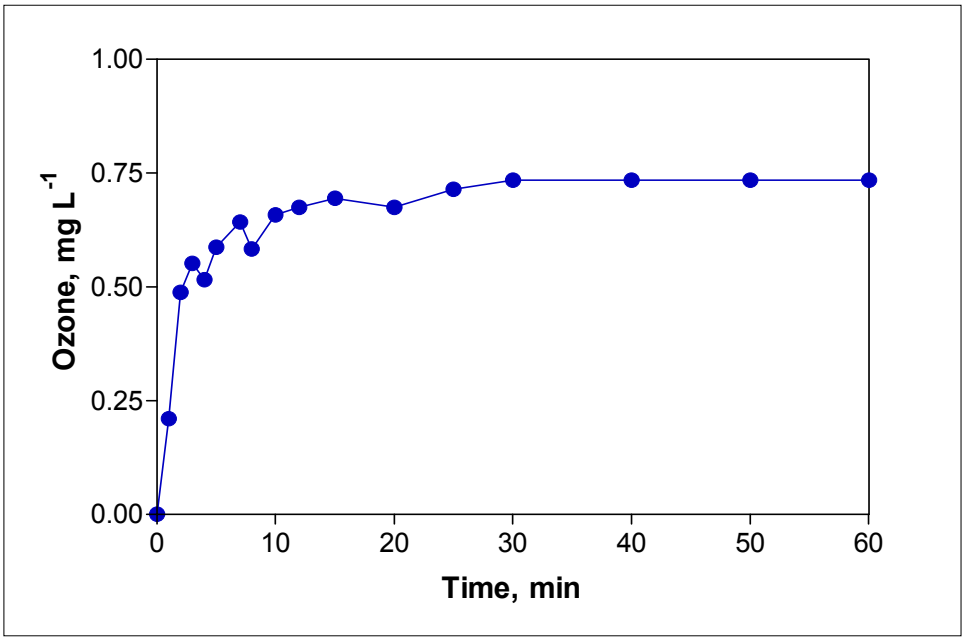

Figure 5.12. Stabilization of ozone in milli-Q water at pH=6.0 during 60 min ozonation at 4.05 mg min^{-1}.

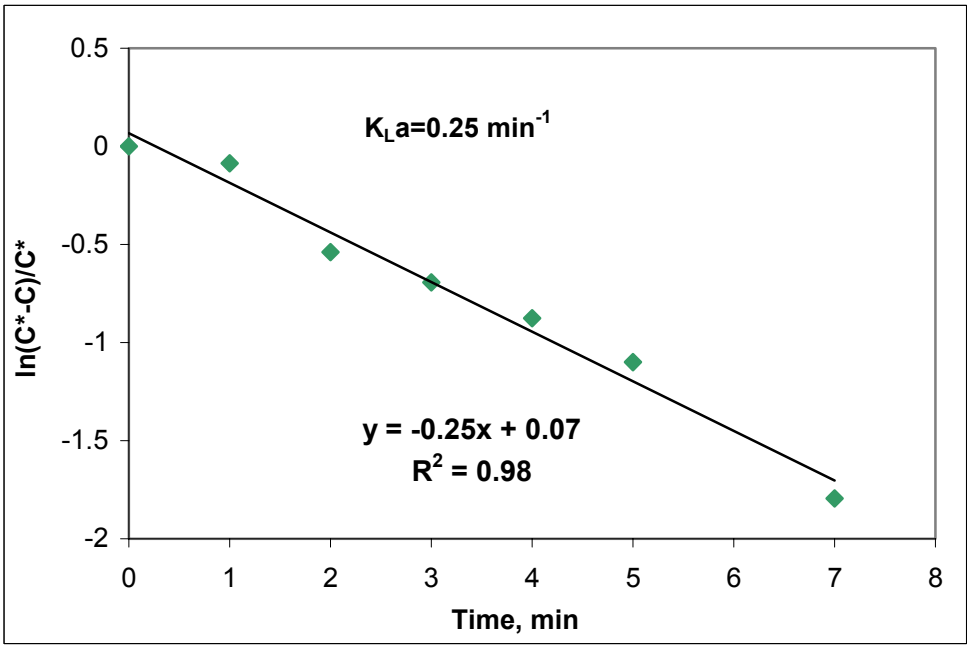

Figure 5.13. Estimation of ozone mass transfer rate coefficient.

We found that unlike the trend in pure water, the concentration of ozone in solutions of BPA increased during initial contact and stabilized at 0.05 mg l^{-1} during t =1-3 min. It was after the 4th min of contact when more than 90 % of BPA was decomposed that ozone began to accumulate in solution. Comparative variations in concentrations of ozone and BPA concentrations are presented in Figure 5.14.

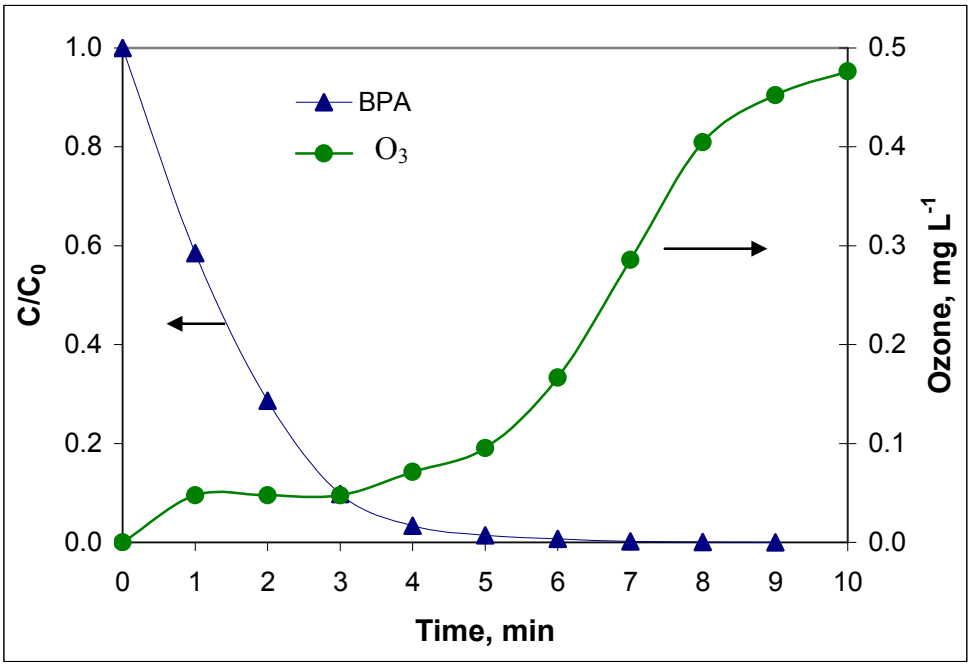

Figure 5.14. Comparative profiles of BPA decay (C_0=44 μM) and ozone accumulation during 10 min ozonation at 4.05 mg min^{-1}.

5.2.3.3. Reaction Kinetics. Oxidation of BPA with ozone at non-alkaline solutions and the rate of oxidative decomposition may be simply described by Equations 5.12 and 5.13, respectively:

$$BPA + O_3 \rightarrow P_{oxid} \qquad (5.12)$$

$$r_{BPA} = -\frac{d[BPA]}{dt} = k_{BPA-O_3}[O_3][BPA] = k'[BPA] \qquad (5.13)$$

where P_{oxid} is a generic term to represent the oxidation byproducts, r_{BPA} or d[BPA]/dt is the rate of reaction or the time rate of BPA decay (M s^{-1}), k_{BPA-O3} is the bimolecular rate constant of BPA with ozone (M^{-1} s^{-1}), k' is the pseudo-first order BPA degradation rate coefficient (s^{-1}) and [O_3], [BPA] are molar concentrations of aqueous ozone and BPA at time t, respectively (M). A more accurate rate expression would also include terms related to the reactions of OH radicals that form upon the decomposition of ozone and CO_3 species that form upon mineralization of organic matter (there was no contact with air to allow atmospheric dissolution of CO_2). On the other hand, Equation 5.13 can provide a fairly good estimate of the bimolecular rate constant (of BPA with ozone) provided that the following are true: i) the rate of O_3 formation/consumption is at steady state; ii) the solution is not deficient in BPA and the rate of BPA oxidation is relatively slow; iii) the solution is acidic and the rate of OH radical formation can be neglected; iv) the rate of ozone scavenging is insignificant.

The first and second conditions were satisfied between t=1-3 min, at which the concentration of ozone was very stable (as was shown in Figure 5.14), the rate of reaction of BPA was slow and there was sufficient BPA in solution. We assumed that the third condition was also satisfied within the same time period, because the solution pH reached a value of 4.0 at t=2 min. Finally, the last condition is fairly satisfied based on the fact that mineralization at early contact is extremely slow and the conditions are highly acidic to prevent sufficient formation of carbonate species, which may consume some of the ozone.

In accordance, the bimolecular rate constant was estimated by Equation 5.13 (using 9.92×10^{-7} M for [O_3] and 0.011 s^{-1} for k') as 1.11×10^4 $M^{-1}s^{-1}$, which is in good agreement with the value reported in the literature for pH 2 (1.3×10^4 $M^{-1}s^{-1}$); and in fair agreement with that for 2.5<pH<5.0 (2.3-5.5$\times 10^4$ $M^{-1}s^{-1}$) (Lee et al., 2003; Deborde et al., 2005). On the other hand, our estimated value is more than one order of magnitude smaller than that reported for pH 6 (4×10^5 $M^{-1}s^{-1}$), two orders of magnitude smaller than that for pH 7 (1-10$\times 10^6$ $M^{-1}s^{-1}$), and 5 orders of magnitude smaller than that for pH 12 (1.6×10^9 $M^{-1}s^{-1}$) (Deborde et al., 2005; Huber et al., 2003; Lee et al., 2003), signifying the enormous impact of pH elevations on acceleration of ozone reactions.

5.2.3.4. Mineralization and pH Effect. The overall degradation of BPA was monitored by the degree of mineralization during 60 min ozonation initiated at pH=3.0, pH=6.0 and pH=11.0. The data are presented in Figure 5.15. It was found that mineralization was most rapid at pH 6, but only during the first 10 min of contact when BPA was not completely converted. The process was significantly slowed down with further contact most likely due to the competition and lower reactivity of the byproducts with molecular ozone. On the other hand, the largest degree of mineralization after 60 min ozonation was accomplished by ozonation at pH 11, although the initial rate was slower than that observed at pH 6. The enhancement is a consequence of rapid decomposition of ozone and the formation of excess OH radicals, which must have reacted with the intermediate products (of BPA oxidation) more readily than ozone. The slower rate of mineralization during the first 10 min (than that at pH 6) can be attributed to: i) the larger concentration of CO_3 radicals that may consume a significant fraction of OH radicals and ii) the likely preference of BPA for electrophilic reactions by ozone over cyclo-addition reactions by •OH. Finally, total mineralization was lowest at pH 3 owing to the extreme stability of ozone in this condition. Relative fractions of mineralization after 60 min ozonation at initial pH levels of 3, 6 and 11 were 17%, 25% and 35%, respectively.

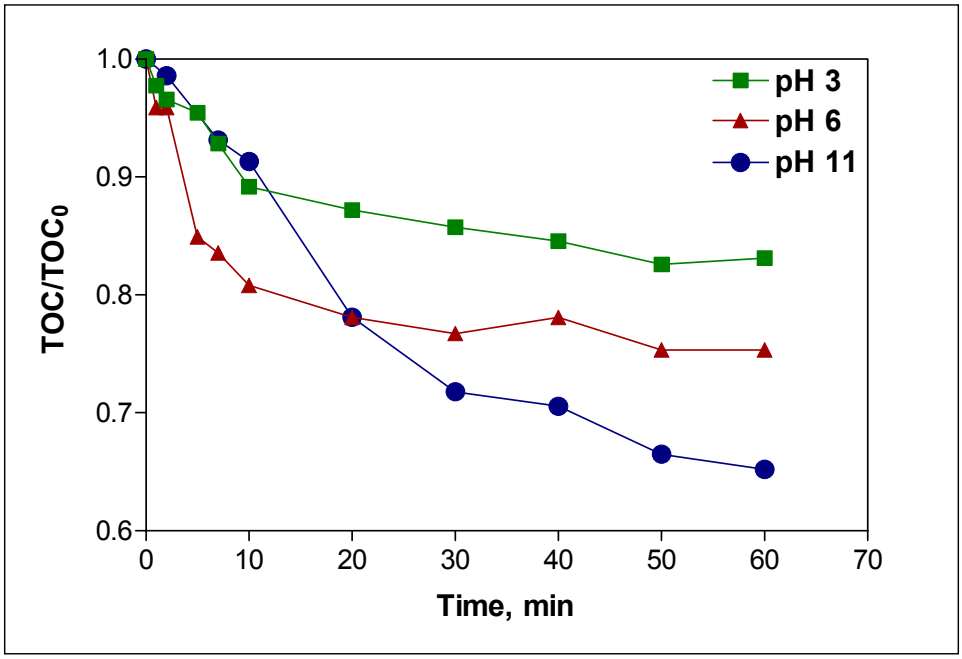

Figure 5.15. Normalized plots of residual TOC at acidic, near-neutral and basic pH (BPA_0 = 44 μM, O_3 = 4.05 mg min^{-1}).

5.2.3.5. By-product Analysis. The intermediate products of BPA oxidation were investigated in test samples of 440 μM (10 times more concentrated than the working concentration) to assure the formation of detectable and identifiable peaks. Samples (initial pH=6) were ozonated for various time periods to generate different effluents for GC-MS. The chromatograms corresponding to 0 and 60 min ozonation are presented in Figure 5.16. It was found that the main fragment (m/z) of BPA was 228, and those of the intermediates were as listed in Table 5.6 together with their relative abundance and identities obtained from spectra libraries.

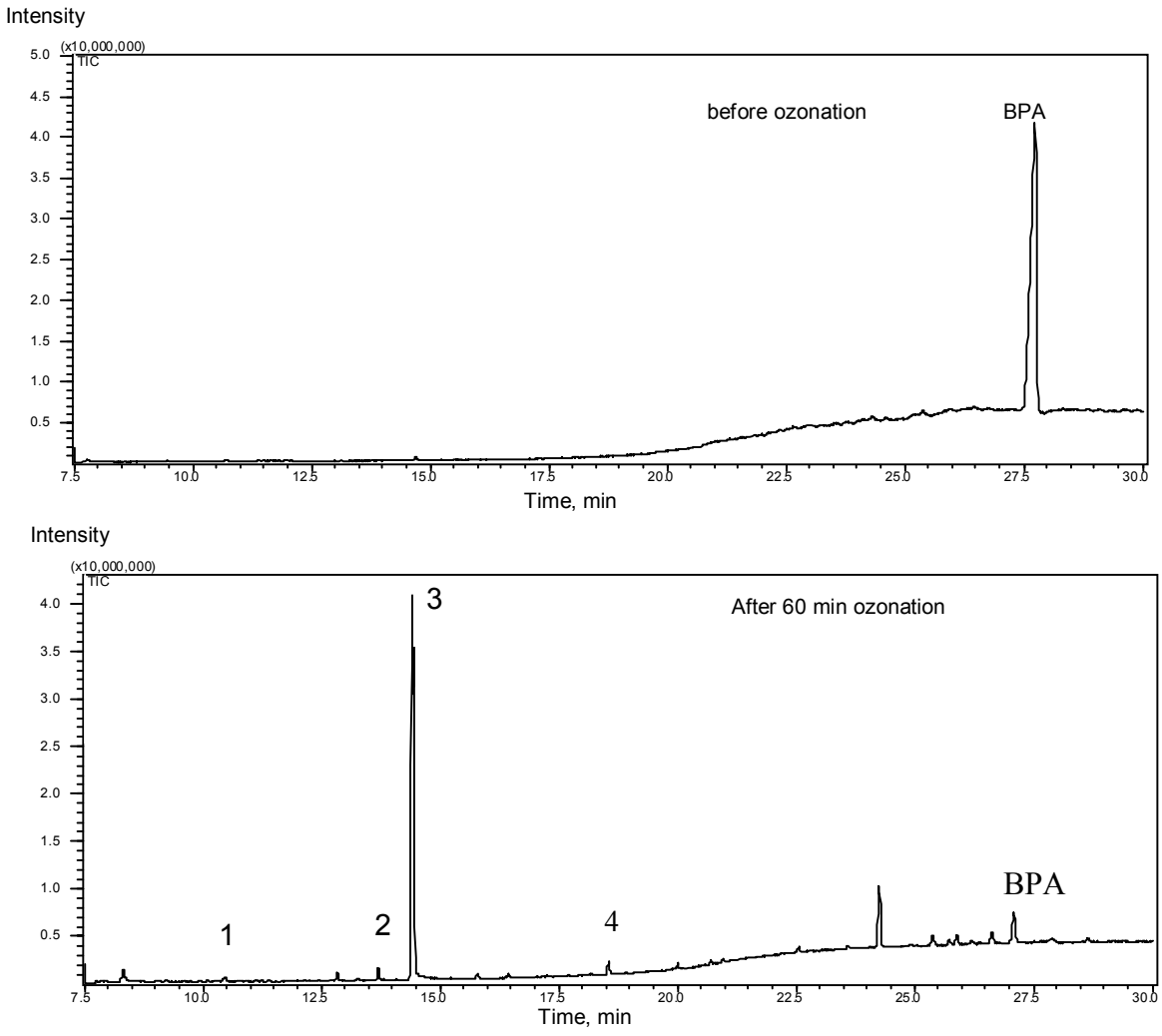

Figure. 5.16. GC-MS chromatograms of 440 μM BPA before and after 60 min ozonation at pH=6. The labeled peaks are those that could be identified by the spectral library.

In the 60th min effluent, the first product (Peak 4) with m/z=135 was identified as p-tert-butylphenol. The next one (Peak 3) with highest intensity and m/z=134 was 2-methyl-2,3-dihydrobenzofuran, which was detected by other researchers in the oxidation of BPA by photo-fenton process (Katsumata et al., 2004). Finally, two additional peaks detected at m/z=110 and m/z=116 were identified as hydroquinone and n-butyl-acetate, respectively.

Table 5.6. Main fragment analysis (m/z) and relative abundances (%) of the oxidation by-products of BPA.

Peak name	Retention time	By-product	m/z (% abundance)
1	10.44	 n-butyl-acetate	116 (<1%), 43(100)
2	13.70	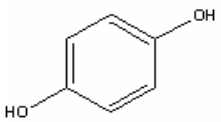 hydroquinone	110(100)
3	14.44	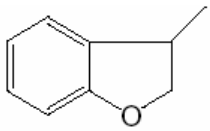 2-methyl-2,3-dihydrobenzofuran	134(100), 119(85), 91(40)
4	18.55	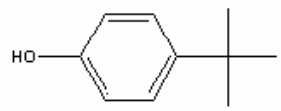 p-tert-butylphenol	150(<1%), 135(100), 107(42)
BPA	27.09	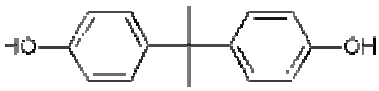	228(12), 213(100), 119(27)

As a result, we propose that the oxidation of BPA by ozone at acidic pH proceeds in the following sequence: i) formation of p-tertbutylphenol; ii) formation of hydroquinone, leading to phenols by the loss of a –OH group (phenols were not detected probably because their formation and conversion occurred very shortly); iii) formation of methylbenzofurans; and iv) loss of aromatic properties leading to the formation of n-butyl acetates. Literature survey of the identified by-products revealed that none of them were classified as endocrine disruptors.

5.2.4. Conclusions

The study has shown that bisphenol A originally at pH=6 was totally oxidized by 10 min ozonation at 4.05 mg O_3 min^{-1}. The rate of oxidation was pseudo-first order and accelerated by increasing rates of ozone addition and decreasing concentrations of BPA input. The bimolecular rate constant was estimated by ignoring the reaction of OH radicals based on the observation that the solution became acidic during initial contact and the concentration of OH radicals is negligible at such. The estimation was made for a specific condition, where the concentration of dissolved ozone was constant, the rate of reaction was slow and there was sufficient amount of BPA in solution. The estimated value of the rate constant ($1.11x10^4$ $M^{-1}s^{-1}$) was in good agreement with the values reported for acidic pH levels, but much lower than that reported for pH 12, as a consequence of reduced reactivity of ozone at acidic pH. The mineralization process was also pH dependent and increased considerably when ozonation was initiated at pH 11, showing the preference of the intermediate by-products for addition reactions by OH radicals over electrophilic reactions with ozone. Finally, the by-products of oxidation in successive order of formation were p-tert-butylphenol; hydroquinone; methyl-dihydrobenzofuran and n-butyl acetate, and none of them are classified as endocrine disruptors.

5.3. Combined Ultrasound and Ozone Application

This section covers a study of ozone-ultrasound combination in reactor USOz to assess the improvement in ozone-mediated elimination of BPA by ultrasound. The results of this study were presented in the COST D32 workshop in Dundee in June 2007.

5.3.1. Background

Research has shown that combined operation of sonolysis and ozonation renders synergistic effects in organic matter destruction (Olson and Barbier, 1994, Kang and Hoffmann, 1998, Gültekin and Ince, 2006). The synergy is partly due to excess hydroxyl radicals formed upon thermal decomposition of ozone in the gas phase (Reactions 5.14-5.15) and partly to increased mass transfer of ozone in solution by mechanical effects of ultrasound (Olson and Barbier, 1994, Kang and Hoffmann, 1998):

$$O_3 +))) \longrightarrow O_2(g) + O(^3P)(g) \quad (5.14)$$

$$O(^3P)(g) + H_2O\,(g) \longrightarrow 2{\bullet}OH \quad (5.15)$$

5.3.2. Experimental

Experiments were carried out in USOz. Test solutions of 100 mL were prepared from the BPA stock using ultra pure milli-Q water. The concentration of BPA in all runs was 10 μM. Ozone was generated electrically from dry pure oxygen at a flow rate of 0.75 L min^{-1} yielding an ozone output concentration of 2 g m^{-3} O_2.

5.3.3. Results and Discussion

5.3.3.1. Rate of BPA Removal. The rate of BPA removal by combined ultrasound and ozonation was pseudo-first order at all pH test levels (pH= 3, 6 and 10.5). The profiles of BPA decay with varying pH in single ultrasound and combined ultrasound-ozonation schemes are presented in Figure 5.17. Comparative estimates of the first order rate constants at each test pH are listed in Table 5.7.

The results showed that addition of ozone at pH 3 was not effective although ultrasound increases the mass transfer rates of gases into solution. Thus, the inefficiency was due to the stability of ozone at acidic pH and to its potential to scavenge some of the OH radicals generated by ultrasound. At pH 6, the rate of BPA decay increased by 1.33 fold due to larger decomposition of ozone to yield additional oxidizing species such as peroxyl, superoxide and hydroxyl radicals. At pH 10.5, the relative rate of BPA removal was 14.4 times larger than that in ultrasound alone as a consequence of its priority to decompose.

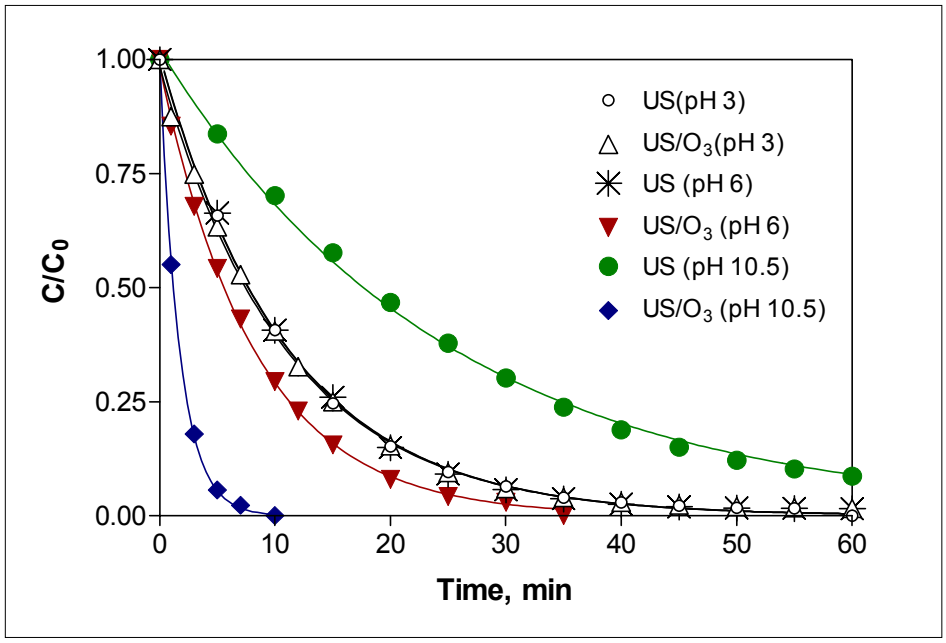

Figure 5.17. Comparative rates of BPA decay by single ultrasound and combined ultrasound-ozonation at pH 3, 6 and 10.5 (BPA=10 µM, O_3=2 g m^{-3}).

Table 5.7. Comparison of BPA degradation rate constants in ultrasound and ultrasound/ozone combined application.

pH	k'x10^{-2}, min^{-1}	
	US	US/Ozone
3.0	9.14±0.13	9.08±0.13
6.0	9.18±0.16	12.18±0.18
10.5	4.05±0.07	58.14±0.76

5.3.3.2. Sonochemical Product Yield. The effect of ozone addition to the ultrasonic reactor was also evaluated by comparing the relative sonochemical product yields. The results are presented in a bar chart in Figure 5.18 for three pH levels. The values correspond to the yields obtained in 10 min reaction time, because the concentration of BPA could not be detected at longer contact times of combined operation at pH 10.5. Comparative estimates of product yields at each test pH are listed in Table 5.8. We found that maximum product yield was attained at pH 10.5 in ultrasound/ozone combined system.

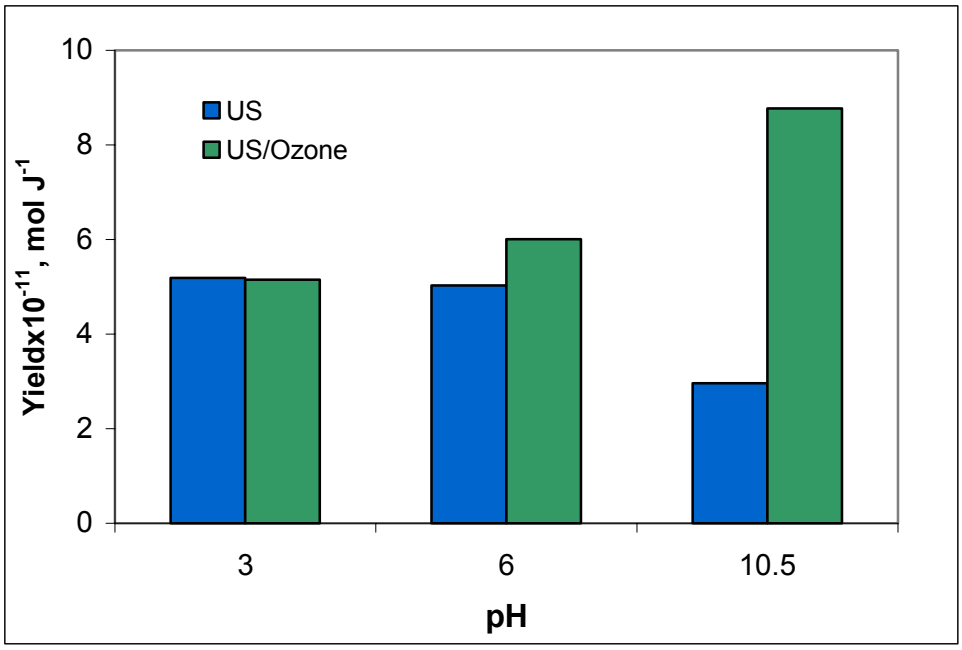

Figure 5.18. Variation of 10-min product yield with pH in ultrasound and ultrasound/ozone systems.

Table 5.8. Comparative sonochemical product yields in single ultrasound and ultrasound/ozone combined applications.

pH	10-min sonochemical yield $x10^{-11}$, mol J^{-1}	
	US	US/Ozone
3.0	5.19	5.15
6.0	5.03	6.00
10.5	2.96	8.77

5.3.4. Conclusions

It was found that injection of ozone at a flow rate of 0.75 L min^{-1} to an ultrasonic reactor (US2) at pH 10.5 produced a synergistic effect as a consequence of generation of excess reactive species by aqueous and thermal decomposition of ozone coupled with enhanced mass transfer of gaseous ozone to the solution.

6. NONYLPHENOL

This chapter covers contents of the manuscript "Ultrasonic degradation of nonylphenol in water: impacts of operating parameters", which was submitted in March 2008 and is currently under review.

6.1. Background

Alkylphenols (AP) comprise one of the most important groups of synthetic EDCs and are of particular interest due to their widespread occurrence in the environment as AP or alkylphenol polyethoxylates (APEO). The presence of APs and their ethoxylated forms in the environment is due to municipal/industrial effluent discharge following incomplete/inefficient degradation in conventional treatment processes. Runoff from terrestrial sources by application of sewage or industrial sludge is also a significant source of AP in aquatic systems (Canadian Council of Ministers of the Environment, 2001).

The majority of research on APEO and AP destruction in the water environment is focused on nonylphenols (NP), which enter the environment directly through wastewater streams or indirectly with NPEOs. Under anaerobic conditions such as those found in sewers, sediments and bio-treatment operations, NPEO is rapidly oxidized to NP, which is quite stable in natural systems and exhibits aquatic toxicity and estrogenic activity (Comber et al., 1993; McLeese et al., 1981; Soto et al., 1995). It is also reported that NPs stimulate the growth of human MCF-7 cell lines (Soto et al., 1991) and the production of vitellogenin by some rainbow trout (Jobling and Sumpter, 1993; Flouriot et al., 1995), and cause reproductive disorders in aquatic invertebrates and fish (Jobling et al., 1996).

Ultrasonic irradiation of liquids is a promising advanced oxidation technique for the elimination of refractory organics by which hydroxyl radicals are produced from the thermal fragmentation of water molecules. Addition of chemical reagents (e.g. ozone, Fe^{2+}, Cu^{2+}), UV light and solid particles has been demonstrated to enhance the efficiency of sonochemical decay processes (De Visscher and Van Langenhove, 1998; Entezari et al., 2003; Tezcanli-Guyer and Ince, 2004; Ku et al., 2005; Kim et al., 2007). When the reagent

is Fe^{2+}, a series of chain reactions typical of the Fenton process occurs to yield hydroxyl and peroxyl radicals from the reductive cleavage of H_2O_2 (Walling, 1975; Neyens et al., 1996):

$$H_2O +))) \rightarrow \bullet OH + \bullet H \quad (6.1)$$

$$\bullet OH + \bullet OH \rightarrow H_2O_2 \quad (6.2)$$

$$Fe^{2+} + H_2O_2 \rightarrow Fe^{3+} + \bullet OH + OH^- \quad (6.3)$$

$$Fe^{3+} + H_2O_2 \rightarrow Fe^{2+} + \bullet HO_2 + H^+ \quad (6.4)$$

$$Fe^{3+} + \bullet HO_2 \rightarrow Fe^{2+} + H^+ + O_2 \quad (6.5)$$

Similar effects are accomplished in the presence of Cu^{2+} through a "Fenton-like" process involving the reduction and oxidation of the metal by ultrasound-generated H_2O_2 and the production of peroxyl and hydroxyl radicals (Entezari et al., 1994; Skoumal et al., 2006):

$$Cu^{2+} + H_2O_2 \rightarrow Cu^+ + \bullet HO_2 + H^+ \quad (6.6)$$

$$Cu^+ + H_2O_2 \rightarrow Cu^{2+} + \bullet OH + OH^- \quad (6.7)$$

$$Cu^{2+} + \bullet HO_2 \rightarrow Cu^+ + O_2 + H^+ \quad (6.8)$$

The aim of this study was to investigate the following issues regarding the sonochemical destruction of 4-n-nonylphenol (4-NP) in water: i) the operating parameters as contaminant concentration, sparge gases, frequency and pH; ii) the reaction sites (as the bulk solution and the bubble-liquid interface) and pathways (as •OH-mediated oxidation, thermal reactions and hydrolysis); iii) the impacts of chemical reagent addition as Na_2CO_3, tertiary butyl alcohol, ferrous sulfate and copper sulfate.

6.2. Experimental

The majority of the experiments were carried out in US1 where the power density was 0.46 W mL^{-1}. In addition, some experiments were run in US3 where the power density was 0.23 W mL^{-1}. The physical properties of 4-NP were reported as follows: MW= 220.35 g mol^{-1}, pKa=10.7, $p_i = 7.1x10^{-7}$ atm (Boublik et al., 1984), solubility = 5.43 mg l^{-1} (Ahel

and Giger, 1993a), log K_{ow} = 4.48 (Ahel and Giger 1993b). The concentration of 4-NP and the pH in all test solutions was 100 μM and 6.0, respectively except in those experiments carried out to study the effect of concentration, pH and divalent cations on the rate of NP decay. Impacts of pH and sparge gas were examined by sonication of the test solutions in US1 at pH 3.0, 6.0 and 10.8 and by continuous bubbling of the test solutions with argon, air or oxygen. Samples were also sonicated in US3 at acidic and alkaline pH to investigate the effect of frequency. Impacts of Fe^{2+} and Cu^{2+} were tested in US1 by sonicating the test solutions in presence of 0.01, 0.05, 0.1, 0.25, and 0.5 mM Fe^{2+} and 0.005, 0.01, 0.05, 0.1, 0.25 and 0.5 mM Cu^{2+} at pH 3 without the addition of H_2O_2. The experiments were repeated by adding increasing doses of H_2O_2 to maintain H_2O_2/Fe^{2+} and H_2O_2/Cu^{2+} molar ratios of 10:1, 20:1, 40:1 and 10:1, 20:1, respectively. The effect of aqueous phase OH radical scavenging by CO_3^{-2} was investigated in US1 in presence of 5 mM Na_2CO_3 and that of interfacial OH scavenging was studied in both reactors by the addition of 1 mM t-butyl alcohol.

6.3. Results and Discussion

6.3.1. Impact of Concentration

Oxygen-saturated solutions of 4-NP at 40, 100, 220 and 480 μM were sonicated in US1 for 45 min under continuous O_2 injection while monitoring the residual concentration of the compound within short intervals. The data is presented in Figure 6.1. Concentration-time data showed that the rate of 4-NP decay was pseudo-first order and thus the apparent rate constants were estimated by equation 6.9, where k' is the pseudo 1st order rate constant (min^{-1}), t is the sonication time (min), C_0 and C are the concentrations of 4-NP at time zero and t, respectively.

$$\ln\left(\frac{C}{C_0}\right) = -k' t \qquad (6.9)$$

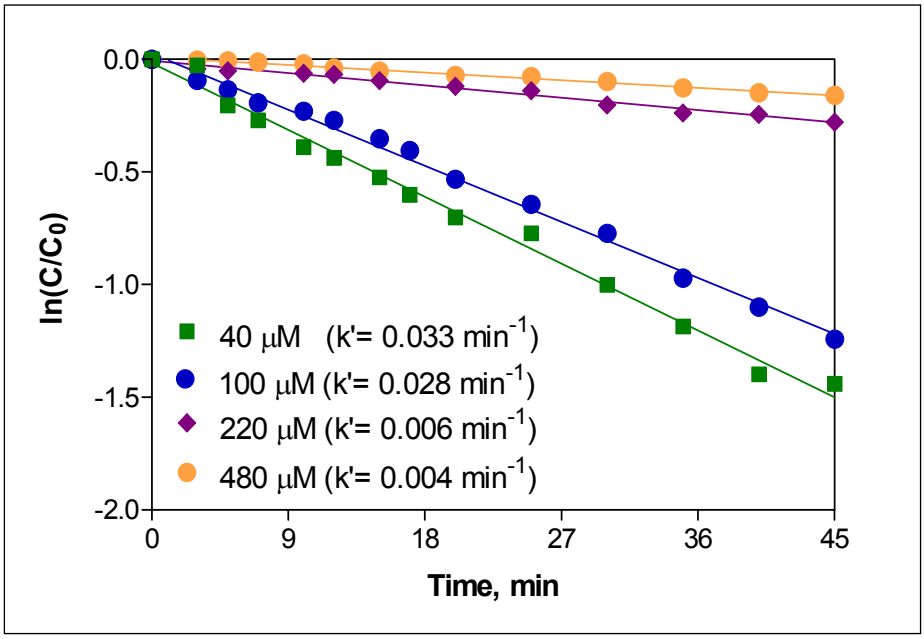

Figure 6.1. Impact of concentration on the decay of 4-NP during 45 min sonication in US1 and O_2 bubbling (0.25 l min^{-1}).

The exponential character of the rate implies that pyrolysis is a potential reaction pathway in the overall destruction of the compound, as was also reported in the literature regarding exponential reaction kinetics under ultrasonic destruction of organic contaminants (De Visscher et al., 1996; Vinodgopal et al., 2001). Otherwise, the reaction would have followed zero-order kinetics, since sonication time is a direct measure of the power density in solution.

The effect of concentration was further assessed in terms of the initial rate of 4-NP decomposition ($0 < t \leq 5$ min) and found that the rate reached a maximum at $C_0 = 100$ μM and reduced rapidly as the concentration was further increased (data shown in Figure 6.2). It was found that there were two distinct concentration regimes affecting the sonochemical decomposition rate of 4-NP: at $0<C_0\leq100$ μM the rate was steeply increased with concentration, while at $100<C_0\leq480$ μM it suffered a steep decrease. Such a relation reminds of saturating binding reactions that are characterized by a maximum at a critical concentration of the substrate and a decline above that level upon saturation of the binding sites.

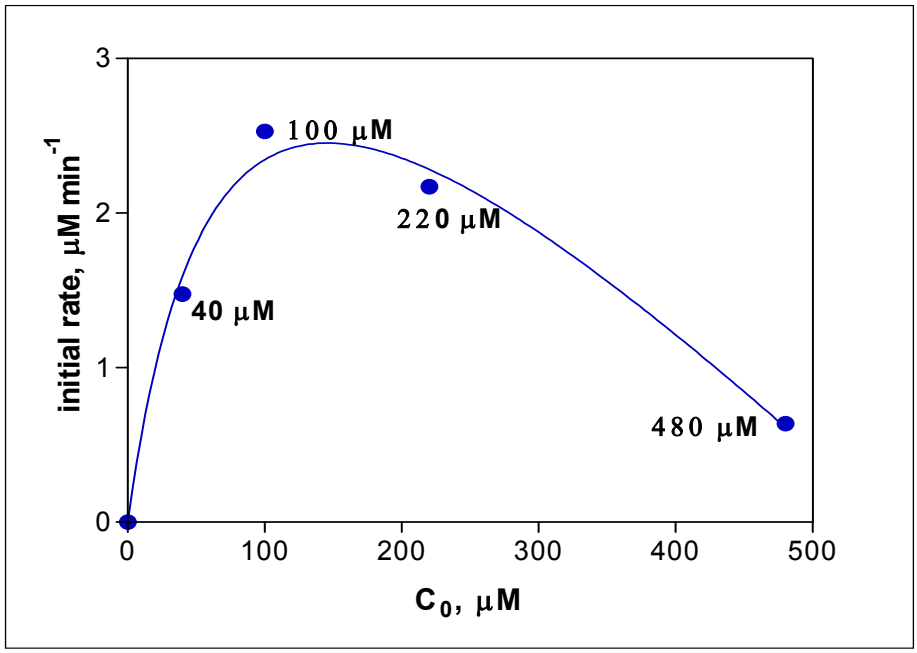

Figure 6.2. Variation of the initial rate of 4-NP decay with concentration.

Similar to this phenomenon is chemical/physical adsorption, where at equilibrium the sites of adsorption are physically saturated. Assuming that the bubble-liquid interface is a highly potential adsorption/reaction site in sonochemical reactions, the data in Figure 6.2 were fit (by Graphpad Prism, 2000) to the well-known Langmurian rate expression defined for heterogeneous reaction systems:

$$r = k\theta = \frac{kKC_0}{(1 + KC_0)} \qquad (6.10)$$

where: r is the rate of 4-NP decay, θ is the fraction of 4-NP in the interfacial surface to that in the bulk liquid, K is the Langmuir coefficient, C_0 is the concentration of 4-NP in solution at time zero and k is a proportionality constant.

The good fit of our data to Equation 6.10 (R^2=0.98) can be explained by the amphiphilic structure of 4-NP, characterized by a hydrophobic linear alkyl chain (log K_{ow} = 4.48) and a hydrophilic phenol moiety (log K_{ow}=1.46). This implies that while one end (the alkyl chain) of the compound readily turns towards the interfacial area for adsorption

at the interface, the other (phenolic part) tends to remain in the bulk solution. In that sense, the reaction is likely initiated by the adsorption of the nonyl tail at the gas-liquid interface and proceeds via: i) oxidation of the tail at the bubble-liquid sheath (where the concentration of OH radicals is very high); ii) cleavage of the covalent bond between the alkyl and phenol groups; iii) diffusion of the volatile oxidation byproducts into the cavity bubbles; and iv) oxidation of the phenol moiety in the bulk solution or the interface via radical reactions. Note that direct diffusion of 4-NP into the bubbles is unlikely due to its low volatility (P_i = 7.1x10^{-7} atm), which was verified in a 1-h silent control experiment open to the atmosphere, where no change in the concentration of 4-NP was recorded.

The sharp deceleration of the initial rate at higher concentrations (C_0>100 μM) must be the consequence of competitive adsorption upon reduced number of available adsorption sites and gradual saturation of the cavity surfaces leading to lower collapse temperatures (less violent collapse) and lower yield of OH radicals. It should also be noted that a fraction of hydrophilic compounds at relatively high concentrations may also reach the gas-liquid interface, thus further enhancing the degree of competition (Serpone et al, 1994; Kidak and Ince, 2006). This also explains why the initial rate of reaction was more rapid at C_0=100 μM than at C_0=40 μM during 0< t≤ 5 min, while the overall rate (0< t≤45 min) at C_0=100 μM was slightly slower; that some of the phenolic moieties at the higher concentration have migrated to the interfacial area after longer contact.

6.3.2. Effect of Saturating Gas

The effect of saturating gas was investigated by continuous bubbling of oxygen, argon or air at 0.25 L min^{-1}. The fraction of 4-NP remaining and the estimated apparent rate constants during sonication under different gas atmospheres is presented in Figure 6.3.

It was found that gases affected the rate of decomposition in the order: O_2>Ar>air. This finding contradicts that of Yim et al. (2003), who have reported that sonochemical rate (at 200 kHz) of 4-NP destruction under argon is larger than that under air or O_2 atmospheres. They attributed their result to the well-known effects of polytrophic gas ratio (γ) and thermal conductivity (σ). Values of γ and σ for argon, air and oxygen are respectively 1.67, 1.40 and 1.40; 179x10^{-4}, 259x10^{-4}, and 265x10^{-4} Wm^{-1}K^{-1}. In theory,

more extreme collapse conditions are expected in the presence of argon gas, which has the highest γ and the lowest σ compared to air and O_2. The more rapid reaction observed in this study under O_2 atmosphere despite its less favorable gas properties (than Ar) must therefore be explained by the formation of excess reactive species such as •O, •OH and $•HO_2$ that may react both with the phenolic component in solution and the nonyl chain at the interface. The fact that the rate was lowest under air atmosphere (despite similar gas properties as O_2) must be due to OH radical scavenging potential of the sonolysis products of nitrogen gas in or outside of a collapsing bubble, as was also reported in the literature (Hart and Henglein, 1986; Yim et al., 2003).

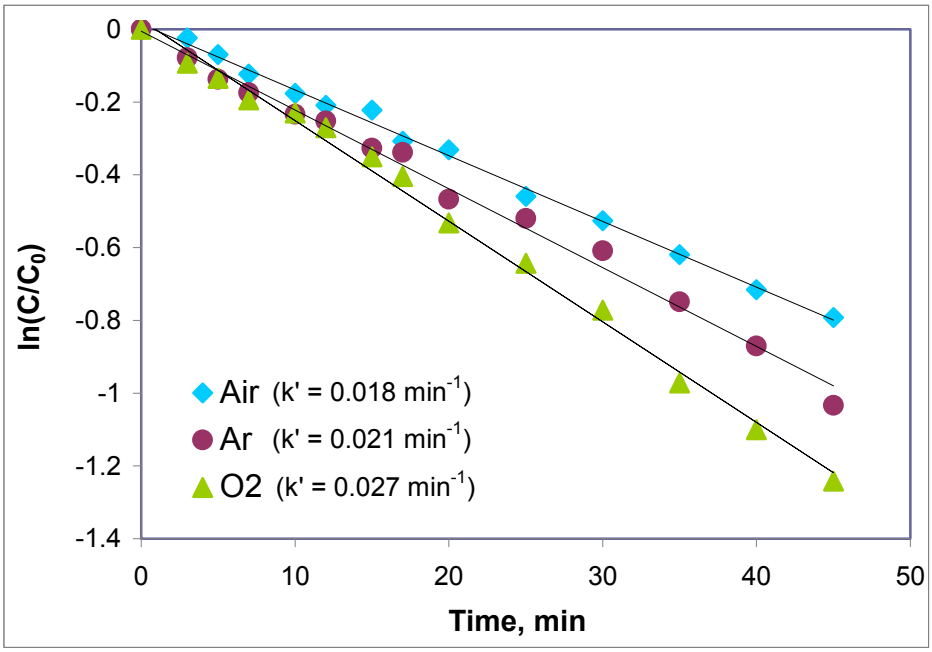

Figure 6.3. The impact of sparge gas on the rate of 4-NP destruction in US1 (C_0=100 μM, gas flow rate=0.25 L min^{-1}).

6.3.3. Effect of pH

The degradation of 4-NP at acidic, near-neutral and alkaline pH (3.0, 6.0 and 10.8) is presented in Figure 6.4. The data show that the rate of reaction was slowest at pH 6 and increased by 2.2-fold and 4-fold, respectively upon acidification (with H_2SO_4) and alkalinization (with NaOH). In the former, acceleration is due to enriched hydrophobicity of the phenolic moiety that eased its approach to the interfacial area, where the

concentration of OH radicals is much higher than that in the bulk solution (Petrier and Francony, 1997). In the latter case with NaOH, deprotanation of phenol-OH produces an anionic moiety (phenolate), which has a much higher preference to remain in the bulk solution than the uncharged moiety. Hence at pH 10.8, while one end (the strongly hydrophilic phenolate) pulls the molecule away from the negatively charged gaseous bubbles, the other (the strongly hydrophobic alkyl chain) is pushing it towards them. A major cause of the sharp acceleration of the reaction rate by alkalinization must be the outcome of these opposing forces acting at the two ends of the molecule. At such, the covalent bond connecting the two moieties are more rapidly cleaved and the alkyl group undergoes a faster decomposition, allowing more OH radicals to be available and releasing reactive species such as methyl and longer alkyl radicals (Yim et al., 2003) that may also contribute to the oxidation of the remaining molecule.

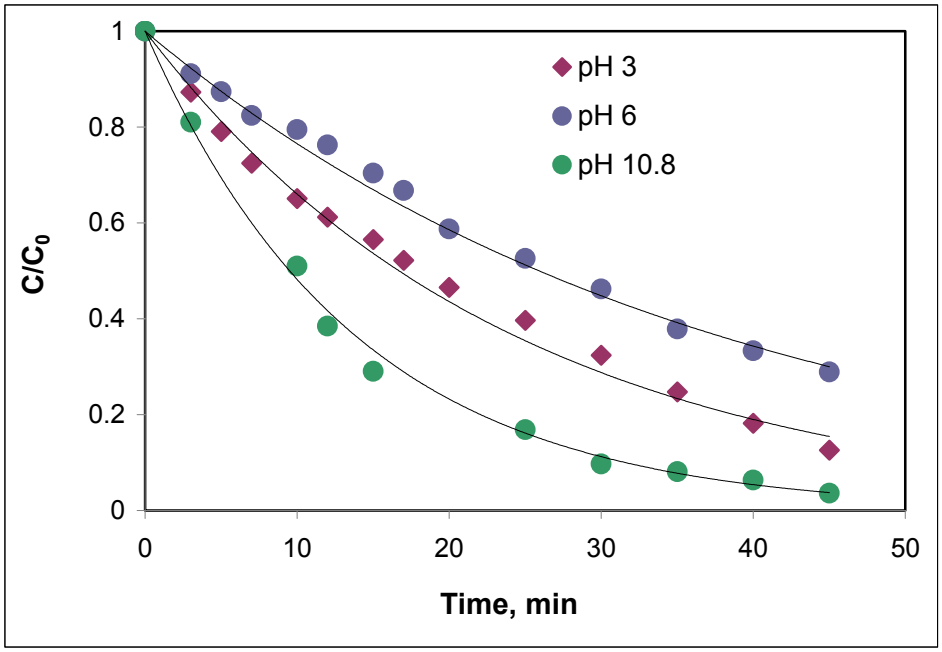

Figure 6.4. The effect of pH on the rate of 4-NP decay (C_0=100 μM) in US1 during O_2 injection at 0.25 L min^{-1}.

The GC chromatograms of the acidic and alkaline samples collected at various time intervals from the reactor were too complex to identify any decomposition byproducts, except for a single peak detected at a retention time of 14.54 min in both samples. The peak was identified as p-benzoquinone (p-BQ) and found to disappear more rapidly in the

alkaline samples sonicated longer than 30 min. The formation of BQ is a strong evidence of OH radical addition to the phenolic group following the cleavage of the alkyl chain and the production of hydroxyhydroquinone. Percent distribution of p-BQ in samples collected at 10, 30 and 45 min is given in Table 6.1. Faster decline of p-BQ after 30 min sonication at pH 10.8 verifies the above discussion that all or a large fraction the alkyl moiety has been decomposed by that time so that more OH radicals and other reactive species were available for the remaining components. Note that pH remained nearly constant throughout the sonication time in both solutions.

Table 6.1. pH-related distribution of p-BQ after 10, 30 and 45 min sonication of 4-NP.

Sonication time (min)	**% Benzoquinone**	
	pH 3	**pH 10.8**
10	100	100
30	50	45
45	28	12

Acceleration of 4-NP destruction in alkaline conditions may also be linked to the literature on sonolytic enhancement of hydrolysis reactions of some organic compounds in alkaline conditions (Thompson et al., 1953; Moon et al., 1979; Kristol et al., 1981). A group of researchers explained the enhancement by the existence of supercritical water (Hua et al., 1995), while others questioned it (Ando et al., 1998; Tauber et al., 1999b). More recently, it was demonstrated that sonolytic hydrolysis of phthalic acid esters was largely accelerated by alkaline pH with a 44°C increase in the reaction temperature compared to hydrolysis without ultrasound (Yim et al., 2002). In the same study it was suggested that accelerated hydrolysis may be due to the existence of a sphere (within the interfacial and the supercritical regions) in which a temperature higher than that in the bulk solution exists. In accordance, we may assume that the observed enhancement in the destruction of 4-NP by alkalinization does not only arise from the rapid cleavage of the covalent bond (as discussed above), but also from the dissipation of heat in the vicinity of collapsing bubbles that enhances the hydrolysis of the compound.

6.3.4. Assessment of the Reaction Sites

To assess the degradation pathway of 4-NP and the potential reaction sites, the role of OH radicals was thoroughly investigated via monitoring the rate of reaction in the presence of: i) effective sinks and sources of hydroxyl radicals in the bulk solution (e.g. carbonates and Fenton reagents, respectively); ii) effective sinks of hydroxyl radicals at the hot interfacial sheath (e.g. t-butyl alcohol).

6.3.4.1. The Bulk Solution.

Addition of Na_2CO_3. Based on the well known reactivity of carbonate species with OH radicals ($k=3.9\times10^8$ $M^{-1}s^{-1}$, (Buxton et al., 1988)), the concentration of 4-NP in the presence of 5 mM CO_3^{2-} was monitored during 45 min sonication in US1. The data are presented in Figure 6.5 together with two data sets corresponding to zero carbonates (at pH 6 and at pH=10.8 - adjusted with NaOH).

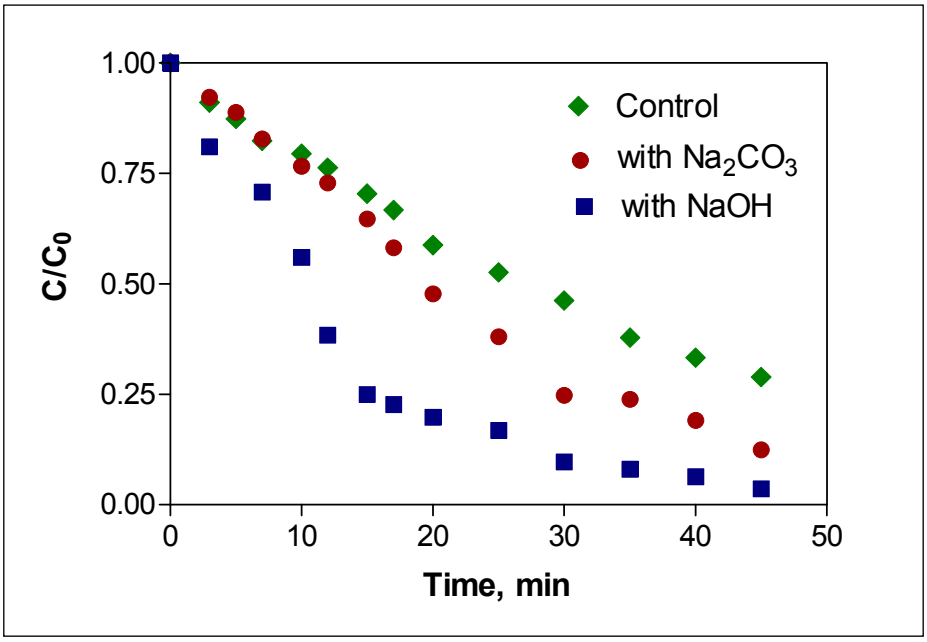

Figure 6.5. Degradation of 4-NP (C_0=100 μM) by ultrasound at basic pH adjusted with Na_2CO_3 (5 mM) and NaOH (1 mM OH^-).

It was found that the presence of carbonates did not affect the rate of 4-NP decay during the first 10 min, but accelerated it by 40% thereafter. Equal rates of decomposition at early sonication can be explained by either or both of the following: i) insignificant degree of competition for OH radicals at the applied CO_3^{2-} dose; ii) insignificant degree of OH radical ejection to the bulk solution at the applied frequency. As discussed in section 5.1.1 (bisphenol A sonication at 300 kHz), it was found that an equivalent concentration of carbonates led to 50 % suppression of the decomposition rate of the compound (Gultekin and Ince, 2008). The opposing trend observed here must be due to differences in the hydrophobicity and structural properties of the compounds as well as different frequencies, which dictate the conditions of collapse and the fate of OH radicals in sonochemical reaction systems. At 20 kHz irradiation, bubble-life time is at least two orders of magnitude longer than that at larger frequencies, so that a significant fraction of hydroxyl radicals react or recombine in the cavity bubbles or at the interfacial sheath before they can escape to the bulk solution. Hence, a moderate concentration of a hydroxyl radical scavenger in a solution irradiated by 20 kHz ultrasound would not reduce the rate of sonochemical decay of a hydrophobic compound, which exists and reacts mainly at the bubble-liquid interface.

The observed rate enhancement after 10 min sonication can be explained by reduced bubble coalescence in presence of inorganic salts that leads to enlarged surface areas and increased rates of mass transfer (Craig et al. 1993). At longer contact, the contribution of excess oxidants produced by oxidation of carbonate and the target compound (carbonate and alkyl radicals, respectively) should also be accounted for as potential accelerators of the rate.

Comparison of the reaction rates in Na_2CO_3 (pH=10.76) and NaOH (pH=10.8) containing solutions in Figure 6.5 showed that the degradation of 4-NP in the latter was more than 50 % faster despite the equivalent pH levels. Based on the previous discussion about effects of enhanced hydrolysis and deprotonation at alkaline pH, one would expect similar rates in both solutions. The observed difference, therefore, must be the outcome of: i) hindered hydrolysis of 4-NP in presence of Na_2CO_3; ii) lower solubility of Na_2CO_3 at high temperatures that may reduce the collapse temperature. The latter is based on the fact that the solubility of Na_2CO_3 decreases with increasing temperatures and is zero at the

supercritical level (Jayaweera, 2003). At such, the vapor pressure of water is 220 atm, whereas that in the presence of NaOH is only 100 atm . If we assume the presence of a sphere between the interfacial and the supercritical regions as suggested by Destaillats et al. (2003), then we would expect more water vapor inside the cavities in a solution containing Na_2CO_3 than that with NaOH, and less energy available at collapse (through a cushion effect).

Addition of salts of Fe^{2+}, Cu^{2+}. The role of aqueous phase OH radicals was also investigated by the addition of OH radical sources into solution that reacted in accordance with equations 6.1-6.8, which describe a series of chain reactions initiated by the oxidation or reduction of Fe^{2+} and Cu^{2+}, respectively followed by catalytic decomposition of hydrogen peroxide. Note that Fenton or Fenton-like reactions are easily initiated in sonicated water without H_2O_2 addition, owing to its onsite generation via equation 6.2. The major control parameter in such reaction systems is the dose of the reagent or its ratio to that of 4-NP to prevent termination of the chain via excess consumption of hydroxyl radicals. Variation of the pseudo-first order 4-NP degradation rate with the initial Fe^{2+} and Cu^{2+} concentrations is presented in Figure 6.6

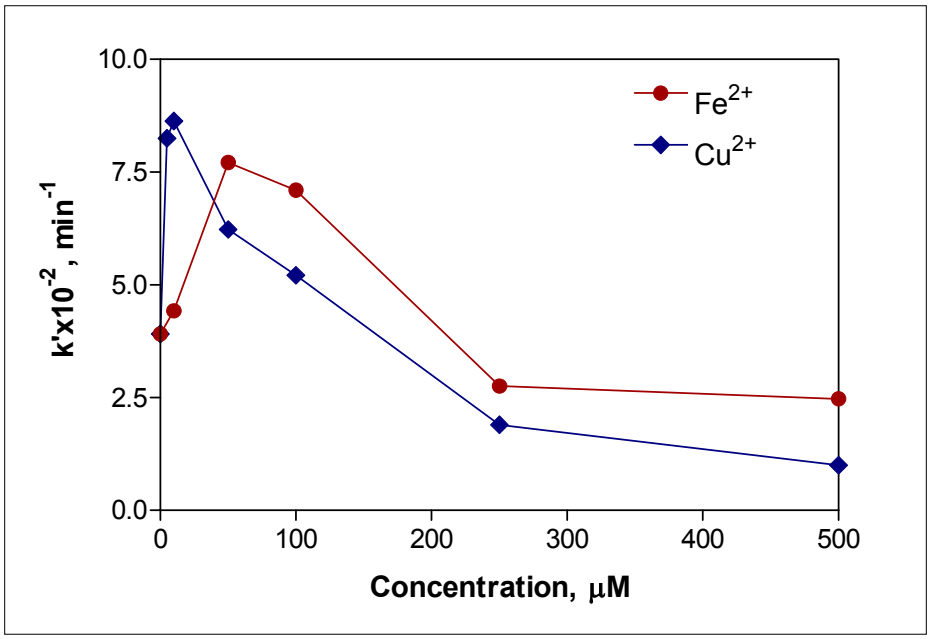

Figure 6.6 Variation of 4-NP decay rate constant in US1 with the concentration of Fe^{2+} and Cu^{2+} (C_0=100 µM, pH=3, t=45 min).

The data show that the rate increases with increasing concentrations of the metals and reaches a maximum at 0.05 mM Fe^{2+} and 0.01 mM Cu^{2+}, corresponding to effective doses of 0.127 g/g NP and 0.029 g/g NP, respectively. At larger concentrations, the effect was found to reverse due to the consumption of some hydroxyl radicals by the excess of metal ions. More significantly, the figure shows that the rate of destruction of 4-NP increases by the addition of excess OH radicals to the solution, indicating the potential of aqueous phase OH radical reactions in the reaction pathway. The fact that the rate also increased in the presence of OH radical sinks does not conflict with this indication, but rather it signifies that oxidation by OH radicals in the bulk solution at 20 kHz does not contribute to the overall reaction unless the radicals are made available by the addition of effective sources of these radicals.

The above indication was further verified by running Fenton (and Fenton-like) reactions in the presence of excess H_2O_2 that was provided by the addition of 0.5, 1, and 2 mM H_2O_2 to yield $H_2O_2/Metal^{2+}$ molar ratios of 10:1, 20:1, and 40:1, respectively. The data showed that the rate of 4-NP decomposition increased with H_2O_2 addition and reached a maximum at a dose of 10:1 H_2O_2/Fe^{2+} and 10:1 H_2O_2/Cu^{2+}, which provided 91 % and 4.6 % enhancement, respectively relative to the rates observed in the absence of external H_2O_2. Note that a much lower effect in presence of copper is due to a much lower dose added to the solution. It was also found that higher doses of H_2O_2 slightly reduced the rate of reaction, as a consequence of OH radical scavenging by excess H_2O_2 as (Ince, 1999):

$$H_2O_2 + \bullet OH \rightarrow \bullet O_2H + H_2O \qquad (6.11)$$

In summary, aqueous phase OH radicals do not take a considerable part in the overall decay of 4-NP by 20 kHz ultrasonic irradiation (due to their limited quantity) unless they are generated or regenerated by the addition of optimal quantities of Fenton and Fenton-like reagents.

6.3.4.2. The Interface.

Addition of tert-butanol. The role of strong OH radical scavengers at the interfacial area was investigated at pH 3 and pH 10.8 in the presence of t-butanol by monitoring the

concentration of 4-NP during 45 min sonication in US1 and US3. The data generated in US1 are presented in Figure 6.7.

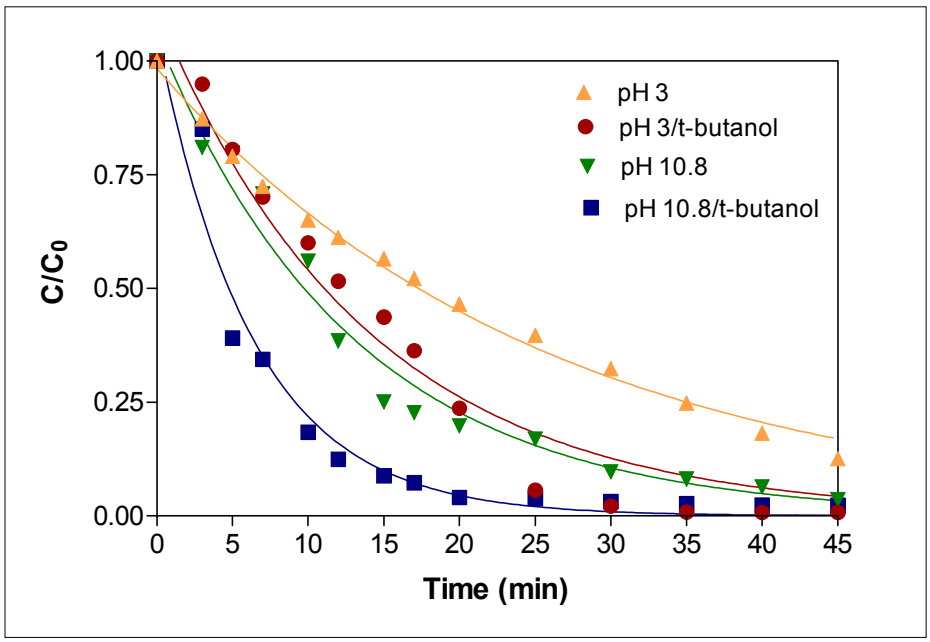

Figure 6.7. The interactive impact of tert-butanol and pH on sonochemical rate of 4-NP decay in US1 (C_0=100 μM, t-butanol=1 mM).

Contrary to the expected deceleration, we found that the rate of 4-NP decay increased with t-butanol addition at both of the pH levels, and the acceleration was much sharper at alkaline pH. Enhanced rate of reaction in presence of t-butanol is contradictory to the findings of Yim et al. (2003) who have reported that sonochemical decomposition of alkylphenols is slowed down by t-butanol addition. The contradiction between their and our results must be due to the difference in the applied molar ratio of t-butanol:NP (100 or 500 in the study of Yim et al. (2003), 10 in this study) and the difference in the applied frequencies. Our data clearly indicate that at low doses of t-butanol there is no competition for interfacial OH radicals, which is consistent with the relative hydrophobicities of the compounds (log K_{ow}=0.4 and 4.48 for t-butanol and 4-NP, respectively). Accelerated rate of 4-NP decay is most likely due to rapid decomposition of t-butanol to produce methyl radicals, which are reported as the essential products of high-temperature pyrolysis of t-butanol (Tauber et al. 1999a). Regarding the frequency as another parameter of significance that may lead to contradictory results, we found that the frequency of

irradiation was 200 kHz in the study of Yim et al. (2003) reporting suppression of the rate, whereas our data were generated at 20 kHz.

To assess the relative impact of low and high frequencies, we monitored the concentration of 4-NP also in US3 (861 kHz) during 45 min sonication in the absence and presence of t-butanol (molar ratio of t-butanol:NP = 10). We found that at alkaline pH the rate of degradation by high frequency irradiation was nearly twice slower in the absence of t-butanol and 5 times slower in its presence. Estimated apparent rate constants under each test condition in the two reactors are listed in Table 6.2. Higher rates under 20 kHz irradiation are due to: (i) higher collapse temperatures leading to higher efficiency of thermal reactions and (ii) longer bubble-life and collapse durations that allow longer exposure of hydrophobic compounds to the hot interfacial conditions (Mason, 1990; Petriér et al., 1994). Hence, under high frequency ultrasound the interfacial area is not as effective a reaction site as it is under low frequency. However, a larger fraction of OH radicals are ejected to the bulk solution to improve the oxidation efficiency of the hydrophilic constituents. The fact that the rate of reaction in US3 was slow despite increased efficiency of OH radical ejection to the bulk solution verifies our hypothesis that 4-NP exists mainly in the vicinity of the bubbles and consumes most of the radicals there. As such, the presence of t-butanol inside or just near a cavity suppresses the rate of 4-NP destruction via incomplete/inefficient pyrolysis of the former within the short collapse time, resulting in a strong competition for OH radicals at the interface.

Table 6.2. Interactive effects of frequency and tert-butanol on the rate of 4-NP decay (C_0=100 μM).

Applied frequency	**k'x10^{-2} (min^{-1})**			
	t-butanol/NP=0		**t-butanol/NP=1.0**	
	pH=3.0	**pH=10.8**	**pH=3.0**	**pH=10.8**
20 kHz	3.91	7.68	7.24	15.80
861 kHz	2.71	3.64	2.08	3.18

6.4. Conclusions

The results have shown that destruction of 4-n-nonylphenol in US1 was more efficient under oxygen atmosphere than argon or air and, at highly basic pH. The enhancement at alkaline conditions was related to increased hydrolysis and easier cleavage of the covalent bond that connected the two ends of the molecule. The presence of Na_2CO_3 did not retard the rate of decomposition, showing the insignificance of OH radical reactions in the bulk solution. However, such reactions were of value in the presence of excess OH radicals made available by the addition of divalent salts of iron and copper. The decomposition of the compound was further accelerated in presence of tert-butanol, which was reported in the literature to suppress the decay of alkylphenols by ultrasound. The disagreement was based on the large discrepancy between the applied doses of tert-butanol and the frequency of irradiation. The latter was verified by running the reaction in a high frequency reactor (US3), where the rate was slower and adversely affected by the addition of tert-butanol.

7. AZO DYES

7.1. Degradation of C.I. Acid Orange 8 by Ultrasound, Ozone and Ultrasound/Ozone Combination

The study presented in this section covers partly the article entitled "Degradation of Aryl-Azo-Naphthol Dyes by Ultrasound, Ozone and Their Combination: Effect of α-Substituents", which is published in Ultrasonics Sonochemistry in 2006 (Gultekin and Ince, 2006).

7.1.1. Introduction

Textile dyehouse effluents contain wasted dyestuff in quantities directly related to the degree of imperfect fixing, and thus are difficult to treat by conventional processes involving biological and chemical methods. When these effluents are discharged into water without proper treatment, the dyes are transported over long distances because of their high solubility, and some are hydrolyzed or anaerobically metabolized to form carcinogenic end products (Tezcanli-Guyer and Ince, 2003; Sharma et al., 2002). Moreover, dyeing mills consume such large amounts of water that in-plant water recycling, which requires proper decontamination of all effluents, is a crucial step in dyehouse wastewater management (Ince and Tezcanli-Güyer, 2004).

Lab-scale application of advanced oxidation processes (AOPs) using a source of ultraviolet light and oxidizing chemicals such as ozone, hydrogen peroxide and Fenton's reagent are found extremely effective for decolorizing dyeing mill effluents (Ince et al., 1997; Arslan and Balcioglu, 1999; Gouldm and Groff, 1987). AOPs are based on in-situ generation of very reactive free radicals such as the hydroxyl radical (•OH), which owing to its non-selectivity is an exceptionally powerful oxidant. The use of ultrasound to generate hydroxyl radicals is a relatively novel technique in AOP, and the method has attracted attention particularly for its decolorization effects (Vinodgopal et al., 1998; Joseph et al., 2000; Sivakumar and Pandit, 2001; Ge and Qu, 2003; Tezcanli-Güyer and Ince, 2004; Rehorek et al., 2004).

The phenomenon responsible for hydroxyl radical formation during sonication of water is cavitation, which consists of the formation, growth and expansion of micro bubbles within the compression-rarefaction cycles of acoustic waves (Suslick, 1990). When these bubbles expand to sufficiently large sizes, they collapse by violent implosions to release extreme temperatures and pressures at local hot spots in the liquid. Under these conditions, molecules of water entrapped in the gaseous bubble interiors dissociate into hydroxyl and hydrogen radicals, which undergo a number of chain reactions including the generation of H_2O_2 (Mason, 1999).

The use of ozone in AOP is widely popular with the advantage that ozone reacts with organic compounds either directly at acidic/neutral conditions and/or indirectly by decomposition at highly alkaline pH (Chu and Ma, 2000). The rate-limiting parameter in decolorization of azo dye solutions by ozone is the mass transfer rate of ozone in the solution (Shu and Huang, 1995). Combined operation of sonolysis and ozonation renders synergistic effects in organic matter destruction (Olson and Barbier, 1994; Kang and Hoffmann, 1998; Ince and Tezcanli, 2001). The synergy is partly due to excess hydroxyl radicals formed upon thermal decomposition of ozone in the gas phase (Reactions 9.1-9.2), and partly to increased mass transfer of ozone in solution by mechanical effects of ultrasound (Olson and Barbier, 1994; Kang and Hoffmann, 1998):

$$O_3 +))) \rightarrow O_2\,(g) + O(^3P)(g) \qquad (7.1)$$

$$O\,(^3P)(g) + H_2O\,(g) \rightarrow 2{\bullet}OH \qquad (7.2)$$

The objective of this study was to investigate and compare the effects of ultrasound (US), ozone (O_3) and their combination (US/O_3) on the degradation of aryl-azo-naphthol dyes. The test dye C.I. Acid Orange 8 (AO8) selected from commercial dyestuff was a mono-azo water soluble dye that is widely consumed in the textile industry for its bright color and good fastness properties (U.S. EPA, 1996).

7.1.2. Materials and Methods

C.I. Acid Orange 8 (MW=364.4 g mol^{-1}) was obtained from Aldrich in 65% purity and used without further purification. The molecular structure of the dye in equilibrium between its azo and hydrazone tautomers is given Figure 7.1:

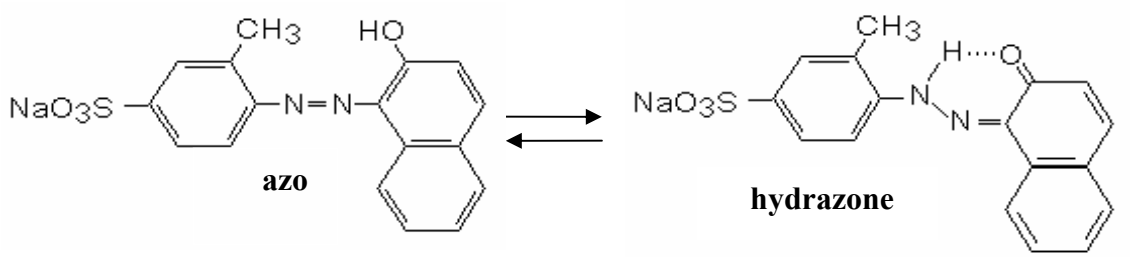

Figure 7.1. Azo and Hydrazone Forms of C.I. Acid Orange 8 (AO8)

The experiments were carried out in a 150 mL glass reactor surrounded by a cooling jacket and consisting of a plate type transducer emitting ultrasonic waves at 300 kHz as generated by electricity at 25 W. Argon was injected during all single US operations to enhance bubble formation and to compensate for degassing effects. The ultrasonic power input in the reactor was 0.190 W mL^{-1} as determined by calorimetry (Mason et al., 1992). Ozone was generated electrically from dry pure oxygen using an Ozone Lab-100 model generator.

7.1.2.1. Procedure. A 3 mM stock solution was made by dissolving 0.168 g of AO8 in 100 mL of boiling ultra pure milli-Q water during magnetic stirring, and stored in the dark at 4ºC prior to use. Dye solutions of various strengths were prepared from the stock by proper dilutions with milli-Q water followed by 1-hour aeration. The pH of all test solutions after saturation with air was 5.0 and no pH adjustment was made in any test scheme.

The procedure consisted of selection of the initial dye and ozone concentrations; and exposure of 100 mL air-saturated test solutions to US, O_3 and US/O_3 combination, respectively at optimized conditions. In all schemes, samples were collected at various times during operation and analyzed for color, UV absorbance, total organic carbon (TOC)

and H_2O_2. The performance of the systems for color decay was assessed by the degree of reduction in the maximum absorbance of the dye in the visible band during 30 min operation, while aromatic and naphthol ring degradation were determined by the abatements at UV-254 and UV-312 nm bands, respectively. The formation of hydroxyl radicals was assessed indirectly by monitoring the concentration of H_2O_2 in the reactor. The capability of experimental schemes for mineralization was investigated by monitoring the TOC of effluent samples during 60 min exposure of the dye solutions to each test scheme.

7.1.2.2. Analytical. The visible and UV absorbance of effluent samples were analyzed using a Unicam Heλios Alpha/Beta double beam spectrophotometer. Total Organic Carbon was monitored by a Shimadzu TOC-V CSH analyzer operating in the non-purgable organic carbon (NPOC) mode. Hydrogen peroxide was determined colorimetrically by the potassium iodide method (Klassen et al., 1994).

7.1.3. Results and Discussion

7.1.3.1. Selection of the Optimum Dye and Ozone Concentrations. Air-saturated solutions of AO8 at 20, 30 and 40 μM were irradiated with ultrasound for 30 min, and time-dependent decay of their visible absorbance was monitored in samples withdrawn from the reactor at 5-min intervals. The plot and analysis of absorbance-time data showed that the rate of color degradation was pseudo-first order with respect to the maximum absorbance of the dye, as presented in Figure 7.2. The coefficients of color decay rate were estimated by fitting the data to the 1st order rate expression:

$$-\frac{dA}{dt} = k' A \tag{7.3}$$

where: A is the maximum absorbance of the dye solution in the visible band at time t and k' is the first order absorbance decay coefficient ($time^{-1}$). It was found that the rate of bleaching was decelerated by increasing concentrations of the dye (20μM>30μM>40μM); nevertheless the working concentration was selected as 30 μM to simulate typical dye concentrations found in dyeing mills after rinsing (PISA Textile, 2004).

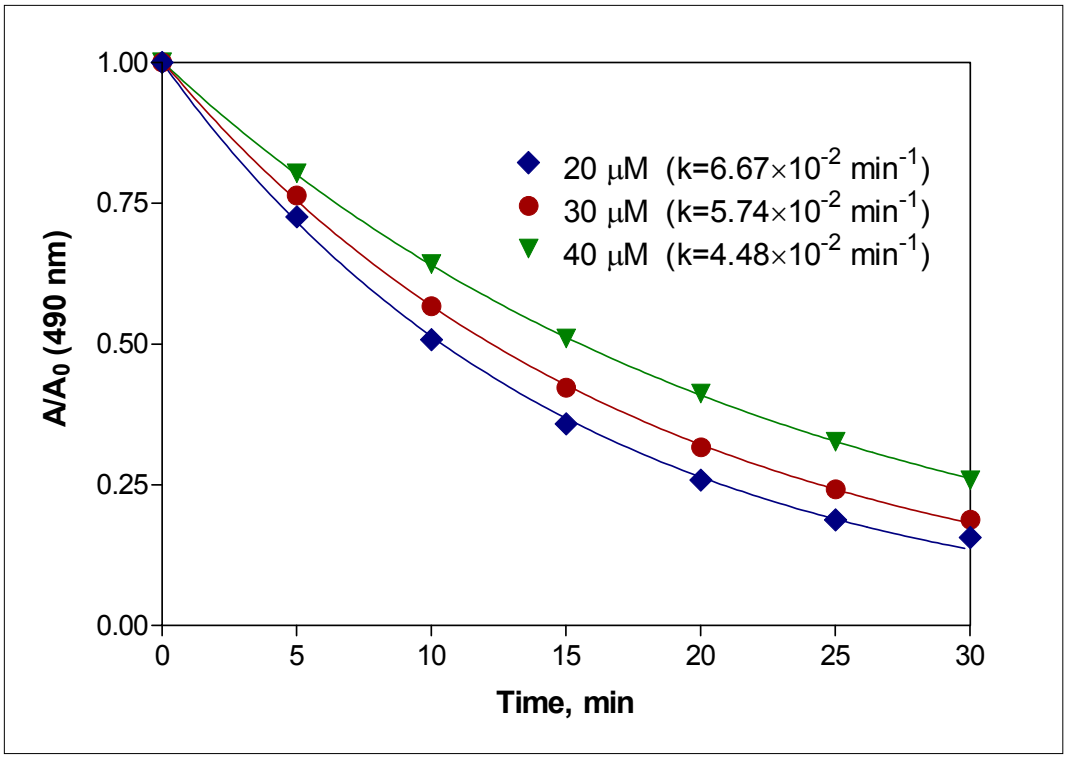

Figure 7.2. Effect of initial dye concentration on the rate of color decay by ultrasound. The solid lines represent the fit of experimental data to the integrated form of Equation (7.3).

The operating ozone concentration was selected by choosing the lowest value that the generator allowed followed by monitoring the rate of color decay at this and higher ozone concentrations during 30 min ozonation without ultrasound. Profiles of color decay and estimated rate coefficients at 2, 4, 6 and 8 g m^{-3} ozone concentrations are presented in Figure 7.3. Note that decolorization was slowest at the minimum ozone concentration of the device- 2 g O_3 m^{-3} (corresponding to an oxygen flow of 0.75 L min^{-1}), however the estimated rate coefficient at this concentration was nearly twice the coefficient in sonicated dye solutions within the same contact. Nevertheless, 2 g m^{-3} was selected as the operational ozone concentration, since it was not possible to operate the ozone generating device at a lower value.

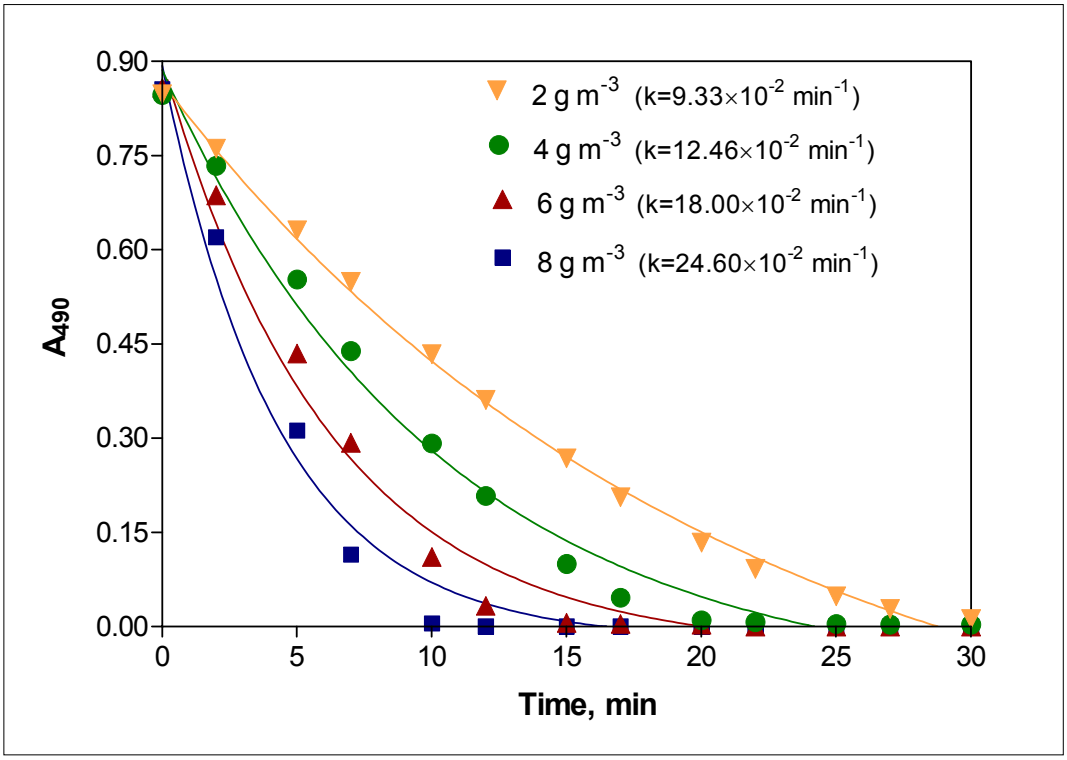

Figure 7.3. The effect of ozone concentration on the rate of color decay during 30 min ozonation of AO8 without ultrasound.

7.1.3.2. Alterations in the Dye Spectrum During US and O_3 Applications. The UV-visible spectrum of the dye dissolved in milli-Q water showed that it had two absorption peaks in the visible band: a maximum at 490 nm and a minimum at 412 nm, which indicate the relative distribution of the hydrazone and azo tautomers, respectively (Sharma et al., 2002). In addition, it absorbed UV light at 312 nm and 254 nm, which correspond respectively to the naphthol and benzene components in its molecular structure. Comparative decay of UV-visible absorption of AO8 (initially at 30 μM) before and during 30 min sonication and ozonation are presented in Figure 7.4. In both operations, the visible absorbance at 490 nm was found to decay considerably, but ozone was considerably more effective than ultrasound. On the other hand, the decay at 412 nm- representing the absorption of the azo tautomer was much more pronounced in the ozone scheme than in US. This implies the relatively higher reactivity of the azo form with molecular ozone (since decomposition of O_3 to •OH is restricted by the acidic pH level) than with the hydroxyl radical, which is the predominant oxidative species in sonochemical degradation of hydrophilic compounds.

The figure also shows that in both schemes the major process is decolorization rather than UV absorption decay, suggesting that the priority of oxidation is the chromophore, irrespective of the active oxidative species.

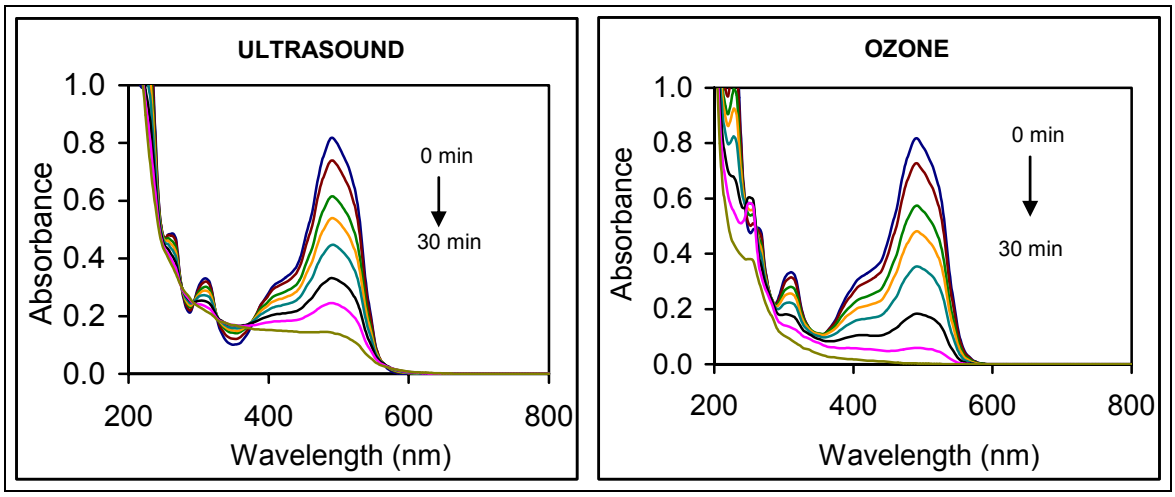

Figure 7.4. The UV-visible spectrum of AO8 at time 0, 2, 5, 7, 10, 15, 20 and 30 min during sonolysis and ozonation.

7.1.3.3. US/O_3 Combination and Comparison with Single Schemes. Simultaneous operation of sonolysis and ozonation for 30 min yielded total decolorization, 72% reduction in UV_{312} and 50% reduction in UV_{254} absorption bands. The corresponding fractions of decay in color, 312 nm and 254 nm by ozonation within the same contact were 95%, 75% and 22%, respectively. Hence, the performances of O_3 and US/O_3 schemes for visible and UV_{312}-band decay were similar, but the latter was at least twice more effective in total absorption abatement at 254 nm. Comparative profiles of visible and UV absorption decay under simultaneous and single operations of US and O_3 during 30 min contact is presented in Figure 7.5.

Note that the decay curve for 254 nm is exponential in US and US/O_3 operations, but parabolic in the O_3 scheme as the indication of the relatively low reduction at 254 nm. The first part of the curve, i.e. the increase during the initial 17 min may be due to the formation of two benzene rings by fragmentation of the naphthalene component, and/or the production of some aromatic/olefinic oxidation intermediates that also absorb at 254 nm. It is remarkable, however that the decay at this absorption by the combined scheme is larger

than the sum of the decay by the single schemes. This can be explained by the synergy of excess hydroxyl radicals and other oxidative species such as singlet oxygen, peroxy and/or superoxide that unlike hydroxyl radicals may accumulate in solution.

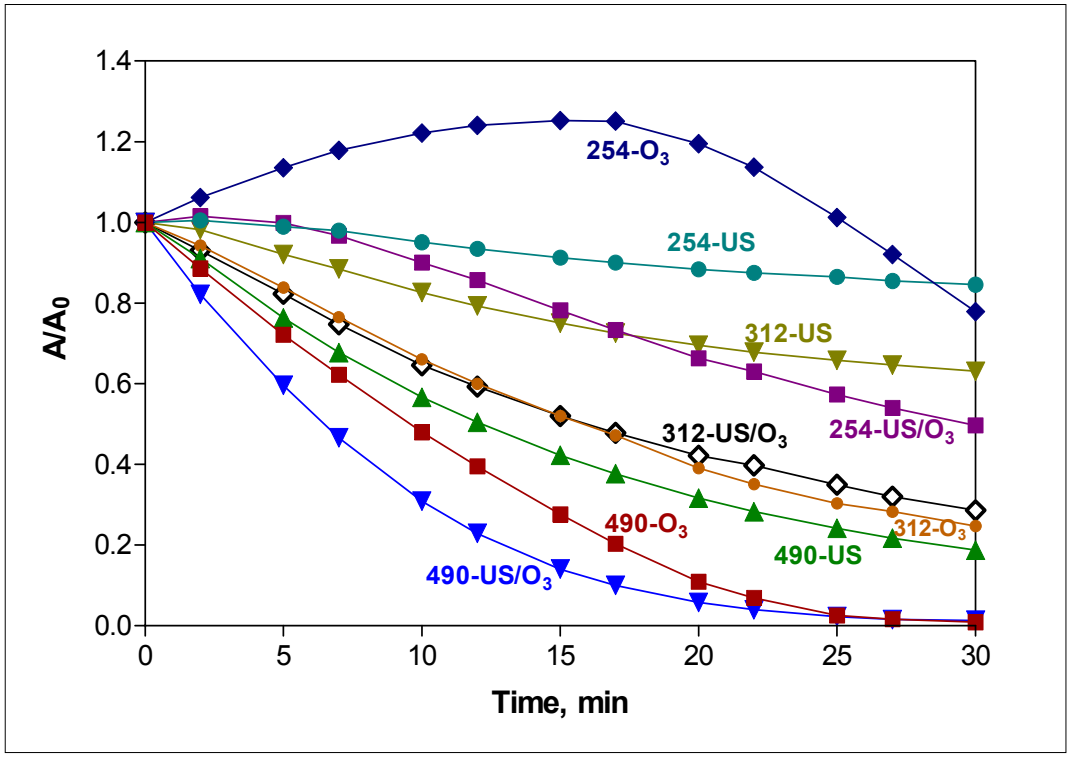

Figure 7.5. Profiles of visible and UV absorption decay during 30 min contact of AO8 with US, O_3 and US/O_3 combined schemes.

7.1.3.4. Hydrogen Peroxide Formation. The buildup of hydrogen peroxide was monitored as an indirect measure of hydroxyl radical production in the test schemes. Upon generation and ejection to the solution, these radicals recombine to yield H_2O_2 and/or unselectively react with dissolved solutes in the bulk. The profile of H_2O_2 buildup during 30 min application of US, O_3 and US/O_3 test schemes in the presence and absence of AO8 is presented in Figure 7.6.

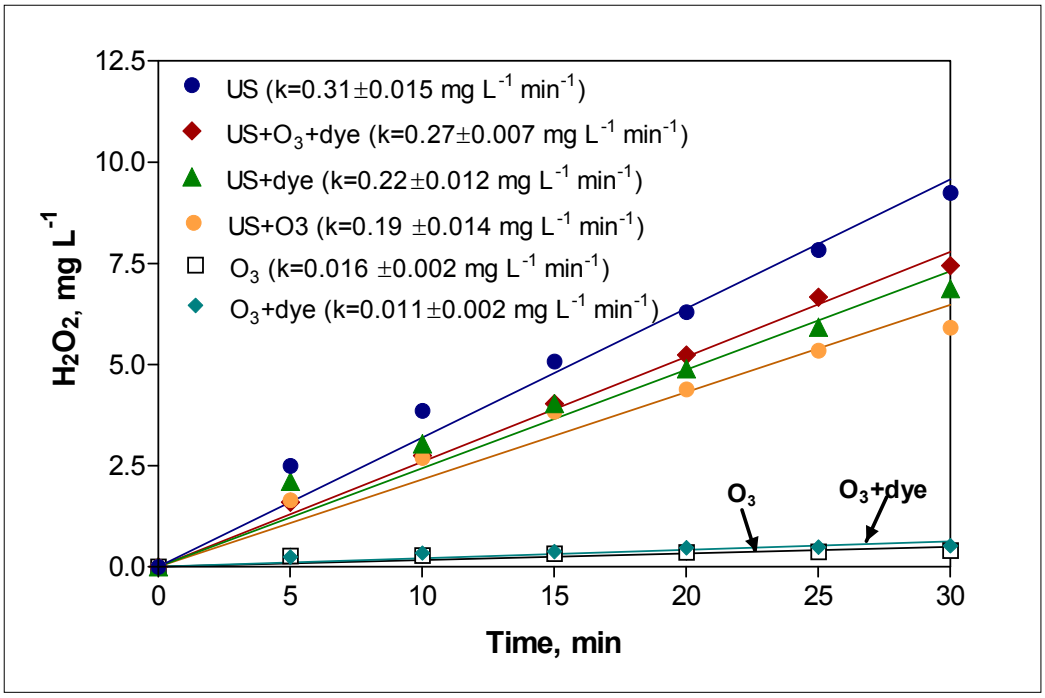

Figure 7.6. Net rate of H_2O_2 production in the test schemes with and without the dye. The solid lines represent linear regression fits, with correlation coefficients $r^2 \geq 0.98$.

The formation of hydrogen peroxide by ozonation without ultrasound was negligible as indicated by the low values of the rate coefficients in ozonated solutions, confirming the previous discussion on the dominance of molecular ozone in these schemes as the major oxidation species. Maximum production was observed in sonicated water containing no dye and no ozone. When the dye was added, the rate was lowered due to scavenging of some hydroxyl radicals by the parent dye and its oxidation by-products. Further reduction in H_2O_2 formation was observed when pure water was sonicated during continuous ozonation, despite the expected increase in hydroxyl radical generation by potential decomposition of ozone in gaseous cavity bubbles. This can be explained by the fact that ozone also is a scavenger of OH radicals although at a slower rate than that of azo dyes (about one order of magnitude), but the effect is magnified with time because here the aqueous ozone tends to accumulate since there are no organic constituents in solution to react with. On the contrary, in the US/dye scheme the scavenger (dye) depletes in time so that more •OH is available for H_2O_2 formation. In the combined US/O_3 scheme with the dye, the net rate of hydrogen peroxide production was larger than in US/O_3 scheme as a result of reduced scavenging of •OH by ozone, which is consumed by reactions with the

dye. Some of the key reactions and their bimolecular rate coefficients to assess their relative contributions to the net rate of H_2O_2 formation are given in Equations 7.4-7.8 (Sharma et al., 2002; Ince and Tezcanli-Güyer, 2004; Destaillats et al., 2000; Sehested et al., 1985).

$$\bullet OH + \bullet OH \rightarrow H_2O_2 \qquad k = 6.0 \times 10^9\ M^{-1}\ s^{-1} \qquad (7.4)$$

$$\bullet OH + \text{dye} \rightarrow [\text{dye-OH adduct}] \rightarrow\rightarrow \text{products} \qquad k = 1.0 \times 10^{10}\ M^{-1}\ s^{-1} \qquad (7.5)$$

$$\bullet OH + O_3 \rightarrow \bullet HO_2 + O_2 \qquad k = 1.1 \times 10^8\ M^{-1}\ s^{-1} \qquad (7.6)$$

$$\bullet OH + H_2O_2 \rightarrow \bullet HO_2 \rightarrow \bullet O_2^- \ (pKa = 4.8) \qquad k = 2.7 \times 10^7\ M^{-1}\ s^{-1} \qquad (7.7)$$

$$O_3 + \text{dye} \rightarrow [\text{dye-ozone}] \rightarrow\rightarrow \text{products} \qquad k = 2.2 \times 10^2\ M^{-1}\ s^{-1} \qquad (7.8)$$

7.1.3.5. Mineralization. The overall degradation or mineralization of the dye solutions was investigated in US, O_3 and US/O_3 test schemes and is presented as a bar chart in Figure 7.7.

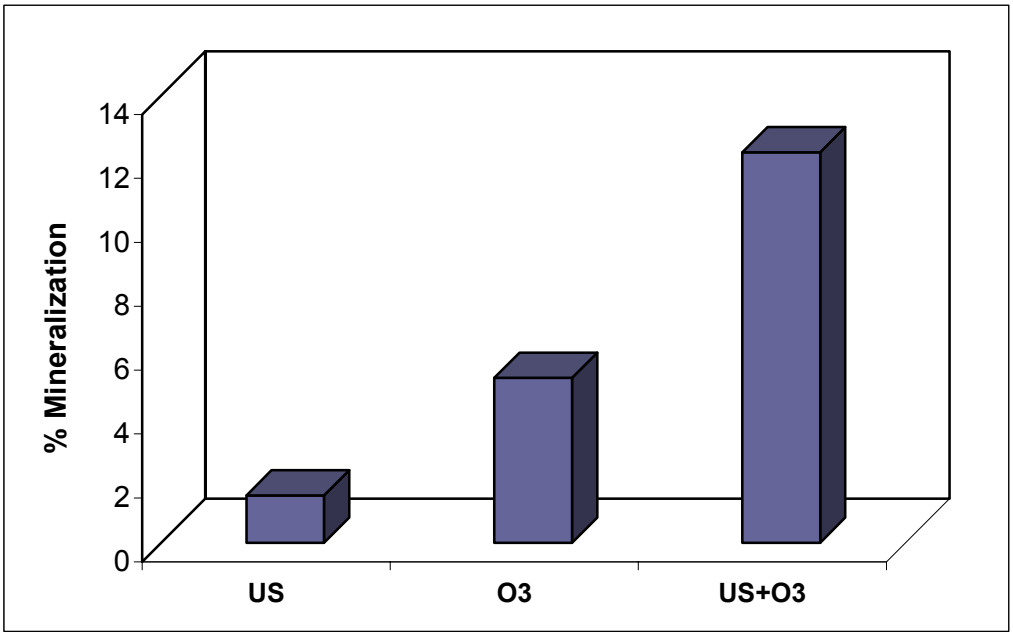

Figure 7.7. Mineralization of AO8 (initial concentration=30 μM) in 1 h contact with single and combined schemes.

It was found that mineralization by sonication alone was negligible as a consequence of limitations in the generation and ejection of •OH into the bulk solution, as well as the hydrophilicity of the dyes. Although some thermal decomposition of azo dyes

may take place at the gas-liquid interface, it must be kept in mind that the potential products (acetylenes and aldehydes) will still exhibit as total organic carbon. Mineralization in the O_3 scheme was more efficient, but not sufficient despite the fact that ozonation was quite effective for nearly complete bleaching of the dyes.

The impact of operating US and O_3 simultaneously on total dye mineralization was larger than the impact on decolorization. The synergy may be attributed not only to excess hydroxyl radical generation and increased mass transfer of ozone as discussed previously, but also to new pathways of oxidation that arise by the formation of secondary oxidative species (e.g $\bullet O_2^-$ and $\bullet O_2H$) other than the primary hydroxyl radicals. Moreover, it is possible that while some oxidation byproducts are recalcitrant to reactions with ozone, they may be reactive with these secondary radicals.

7.1.4. Conclusions

Degradation of aryl-azo-naphthol dyes by ultrasound, ozone and a combination of the two in optimized conditions was investigated. The observation that color decay was considerably faster in all test schemes than the decay of aromatic/naphthalene components was attributed to the priority of chromophore destruction in all oxidation pathways. The effectiveness of ultrasound was lower than ozone for bleaching and mineralization, but ozone/ultrasound combination was found more efficient than the additive effects of single operations. The synergy was attributed to enhanced mass transfer of ozone to accelerate its direct reactions with the parent dye, and the generation of excess radical species upon its thermal decomposition in collapsing cavity bubbles.

Monitoring of hydrogen peroxide concentration during sonolysis, ozonation and simultaneous operation of the two showed that the net rate of H_2O_2 formation was a maximum during sonication of deionized water containing no dye and no ozone, and slowest during ozonation without ultrasound. The observation was explained by scavenging of ultrasound-generated hydroxyl radicals by ozone and the dye, and the increase in hydrogen peroxide during combined sonolysis and ozonation was attributed to reduced scavenging effects upon depletion of ozone by thermolysis and direct reactions.

7.2. Degradation of C.I. Acid Orange 8 by Ultrasound in the Presence of Carbon Tetrachloride and Tertiary-Butyl-Alcohol

This section covers contents of the manuscript "Sonochemical decay of C.I. Acid Orange 8 in water: effects of hydroxyl radical sinks and preservers at the bubble-liquid interface", which was submitted in March 2008 and is currently under review.

7.2.1. Background

It is well known that under ultrasonic irradiation water molecules are thermally fragmented to H and OH radicals. The local concentration of these radicals is a maximum at the time of collapse and a large majority of them will be recombined at the cooler gas-liquid interface before they are ejected out into the bulk solution. A small fraction (depending on the frequency of irradiation and the power applied), however, may accomplish to escape the interfacial sheath and diffuse into solution to initiate a series of oxidation reactions. Hence, if the target of sonication is to destroy low volatility organic chemicals in solution, it is of primary significance to intensify the efficiency of OH radical ejection into the aqueous phase by applying high frequency ultrasound and/or by inhibiting the rate of combination reactions at the interface.

The practice of chemical reagent addition to enhance the rate of sonochemical decomposition of non-volatile compounds and to increase the cost effectiveness of the process has focused on the use of salts, bivalent/zero-valent iron, gaseous ozone and carbon tetrachloride. The effect of CCl_4 is due to its high volatility (vapor pressure = 91 mm Hg at 20°C), which facilitates its diffusion into the gaseous bubble interior to undergo molecular fragmentation. The chemistry of CCl_4 under ultrasonic irradiation is summarized in reactions 7.9-7.16 (Hua and Hoffman, 1996; Tatarova et al., 2004):

$$CCl_4 +))) \rightarrow \bullet Cl + \bullet CCl_3 \quad (7.9)$$

$$CCl_4 +))) \rightarrow Cl_2 + \bullet CCl_2 \quad (7.10)$$

$$\bullet CCl_3 +))) \rightarrow \bullet Cl + \bullet CCl_2 \quad (7.11)$$

$$2\bullet CCl_3 +))) \rightarrow CCl_4 + \bullet CCl_2 \quad (7.12)$$

$$2\bullet CCl_3 +))) \rightarrow C_2Cl_6 \quad (7.13)$$

$$2\bullet CCl_2 +))) \rightarrow C_2Cl_4 \quad (7.14)$$

$$2\bullet Cl +))) \rightarrow Cl_2 \quad (7.15)$$

$$\bullet Cl_2 + H_2O +))) \rightarrow HOCl + HCl \quad (7.16)$$

Enhanced decomposition of organic contaminants by ultrasound in the presence of CCl_4 is due to the production of HOCl, HCl and chlorine containing radicals, all of which are strong oxidizing agents (Wang et al., 2007). In addition, CCl_4 reacts strongly with hydrogen atoms to lower the sink of OH radicals by their combination reaction with hydrogen ($k_{CCl4\text{-}H} = 3.8x10^7$ M s^{-1}, $k_{H\text{-}OH} = 4x10^{10}$ M s^{-1}; Buxton et al., 1988).

The presence of azo dyes in aquatic systems is a serious concern due to their persistent color and potential to form carcinogenic amines upon hydrolysis. Research on the degradability of such dyes by ultrasound has shown that the process is strongly related to the ultrasonic power in solution, the applied frequency, pH, the dye structure and the relative position of the substituents (Ince and Tezcanli-Güyer, 2004; Rehorek et al., 2004; Özen et al., 2005). However, even at optimal conditions at which complete decolorization is accomplished, the degree of mineralization is low unless very long contact is allowed (Vinodgopal et al., 1998) and/or the process is catalyzed by strong chemical agents, such as ferric salts, ozone, H_2O_2 and/or by catalysis with solid particles. The literature on sonochemical decomposition of azo dyes in presence of CCl_4 is limited, and the most recent publication has reported the effects of operational parameters such as pH, dye concentration and OH scavenging on the degradation of methyl orange by 20 kHz ultrasound (Wang et al., 2007).

The aim of this study was to evaluate the relative impacts of carbon tetrachloride and tertiary butyl alcohol (a strong scavenger of OH radicals at the gas-liquid interface) addition on the degradation of azo dyes in US2 and to assess the potential reaction sites. The test dye was C.I. Acid Orange 8 (AO8), which is a highly soluble aryl-azo-naphthol dye consumed widely in textile dyeing operations for its bright color and good fastness properties.

7.2.2. Experimental

Sonication experiments were carried out in US2. Dye solutions of 100 mL were aerated prior to sonication and argon gas was injected continuously into the reactor during sonication. The dye concentration and the contact time in all experiments were 30 μM and 30 min, respectively unless otherwise indicated. The procedure consisted of exposing AO8 solutions to ultrasound in the presence of 0, 105, 310, 520, 730, 1040, 2070 and 5200 μM CCl_4 and the degree of dye removal in each set was monitored by the abatement in the visible and UV absorption of the solutions. The effect of OH radical scavenging at the bubble-liquid interface was investigated by running the reactions successively in the presence of 105, 210, 315, 525 and 1050 μM tert-butanol.

7.2.3. Results and Discussion

7.2.3.1. Decomposition of the Dye in the Bulk Solution. AO8 had three absorption maxima in its UV-visible spectrum: two in the UV-band and one in the visible. The peaks at 254 and 312 nm reflected the absorption of aryl and naphthol groups, respectively while that at 490 nm was due to the absorption of the chromophore, which was made of a N=N moiety attached to the aryl and naphthol carbons. It was found that ultrasound rendered more than 80 % abatement in the visible absorption of the dye and about 20 % and 40 % abatement in the absorption of UV-254 and UV-312 bands, respectively. The UV-visible spectrum of the dye during 30 min exposure to ultrasound are presented in Figure 7.8.

Monitoring of the residual dye concentration during sonication of the dye solutions in presence of increasing concentrations of CCl_4 showed that within a range of 105-1040 μM, CCl_4 sharply accelerated the rate of dye degradation and almost complete (99%) decolorization was achieved in the presence of 2070 μM CCl_4. Knowing that sulfonated azo dyes are decomposed much faster by sonication at acidic solutions (upon neutralization of the negatively charged SO_3 group and the enrichment of hydrophobicity, Ince and Tezcanli-Güyer, 2004), we checked the pH of the test samples during the course of reaction. We found that pH dropped from an initial value of 6.34 to 3.73 and 6.05, respectively after 1 min sonication with and without CCl_4 (2070 μM). The initial deviation from neutrality was due to air equilibration of the test samples, while further reduction

after 1 min sonication without CCl_4 is a consequence of deprotonation (of naphthol-OH). On the other hand, the sharp drop in pH after 1 min sonication with CCl_4 is due to reactions (7.9-7.16) that produce hypochlorous and hydrochloric acids. After 10 min sonication pH was 4.37 without CCl_4 indicating the formation of organic acids as products of dye sonolysis, and 2.92 with CCl_4 as a consequence of the formation of organic and inorganic acids.

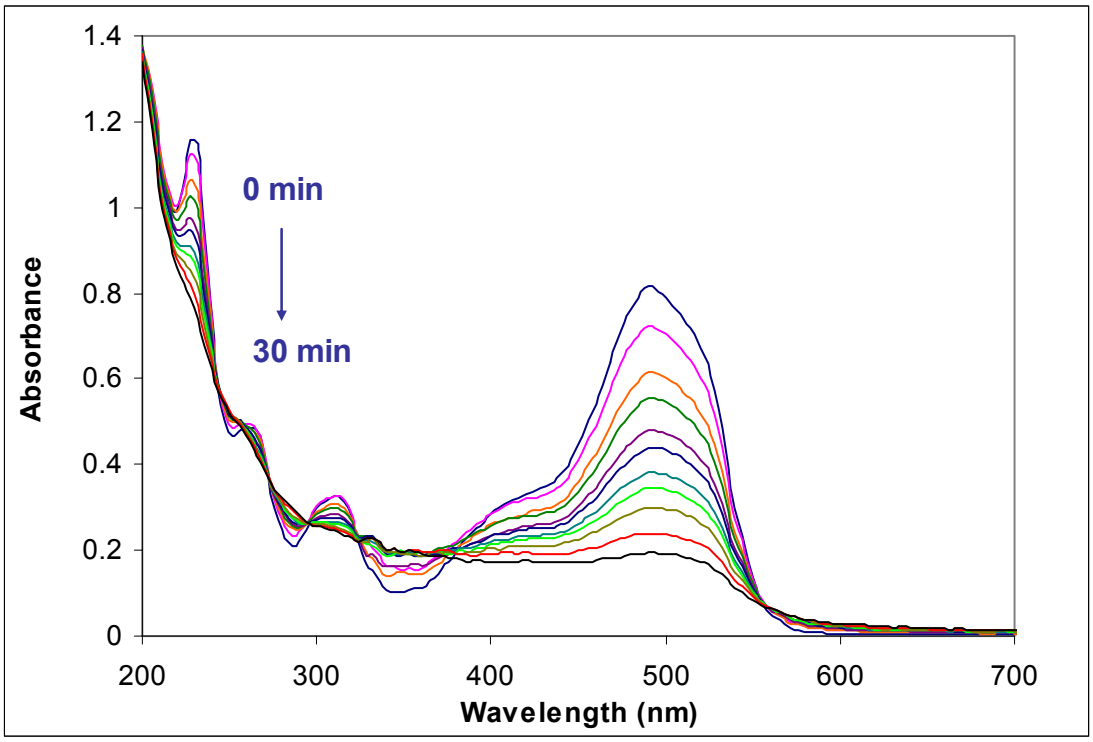

Figure 7.8. The UV visible spectrum of AO8 during 30 min sonication in US2.

The rate of decolorization was pseudo-first order in the visible absorbance of the dye at all conditions so that rate coefficients were estimated by non-linear regression of absorbance-time data using the integrated expression of the first order rate law:

$$k' = \frac{1}{t} \ln\left(\frac{A_t}{A_0}\right) \tag{7.17}$$

where: A_0 and A_t are the absorbance (490 nm) of the dye solution at time 0 and t, respectively and k' is the pseudo-first order absorbance decay coefficient. Variation of k'

with the initial concentration of CCl_4 in the reactor is presented in Figure 7.9. The data show that there are three concentration regimes that induce different impacts on the rate of dye degradation: i) 0-1040 µM range, where the effect is steep acceleration; ii) 1040-2500 µM range, where the effect is moderate acceleration; and iii) 2500-6000 µM range, where the effect is trace acceleration.

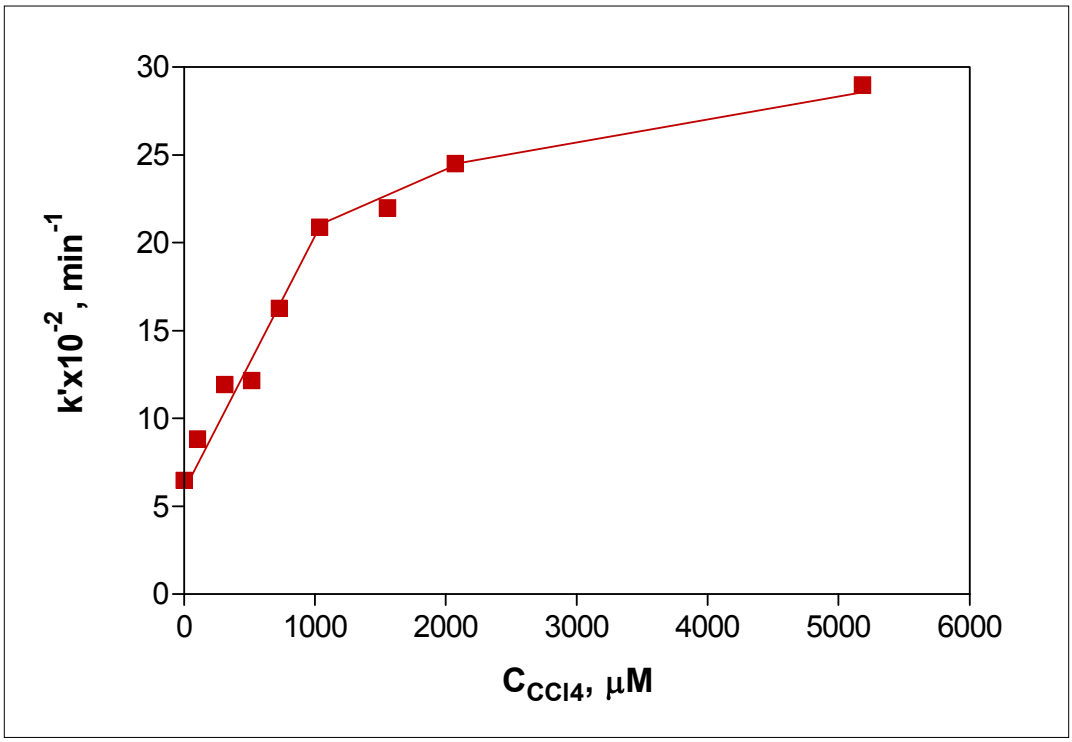

Figure 7.9. Variation of decolorization rate coefficient with the concentration of CCl_4.

It was found that the dose of CCl_4 induced dissimilar effects on the decay of color and UV absorbance, as demonstrated by the bar chart in Figure 7.10. The data show that after 30 min reaction total color decay with ultrasound alone and ultrasound+2070 µM CCl_4 was 84 % and 99.5 %, respectively and was not altered by further addition of CCl_4. On the other hand, fractions of naphthol and aryl ring decay without CCl_4 were 39 % and 18 % and increased to 68 % and 36 %, respectively in presence of CCl_4. However, at 5200 µM CCl_4 the effect was reversed most probably due to the formation of large concentrations of OH radical scavengers (e.g. trichloromethyl radical and hydrogen peroxide). The fact that decolorization of the dye at all conditions including the absence of CCl_4 is considerably larger than the decay of aryl and naphthol groups is due to the higher

priority of OH radicals to attack the azo group rather than the aromatic rings (Özen et al., 2005). Note also that, the lower fraction of abatement in UV-254 than UV-312 band is because the former reflects not only the absorption of aryl groups but also that of total organic carbon, and mineralization is a very slow process relative to the oxidation of parent compounds.

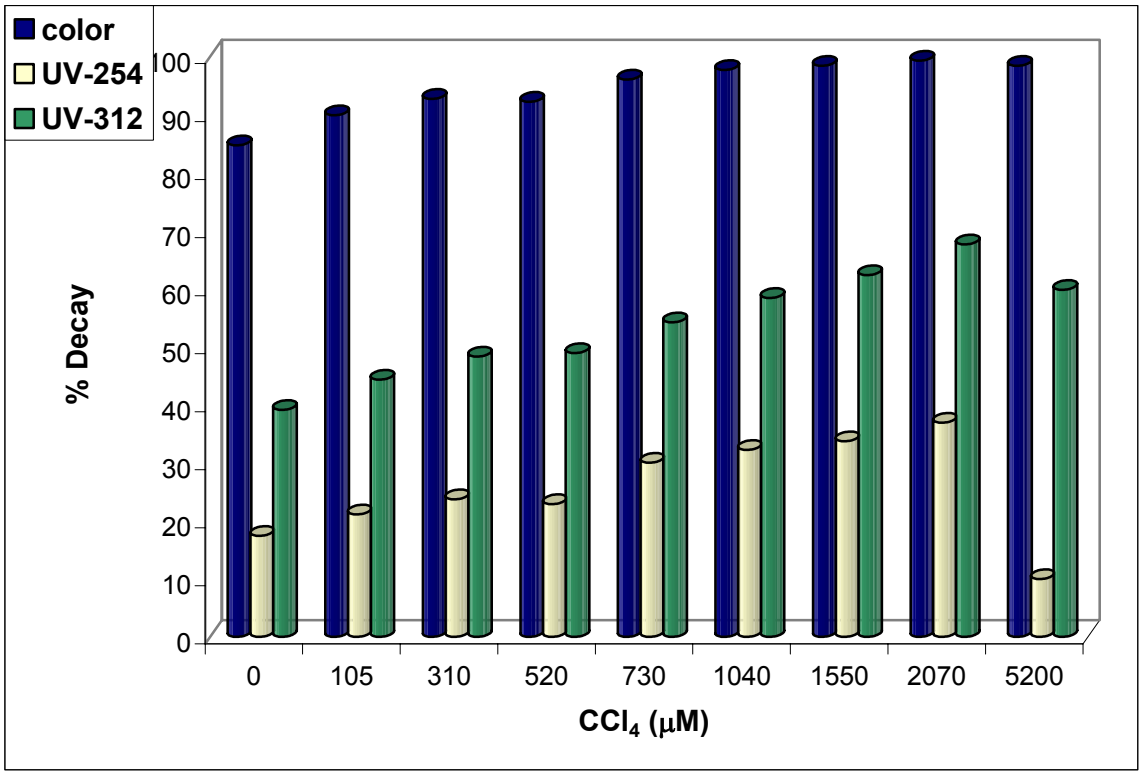

Figure 7.10. Relative fractions of UV and visible absorption abatement after 30 min sonication in the presence of low, medium and high concentrations of CCl_4.

To track the variation of OH radical concentration in solution with the applied test conditions we monitored the quantity of H_2O_2 during sonication of: i) milli-Q water (Control); ii) milli-Q water + dye; iii) milli-Q water + CCl_4; and iv) milli-Q water + dye + CCl_4. The concentration of CCl_4 in iii) and iv) was 2070 μM, because the degree of decomposition in all three components of the dye was a maximum at this level. The data are presented in Figure 7.11.

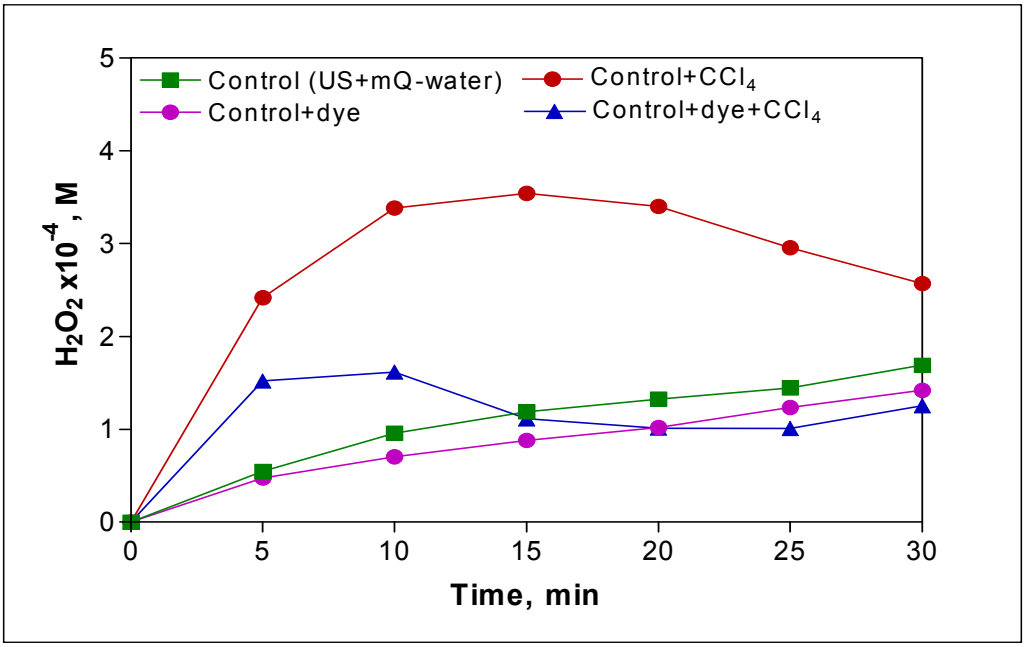

Figure 7.11. Relative rates of H_2O_2 formation during 30 min sonication of pure water, dye-spiked water, CCl_4-spiked water and dye+CCl_4-spiked water. (Initial concentrations were: CCl_4 = 2070 μM, AO8 = 30 μM.)

The profile of H_2O_2 accumulation in control and control+dye sets were similar, and the slightly lower rate of formation in the latter is due to partial consumption of OH radicals by the dye. Largest H_2O_2 concentrations were determined in control+CCl_4 set, where initially the quantity of OH radical scavengers was zero and the reaction of CCl_4 with hydrogen atoms (produced by water fragmentation) resulted in a large reserve of OH radicals. In accordance, the sharp increase in H_2O_2 formation in this set during the first 10 min can be attributed to the following reactions (Buxton et al., 1988):

$$CCl_4 + \bullet H \rightarrow H^+ + Cl^- + \bullet CCl_3 \rightarrow Cl_3^- \qquad (k=3.8\text{x}10^7\ M^{-1}s^{-1}) \qquad (7.18)$$

$$Cl_3^- + \bullet H \rightarrow H^+ + \bullet Cl_2^- + Cl^- \qquad (k=6\text{x}10^{10}\ M^{-1}s^{-1}) \qquad (7.19)$$

On the other hand, the relative steadiness in H_2O_2 between 10 and 15 min and the decline thereafter must be due to the decomposition of CCl_4 (reduced hydrogen sink) and the accumulation of trichloromethyl radical, which at large concentrations is a source of OH radical sink (Hung and Hoffmann, 1998). Furthermore, it should be noted that H_2O_2 may

also scavenge OH radicals when it exists above a critical concentration (Ince, 1999). To conclude, the decline in the net rate of H_2O_2 formation after 15 min sonication must be attributed to the following competing reactions (Buxton et al., 1988; Hung and Hoffmann, 1998):

$$\bullet CCl_3 + \bullet OH \rightarrow HOCCl_3 \qquad (k=10^6\text{-}10^7\ M^{-1}\ s^{-1}) \qquad (7.20)$$

$$H_2O_2 + \bullet OH \rightarrow H_2O + \bullet HO_2 \qquad (k= 2.7x10^7\ M^{-1}\ s^{-1}) \qquad (7.21)$$

In set iv, where sonication run out in combined presence of AO8 and CCl_4, the rate of H_2O_2 formation during early contact was slower than that in the absence of the dye due to rapid consumption of OH radicals by the dye components, particularly the chromophore (Buxton et al., 1988; Destaillats et al., 2000):

$$Dye + \bullet OH \rightarrow Dye\text{-}OH\ adduct \qquad (k= 10^{10}\text{-}10^{11}\ M^{-1}\ s^{-1}) \qquad (7.22)$$

The slight increase in H_2O_2 after 25 min sonication can be attributed to 85 % completion of decolorization by that time. The quantity of OH radicals in solution (estimated by H_2O_2 equivalents) in each set at t =10, 15, 20 and 30 min is listed in Table 7.1. Note that this method of •OH estimation provided excellent correlation (r^2=0.98) with that of iodide dosimetry proposed in the literature (Iida et al., 2005).

Table 7.1. Variation of OH radical concentration with solution matrix.

Test Scheme	**•OH x10^{-4} (M)**			
	10 min	**15 min**	**20 min**	**30 min**
1.Control (US/MQ-water)	1.12	1.39	1.55	1.98
2.Control+CCl_4 (2070µM)	3.96	4.14	3.98	3.01
3.Control+dye (30 µM)	0.83	1.03	1.19	1.66
4.Control+dye+CCl_4	1.89	1.30	1.19	1.47

Table 7.1 shows that the amount of OH radicals in the presence of CCl_4 (and no OH scavengers) is 3 times and 1.5 times larger than that in the control after 10 min and 30 min reaction, respectively. Note also that at t=10 min the concentration of •OH in set 3 (containing no CCl_4) is 56 % lower than that in set 4 (with CCl_4); at t= 15 min it is 21%

lower; at t=20 min it is equal; and t=30 min it is 13 % higher. The profile reflecting a steady decline in the quantity of OH radicals with time in set 4 is the consequence of the elimination of CCl_4 upon which the quantity of free hydrogen radicals increases. On the other hand, the steady increase in OH radicals in set 3 with prolonged sonication is due to the progress and partial completion of decolorization, which is a major •OH consuming process.

7.2.3.2. Does AO8 undergo decomposition at the bubble-liquid interface?. Owing to the very high solubility of azo dyes, it is expected that the prime reaction site for their sonolytic decomposition is the bulk liquid. It is also reported that in concentrated solutions of highly soluble organic compounds, some of the solutes may migrate to the bubble-liquid interface, where they also undergo pyrolytic or oxidative decomposition (Serpone et al, 1994). When the organic solute is a sulfonated azo dye such as AO8, diffusion to the interfacial area is further facilitated in acidic solutions (as previously discussed), which results in hydrophobic enrichment of the solute. To assess the degradability of AO8 at the interfacial area, we monitored the rate of decolorization during sonication in presence of tertiary butyl alcohol, which is a highly volatile compound that readily diffuses to the gaseous bubble through the bubble-liquid sheath (Nagata et al., 1996). Relative rates of color decay in presence of varying concentrations of t-butanol are presented in Figure 7.12.

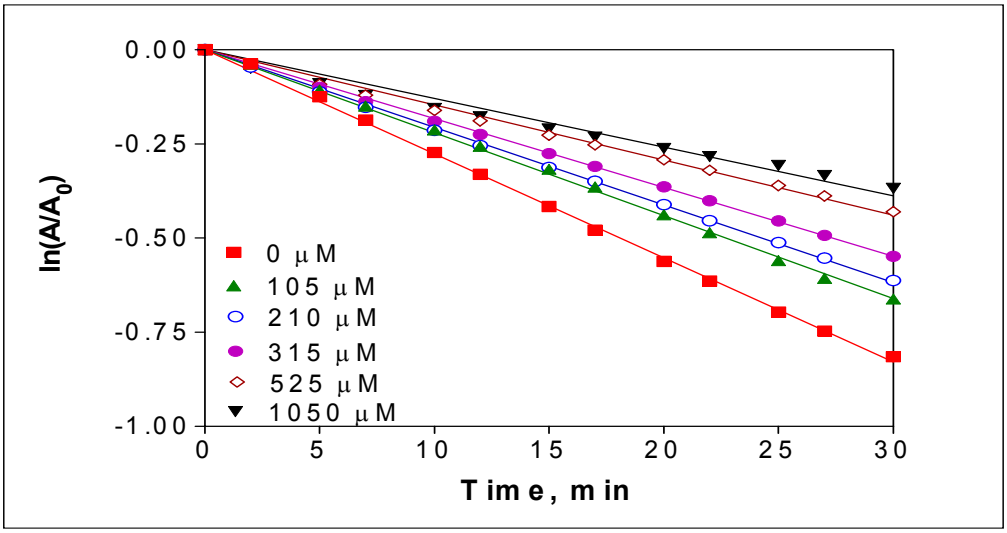

Figure 7.12. Log-linear variation of the visible absorbance of AO8 (C_0 = 30 µM) with increasing concentrations of t-butanol.

The observed deceleration in the rate of bleaching with increasing concentrations of t-butanol may be attributed to the following: i) the competition of the dye and t-butanol for OH radicals at the interfacial area; ii) lower rate of OH radical ejection to the bulk solution due to enhanced consumption in or outside the collapsing bubbles. To assess the validity of the second hypothesis, we monitored the concentration of H_2O_2 during sonication of milli-Q water spiked with the test concentrations of t-butanol, and found that the rate of H_2O_2 formation was not affected by t-butanol concentrations lower than 1050 μM (data not shown), but suppressed by about 35 % at 1050 μM t-butanol (Figure 7.13). However, dye degradation was not only retarded in the presence of 1050 μM t-butanol as shown in Figure 7.12, but also in that of lower concentrations (data not shown), whereby OH radical concentration in solution was unchanged. Thus, the inhibition at low concentrations of t-butanol is mainly due to the competition at the bubble-liquid sheath, signifying the importance of interfacial oxidation as a major reaction pathway in the sonolytic decay of AO8. At higher concentrations of t-butanol, leading to lower OH radicals in the solution bulk, the dye suffered competitive inhibition not only at the interfacial area, but also in the bulk solution.

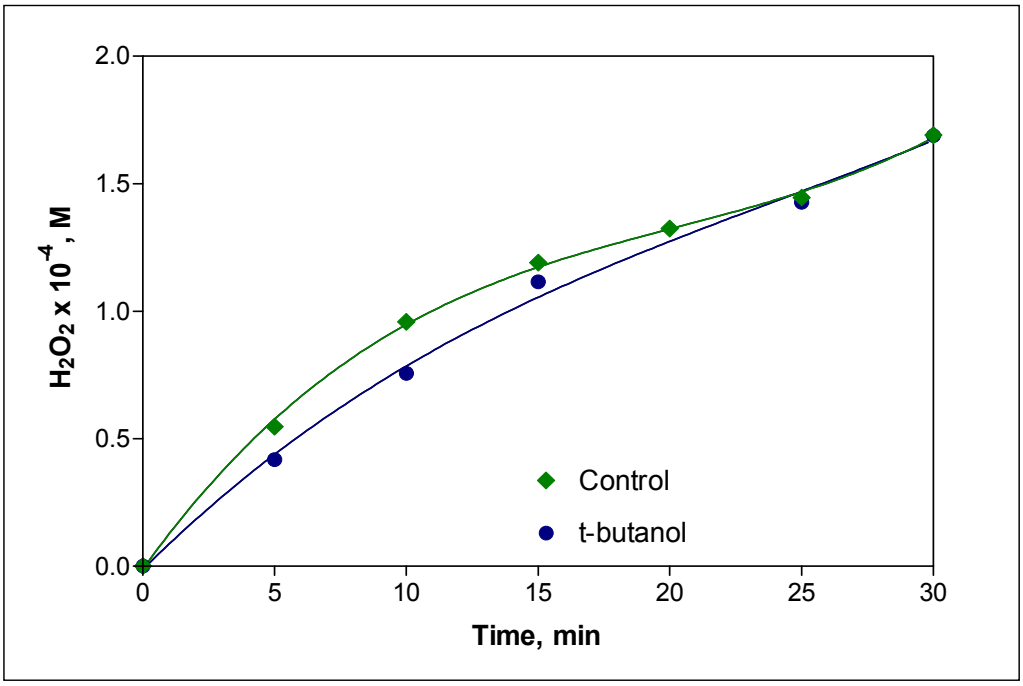

Figure 7.13. Impact of 1050 μM t-butanol on the rate of H_2O_2 accumulation in solution. The solid lines represent the fitted polynomial (r'=0.996) with slopes 0.00032 and 0.00019 for Control and t-butanol.

It was found that the rate of dye degradation was also retarded by increasing the initial dye concentration, and the effect of t-butanol at such was magnified via: i) enhanced competition for OH radicals and the adsorption sites at the interfacial sheath; and ii) increased physical barriers to mass transfer at the bubble-liquid interface. Comparative estimates of pseudo-first order decay rate constants of the three dye components at each test concentration are listed in Table 7.2. Note that combined effect of excess dye and t-butanol addition was more drastic on decolorization of the dye than the decay of UV absorption.

Table 7.2. Impact of initial dye concentration on the rate of decomposition in presence of 1050 μM t-butanol.

Dye Conc.	**k'x10^{-2} (min^{-1})**					
	COLOR		**UV-312**		**UV-254**	
	US alone	**US + t-butanol**	**US alone**	**US + t-butanol**	**US alone**	**US + t-butanol**
30 μM	6.48	2.78	1.82	1.18	0.72	0.13
50 μM	4.95	1.88	1.52	0.97	0.46	0.17
100 μM	3.12	0.83	1.16	0.50	0.25	0.07

Finally, we monitored the rate of dye degradation during sonication in the concurrent presence of a hydroxyl radical reserve (CCl_4) and a hydroxyl radical sink (tert-butanol), and found that the effect was antagonistic. The data are displayed in Table 7.3 in terms of relative bleaching rate constants at various experimental conditions.

Table 7.3. Comparison of pseduo-first order decolorization rate coefficients of AO8 (C_0=30μM) by ultrasound in presence of CCl_4, t-butanol and both.

Condition	**k' x 10^{-2} (min^{-1})**
US	6.48 ± 0.08
US/CCl_4	24.51± 0.69
US/t-butanol	2.78 ± 0.10
US/CCl_4/t-butanol	4.74 ± 0.53

It was found that while decolorization of the dye was enhanced by 278 % in presence of CCl_4 only, it was retarded by 27 % in the presence of both reagents. This means that sonolytic fragmentation of CCl_4 is remarkably suppressed by the presence of t-butyl alcohol via the competition for adsorption sites and OH radicals and the formation of excessive volatile oxidation byproducts, which by diffusion into the gaseous bubbles reduce the bubble temperature and the violence of collapse.

7.2.4. Conclusions

The degradation of C.I. Acid Orange 8 by ultrasonic irradiation in US2 was remarkably enhanced by the addition of CCl_4 and reached a maximum in presence of 2070 μM CCl_4. Addition of tertiary butyl alcohol as a strong OH radical scavenger at the bubble-liquid interface was found to decelerate the rate- particularly that of color decay, showing that the dye did not undergo oxidation only in the bulk solution, but also in the interfacial area. The suppression was magnified in more concentrated dye solutions at which more of the dye molecules may reach the interfacial sheath, but less are able to undergo reaction. In the presence of both reagents at their most effective concentrations the rate of decolorization was 27 % lower than that in control (ultrasound alone), showing that t-butanol was more reactive than CCl_4, i.e. impacts of OH radical scavenging were larger than those of OH radical preserving. The enrichment and accumulation of the volatile oxidation byproducts in the cavity bubbles (that reduce bubble temperatures) should also be accounted for as a potential source of rate reduction.

CHAPTER 8. CONCLUSIONS AND RECOMMENDATIONS

Contamination of the water environment with endocrine disrupting compounds worldwide has raised significant public concern due to their initiation of hormone-like activities even at trace concentrations. Research has shown that advanced oxidation processes, which generate very active oxidative species such as the hydroxyl radical, have the potential to completely eliminate these compounds if not to mineralize. Fortunately, research on the products of oxidation has shown that they do not exhibit "endocrine disrupting" character. In this regard, this study was aimed to investigate the degradability of two classified and one non-classified group of endocrine disruptors by ultrasonic cavitation, ozonation and combinations of ultrasound with ozone and/or Fenton reactions.

A brief summary of the main findings is given in the following sections:

1. Bisphenol A

Sonication

- The pseudo-first order decomposition of BPA decreased with increases in initial concentration, pH and the presence of hydroxyl radical scavengers. More rapid reactions at acidic pH were attributed to enhanced hydrophobicity of the solution that enabled a larger fraction of BPA molecules to migrate towards the bubble-liquid interface, where the concentration of hydroxyl radicals is a maximum.
- BPA degradation was faster under air atmosphere than argon or oxygen atmospheres due to generation of nitric acid and excess radical species (e.g. •OH, $\bullet NO_2$, $\bullet NO_3$).
- The rate inhibitive impact of t-butanol (a strong scavenger of •OH at the bubble-liquid interface) was larger than that of carbonate (a strong scavenger of •OH in the bulk solution) showing that in addition to the aqueous phase, the interfacial area is a major reaction site for the sonochemical degradation of BPA.

- The effect of frequency on the rate of BPA reactions was as the following: 300 kHz>861 kHz>1145 kHz>577 kHz.
- At very low concentrations of BPA such as those found in natural waters, no mineralization is accomplished by 8 h sonication, but at larger concentrations nearly 30 % of organic carbon is converted to CO_2 within the same contact.
- Pulsed mode of sonication is a potential method of increasing the cost effectiveness of ultrasonic systems, but the selection of the right pulse and interval lengths is of great importance.

Ozonation

- The rate of oxidation at acidic pH was accelerated by increasing rates of ozone addition and decreasing concentrations of BPA. The bimolecular rate constant of BPA with O_3 was 1.11×10^4 $M^{-1}s^{-1}$, which was in good agreement with the values reported in the literature.
- Maximum degree of mineralization was accomplished at highly alkaline pH, although BPA degradation at such was not a maximum. The different profiles was attributed to non-reactivity of the oxidation by-products of BPA with molecular ozone, which is the dominant species at acidic pH.
- Ozonation by-products of oxidation in successive order of formation were p-tert-butylphenol; hydroquinone; methyl-dihydrobenzofuran and n-butyl acetate, and none of them are endocrine disruptors.

Ultrasound-Ozone Combination

- Maximum reaction rates and sonochemical product yields were observed at alkaline pH due to enhanced mass transfer and enhanced decomposition of ozone in the aqueous and gas phases.

2. Nonylphenol

- The initial rate of 4-NP decay increased between $0<C_0<100$ μM, but rapidly declined as C_0 was further increased due to enhanced competition for adsorption sites and saturation of the cavity surfaces.
- Maximum decomposition occurred in presence of oxygen bubbling, despite its less favorable gas properties than argon, as attributed to the formation of additional reactive species under oxygenation. Alkaline pH facilitated the decomposition process by enhanced hydrolysis and facilitated cleavage of the covalent bond connecting the hydrophilic and hydrophobic tails of the molecule.
- The presence of moderate concentrations of Na_2CO_3 did not inhibit the decomposition of NP, but the addition of Fenton and Fenton like reagents at optimal doses enhanced the process.
- The reactions were further accelerated during sonication at 20 kHz in the presence of low doses of t-butanol, which is a strong scavenger of OH radicals at the bubble-liquid interface. However, the rate was remarkably slowed down by the same quantity of t-butanol under 861 kHz irradiation. The opposing tendencies at two extreme frequencies were attributed to differences in bubble character, collapse violence and the differences in the quantity of OH radicals.

3. C.I. Acid Orange 8

- Higher decolorization and mineralization was accomplished by combined ultrasound/ozone application than by singly applied ultrasound or ozonation.
- Dye degradation was remarkably enhanced by the addition of 2070 μM carbon tetrachloride upon the production of inorganic acids and the consumption of H radicals, which are major sinks of OH radicals in sonochemical reaction systems.
- Addition of t-butanol decelerated the rate of dye degradation and the suppression was higher in more concentrated dye solutions at which more of the dye molecules approached the interfacial sheath, but less were able to undergo reaction. This was related to enhanced competition for hydroxyl radicals and sites of adsorption at the interfacial sheath.

Recommendations

More research is required on the following issues to complete the reasearch:

- The effects of solution matrix, i.e decomposition of the endocrine disruptors in the presence of substances that are typical of natural water composition.
- The interaction of other endocrine disruptors in solution, since natural waters contain complex mixtures of such compounds.
- Development of easy and reliable screening tools to assess the endocrine activity of the treated samples.

REFERENCES

Adewuyi, Y.G., 2001. Sonochemistry: Environmental science and engineering applications. Industrial and Engineering Chemistry Research, 40, 4681-4715.

Ahel, M., Giger, W., 1993a. Aqueous solubility of phenols and alkylphenol polyethoxylates between water and organic solvents. Chemosphere, 26, 1461-1470.

Ahel, M., Giger, W., 1993b. Partitioning of alkylphenols and alkylphenol polyethoxylates between water and organic solvents. Chemosphere, 26, 1471-1478.

Ahel, M., Giger, W., Schaffner, C., 1994. Behaviour of alkylphenol polyethoxylate surfactants in the aquatic environment-II. Occurrence and transformation in rivers. Water Research, 28, 1143-1152.

Alexander, H.C., Dill, D.C., Smith, L.W., Guiney, P.D., Dorn, P.B., 1988. Bisphenol A: Acute aquatic toxicity. Environmental Toxicology and Chemistry, 7, 19-26.

Alum, A., Yoon, Y., Westerhoff, P., Abbaszadegan, M., 2004. Oxidation of bisphenol A, 17β-estradiol, and 17α-ethynyl estradiol and byproduct estrogenicity. Environmental Toxicology, 19, 257-264.

Alvares, A.B.C., Diaper, C., Parsons, S. 2001. Partial oxidation by ozone to remove recalcitrance from wastewaters-A review, Environmental Technology, 22, 409–427.

Andersson, T., Forlin, L., Harig, I., Larsson, A., 1988. Physiological disturbances in fish living in coastal water polluted with bleached kraft mill effluents. Canadian Journal of Fisheries and Aquatic Sciences, 45, 1525-1536.

Ando, T., Fujita, M., Kimura, T., Kondo, Y., 1998. Decarboxylation of 6-Nitrobenzisoxazole-3-carboxylate with ultrasonic irradiation. The possibility of the formation of supercritical water. Journal of Organic Chemistry, 63, 6048-6049.

Anotai, J., Wuttipong, R., Visvanathan, C., 2007. Oxidation and detoxification of pentachlorophenol in aqueous phase by ozonation. Journal of Environmental Management, 85, 345-349.

APHA/AWWA/WPCP, 1992. Standard Methods for the Examination of Water and Wastewater, 17th Edition, American Public Health Association, Washington DC.

Arslan, I., Akmehmet Balcioglu, I., 1999. Degradation of commercial reactive dyestuffs by heterogenous and homogenous advanced oxidation processes: a comparative study. Dyes and Pigments, 43, 95-108.

Arslan-Alaton, I., Caglayan, A.E., 2006. Toxicity and biodegradability assessment of raw and ozonated procaine penicillin G formulation effluent. Ecotoxicology and Environmental Safety, 63, 131-140.

Bailey, V., Lackner, H., 1995. Emerging Technology Summary: X-Ray Treatment of Organically Contaminated Aqueous Solutions, Prepared for U.S. Environmental Protection Agency Office of Research and Development Superfund Innovative Technology Evaluation Program.

Bajt, O., Mailhot, G., Bolte, M., 2001. Degradation of dibutyl phthalate by homogeneous photocatalysis with Fe(III) in aqueous solution. Applied Catalysis B: Environmental, 33, 239-248.

Barbier, P., Pétrier, C., 1996. Study at 20 kHz and 500 kHz of the ultrasound-ozone advanced oxidation system: 4-nitrophenol degradation. Journal of Advanced Oxidation Technologies, 1, 154-161.

Bayer-Leverkusen, 1989. Grunddatensatz für Altstoffe über 1000 JATO. In SIDS Profile for Bisphenol A, Dow Europe, Horgen, Switzerland.

Beckett, M. A., Hua, I., 2001. Impact of ultrasonic frequency on aqueous sonoluminescence and sonochemistry. Journal of Physical Chemistry A, 105, 3796-3802.

Belfroid, A.C., Van der Horst, A., Vethaak, A.D., Schäfer, .J., Rijs, G.B.J., Wegener, J., Cofino, W.P., 1999. Analysis and occurrence of estrogenic hormones and their glucuronides in surface water and wastewater in The Netherlands. Science of the Total Environment, 225, 101-108.

Belfroid, A., van Velzen, M., van der Horst, B., Vethaak, D., 2002. Occurrence of bisphenol A in surface water and uptake in fish: evaluation of field measurements. Chemosphere, 49, 97-103.

Bielski, B.H.J., Cabelli, D.E., Arudi, R.L., 1985. Reactivity of HO_2/O_2^- radicals in aqueous solution. Journal of Physical Chemistry Reference Data, 14, 1041-1100.

Blackburn, M.A., Waldock, M.J., 1995. Concentrations of alkylphenols in rivers and estuaries in England and Wales. Water Research, 29, 1623-1629.

Bolton, J.R., Bircher, K.G., Tumas, W., Tolman, C.A., 1996. Figures-of-Merit for the Technical Development and Application of Advanced Oxidation Processes. Journal of Advanced Oxidatin Technologies, 1, 13-17.

Boublik, T., Fried, V., Hala, E. (Eds), 1984. The Vapour Pressures of Pure Substances, Second Ed., Elsevier, Amsterdam, the Netherlands.

Brotons, J.A., Olea-Serrano, M.F., Villalobos, M., Pedraza, V., Olea, N., 1995. Xenoestrogens released from lacquer coatings in food cans. Environmental Health Perspectives, 103, 608-612.

Buxton, G.V., Greenstock, C.L., Helman, W.P., Ross, A.B., 1988. Critical review of rate constants for reactions of hydrated electrons, hydrogen atoms and hydroxyl radicals ($\bullet OH/\bullet O^-$) in aqueous solution. Journal of Physical Chemistry Reference Data, 17, 513-886.

Calafat, A.M., Kuklenyik, Z., Reidy, J.A., Caudill, S.P., Ekong, J., Needham, J.L., 2005. Urinary concentrations of bisphenol A and 4-nonylphenol in a human reference population.

Environmental Health Perspectives, 113, 391-395.
Canadian Council of Ministers of the Environment, 2001. Canadian Water Quality Guidelines for the Protection of Aquatic Life, Nonylphenol and Its Ethoxylates.

Carson, R. (Ed.), 1962. Silent Spring, Houghton Mifflin, Boston.

Chen, P.J., Linden, K.G., Hinton, D.E., Kashiwada, S., Rosenfeldt, E.J., Kullman, S.W., 2006. Biological assessment of bisphenol A degradation in water following direct photolysis and UV advanced oxidation. Chemosphere, 65, 1094-1102.

Chen, P.J., Rosenfeldt, E.J., Kullman, S.W., Hinton, D.E., Linden, K.G., 2007. Biological assessments of a mixture of endocrine disruptors at environmentally relevant concentrations in water following UV/H_2O_2 oxidation. Science of the Total Environment, 376, 18-26.

Chiang, K., Lim, T. M., Tsen, L., Lee, C. C., 2004. Photocatalytic degradation and mineralization of bisphenol A by TiO_2 and platinized TiO_2. Applied Catalysis A: General, 261, 225-237.

Chin, S.S., Lim, T.M., Chiang, K., Fane, A.G., 2007. Hybrid-low pressure submerged membrane photoreactor for the removal of bisphenol A. Desalination, 202, 253-261.

Chiou, C.S., Chen, Y.H., Chang, C.T., Chang, C.Y., Shie, J.L., Li, Y.S., 2006a. Photochemical mineralization of di-n-butyl phthalate with H_2O_2/Fe^{3+}. Journal of Hazardous Materials, B135, 344-349.

Chiou, C.S., Shie, J.L., Chang, C.Y., Liu, C.C., Chang, C.T., 2006b. Degradation of di-n-butyl phthalate using photoreactor packed with TiO_2 immobilized on glass beads. Journal of Hazardous Materials, B137, 1123-1129.

Chu, W., Ma, C.W., 2000. Quantitative prediction of direct and indirect dye ozonation kinetics. Water Research, 34, 3153-3160.

Colarusso, P., Serpone, N., 1996. Sonochemistry effects of ultrasound on homogeneous chemical reactions and in environmental detoxification. Research on Chemical Intermediates, 22, 61-89.

Colborn, T., Dumanoski, D., Myers, J. P. (Eds), 1996. Our Stolen Future, Plume Publishing, New York.

Coleman H.M., Chiang, K., Amal, R., 2005. Effects of Ag and Pt on photocatalytic degradation of endocrine disrupting chemicals in water. Chemical Engineering Journal, 113, 65-72.

Comber, M.H.I., Williams, T.D., Stewart, K.M., 1993. The effect of nonylphenol on *Daphnia magna*. Water Research, 27, 273-276.

Cook, J. W., Dodds, E. C., Hewett, C. L., Lawson, W., 1934. Estrogenic activity of some condensed ring compounds in relation to their other biological activities. Proceedings of the Royal Society of London, B114, 272-286.

Craig, V. S. J., Ninham, B. W., Pashley, R. M., 1993. The effect of electrolytes on bubble coalescence in water. Journal of Physical Chemistry, 97, 10192-10197.

Crain, D.A., Eriksen, M., Iguchi, T., Jobling, S., Laufer, H., LeBlanc, G.A., Guillette Jr., L.J., 2007. An ecological assessment of bisphenol-A: Evidence from comparative biology. Reproductive Toxicology, 24, 225-239.

Crum, L. A., 1994. Sonoluminescence, sonochemistry, and sonophysics. Journal of the Acoustical Society of America, 95, 559-562.

Daborn, L. A., 1999. “Endocrine Disruption: Changing Times”, Conservation Council of New Brunswick, http://www.elements.nb.ca/theme/toxics/lia/lia.htm.

Dahlem, O., Demaiffe, V., Halloin, V., Reisse, J., 1998. Direct sonication system suitable for medium-scale sonochemical reactors. AlChE Journal, 44, 2724-2730.

D'Ascenzo, G., Di Corcia, A., Gentili, A., Manzini, R., Mastropasqua, R., Nazzari, M., Samperi, R., 2003. Fate of estrogen conjugates in municipal sewage transport and treatment facilities. Science of the Total Environment, 302, 199-209.

De Visscher, A., Van Eenoo, P., Drijvers, D., Van Langenhove, H., 1996. Kinetic model for the sonochemical degradation of monocyclic aromatic compounds in aqueous solution. Journal of Physical Chemistry, 100, 11636-11642.

De Visscher, A.; Van Langenhove, H., 1998. Sonochemistry of organic compounds in homogeneous aqueous oxidising systems. Ultrasonics Sonochemistry, 5, 87-92.

Deborde, M., Rabouan, S., Duguet, J.P., Legube, B., 2005. Kinetics of aqueous ozone-induced oxidation of some endocrine disruptors. Environmental Science and Technology, 39, 6086-6092.

Destaillats, H., Colussi, A.J., Joseph, J.M., Hoffmann, M.R., 2000. Synergistic effects of sonolyis combined with ozonolysis for the oxidation of azobenzene and methyl orange. Journal of Physical Chemistry, 104: 8930-8935.

Destaillats, H., Turjanski, A. G., Estrin, D. A., Hoffmann, M. R., 2002. Molecular Structure Effects on the Kinetics of Hydroxyl Radical Addition to Azo Dyes. Journal of Physical Organic Chemistry, 15**,** 287-292.

Destaillats H., Hoffmann, M. R., Wallace, H. C., 2003. Sonochemical Degradation of Pollutants. In Tarr M. A. (Ed.), Chemical Degradation Methods for Wastes and Pollutants-Environmental and Industrial Applications, 201-233, Marcel Dekker, Inc., New York.

Drijvers, D., van Langenhove, H., Beckers, M., 1999. Decomposition of phenol and trichloroethylene by the ultrasound/H_2O_2/CuO process. Water Research, 33, 1187-1194.

Entezari, M. H., Petrier, C., Devidal, P., 2003. Sonochemical degradation of phenol in water: a comparison of classical equipment with a new cylindrical reactor. Ultrasonics Sonochemistry, 10, 103-108.

Fatoki, O.S., Vernon, F., 1990. Phthalate esters in rivers of the greater Manchester area, U.K. Science of The Total Environment, 95, 227-232.

Fischer C.H., Hart, E.J., Henglein, A., 1986. Ultrasonic irradiation of water in the presence of $^{18,18}O_2$: Isotope exchange and isotopic distribution of H_2O_2. Journal of Physical Chemistry, 90, 1954-1956.

Flouriot, G., Pakdel, F., Ducouret, B., Valotaire, Y., 1995. Influence of xenobiotics on rainbow trout liver estrogen receptor and vitellogenin gene expression. Journal of Molecular Endocrinology, 15, 143–151.

Fromme, H., Küchler, T., Otto, T., Pilz, K., Müller, J., Wenzel, A., 2002. Occurrence of phthalates and bisphenol A and F in the environment. Water Research, 36, 1429-1438.

Fry, D.M., Toone, C.K., 1981. DDT-induced feminization of gull embryos. Science, 231, 919-924.

Fry, D.M., Toone, C.K., Speich, S.M., Peard, R.J., 1987. Sex ratio skew and breeding patterns of gulls: Demographic and toxicological considerations. Studies in Avian Biology, 10, 26-43.

Fukahori, S., Ichiura, H., Kitaoka, T., Tanaka, H., 2003. Capturing of bisphenol A photodecomposition intermediates by composite TiO_2-zeolite sheets. Applied Catalysis B: Environmental, 46, 453-462.

Ge, J., Qu, J., 2003. Degradation of azo dye acid red B on manganese dioxide in the absence and presence of ultrasonic irradiation. Journal of Hazardous Materials, B100, 197-207.

Gill, W.B., Schumacher, F.B., Bibbo, M., Straus, F.H., Schoenberg, H.W., 1979. Association of diethylstilbestrol exposure in utero with cryptorchidism, testicular hypoplasia and semen abnormalities. The Journal of Urology, 122, 36-39.

Glaze, W.H., Kang, J.W., Chapin, D.H., 1987. The chemistry of water treatment processes involving ozone, hydrogen peroxide and ultraviolet radiation. Ozone Science and Engineering, 9, 335-352.

Gogate, P.R., Pandit, A.B., 2004. A review of imperative technologies for wastewater treatment I: Oxidation technologies at ambient conditions. Advances in Environmental Research, 8, 501-551.

Gomes, R.L., Lester, J.N., 2003. Endocrine disruptors in Receiving Waters, In: Birkett J.W., Lester, J.N. (Eds.), Endocrine Disruptors in Wastewater and Sludge Treatment Processes, 177-217, CRC Press, Boca Raton, Florida.

Gottschalk C., Libra, J. A., Saupe, A. (Eds.), 2000. Ozonation of Water and Wastewater - A Practical Guide to Understanding Ozone and its Application, Wiley-VCH, Weinheim, Germany.

Gouldm, J.P., Groff, K.A., 1987. The kinetics of ozonolysis of synthetic dyes. Ozone Science and Engineering, 9, 153-164.

Gözmen, B., Oturan, M.A., Oturan, N., Erbatur, O., 2003. Indirect electrochemical treatment of bisphenol A in water via electrochemically generated Fenton's reagent. Environmental Science and Technology, 37, 3716-3723.

Gray, M.A., Metcalfe, C.D., 1997. Induction of testis-ova in japanese medaka (Oryzias latipes) exposed to p-nonylphenol. Environmental Toxicology and Chemistry, 16, 1082-1086.

Gray, K. A., Cleland, M. R., 1998. Environmental radiolysis for soil and sediment treatment: a review of chemistry, design and economic issues. Journal of Advanced Oxidation Technologies, 3, 22-36, 1998.

Guillette, L.J.Jr., Gross, T.S., Masson, G.R., Matter, N.M., Percival, H.F., Woodward, A.R., 1994. Developmental abnormalities of the gonad and sex hormone concentrations in

juvenile alligators from contaminated and control lakes in Florida. Environmental Health Perspectives, 104, 680-688.

Guillette, L.J.Jr., Pickford, D.B., Crain, D.A., Rooney, A.A., Percival, H.F., 1996. Reduction in penis size and plasma testosterone concentrations in juvenile alligators living in a contaminated environment. General and Comparative Endocrinology, 101, 32-42.

Gultekin, I., Ince, N.H., 2006. Degradation of aryl-azo-naphthol dyes by ultrasound, ozone and their combination: Effect of α-substituents. Ultrasonics Sonochemistry, 13, 208-214.

Gultekin, I., Ince, N.H., 2008. Ultrasonic destruction of bisphenol-A: the operating parameters. Ultrasonics Sonochemistry, 15, 524–529.

Gültekin, I., Mavrov, V., Ince, N.H., Oxidation of bisphenol A by ozonation, unpublished data.

Harris, C.A., Henttu, P., Parker, M.G., Sumpter J.P., 1997. The estrogenic activity of phthalate esters in vitro. Environmental Health Perspectives, 105, 802-811.

Hart, E. J., Henglein, A., 1985. Free radical and free atom reactions in the sonolysis of aqueous iodide and formate solutions. Journal of Physical Chemistry, 89, 4342-4347.

Hart, E.J., Henglein, A., 1986. Sonolytic decomposition of nitrous oxide in aqueous solution. Journal of Physical Chemistry, 90, 5992–5995.

Hart, E.J., Fischer, C.H., Henglein, A., 1986. Isotopic exchange in the sonolysis of aqueous solutions containing nitrogen-14 and nitrogen-15 molecules. Journal of Physical Chemistry, 90, 5989-5991.

Herbst, A.L., Senekjian, E.K., Frey, K., 1989. Abortion and pregnancy loss among diethylstilbestrol-exposed women. Seminars in Reproductive Endocrinology, 7, 124-129.

Henglein, A., 1987. Sonochemistry: historical developments and modern aspects, Ultrasonics, 25, 6-16.

Henglein, A., Ulrich, R., Lilie, J., 1989. Luminescence and Chemical Action by Pulsed Ultrasound. Journal of American Chemical Society, 111, 1974-1979.

Herbst, A.L., Ulfelder, H., Poskanzer, D.C., 1971. Adenocarcinoma of the vagina. Association of maternal stilbesterol therapy with tumor appearance in young women. The New England Journal of Medicine, 284, 878-881.

Horikoshi, S., Tokunaga, A., Hidaka, H., Serpone, N., 2004. Environmental remediation by an integrated microwave/UV illumination method VII. Thermal/non-thermal effects in the microwave-assisted photocatalyzed mineralization of bisphenol-A. Journal of Photochemistry and Photobiology A: Chemistry, 162, 33-40.

P.H. Howard (Ed.), 1989. Handbook of Environmental Fate and Exposure Data for Organic Chemicals, Vol. I., Lewis Publishers, Chelsea, Michigan.

Hua I, Höchemer R.H., Hoffmann, M.R., 1995. Sonolytic hydrolysis of p-nitrophenyl acetate: The role of supercritical water. Journal of Physical Chemistry, 99, 2335-2342.

Hua, I., Hoffmann, M.R., 1996. Kinetics and mechanism of the sonolytic degradation of CCl_4: intermediates and byproducts. Environmental Science and Technology, 30, 864-871.

Hua, I., Hoffmann, M.R., 1997. Optimization of ultrasonic irradiation as an advanced oxidation technology. Environmental Science and Technology, 31, 2237-2243.

Huber, M.M., Canonica, S., Park, G.Y., von Gunten, U., 2003. Oxidation of pharmaceuticals during ozonation and advanced oxidation processes. Environmental Science and Technology, 37, 1016-1024.

Hung, H.M., Hoffmann, M.R., 1998. Kinetics and mechanisms of the enhanced reductive degradation of CCl_4 by elemental iron in the presence of ultrasound. Environmental Science and Technology, 32, 3011-3016.

Hung, H., Ling, F.H., Hoffmann, M.R., 2000. Kinetics and mechanism of the enhanced reductive degradation of nitrobenzene by elemental iron in the presence of ultrasound. Environmental Science and Technology, 34, 1758-1763.

Hustert, K., Moza, P.N., 1988. Photocatalytic degradation of phthalates using titanium dioxide in aqueous solution. Chemosphere, 17, 1751-1754.

IEH (Institute for Environment and Health), 2005. Chemicals Purported to be Endocrine Disruptors: A Compilation of Published Lists (Web Report W20), Leicester, UK, MRC Institute for Environment and Health, http://www.le.ac.uk/ieh.

Iida, Y., Yasui, K., Tuziuti, T., Sivakumar, M., 2005. Sonochemistry and its dosimetry. Microchemical Journal, 80, 159-164.

Ike, M., Asano, M., Belkada, F.D., Tsunoi, S., Tanaka, M., Fujita, M., 2002. Degradation of biotransformation products of nonylphenol ethoxylates by ozonation and UV/TiO_2 treatment. Water Science and Technology, 46, 127-132.

Ince, N.H., Stefan, M.I., Bolton, J.R., 1997. UV/H_2O_2 degradation and toxicity reduction of textile azo dyes: remazol black-B, a case study, Journal of Advanced Oxidation Technologies 2, 442-448.

Ince, N.H., 1999. Critical effect of hydrogen peroxide in photochemical dye degradation. Water Research, 33, 1080-1084.

Ince, N.H., Apikyan, I.G., 2000. Combination of activated carbon adsorption with light-enhanced chemical oxidation via hydrogen peroxide. Water Research, 34, 4169-4176.

Ince NH, Tezcanli G., 2001. Reactive dyestuff degradation by combined sonolysis and ozonation. Dyes Pigments, 49, 145-153.

Ince, N.H., Tezcanli, G., Belen, R.K., Apikyan, I.G., 2001. Ultrasound as a catalyzer of aqueous reaction systems: the state of the art and environmental applications. Applied Catalysis B: Environmental, 29, 167-176.

Ince, N.H., Tezcanli-Güyer, G., 2004. Impacts of pH and molecular structure on ultrasonic degradation of azo dyes. Ultrasonics, 42, 591-596.

Ioan, I., Wilson, S., Lundanes, E., Neculai, A., 2007. Comparison of Fenton and sono-Fenton bisphenol A degradation. Journal of Hazardous Materials, 142, 559-563.

Irmak, S., Erbatur, O., Akgerman, A., 2005. Degradation of 17β-estradiol and bisphenol A in aqueous medium by using ozone and ozone/UV techniques. Journal of Hazardous Materials, 126, 54-62.

Jayaweera, I., 2003. Supercritical Water Oxidation Technology, In Tarr, M.A. (Ed.), Chemical Degradation Methods for Wastes and Pollutants-Environmental and Industrial Applications, 121-163, Marcel Dekker, Inc., New York.

Jiang, J.Q., Yin, Q., Zhou, J.L., Pearce, P., 2005. Occurrence and treatment trials of endocrine disrupting chemicals (EDCs) in wastewaters. Chemosphere, 61, 544-550.

Jintelmann, J., Katayama, A., Kurihara, N., Shore, L., Wenzel, A., 2003. Endocrine disruptors in the environment. Pure and Applied Chemistry, 75, 631-681.

Jobling, S., Sumpter, J.P., 1993. Detergent components in sewage effluent are weakly estrogenic to fish: an in vitro study using rainbow trout (oncorhynchus mykiss) hepatocytes. Aquatic Toxicology, 27, 361–372.

Jobling, S., Sheahan, D., Osborne, J.A., Matthiessen, P., Sumpter, J.P., 1996. Inhibition of testiculary growth in rainbow trout (oncorhynchus mykiss) exposed to estrogenic alkylphenolic chemicals. Environmental Toxicology and Chemistry, 15, 194–202.

Joseph, J.M., Destaillats, H., Hung, H.M., Hoffmann, M.R., 2000. The sonochemical degradation of azobenzene and related azo dyes: rate enhancements via Fenton's reactions. Journal of Physical Chemistry A, 104, 301-307.

Kamiya, T., Yamauchi, T., Hirotsuji, J., Fujita, M., 2005. Ozone-based decomposition of main endocrine disruption chemicals in sewage effluent. Ozone Science and Engineering, 27, 389-395.

Kaneco, S., Rahman, M. A., Suzuki, T., Katsumata, H., Ohta, K., 2004. Optimization of solar photocatalytic degradation conditions of bisphenol A in water using titanium dioxide. Journal of Photochemistry and Photobiology A: Chemistry, 163, 419-424.

Kaneco, S., Katsumata, H., Suzuki, T., Ohta, K., 2006. Titanium dioxide mediated photocatalytic degradation of dibutyl phthalate in aqueous solution – kinetics, mineralization and reaction mechanism. Chemical Engineering Journal, 125, 59-66.

Kang, J.W., Hoffmann, M.R., 1998. Kinetics and mechanism of the sonolytic destruction of methyl-tert-butyl ether by ultrasonic irradiation in the presence of ozone, Environmental Science and Technology 32, 3194-3199.

Katsumata, H., Kawabe, S., Kaneco, S., Suzuki, T., Ohta, K., 2004. Degradation of bisphenol A in water by the photo-Fenton reaction. Journal of Photochemistry and Photobiology A: Chemistry, 162, 297-305.

Kidak, R., Ince, N.H., 2006. Effects of operating parameters on sonochemical deceomposition of phenol, Journal of Hazardous Materials B, 137, 1453-1457.

Kim, J., Korshin, G.V., Velichenko, A.B., 2005. Comparative study of electrochemical degradation and ozonation of nonylphenol. Water Research, 39, 2527-2534.

Kim, J. K., Martinez, F., Metcalfe, I. S., 2007. The beneficial role of use of ultrasound in heterogeneous Fenton-like system over supported copper catalysts for degradation of p-chlorophenol. Catalysis Today, 124, 224–231.

Kitajima, M., Hatanaka, S., Hayashi, S., 2006. Mechanism of O_2-accelerated sonolysis of bisphenol A. Ultrasonics, 44, 371-373.

Klassen, N.V., Marchington, D., McGowan, H.C.E., 1994. H_2O_2 determination by the I_3^- method and by $KMnO_4$ titration. Analytical Chemistry, 66, 2921-2925.

Kohtani, S., Koshiko, M., Kudo, A., Tokumura, K., Ishigaki, Y., Toriba, A., Hayakawa, K., Nakagaki, R., 2003. Photodegradation of 4-alkylphenols using $BiVO_4$ photocatalyst under irradiation with visible light from a solar simulator. Applied Catalysis B: Environmental, 46, 573-586.

Kohtani, S., Hiro, J., Yamamoto, N., Kudo, A., Tokumura, K., Nakagaki, R., 2005. Adsorptive and photocatalytic properties of Ag-loaded $BiVO_4$ on the degradation of 4-n-alkylphenols under visible light irradiation. Catalysis Communications, 6, 185-189.

Kolpin, D.W., Furlong, E.T., Thurman, E.M., Zaug, S.D., Barber, L.B., Buxton, H.T., 2002. Pharmaceuticals, hormones and other organic wastewater contaminants in US streams, 1999-2000. A national reconnaissance. Environmental Science and Technology, 36, 1202-1211.

Kontronarou, A., Mills, G., Hoffmann, M. R., 1991. Ultrasonic irradiation of p-nitrophenol in aqueous solution. Journal of Physical Chemistry, 95, 3630-3638.

Korshin, G.V., Kim, J., Gan, L., 2006. Comparative study of reactions of endocrine disruptors bisphenol A and diethylstilbestrol in electrochemical treatment and chlorination. Water Research, 40, 1070-1078.

Kosky, P.E., Guggenheim, E.A., 1991. The aqueous phase in the interfacial synthesis of polycarbonates. 1. Ionic equilibria and experimental solubilities in the BPA-NaOH-H_2O system. Industrial and Engineering Chemistry Research, 30, 462-467.

Krishnan, A.V., Stathis, P., Permuth, S.F., Tokes, L., Feldman, D., 1993. Bisphenol-A: an estrogenic substance is released from polycarbonate flasks during autoclaving. Endocrinology, 132, 2279-2286.

Kristol, D.S., Klotz, H., Parker, R.C., 1981. The effect of ultrasound on the alkaline hydrolysis of nitrophenyl esters. Tetrahedron Letters, 22, 907-908.

Ku, Y., Tu, Y., Ma, C., 2005. Effect of hydrogen peroxide on the decomposition of monochloropehenols by sonolysis in aqueous solution. Water Research, 39, 1093-1098.

Kurinobu, S., Tsurusaki, K., Natui, Y., Kimata, M., Hasegawa, M., 2007. Decomposition of pollutants in wastewater using magnetic photocatalyst particles. Journal of Magnetism and Magnetic Materials, 310, 1025-1027.

Lau, T.K., Chu, W., Graham, N., 2005. The degradation of endocrine disruptor di-n-butyl phthalate by UV irradiation: A photolysis and product study. Chemosphere, 60, 1045-1053.

Lee, J., Park, H., Yoon, J., 2003. Ozonation characteristics of bisphenol A in water. Environmental Technology, 24, 241-248.

Lee, J.M., Kim, M.S., Kim, B.W., 2004. Photodegradation of bisphenol-A with TiO_2 immobilized on the glass tubes including the UV light lamps. Water Research, 38, 3605-3613.

Leighton T. G. (Ed.), 1994. The Acoustic Bubble, Academic Press, Harcourt Brace&Company, London.

Lenz, K., Beck, V., Fuerhacker, M., 2004. Behaviour of bisphenol A (BPA), 4-nonylphenol (4-NP) and 4-nonylphenol ethoxylates (4-NP1EO, 4-NP2EO) in oxidative water treatment water processes. Water Science and Technology, 50, 141-147.

Lepoint, T., Mullie, F., 1994. What Exactly is Cavitation Chemistry. Ultrasonics Sonochemistry, 1, 13-22.

Lepoint-Mullie, F., De Pauw, D., Lepoint, T., 1996. Analysis of the New Electrical Model of Sonoluminescence. Ultrasonics Sonochemistry, 3, 73-76.

Li, L., Zhu, W., Chen, L., Zhang, P., Chen, Z., 2005. Photocatalytic ozonation of dibutyl phthalate over TiO_2 film. Journal of Photochemistry and Photobiology A: Chemistry, 175, 172-177.

Li, L., Zhu, W., Zhang, P., Zhang, Q., Zhang, Z., 2006. AC/O_3-BAC processes for removing refractory and hazardous pollutants in raw water. Journal of Hazardous Materials, B135, 129-133.

Mailhot, G., Sarakha, M., Lavedrine, B., Cáceres, J., Malato, S., 2002. Fe(III)-solar light induced degradation of diethyl phthalate (DEP) in aqueous solutions. Chemosphere, 49, 525-532.

Makkino, K., Mossoba, M.M., Riesz, P., Chemical effects of ultrasound on aqueous solutions. Evidence for hydroxyl and hydrogen free radicals by spin trapping. Journal of American Chemical Society, 104, 3537-3539, 1982.

Mahamuni, N.N., Pandit, A.B., 2006. Effect of additives on ultrasonic degradation of phenol. Ultrasonics Sonochemistry, 13, 165-174.

Margulis, M.A., 1992. Fundamental Aspects of Sonochemistry. Ultrasonics, 30, 152-155.

Margulis, M.A., (Ed.), 1995. Sonochemistry and Cavitation, Gordon and Breach Science Publishers, Amsterdam.

Mason, T.J. (Ed.), 1990. Chemistry with Ultrasound - Critical Reports on Applied Chemistry, Volume 28, Society of Chemical Industry, Elsevier Applied Science, London.

Mason, T.J., Lorimer, J.P., Bates, D.M., 1992. Quantifying sonochemistry: casting some light on a black art. Ultrasonics, 30, 40-42.

Mason, T.J., Lorimer J.P., Bates, D.M., Zhao, Y., 1994. Dosimetry in sonochemistry: The use of aqueous terephthalate ion as a fluorescence monitor. Ultrasonics Sonochemistry, 1, 91-95.

Mason, T.J., Luche, J.L., 1997. Ultrasound as a New Tool for Synthetic Chemists. In van Eldik, R., Hubbard, C.D. (Eds.), Chemistry Under Extreme or Non-Classical Conditions, Chapter 8, 317-380, John Wiley & Sons. Inc., New York.

Mason, T.J., Cordemans de Meulenaer, E., 1998. Practical Considerations for Process Optimization. In Luche, J.L. (Ed.), Synthetic Organic Sonochemistry, Chapter 8, 301-329, Plenum Press, New York.

Mason, T. J. (Ed.), 1999. Sonochemistry, Oxford University Press Inc., New York.

Mason, T.J., Lorimer, J.P. (Eds), 2002. Applied Sonochemistry – The Uses of Power Ultrasound in Chemistry and Processing, Wiley-VCH, Weinheim.

Mason, T.J., Peters, D. (Eds), 2002. Practical Sonochemistry: Uses and Applications of Ultrasound, Second Edition, Horwood Publishing, Chichester.

Masten, S.J., Davies, S.H., 1993. The use of ozonation to degrade organic contaminants in wastewaters. Environmental Science and Technology, 28, 180-185.

McLeese, D.W., Zitko, V., Sergeant, D.B., Burridge, L., Metcalfe, C.D., 1981. Lethality and accumulation of alkylphenols in aquatic fauna. Chemosphere, 10, 723-730.

Mead, L., Sutherland, R.G., Verrall, R.E., 1976. The effect of ultrasound on water in the presence of dissolved gases**.** Canadian Journal of Chemistry, 54, 1114-1120.

Metzler, M., Pfeiffer, E., 2001. Chemistry of Natural and Antropogenic Endocrine Active Compounds, In Metzler, M. (Ed.), Endocrine Disruptors Part I, 63-80, Springer, Germany.

Mocarelli, P., Brambilla, P., Gerthoux, P.M., Patterson, D.G., Jr., Needham, L.L., 1996. Change in sex ratio with exposure to dioxin. The Lancet, 348, 401-416.

Moon, S., Duchin, L.,Cooney, J.V., 1979. Application of ultrasound to organic reactions: ultrasonic catalysis on hydrolysis of carboxylic acid esters. Tetrahedron Letters, 20, 3917-3920.

Morrison, P.A., Leatherland, J.F., Sonstegard, R.A., 1985. Plasma cortisol and sex steroid levels in great lakes coho salmon (Oncorhynchus kisutch walbaum) in relation to fecundity and egg survival. Comparative Biochemistry and Physiology, 80A, 61-68.

Muneer, M., Theurich, J., Bahnemann, D., 2001. Titanium dioxide mediated photocatalytic degradation of 1,2-diethyl phthalate. Journal of Photochemistry and Photobiology A: Chemistry, 143, 213-219.

Nagata, Y., Hirai, K., Bandow, H., Maeda, Y., 1996. Decomposition of hydrobenzoic and humic acids in water by ultrasonic irradiation. Environmental Science and Technology, 30, 1133-1138.

Nakashima, T., Ohko, Y., Tryk, D.A., Fujishima, A., 2002. Decomposition of endocrine-disrupting chemicals in water by use of TiO_2 photocatalysts immobilized on polytetrafluoroethylene mesh sheets. Journal of Photochemistry and Photobiology A: Chemistry, 151, 207-212.

Naylor, C.G., Mierure, J.P., Weeks, J.A., Castaldi, F.J., Romano, R.R., 1992. Alkyphenol ethoxylates in the environment. Journal of the American Oil Chemists Society, 69, 695-793.

Neamtu, M., Frimmel, F.H., 2006a. Degradation of endocrine disrupting bisphenol A by 254 nm irradiation in different water matrices and effect on yeast cells. Water Research, 40, 3745-3750.

Neamtu, M., Frimmel, F.H., 2006b. Photodegradation of endocrine disrupting chemical nonylphenol by simulated solar UV-irradiation. Science of the Total Environment, 369, 295-306.

Negishi, K., 1961. Experimental Studies on Sonoluminescence and Ultrasonic Cavitation. Journal of the Physical Society of Japan, 16, 1450-1465.

Neppiras, E. A., 1980. Acoustic Cavitation. Physical Reports, 61, 159-251.

Neyens, E., Baeyens, J.A, 2003. Review of classic Fenton's peroxidation as an advanced oxidation technique. Journal of Hazardous Materials, B98, 33-50.

Nilsson, C., 1994. Phthalic acid esters used as plastic additives: comparisons of toxicological effects. Swedish National Chemicals Inspectorate, Solna.

Nimrod, A.C., Benson, W.H., 1996. Environmental estrogenic effects of alkylphenol ethoxylates. Critical Reviews in Toxicology, 26, 335-364.

Ning, B., Graham, N.J.D., Zhang, Y., 2007. Degradation of octylphenol and nonylphenol by ozone-Part I: Direct reaction. Chemosphere, 68, 1163-1172.

Noltingk, B.E., Neppiras, E.A., 1950. Cavitation Produced by Ultrasonics. Proceedings of Physical Society, B63, 674-685.

Oakes, J., Gratton, P., 1998. Kinetic Investigations of Azo Dye Oxidation in Aqueous Media. Journal of the Chemical Society- Perkin Transactions 2, 1857-1864.

Oh, B.S., Jung, Y.J., Oh, Y.J., Yoo, Y.S., Kang, J.W., 2006. Application of ozone, UV and ozone/UV processes to reduce diethyl phthalate and its estrogenic activity. Science of the Total Environment, 367, 681-693.

Ohko, Y., Ando, I., Niwa, C., Tatsuma, T., Yamamura, T., Nakashima, T., Kubota, Y., Fujishima, A., 2001. Degradation of bisphenol A in water by TiO_2 photocatalyst. Environmental Science and Technology, 35, 2365-2368.

Okamoto, Y., Hayashi, T., Toda, C., Ueda, K., Hashizume, K., Itoh, K., Nishikawa, J., Nishihara, T., Kojima, N., 2006. Formation of estrogenic products from environmental phthalate esters under light exposure. Chemosphere, 64, 1785-1792.

Okitsu, K., Iwasaki, K., Yobiko, Y., Bandow, H., Nishimura, R., Maeda, Y., 2005. Sonochemical degradation of azo dyes in aqueous solution: a heterogeneous kinetics model taking into account the local concentration of OH radicals and azo dyes. Ultrasonics Sonochemistry, 12, 255-262.

Olson, T.M., Barbier, P.F., 1994. Oxidation kinetics of natural organic matter by sonolysis and ozone. Water Research, 28, 1383-1391.

Ooka, C., Yoshida, H., Horio, M., Suzuki, K., Hattori, T., 2003. Adsorptive and photocatalytic performance of TiO_2 pillared montmorillonite in degradation of endocrine disruptors having different hydrophobicity. Applied Catalysis B: Environmental, 41, 313-321.

Ooka C., Yoshida, H., Suzuki, K., Hattori, T., 2004. Highly hydrophobic TiO_2 pillared clay for photocatalytic degradation of organic compounds in water. Microporous and Mesoporous Materials, 67, 143-150.

Özen, A.S., Aviyente, V., Klein. R.A., 2003. Modeling the oxidative degradation of azo dyes : a density functional theory study. Journal of Physical Chemistry A, 107, 4898-4907.

Özen, A.S., Aviyente, V., Tezcanli-Güyer, G., Ince, N.H., 2005. Experimental and modeling approach to decolorization of azo dyes by ultrasound: degradation of the hydrazone tautomer. Journal of Physical Chemistry A, 109, 3506-3516.

Panter, G.H., Thompson, R.S., Beresford, N., Sumpter, J.P., 1999. Transformation of non oestrogenic steroid metabolite to an estrogenically active substance by minimal bacterial activity. Chemosphere, 38, 3579-3596.

Parsons, S.A., Williams, M., 2004. Introduction, In Parsons, S. (Ed.), Advanced Oxidation Processes for Water and Wastewater Treatment, 1-6, IWA Publishing, London, UK.

Pawlowski, S., Islinger, M., Völkl, A., Braunbeck, T., 2000. Temperature-dependent vitellogenin-mRNA expression in primary cultures of rainbow trout (Oncorhynchus mykiss) hepatocytes at 14 and 18 degrees C. Toxicology in Vitro, 14, 531-540.

Pelizetti, E., Minero, C., Maurino, V., Sclafani A., Hidaka, H., Serpone, N., 1989. Photocatalytic degradation of nonylphenol ethoxylated surfactants. Environmental Science and Technology, 23, 1380-1385.

Perez, P., Pulgar, R., Olea-Serrano, F., Villalobos, M., Rivas, A., Metzler, M., Pedraza, V., Olea, N., 1998. The estrogenicity of bisphenol A-related diphenylalkanes with various substituents at the central carbon and the hydroxy groups. Environmental Health Perspectives, 106, 167-174.

Perry, R.H., Green, D. (Eds), 1984. Perry's Chemical Engineers' Handbook, Sixth Edition, McGraw-Hill, Malaysia.

Pétrier, C., Micolle, M., Merlin, G., Luche, J. L., Reverdy, G., 1992. Characteristics of pentachlorophenate degradation in aqueous solution by means of ultrasound. Environmental Science and Technology, 26, 1639-1642.

Petrier, C., Lamy, M.F., Francony, A., Benahcene, A., David, B., Renaudin, V., Gondrexon, N., 1994. Sonochemical degradation of phenol in dilute aqueous solutions: comparison of the reaction rates at 20 kHz and 487 kHz. Journal of Physical Chemistry, 98, 10514-10520.

Petrier, C., Francony, A., 1997. Ultrasonic waste-water treatment: incidence of ultrasonic frequency on the rate of phenol and carbon tetrachloride degradation. Ultrasonics Sonochemistry, 4, 295-300.

Petrier, C., Luche, J.L., 1998. Sonochemistry of Solutions. In Luche, J.L. (Ed.), Synthetic Organic Sonochemistry, Chapter 2, 51-90, Plenium Press, New York.

Pignatello, J.J., 1992. Dark and photoassisted Fe^{3+}-catalyzed degradation of chlorophenoxy herbicides by hydrogen peroxide. Environmental Science and Technology, 26, 944-951.

Private communication, 2004. PISA Textile Corp., Istanbul.

Psillakis, E., Mantzavinos, D., Kalogerakis, N., 2004. Monitoring the sonochemical degradation of phthalate esters in water using solid-phase microextraction. Chemosphere, 54, 849-857.

Rayleigh, O.M., 1917. On the pressure developed in a liquid during the collapse of a spherical cavity. Philosophical Magazine Series, 34, 94-98.

Rehorek, A., Tauber, M., Gübitz, G., 2004. Application of power ultrasound for azo dye degradation. Ultrasonics Sonochemistry, 11, 177-182.

Reisse, J., 1995. Proceedings of the 15th International Congress on Acoustics, Trondheim, Norway, 409.

Riesz, P., Kondo, T., Krishna, C.M., 1990. Sonochemistry of volatile and nonvolatile solutes in aqueous solutions. Ultrasonics, 28, 295-303.

Riesz, P., Mason, T.J. (Ed.), 1991. Advances in Sonochemistry, Vol. 2, JAI Press, London.

Rosenfeldt, E.J., Linden, K.G., 2004. Degradation of endocrine disrupting chemicals bisphenol A, ethinyl estradiol, and estradiol during UV photolysis and advanced oxidation processes. Environmental Science and Technology, 38, 5476-5483.

Routledge, E.J., Sumpter, J.P., 1996. Estrogenic activity of surfactants and some of their degradation products assessed using a recombinant yeast screen. Environmental Toxicology and Chemistry, 15, 241-248.

RTECS, 1997. Registry of Toxic Effects of Chemical Substances, National Institute for Occupational Safety and Health, Ohio.

Ruppert, G., Bauer, R., 1993. The photo-Fenton reaction-an effective photochemical wastewater treatment process. Journal of Photochemistry and Photobiology A: Chemistry, 73, 75-78.

Sehested, K., Holman, J., Bjergbahhe, E., Hart, E.J., 1984. A pulse radiolytic study of the reaction $OH+O_3$ in aqueous medium. Journal of Physical Chemistry, 88, 4144-4147.

Sehgal, C., Yu, T.J., Sutherland, R.G., Verrall, R., 1982. Use of 2,2-diphenyl-1-picrylhydrazyl to investigate the chemical behavior of free radicals induced by ultrasonic cavitation. Journal of Physical Chemistry, 68, 2982-2986.

Serpone, N., Terzian, R., Hidaka, H., Pelizetti, E., 1994. Ultrasonic induced dehalogenation and oxidation of 2-chlorophenol, 3-chlorophenol, and 4-chlorophenol in air-equilibrated aqueous media. Similarities with irradiated semiconductor particulates. Journal of Physical Chemistry, 98, 2634-2640.

Sharma, K.K., Rao, B.S.M., Mohan, H., Mittal, J.P., Oakes, J., Neill, P.O., 2002. Free-radical-induced oxidation and reduction of 1-arylazo-2-naphthol dyes: a radiation chemical study, Journal of Physical Chemistry A, 106, 2915-2923.

Sharpe, R.M., Shakkebaek, N.E., 1993. Are estrogens involved in falling sperm counts and disorder of the male reproductive tract?. The Lancet, 341, 1392-1395.

Shu, H.Y., Huang, C.R., 1995. Degradation of commercial azo dyes in water using ozonation and UV enhanced ozonation process. Chemosphere, 31, 3813-3825.

Sigma-Aldrich, 2004. Tert-Butanol Material Safety Data Sheet.

Sivakumar, M., Pandit, A.B., 2001. Ultrasound enhanced degradation of Rhodamine B: optimization with power density. Ultrasonics Sonochemistry, 8, 233-240.

Skoumal, M., Cabot, P., Centellas, F., Arias, C., Rodríguez, R.M., Garrido, J.A., Brillas, E., 2006. Mineralization of paracetamol by ozonation catalyzed with Fe^{2+}, Cu^{2+} and UVA light. Applied Catalysis B: Environmental, 66, 228-240.

Soto, A.M., Justicia, H., Wray, J.W., Sonnenschein C., 1991. p-nonyl-phenol: an estrogenic xenobiotic released from modified polystyrene. Environmental Health Perspectives, 92, 167–173.

Soto, A.M., Sonnenschein, C., Chung, K.L., Fernandez, M.F., Olea, N., Serrano, F.O., 1995. The e-screen assay as a tool to identify estrogens: an update on estrogenic environmental pollutants. Environmental Health Perspectives, 103, 113-122.

Spelsberg, T.C., Riggs, B.L., 1987. Evidence of estrogen receptors in normal human osteoblast-like cells. Science, 241, 84-86.

Staehelin, J., Hoigné, J., 1982. Decomposition of ozone in water: rate of initiation by hydroxide ions and hydrogen peroxide. Environmental Science and Technology, 16, 676-681.

Staples, C.A., Dorn, P.B., Klecka, G.M., O'Block, S.T., Harris, L.R., 1998. A review of the environmental fate, effects, and exposures of bisphenol A. Chemosphere, 36, 2149-2173.

Staples, C.A., Parkerton, T.F., Peterson, D.R., 2000. A risk assessment of selected phthalate esters in North American and Western European surface waters. Chemosphere, 40, 885-891.

Steinmetz, R., Brown, N.G., Allen, D.L., Bigsby, R.M., Ben-Jonathan, N., 1997. The environmental estrogen bisphenol A stimulates prolactin release in vitro and in vivo. Endocrinology, 138, 1780-1786.

Stroud, S. W., 1940. Metabolism of the parent compounds of some of the simpler sythetic estrogenic hydrocarbons. Journal of Endocrinology, 2, 55-62.

Suslick, K.S., Hammerton, D.A., Cline, R.E., 1986. Sonochemical Hot Spot. Journal of American Chemical Society, 108, 5641-5642.

Suslick, K.S., 1990. Sonochemistry. Science, 247, 1439-1445.

Suslick, K.S., Doktycz, S.J., Flint, E.B., 1990. On the origin of sonoluminescence and sonochemistry. Ultrasonics, 28, 280-290.

Suslick, K.S., 2006. "The Chemistry of Ultrasound", http://www.scs.uiuc.edu/suslick/britannica.html

Synder, S.A., Westerhoff, P., Yoon, Y., Sedlak, D.L., 2003. Pharmaceuticals, personal care products, and endocrine disruptors in water: Implications for the water industry. Environmental Engineering Science, 20, 449-469.

Takeuchi, T., Tsutsumi, O., 2002. Serum bisphenol A concentrations showed gender differences, possibly linked to androgen levels. Biochemical and Biophysical Research Communications, 291, 76-78.

Tan, G.H., 1995. Residue levels of phthalate esters in water and sediment samples from the Klang River basin. Bulletin of Environmental Contamination and Toxicology, 54, 171-176.

Tatarova, L.A., Trofimova, K.S., Gorban, A.V., Khaliullin, A.K., 2004. Reaction of carbon tetrachloride with hydrogen peroxide. Russian Journal of Organic Chemistry, 40, 1403-1406.

Tauber, A., Mark, G., Schumann, H., Sonntag, C., 1999a. Sonolysis of tert-butyl alcohol in aqueous solution. Journal of the Chemical Society, Perkin Transactions 2, 1129-1135.

Tauber, A., Schuchmann, H.P., von Sonntag, C., 1999b. Sonolysis of aqueous 4-nitrophenyl acetate - no evidence for hydrolysis induced by transient supercriticality. Chemistry-A European Journal, 5, 2198-2202.

Ternes, T.A., Kreckel, P., Mueller, J., 1999. Behaviour and occurrence of oestrogens in municipal sewage treatment plants-II. Aerobic batch experiments with activated sludge. Science of the Total Environment, 225, 91-99.

Tezcanli-Guyer, G., Ince, N.H., 2003. Degradation and toxicity reduction of textile dyestuff by ultrasound. Ultrasonics Sonochemistry, 10, 235-240.

Tezcanli-Güyer, G., Ince, N.H., 2004. Individual and combined effects of ultrasound, ozone and UV irradiation: a case study with textile dyes. Ultrasonics, 42, 603-609.

Thompson, D., Vilbrandt, F.C., Gray, W.C., 1953. The effect of insonation on the specific reaction rate constant in the acid hydrolysis of ethyl acetate. Journal of the Acoustical Society of America, 25, 485-490.

Thuren, A., 1986. Determination of phthalates in aquatic environments. Bulletin of Environmental Contamination and Toxicology, 36, 33-40.

U.S. Department of Health, Education and Welfare (DHEW), 1978. 13-Week Subchronic Toxicity Studies of Direct Blue 6, Direct Black 38 and Direct Brown 95 Dyes.

U.S. Environmental Protection Agency, 1996. Best Management Practices for Pollution Prevention in the Textile Industry, Eastern Research Group, Inc., Washington DC.

U.S. Environmental Protection Agency, 1997. Special Report on Environmental Endocrine Disruption: An Effects Assessment and Analysis, 630/R-96/012, Washington DC.

U.S. Environmental Protection Agency, 1998. Advanced Photochemical Oxidation Processes, 625/R-98/004, Washington DC.

U.S. Environmental Protection Agency, 2001a. Handbook on Advanced Nonphotochemical Oxidation Processes, 625/R-01/004, Washington DC.

U.S. Environmental Protection Agency, 2001b. Removal of Endocrine Disruptor Chemicals Using Water Treatment Processes, 625/R-00/015, Washington DC.

Verrall, R.E., Sehgal, C., Suslick, K.S. (Ed.), 1988. Sonochemistry: Its Chemical, Physical and Biological Effects, VCH, New York.

Vinodgopal, K., Peller, J., Makagon, O., Kamat, P.V., 1998. Ultrasonic mineralization of a reactive textile azo dye, Remazol Black B. Water Research, 32, 3646-3650.

Vinodgopal, K., Ashokkumar, M., Grieser, F., 2001. Sonochemical degradation of a polydisperse nonylphenol ethoxylate in aqueous solution. Journal of Physical Chemistry B, 105, 3338-3342.

Vitali, M., Guidotti, M., Macilenti, G., Cremisini, C., 1997. Phthalate esters in freshwaters as markers of contamination sources - a site study in Italy. Environment International, 23, 337-347.

vom Saal, F.S., Cooke, P.S., Buchanan, D.L., Palanza, P., Thayer, K.A., Nagel, S.C., Parmigiani, S., Welshons, W.V., 1988. A physiologically based approach to the study of bisphenol A and other estrogenic chemicals on the size of reproductive organs, daily sperm production, and behavior. Toxicology and Industrial Health, 14, 239-260.

von Gunten, U., 2003. Ozonation of drinking water: Part I. Oxidation kinetics and product formation. Water Research, 37, 1443-1467.

Walker, B.S., Janney, J.C., 1990. Estrogenic substances. II. Analysis of plant sources. Endocrinology, 14, 389-392.

Walling, C., 1975. Fenton's reagent revisited. Accounts of Chemical Research, 8, 125-131.

Wang, G., Wu, F., Zhang, X., Luo, M., Deng, N., 2006. Enhanced TiO_2 photocatalytic degradation of bisphenol A by β-cyclodextrin in suspended solutions. Journal of Photochemistry and Photobiology A: Chemistry, 179, 49-56.

Wang, L., Zhu, L., Luo, W., Wu, Y., Tang, H., 2007. Drastically enhanced ultrasonic degradation of methyl orange by adding CCl_4. Ultrasonics Sonochemistry, 14, 253-258.

Watanabe, N., Horikoshi, S., Kawabe, H., Sugie, Y., Zhao, J., Hidaka, H., 2003. Photodegradation mechanism for BPA at the TiO_2/H_2O surfaces. Chemosphere 52, 851-859.

Weavers, L. K., Ling, F. H., Hoffmann, M. R., "Aromatic Compound Degradation in Water Using a Combination of Sonolysis and Ozonolysis," Environmental Science and Technology, 32, 2727-2733, 1998.

Weissler, A., Cooper, H. W., Snyder, S., Chemical Effect of Ultrasonic Waves: Oxidation of Potassium Iodide Solution by Carbon Tetrachloride, J. Am. Chem. Soc., 72, 1769-1775, 1950.

WWF, 2000. European Toxics Programme Report. Bisphenol A-A Known Endocrine Disruptor, UK.

Xie, Y.B., Li, X.Z., 2006. Degradation of bisphenol A in aqueous solution by H_2O_2-assisted photoelectrocatalytic oxidation. Journal of Hazardous Materials, B138, 526-533.

Xu, B., Gao, N.Y., Sun, X.F., Xia, S.J., Rui, M., Simonnot, M.O., Causserand, C., Zhao, J.F., 2007. Photochemical degradation of diethyl phthalate with UV/H_2O_2. Journal of Hazardous Materials, B139, 132-139.

Yamamoto T., Yasuhara A., 1999. Quantities of bisphenol A leached from plastic waste samples. Chemosphere, 38, 2569-2576.

Yamamoto T., Yasuhara A., Shiraishi H., Nakasugi O., 2001. Bisphenol A in hazardous waste landfill leachates. Chemosphere, 42, 415-418.

Yang, G.P., Zhao, X.K., Sun, X.J., Lu, X.L., 2005. Oxidative degradation of diethyl phthalate by photochemically-enhanced Fenton reaction. Journal of Hazardous Materials, B126, 112-118.

Yim, B., Nagata, Y., Maeda, Y., 2002. Sonolytic degradation of phthalic acid esters in aqueous solutions: Acceleration of hydrolysis by sonochemical action. Journal of Physical Chemistry, A106, 104-107.

Yim, B., Yoo, Y., Maeda, Y., 2003. Sonolysis of alkylphenols in aqueous solution with Fe(II) and Fe(III). Chemosphere, 50, 1015-1023.

Ying, G.G., Kookana, R.S., Ru, Y.J., 2002a. Occurence and fate of hormone steroids in the environment. Environment International, 28, 545-551.

Ying, G.G., Williams, B., Kookana, R., 2002b. Environmental fate of alkylphenols and alkylphenol ethoxylates-a review. Environment International, 28, 215-226.

Yunrui, Z., Wanpeng, Z., Fudong, L., Jianbing, W., Shaoxia, Y., 2007. Catalytic activity of Ru/Al_2O_3 for ozonation of dimethyl phthalate in aqueous solution. Chemosphere, 66, 145-150.

Zepp, R.G., Faust, B.C., Hoigne, J., 1992. Hydroxyl radical formation in aqueous reactions (pH 3-8) of iron(II) with hydrogen peroxide: The photo-Fenton reaction. Environmental Science and Technology, 26, 313-319.

Zhan, M., Yang, X., Xian, Q., Kong, L., 2006. Photosensitized degradation of bisphenol A involving reactive oxygen species in the presence of humic substances. Chemosphere, 63, 378-386.

Zhang, L., Kanki, T., Sano, N., Toyoda, A., 2003. Development of TiO_2 photocatalyst reaction for water purification. Separation and Purification Technology, 31, 105-110.

Zhao, X., Yang, G., Wang, Y., Gao, X., 2004. Photochemical degradation of dimethyl phthalate by Fenton reagent. Journal of Photochemistry and Photobiology A: Chemistry, 161, 215-220.

Zheng, W., Maurin, M., Tarr, M.A., 2005. Enhancement of sonochemical degradation of phenol using hydrogen atom scavengers. Ultrasonics Sonochemistry, 12, 313-317.

Zhou, D., Wu, F., Deng, N., Xiang, W., 2004. Photooxidation of bisphenol A (BPA) in water in the presence of ferric and carboxylate salts. Water Research, 38, 4107-4116.

Zollinger, H. 1987. Color-Chemistry-Synthesis: Properties and Applications of Organic Dyes and Pigments, VCH Publishers, New York.

APPENDIX A

BISPHENOL-A CALIBRATION CURVE

Bisphenol-A calibration curve was prepared by injecting BPA solutions of 0.2, 0.5, 2, 5, 20, 40, 60 and 100 μM to the HPLC. Detected peak areas for each standard solution and the corresponding calibration curve is presented in Table A.1 and Figure A.1, respectively.

Table A.1. Detected peak areas during HPLC analysis of standard BPA solutions.

Bisphenol-A Concentration, μM	Peak Area
0.2	14964.0
0.5	36115.2
2	152437.8
5	382404.6
20	1542603.4
40	3206268.2
60	5211327.0
100	8616802.0

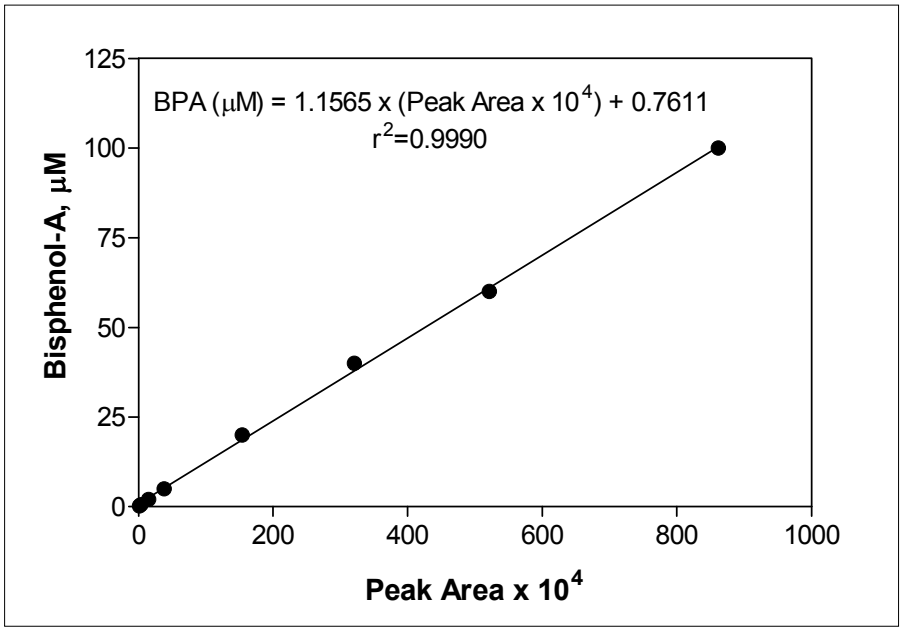

Figure A.1. Bisphenol A calibration curve.

APPENDIX B

4-n-NONYLPHENOL CALIBRATION CURVE

4-n-Nonylphenol calibration curve was prepared by injecting 4-NP solutions of 0.2, 0.5, 2, 5, 10, 20, 60, 100, 250 and 500 µM to the HPLC. Detected peak areas for each standard solution and the corresponding calibration curve is presented in Table B.1 and Figure B.1, respectively.

Table B.1. Detected peak areas during HPLC analysis of standard 4-NP solutions.

Nonylphenol Concentration, µM	Peak Area
0.2	704.1
0.5	1604.6
2	6767.5
5	23486.9
10	49793.5
20	96284.2
60	347510.7
100	663838.0
250	1780271.5
500	3612084.6

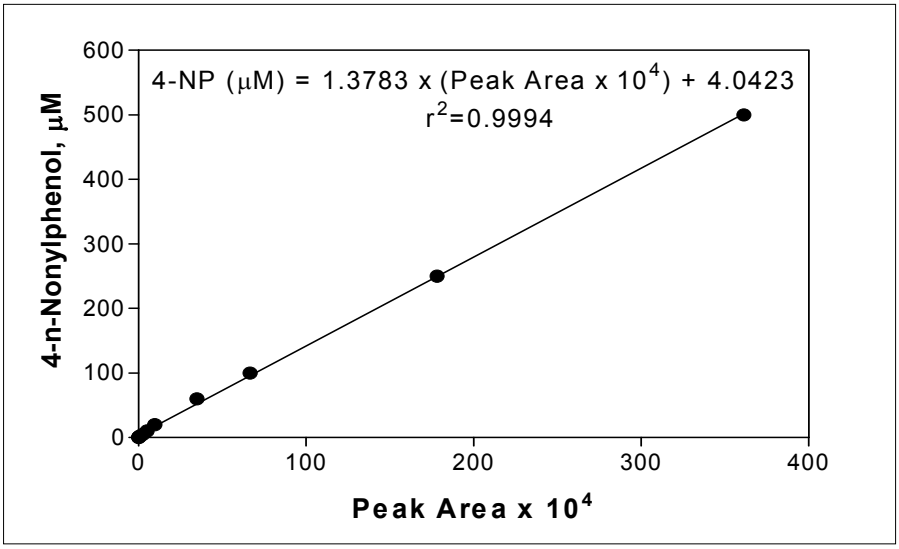

Figure B.1. 4-n-Nonylphenol calibration curve.

APPENDIX C

HYDROGEN PEROXIDE CALIBRATION CURVE

Hydrogen peroxide was analyzed as described in section 4.2.1.3. A calibration curve was prepared by using a series of H_2O_2 solutions and recording the absorbance at 351 nm as presented in Table C.1. The corresponding calibration curve is given in Figure C.1.

Table C.1. H_2O_2 concentrations and corresponing absorbance values at 351 nm used for calibration curve preparation.

H_2O_2 concentration (mg L^{-1})	Absorbance at 351 nm
0.396	0.012
0.791	0.039
1.187	0.062
1.582	0.085
1.978	0.114
2.373	0.138
3.164	0.191
3.955	0.241
7.911	0.505

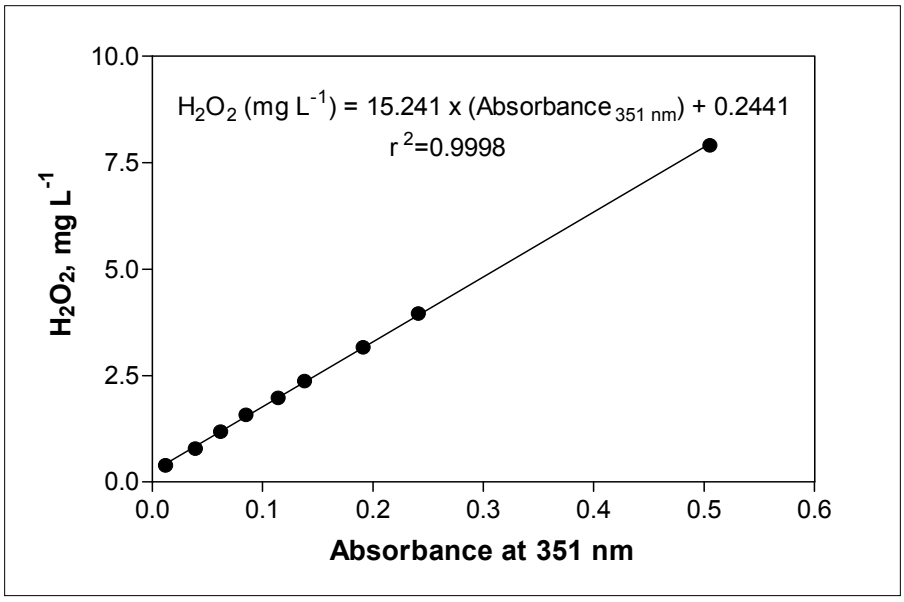

Figure C.1. H_2O_2 calibration curve.